

9th

International Symposium on
Hysteresis Modelling
and Micromagnetics

13-15 May 2013, Taormina, ITALY

HMM 2013



ABSTRACT BOOK



9th

International Symposium on
Hysteresis Modelling
and Micromagnetics

13-15 May 2013, Taormina, ITALY



Co-Chairs

Giovanni FINOCCHIO

*Department of Electronic Engineering, Industrial Chemistry and Engineering
University of Messina*

Giancarlo CONSOLO

*Department of Mathematics and Informatics
University of Messina*

9th

International Symposium on
Hysteresis Modelling
and Micromagnetics

13-15 May 2013, Taormina, ITALY



Scientific Committee

Giovanni FINOCCHIO, *University of Messina, Italy*

Giancarlo CONSOLO, *University of Messina, Italy*

Edward DELLA TORRE, *The George Washington University, Washington DC, USA*

Luis TORRES, *University of Salamanca, Spain*

9th

International Symposium on
Hysteresis Modelling
and Micromagnetics

13-15 May 2013, Taormina, ITALY



Local Organizing Committee

Bruno AZZERBONI, *University of Messina (chair)*

Giancarlo CONSOLO, *University of Messina*

Giovanni FINOCCHIO, *University of Messina*

Anna GIORDANO, *University of Messina*

Carmelo MILAZZO, *University of Messina*

Vito PULIAFITO, *University of Messina*

9th International Symposium on
Hysteresis Modelling
and Micromagnetics
13-15 May 2013, Taormina, ITALY



Editorial Board

Ermanno CARDELLI, *University of Perugia, Italy (chair)*

Franca ALBERTINI, *IMEM CNR Parma, Italy*

Gianfranco DURIN, *INRIM Torino, Italy*

Michela ELEUTERI, *University of Milano, Italy*

Vito PULIAFITO, *University of Messina, Italy*

Ciro VISONE, *University of Sannio, Benevento, Italy*

Roberto ZIVIERI, *University of Ferrara, Italy*

9th International Symposium on
Hysteresis Modelling
and Micromagnetics
13-15 May 2013, Taormina, ITALY



International Steering Committee

L. BENNETT, *The George Washington University, Washington DC, USA (chair)*

G. BERTOTTI, *INRIM Torino, Italy*

M. BROKATE, *TU Munchen, Germany*

E. CARDELLI, *University of Perugia, Italy*

J.R. CARDOSO, *University of Sao Paulo, Brazil*

R. CHANTRELL, *University of York, UK*

E. DELLA TORRE, *The George Washington University, Washington DC, USA*

M. DONAHUE, *NIST Gaithersburg, USA*

J. FIDLER, *Vienna University of Technology, Austria*

G. FRIEDMAN, *Drexel University, Philadelphia, USA*

A. IVANYI, *University of Budapest, Hungary*

H. KRONMULLER, *Max Planck Institut, Stuttgart, Germany*

I. MAYERGOYZ, *The University of Maryland, USA*

R. MCMICHAEL, *NIST Gaithersburg, USA*

I. MULLER, *The Technical University of Berlin, Germany*

C. SERPICO, *University of Naples Federico II, Italy*

J. SPREKELS, *The Weierstrass Institute, Germany*

A. VISINTIN, *University of Trento, Italy*

C. VISIONE, *University of Sannio, Benevento, Italy*

G.T. ZIMANYI, *University of California, Davis, USA*

Current-induced domain wall motion: Intrinsic pinning and two barrier stability

Teruo Ono

Institute for Chemical Research, Kyoto University, Uji, Japan

Electrical displacement of a domain wall (DW) is a prospective method for information processing in new type of magnetic non-volatile memories and logic devices [1-4]. Such novel spintronic devices require a low DW drive current and a high DW de-pinning field for stable information retention.

When a magnetic DW is driven by electric current via adiabatic spin torque, the theory predicts a threshold current even for a perfect wire without any extrinsic pinning [4]. We show the evidence that this intrinsic pinning determines the threshold current, and thus that the adiabatic spin torque dominates the DW motion, in a perpendicularly magnetized Co/Ni nano-wire [5-10].

Furthermore, we experimentally demonstrate that there exist two types of energy barriers, intrinsic and extrinsic, for the DW motion, and determine both barriers quantitatively. Given that the two energy barriers can be tuned independently by proper designing the devices, our finding suggests the possibility of durable spintronic devices with low power consumption.

This work was partly supported by a Grant-in-Aid for Scientific Research (S) and "Funding program for world-leading innovative R & D on science and technology" (FIRST program) from the Japan Society for the Promotion of Science.

-
- [1] A. Yamaguchi et al., Phys. Rev. Lett. 92 (2004) 077205.
 - [2] S. S. P. Parkin et al., Science 320 (2008) 190.
 - [3] D. A. Allwood et al., Science 309 (2005) 1688.]
 - [4] G. Tatara & H. Kohno, Phys. Rev. Lett. 92, (2004)086601.
 - [5] T. Koyama et al., Nature Materials, 10 (2011) 194.
 - [6] T. Koyama et al., Appl. Phys. Lett. 98 (2011) 192509.
 - [7] T. Koyama et al., Appl. Phys. Lett. 98 (2011) 192509.
 - [8] D. Chiba et al., Appl. Phys. Express 3 (2010) 073004.
 - [9] T. Koyama et al., Appl. Phys. Express 1 (2008) 101303.
 - [10] T. Koyama et al., Nature Nanotechnology 7 (2012) 635.

Current Driven Gyrotropic Mode of a Magnetic Vortex as a Non-Isochronous Auto-Oscillator

Andrei Slavin

Oakland University, Rochester, MI 48309

It is shown that the stable current-driven gyrotropic motion of the vortex core in a vortex-state free layer of a spin-torque nano-oscillator can be described in the framework of a standard model of a non-isochronous auto-oscillator. It is also demonstrated that the non-isochronous parameters of the gyrotropic mode auto-oscillator, determining its non-autonomous dynamics under the influence of external signals, can be found from the measurements of the linewidths of higher harmonics of the autonomous current-driven gyrotropic motion.

Magnetic vortex-antivortex dipoles in spin-transfer oscillators

Stavros Komineas^a

^a Department of Applied Mathematics, University of Crete, Heraklion, Greece

Periodic motion of vortices in the GHz range which is induced by spin-transfer-torque give rise to spin-transfer-oscillators (STO). This raises anew the issue of magnetic vortex dynamics.

We assume that spin-polarized current, with in-plane spin-polarization, is injected through a nano-aperture on the top surface of an element. Spin torque acts on a vortex-antivortex (VA) pair where the vortex and the antivortex have opposite polarities. This vortex dipole has the structure of a skyrmion with skyrmion number $\mathcal{N} = 1$. Our study is based on the Landau-Lifshitz-Gilbert-Slonczewski equation. We show that the dipole is set in a steady rotational motion which is induced by two independent forces: the interaction between the two vortices and an external in-plane magnetic field. The nonzero skyrmion number of the vortex dipole is responsible for both forces giving rise to rotational motion. The spin-torque acts to stabilize the motion.

We obtain simple rotational dynamics (steady-state rotation) by taking into account the exchange interaction and an easy-plane anisotropy. We find three types of vortex-antivortex pairs, which may even coexist for the same parameter values, as shown in Fig. 1. This gives bistability and could lead to hysteresis, as has been observed in experiments.

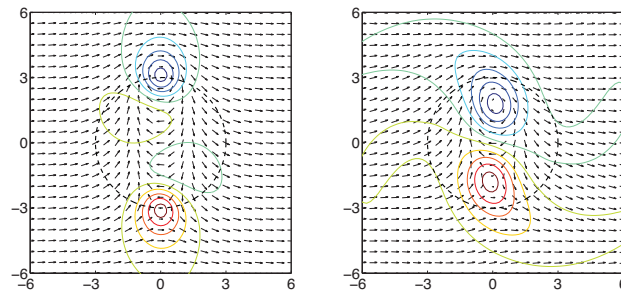


Figure 1: Vector plots for two stable vortex-antivortex pairs in steady-state rotation around a nano aperture (dashed line). Colored lines are contour plots for the perpendicular magnetization component (red: up, blue: down). Both pairs correspond to exactly the same parameter values, but their frequencies of rotation are significantly different.

We derive an exact (virial) relation through which we interpret the skyrmion rotational motion and show the effect of various factors to the rotation frequency. The external magnetic field can be used to tune the frequency of rotation, while the spin-torque affects the frequency indirectly, by tuning the distance between the two vortices.

The present results could be used as a framework for the description of frequency generation by various topological solitons under spin-polarized current.

Spin-orbit Torques in Ferromagnetic Thin Films

I. M. Miron¹, K. Garello², E. Jué¹, G. Gaudin¹, P.-J. Zermatten¹, M. V. Costache², S. Auffret¹,
S. Bandiera¹, B. Rodmacq¹, J. Vogel⁵, S. Pizzini⁵, A. Schuhl⁵, and P. Gambardella^{2,3,4}

¹ SPINTEC, UMR-8191, CEA/CNRS/UJF/GINP, INAC, Grenoble, France

² Catalan Institute of Nanotechnology (ICN-CIN2), Barcelona, Spain

³ Departament de Física, Universitat Autònoma de Barcelona (UAB), Barcelona, Spain

⁴ Institució Catalana de Recerca i Estudis Avançats (ICREA), Barcelona, Spain

⁵ Néel Institute CNRS Grenoble, France

Materials with large coercivity and perpendicular magnetic anisotropy represent the mainstay data storage media, thanks to their ability to retain a stable magnetization state over long periods of time and their compliance with increasing miniaturization steps. A major concern is that the same anisotropy properties that make a material attractive for storage also make it hard to write.

We address this issue by investigating novel spin torque mechanisms based on spin-orbit effects. It is well known that spin-orbit coupling is ultimately responsible for magnetocrystalline anisotropy and damping. Under certain conditions, however, spin-orbit effects might either induce [1,2,3] or enhance [4,5] specific spin torque mechanisms.

We show that in materials lacking inversion symmetry, the spin accumulation induced by the current creates torques on the magnetization. We analyze the expected symmetry of these torques in uniformly magnetized layers as well as magnetic domain walls, and evidence experimentally their existence in agreement with symmetry arguments.

-
1. A. Manchon and S. Zhang, PRB **78** 212405 (2008)
 2. I.M. Miron et al. Nature Materials **9**, 230-234 (2010)
 3. I.M. Miron et al. Nature **476**, 189-193 (2011)
 4. I.M. Miron et al. PRL **102**, 137202 (2009)
 5. I.M. Miron et al. Nature Materials **10**, 419 (2011)

Current-induced domain wall motion along high perpendicular magnetocrystalline anisotropy ferromagnetic stacks

Eduardo Martinez^a, Satoru Emori^b and Geoffrey S. D. Beach^b

^aUniversidad de Salamanca. Salamanca. Spain.

^bMassachusetts Institute of Technology. Cambridge, Massachusetts. USA

The current-induced domain wall motion (CIDWM) along thin ferromagnetic strips with high perpendicular magnetocrystalline anisotropy (PMA) is nowadays a subject of great technological and fundamental interest. For instance, it has been recently shown [1,2] that a current alone drives very efficiently DWs in ultrathin ferromagnetic strips (Co or CoFe) sandwiched between an oxide (AlO or MgO) and a heavy metal (Ta or Pt). The direction of the CIDWM depends on the underneath heavy metal layer [2], being along the electron flow (against the current) in the Ta/CoFe/MgO stack, or along the current (against the electron flow) in the Pt/CoFe/MgO stack.

The high velocity and the direction of the CIDWM along the current in the Pt stack are inconsistent with the conventional spin-transfer torque (STT) theory, and these observations have been attributed to novel contributions due to spin-orbit torques (SOTs) such as the Rashba effect and/or the spin Hall effect (SHE). The Rashba effective field stabilizes Bloch DWs against deformation, permitting high-speed motion via conventional STT if one of the non-adiabatic parameter or the polarization factor has a negative value [1]. On the other hand, the SHE in the heavy metal has been shown strong enough to induce magnetization switching [3], which indicates that it likewise plays a key role in CIDWM. However, the SHE alone can only drive the DW if it adopts a Néel configuration [4], but its direction of motion with respect to the current depends on the internal DW magnetization (Néel right or Néel left) and on the magnetization state at the two domains (up-down or down-up). Considering the cross section of the studied samples, a Néel state is not expected from magnetostatic considerations, unless a strong antisymmetric exchange Dzyaloshinskii-Moriya interaction (DMI) stabilizes the Néel configuration against the Bloch one [5,6].

In this talk, the influence of the spin-orbit torques (Rashba and/or SHE) and the DMI on the current-driven DW dynamics will be analyzed by means of full micromagnetic simulations and the one-dimensional model. In particular, it will be shown that the DMI explains the CIDWM in the Pt/CoFe/MgO system by stabilizing Néel DW with a left-handed chirality [2,5], such that the SHE alone drives it along the current, uniformly and with high efficiency.

-
- [1] I.M. Miron et al. *Nat. Mater.* 10, 419 (2011).
 - [2] S. Emori et al, arXiv:1302.2257 (2013).
 - [3] L. Liu, et al., *Science* 336, 555–558 (2012).
 - [4] A. V. Khvalkovskiy et al. *Phys. Rev. B* 87, 020402 (2013).
 - [5] M. Heine et al. *Phys. Rev. B* 78, 140403 (2008).
 - [6] A. Thiaville et al. *European Physics Letters.* 100, 57002 (2012).

Spin-orbit coupled transport at metallic interfaces

A. Manchon, X. Wang, C. Ortiz-Pauyac, S. Grytsyuk, P. Barba Gonzalez, H. Li, U. Schwingenschlogl

Physical Science and Engineering Division, King Abdullah University of Science and Technology (KAUST), Saudi Arabia
E-mail: aurelien.manchon@kaust.edu.sa

It has been recently demonstrated that appropriately designed spin-orbit coupling (SOC) can be used to generate spin torque (coined as SOC-torque) in a single ferromagnet, without the need of an external polarizer [1-3]. This effect has been observed experimentally in both perpendicular and in-plane magnetic systems, consisting in ferromagnetic metals [4,5] and dilute magnetic semiconductors [6]. Interestingly, due to the complex structure of metallic systems, the microscopic origin of the current-driven magnetization dynamics is still under debate and the contributions of spin Hall and band structure effects are still under intense investigation [7].

In this work, I will address the different origins of the SOC-torque and discuss experimental implications. In a first part, I will introduce a diffusive model for spin Hall effect in metallic bilayers and show how it can generate spin torque, anisotropic magnetoresistance and anomalous Hall effect. The connection between these three effects can be exploited as a probe of the spin Hall origin of the SOC-torque. In a second part, I will address the nature of the band structure of such bilayers in the presence of interfacial symmetry breaking using *ab initio* calculations. It can be shown such an inversion asymmetry in the system produces two important effects: the well-known Rashba field (and related Rashba torque) on the itinerant electrons, and the celebrated Dzyaloshinskii-Moriya interaction on the localized spins. In a third part, I will discuss the nature of the Rashba torque and its complex angular dependence in a simplified 2-dimensional model. Implications in terms of experimental observations will be proposed.

[1] A. Manchon and S. Zhang, Phys. Rev. B 78, 212405 (2008); Phys. Rev. B 79, 094422 (2009).

[2] X. Wang and A. Manchon, Phys. Rev. Lett. 108, 117201 (2012); arXiv:1111.5466.

[3] K. Obata, and G. Tatara, Phys Rev. B 77, 214429 (2008).

[4] I. M. Miron et al., Nature Materials 9, 230 (2010); U. H. Pi et al., Appl. Phys. Lett. 97, 162507 (2010); I. M. Miron, et al. Nature (London) 476, 189 (2011).

[5] L. Liu, et al., Phys. Rev. Lett. 106, 036601 (2011); Science 336, 555 (2012).

[6] A. Chernyshov et al., Nature Physics 5, 656 (2009); M. Endo, F. Matsukura, and H. Ohno, Appl. Phys. Lett. 97, 222501 (2010); Fang et al. Nature Nanotechnology 6, 413 (2011).

[7] P. Haney, K.-J. Lee, H.-W. Lee, A. Manchon and M. D. Stiles, arXiv:1301.4513

Modelling experiments on ultra-fast domain wall dynamics

Mathias Kläui^{a,b}

^aInstitut für Physik, Johannes Gutenberg-Universität Mainz, 55128 Mainz, Germany

^bGraduate School of Excellence Materials Science in Mainz (MAINZ), Johannes Gutenberg-Universität Mainz, 55099 Mainz, Germany

In common micromagnetic simulations, the dynamics due to applied fields and injected spin-polarized currents can be simulated. Particularly exciting spin dynamics can be found in confined spin structures such as domain walls [1]. Field-induced dynamics has been predicted to lead to constant domain wall displacements for field strengths below the Walker Breakdown, while above precessional domain wall motion sets in [1]. We find that in ring structures, even below the Walker breakdown, periodic velocity oscillations occur, which we explain using micromagnetic simulations by the interplay between the acting torque terms. To displace multiple domain walls synchronously by magnetic fields in a wire was previously thought impossible due to a certain field direction favouring domains parallel to the field thus leading to opposite wall motion for adjacent walls. We overcome this problem using specially tailored perpendicular field pulses that displace multiple walls in a wire in the same direction [2].

Since magnetic fields exhibit unfavourable scaling alternative approaches based on spin-currents have emerged. The transfer of angular momentum (“spin transfer torque effect”) leads for instance to current-induced domain wall motion (CIDM) [3]. We find that the previously neglected diffusive torque term [4] that acts as a non-adiabatic torque can play an important role for vortex core displacement. By extending the LLG equation with spin torque terms that depend on the magnetization gradient, the diffusive torque can be modelled. Concurrently we also measure the domain wall magnetoresistance effect in nanoconstrictions and correlate the observed large effects with the domain wall structure [5].

Finally using Free Electron Laser sources, we measure the ultra-fast magnetization dynamics due to superdiffusive spin currents [6]. These are modelled using a Monte Carlo approach of superdiffusive spin transport [7].

-
- [1] M. Kläui, Review in *J. Phys. Cond. Matter* **20**, 313001 (2008).
 - [2] J.-S. Kim, M. Kläui, Patent EP12199318
 - [3] L. Heyne et al., *Phys. Rev. Lett.* **105**, 187203 (2010); M. Eltschka et al., *Phys. Rev. Lett.* **105**, 056601 (2010).
 - [4] A. Manchon, W.-S. Kim, and K.-J. Lee, arXiv:1110.3487
 - [5] A. von Bieren et al., *Phys. Rev. Lett.* **110**, 67203 (2013).
 - [6] B. Pfau et al., *Nature Comm.* **3**, 1100 (2012).
 - [7] M. Battiato et al., *Phys. Rev. Lett.* **105**, 027203 (2010).

Ordered arrays of magnetic nanostructures in thin films: synthesis and modeling

Paola Tiberto, Gabriele Barrera, Federica Celegato, Marco Coisson, Alessandra Manzin, Franco Vinai, Luca Boarino, Natascia De Leo

INRIM, Electromagnetism Division, Torino, Italy

Progress in nanomagnetism has been achieved by the simultaneous advances in nanotechnology that allows the fabrication of novel magnetic nanostructures, as arrays in magnetic thin films. This is primarily motivated by applications such as spintronics, magnetic sensing, and ultrahigh-density magnetic recording. In this context, fabrication process based either on high-resolution planar lithography (i.e. sequential optical, electron-beam and focused ion beam lithography) or large area self-assembly approaches (polystyrene nanospheres or nanotemplates) have played a major role and has been intensively worldwide investigated in the last decade. The accurate control of the arrays nanostructures dimension, distance and ordering together with the thin films composition has led to a variety of new classes of magnetic nanomaterials with a unique combination of remarkable properties: DC magnetotransport, exchange bias, magnetization switching and spin dynamics.

In this talk, a variety of nanostructured arrays on magnetic thin film obtained either by top down or bottom up lithographical techniques will be shown. In the latter case, two multi-step processes exploiting self-assembling of polystyrene nanospheres to create dot and anti-dot arrays in thin films (Co, Ni, Ni₈₀Fe₂₀, Fe₅₀Pd₅₀ and Fe₅₃Pt₄₇) by means of nanosphere lithography will be shown. The first one directly uses polystyrene nanospheres (PN) as a mask to fabricate arrays of magnetic nanoholes and dots. In the second case, the nanospheres are used to design a polymeric mask on a photoresist subsequently used to pattern a magnetic nanostructure on a film. Advantages and disadvantages of the two lithographical techniques will be discussed particularly regarding magnetic response. DC magnetic and magnetotransport properties will be highlighted. In particular hysteresis properties in nanostructures produced either with top-down or bottom up lithographical techniques will be accounted for by using a micromagnetic numerical approach.

Spin wave band structure in one- and bi-component magnonic crystals

Gianluca Gubbiotti^a, Silvia Tacchi^a, Marco Madami^b and Giovanni Carlotti^b

^a Istituto Officina dei Materiali del CNR (CNR-IOM), Unità di Perugia, c/o Dipartimento di Fisica, Via A. Pascoli, I-06123 Perugia, Italy

^b Dipartimento di Fisica, Università di Perugia, Via A. Pascoli, I-06123 Perugia, Italy

Magnonic crystals (MCs) represent a new class of metamaterials with periodically modulated magnetic properties[1,2] where, similarly to light in photonic crystals,[3] the spin waves (SWs) dispersion is characterized by the presence of allowed magnonic states and ranges of forbidden frequencies.[4] The latter are related to the appearance of Brillouin Zones, induced by the artificial periodicity of the pattern geometry. MCs offer better prospects for miniaturization of a new generation of spin logic devices, filters, and waveguides operating in the GHz frequency range.[5] To this respect, knowledge of the magnonic band structure and of the physics underpinning the dispersion curves of magnonic modes is of paramount importance for any desired application.[6] While most of the reported works on MCs are focused on in one-component arrays of identical elements (stripes and dots),[7,8] coupled by dynamical dipolar interaction, and antidot arrays where circular holes are drilled into a continuous ferromagnetic film,[9] there are few reports about bi-component MCs (BMCs). In this presentation, recent results obtained by Brillouin light scattering for the SW band diagram in BMCs, constituted by two magnetic materials with different saturation magnetization and exchange stiffness as well, are reviewed.[10,11]

This work was partially supported by MIUR-PRIN 2010-11 Project2010ECA8P3 "DyNanoMag"

-
- [1] V. V. Kruglyak et al., J. Phys. D: Appl. Phys. 43, 264001 (2010).
 - [2] B. Lenk et al., Phys. Rep. 507, 107 (2011)
 - [3] E. Yablonovitch et al., Phys. Rev. Lett. 63, 1950 (1989).
 - [4] G. Gubbiotti et al., J. Phys. D: Appl. Phys. 43, 264003 (2010).
 - [5] G. A. Melkov et al., J. Appl. Phys. 99, 08P513 (2006).
 - [6] S. Tacchi et al., Phys. Rev. Lett. 107, 127204 (2011).
 - [7] J. Ding et al., Phys. Rev. Lett. 107, 047205 (2011).
 - [8] G. Gubbiotti et al., Appl. Phys. Lett. 90, 092503 (2007).
 - [9] S. Tacchi et al., Phys. Rev. B **86**, 014417 (2012).
 - [10] G. Duerr et al., Appl. Phys. Lett. **99**, 202502 (2011).
 - [11] S. Tacchi et al., Phys. Rev. Lett. **109**, 137202 (2012)

Magnetic reversal modes in magnetic nanowires prepared from ordered hexagonal alumina templates

Yu. P. Ivanov^a, M. Vázquez^a, O. Chubykalo-Fesenko^a

^a Instituto de Ciencia de Materiales de Madrid, CSIC, Cantoblanco, 28049 Madrid, Spain

Magnetic nanowires (NWs) with diameters of the order or less than the single domain limit, as well as their arrays, are very attractive for applications in nanoelectronics, chemical and biological sensing, medicine etc. Using templates, such as hexagonal highly ordered anodic alumina oxide (AAO) membranes, NWs with high aspect ratios can be prepared [1], which is difficult to achieve by other techniques such as conventional lithographic processes. The knowledge of the coercivity mechanism in relation to material and geometry of such NWs and their arrays is important for engineering their magnetic properties for future applications. Powerful instrument to investigate the magnetization reversal modes in NWs as well as their ordered arrays is the micromagnetic simulation [2]. The quantitative agreement between simulation data and experimental ones strongly depends on the inclusion of realistic experimental nanostructure and parameters into the model [2].

We present systematic micromagnetic simulations of most commonly reported experimental electrodeposited nanowires, based on permalloy, nickel, iron and cobalt, with different crystal structures. The dependence of coercivity and remanence on the nanowire diameter, the angular dependence of coercivity and the corresponding reversal modes are presented and discussed. Depending on the crystallographic structure, the nanowires present transverse or vortex domain wall or the vortex structure along the whole nanowire length. In Fig.1 the results are presented as the state diagrams for the reversal modes. The corresponding magnetic force microscopy images of different structures are also evaluated by the micromagnetic simulations.

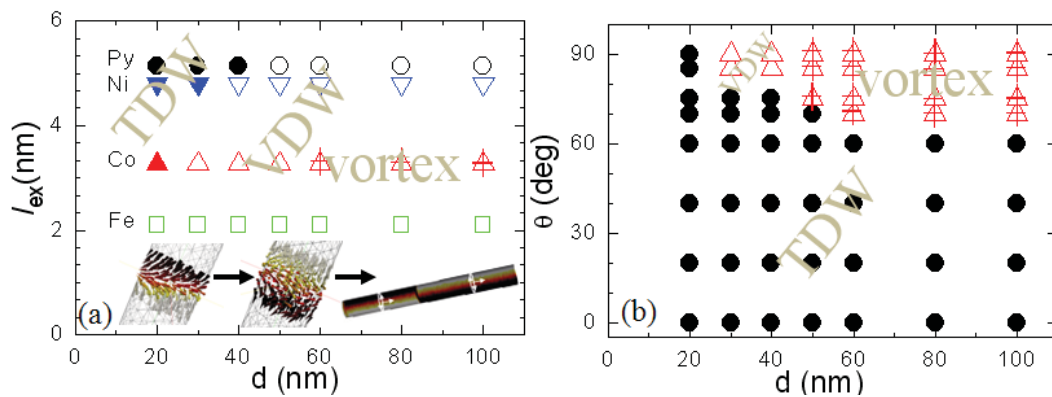


Figure 1: The state diagram of the magnetic reversal modes as a function of the NW diameter in (a) polycrystalline and single crystalline cubic anisotropy NWs and (b) NWs with single crystalline hcp Co and easy axis direction at the angle θ with the NW axis, as a function of the NW diameter. The fill points and open points are TDW and VDW, accordingly. The cross rectangles indicate the area with magnetic vortex state spanning the whole NW length at the remanence. The field is applied parallel to NW axis.

[1] L. G. Vivas et al. Phys. Rev. B 85 (2012), 035439.

[2] L. G. Vivas et al. (2013), accepted in Nanotechnology.

Experimental demonstration of basic mechanisms of magnetization reversal in magnetic microwires

Alexander Chizhik^a, Andrzej Stupakiewicz^b, Arcady Zhukov^{a,c}, Andrzej Maziewski^b, Julian Gonzalez^a

^aUniversidad del País Vasco, UPV/EHU, San Sebastián, Spain

^bLaboratory of Magnetism, University of Białystok, 15-424 Białystok, Poland

^cIKERBASQUE, Basque Foundation for Science, 48011 Bilbao, Spain

The study of magnetization reversal is the key task related to the sensor application of the magnetic microwires. During last years we performed systematically the investigation of the magnetic domain structure and magnetization reversal process in wide series of the glass covered microwires of different compositions, metallic nucleus diameters and glass covering thickness. As a result of this search we have found that the microwire of nominal composition $\text{Fe}_{5,71}\text{Co}_{64,04}\text{B}_{15,88}\text{Si}_{10,94}\text{Cr}_{3,40}\text{Ni}_{0,03}$ and metallic nucleus diameter of 100 μm demonstrates perfect samples of surface magnetic domain structure. Therefore, it was selected as the best specimen for the detailed investigation of the mechanisms of the local magnetization reversal in cylindrically shaped wires.

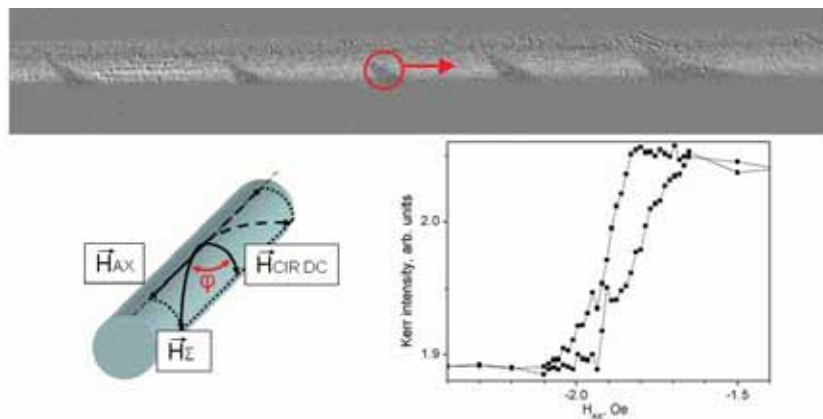


Figure 1. Kerr image of drift of wedged domains; corresponding hysteresis loop and schematic configuration of magnetic field application.

Magnetic domain imaging in the surface of microwires has been performed by means of magneto-optical Kerr effect (MOKE) microscopy [1]. Hysteresis loops were obtained from the magneto-optic intensity as a result of the MOKE images processing. The experiments have been performed in crossed axial and circular magnetic fields (Fig. 1). It was found four different mechanisms of the magnetization reversal as dependence of the external magnetic field configuration: (i) long distance quick motion of the solitary circular domain walls, (ii) the effect of the domain suppression, (iii) the drift of wedged domains (Fig. 1) and (iv) formation and transformation of the vortex domain structure.

The analysis of the obtained results has been performed using the theoretical model based on four magnetization states with different chirality [2]. In this case helical magnetic field induces the co-existence of stable and metastable helical magnetic states in the surface of the microwire which participate in the process of the magnetization reversal.

[1] A. Chizhik, A. Stupakiewicz, A. Maziewski, A. Zhukov, J. Gonzalez, and J. M. Blanco, *Appl. Phys. Lett.* **97** (2010), 012502.

[2] A. Chizhik, V. Zablotskii, A. Stupakiewicz, C. Gómez-Polo, A. Maziewski, A. Zhukov, J. Gonzalez, and J. M. Blanco, *Phys. Rev. B* **82** (2010), 212401.

Dynamical magnetization pinning of the main ferromagnetic resonance mode in a thin circular dot

G.R. Aranda^a, G.N. Kakazei^{b,c}, S.A. Bunyaev^b, V.O. Golub^c, E. Tartakovskaya^c, A. Chumak^d, A. Serga^d, B. Hillebrands^d, K.Y. Guslienko^{a,e}

^a Dpto. Física de Materiales, Universidad del País Vasco, San Sebastian, Spain

^b Dpto. Física da Faculdade de Ciências, IFIMUP–IN, Universidade do Porto, Porto, Portugal

^c Institute of Magnetism, National Academy of Sciences of Ukraine, Kiev, Ukraine

^d Technische Universität Kaiserslautern, Kaiserslautern, Germany

^e IKERBASQUE, The Basque Foundation for Science, Bilbao, Spain

A comprehensive experimental, micromagnetic and analytical investigation of high frequency magnetization dynamics in circular Permalloy ferromagnetic dots as a function of the external magnetic field orientation was carried out [1]. We established the limits for applicability of the simple Kittel's equation for the main resonance field depending on the field orientation and the dot sizes. The square arrays of Permalloy dots with the diameters $2R$ varying from 500 to 4000 nm, thicknesses $L = 40$ and 50 nm and the lattice period of $4R$ to avoid dipolar interdot interactions were prepared in one deposition run to keep the same magnetization and in-plane anisotropy. Room temperature ferromagnetic resonance measurements were done at 9.85 GHz using a standard X-band electron spin resonance spectrometer. Out-of-plane angular dependence of the main resonance peak was measured in the whole range of the field angles $0^\circ \leq \theta \leq 90^\circ$ with respect to the dot plane.

It has been shown that the experimentally observed magnetization dynamics of the main resonance mode can be qualitatively interpreted in terms of varying dipolar boundary conditions for the dynamic magnetization components at the dot lateral edges and described in the terms of pinning of the dynamical magnetization [2]. We calculated the pinning parameter from micromagnetically simulated dynamical magnetization mode profiles, similarly to Ref. [3] and also obtained this parameter from geometrical and magnetic parameters by extension of the theory of in-plane magnetized dots [2]. Micromagnetic simulations also offered the possibility of the direct calculation of local demagnetizing fields that can be compared with approximate analytical calculations. Finally, the values of resonance fields and pinning parameters obtained from the simulations and theory were compared to the ferromagnetic resonance measurements. The pinning parameter can be considered as an indicator of the uniformity of the dynamical magnetization profile and validity of the Kittel approximation.

Regardless non-elliptic dot shape and relatively large dynamical magnetization pinning at the dot lateral edges, the Kittel equation (no pinning) has good accuracy for the description of the experimentally measured main excitation mode in thin dots (the aspect ratios thickness/radius $b = L/R \leq 0.1$) within a wide range of the external field angles $\theta = 7-90^\circ$. Whereas, for the dot aspect ratios $b > 0.1$ and field orientations close to the dot normal ($\theta = 0^\circ$) the strong pinning conditions [4] are more appropriate and a more detailed approach accounting essentially inhomogeneous distribution of the dynamic magnetization is necessary.

-
- [1] G. N. Kakazei et al., Phys. Rev. B **86** (2012), 054419.
[2] K. Y. Guslienko and A. N. Slavin, Phys. Rev. B **72** (2005), 014463.
[3] H. T. Nguyen, T. M. Nguyen, and M. G. Cottam, Phys. Rev. B **76** (2007), 134413.
[4] G. N. Kakazei et al., Appl. Phys. Lett. **85** (2004), 443-445.

Analytical solutions of Helmholtz equations

By

Variational Iteration and Adomian Methods

^aDursun Üstündag, ^bN. Füsün Oyman Serteller,

^aFaculty of Science and Letters, Department of Mathematics, Marmara University, Istanbul, Turkey.

^bFaculty of Technology, Department of Electrical Engineering, Marmara University, Istanbul, Turkey.

In this research, two analytical approximated methods namely variational iteration (VIM) [1] and Adomian's decomposition (ADM) [2] are compared for the solution of initial value problems of Helmholtz equations shown in (1). Some illustrative examples, such as nonhomogeneous hyperbolic telegraph and ecliptic wave equations are presented to show the efficiency of the methods

$$\begin{cases} \frac{\partial^2 u(x, y)}{\partial x^2} + \frac{\partial^2 u(x, y)}{\partial y^2} - 2u(x, y) = (12x^2 - 3x^4) \sin(y), \\ u(0, y) = 0, \quad u_x(0, y) = 0 \end{cases} \quad (1)$$

Below Figure 1 shows that both VIM and ADM are efficient methods by comparing absolute errors in the solution of Helmholtz equation given in (1), which represents electromagnetic systems. However, VIM has merits and advantages over ADM to overcome the difficulties arising in calculation of Adomian Polynomials. Certain extension of this work to other equations is possible and symbolic computation is playing a role both in the theory and practical applications.

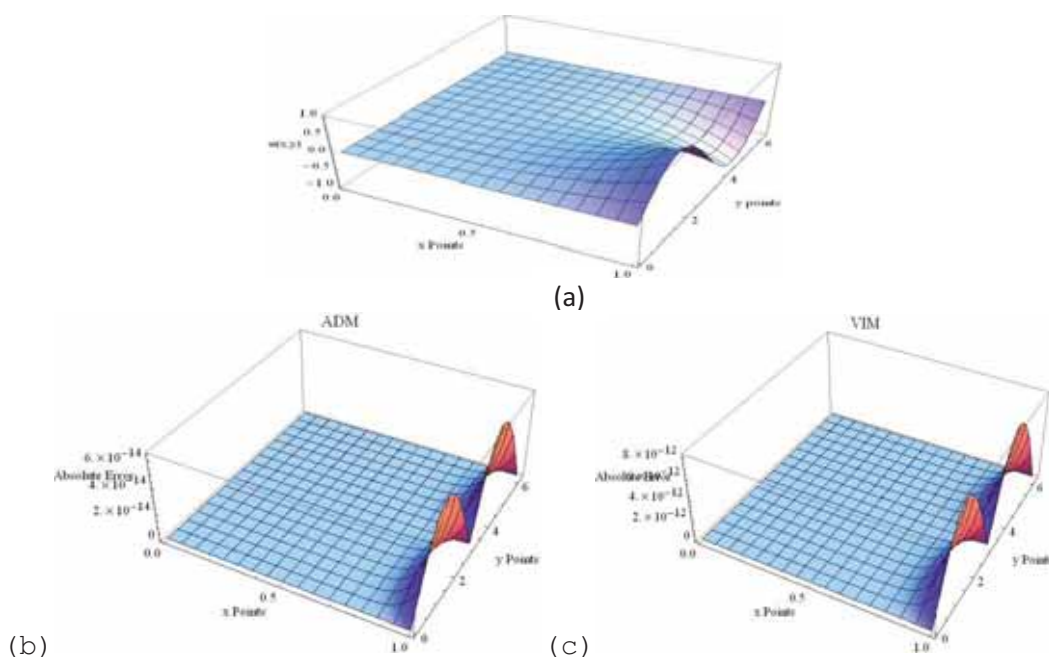


Figure 1. (a) Solution of Equation (1), obtained by using ADM and VIM. (b) and (c) Absolute errors versus with grid points, respectively.

References

- [1] Dehghan, M. and Shakeri, F. Application of He's variational iteration method for solving the Cauchy reaction-diffusion problem. *J Comput Appl Math*, 214, 2 (May 1 2008), pp.435-446.
- [2] Al-Mannai, M. and Khabeev, N. Numerical solution of nonlinear heat problem with moving boundary. *Acta Astronaut*, 70(Jan-Feb 2012),pp 1-5.
- [3] Adomian, G. Solutions of nonlinear PDE. *Appl Math Lett*, 11, 3 (May 1998), pp121-123

Symmetry properties and invariance of vortex-state linearized equations of motion in ferromagnetic dots

Roberto Zivieri^a, Giancarlo Consolo^b

^aDipartimento di Fisica e Scienze della Terra, Università di Ferrara, Ferrara, Italy

^bDipartimento di Scienze per l'Ingegneria e l'Architettura, Università di Messina, Messina, Italy

We prove some discrete space and time symmetries of linearized equations of motion in vortex-state ferromagnetic dots. The space symmetries are strictly related to the vortex-state configuration of the magnetization characterized by a chirality $c = \pm 1$ (counterclockwise or clockwise rotation of the magnetization) and a polarity $p = \pm 1$ (outward or inward core magnetization) and to its nature of axial vector. For a purely conservative dynamics, the linearized equation of motion in vortex-state ferromagnetic dots is written in the approximated form as [1]

$$-\frac{1}{\gamma} \frac{\partial \delta \vec{m}_{\text{OC}}}{\partial t} = \vec{\tau}. \quad (1)$$

where γ is the gyromagnetic ratio, $\delta \vec{m}_{\text{OC}} = (\delta m_u, \delta m_z)$ is the out-of-core (OC) dynamic magnetization and $\vec{\tau} = (\tau_u, \tau_z)$ is the torque. Eq.(1) can be applied to ferromagnetic dots of any shape exhibiting a curling configuration. First, we discuss the space symmetries. By placing the vortex parallel to the reflection plane (xy plane) and by introducing the space reflection operator σ_{xy} , the following symmetry transformation holds: $\sigma_{xy} c = -c$. The c switching leads to a change of sign of the in-plane static magnetization component ($M \rightarrow -M$) and of the in-plane dynamic one, namely $\delta m_u \rightarrow -\delta m_u$ which leads to a change of sign of the corresponding dynamic effective field component $\delta h_u \rightarrow -\delta h_u$. Moreover, there is also the switching $\delta m_v^C \rightarrow -\delta m_v^C$ of the core (C) component $\delta m_v^C = -\delta m_z \cos \theta$ with θ the polar angle. These transformations lead to the invariance of Eq.(1). By placing the vortex perpendicularly to the reflection plane (xy plane), we get $\sigma_{xy} p = -p$. The p switching (vortex core switching) leads to $\delta m_u \rightarrow -\delta m_u$ and to $\delta m_z \rightarrow -\delta m_z$ leaving again the equation of motion invariant. A remarkable physical effect on spin dynamics is the interchange $k_v \rightarrow -k_v$ of the phases of azimuthal vortex modes characterized by the azimuthal number $k_v = \pm 1, \pm 2, \dots$ obtained by using a reflection operator $\bar{\sigma}_{xy}$ in a quantum mechanical scheme such that $\bar{\sigma}_{xy} \delta m_i(k_v) = \delta m_i^*(k_v)$ with $i = u, z$.

We now discuss the time-reversal T symmetry, namely $t \rightarrow -t$. Under this symmetry transformation both the static and dynamic quantities change sign, due to the reversal of angular momentum of electrons, leaving Eq.(1) invariant like in the case of space symmetries. Within a quantum mechanical scheme, according to Wigner anti-unitary operator [2] $T \delta m_i(t) = \delta m_i^*(-t)$, the effect is equivalent to that of $\bar{\sigma}_{xy} (k_v \rightarrow -k_v)$ and leads to a change of the sense of rotation of azimuthal vortex modes including the gyrotropic. Instead, the dynamics of radial modes ($k_v = 0$), is not affected by the T symmetry.

[1] R. Zivieri and F. Nizzoli, Phys. Rev. B **75** (2005), 014411-1-5; *ibidem* Phys. Rev. B **74** (2006), 219901(E).

[2] E.P. Wigner, Group theory and its application to the quantum mechanics, New York, Academic Press (1959), p.325.

On the density of chirality equation in a vortex-state cylindrical ferromagnet

Roberto Zivieri^a

^aDipartimento di Fisica e Scienze della Terra, Università di Ferrara, Ferrara, Italy

An equation for the density of chirality in a circular and cylindrical ferromagnet exhibiting a flux-closure configuration of the magnetization is derived following a semi-classical approach [1]. We outline its derivation in the simplest case, that of a circular ferromagnetic ring exhibiting a vortex-state and neglecting damping. For a classical ferromagnet (FM) in the vortex flux-closure configuration it is useful to write down, in analogy with the classical fluid, a circulation Γ in the form of a line integral $\Gamma = \oint_{\partial S} \vec{M} \cdot d\vec{l}$ where ∂S denotes the contour line of the surface S and \vec{M} is the magnetization

field. By applying the Stokes theorem we get $\oint_{\partial S} \vec{M} \cdot d\vec{l} = \oint_S \vec{\nabla} \times \vec{M} \cdot d\vec{S}$. The density of chirality (or chirality per unit area) is defined as the curl of the magnetization field, viz. $\vec{\omega}_{\text{FM}} = \vec{\nabla} \times \vec{M}(t)$. Taking into account the purely precessional Landau-Lifshitz equation, namely $-\frac{1}{\gamma} \frac{\partial \vec{M}}{\partial t} = \vec{M} \times \vec{H}$ and applying the curl operator on both members yields

$$-\frac{1}{\gamma} \frac{\partial \vec{\omega}_{\text{FM}}}{\partial t} = \vec{M} (\vec{\nabla} \cdot \vec{H}) - \vec{H} (\vec{\nabla} \cdot \vec{M}) + (\vec{H} \cdot \vec{\nabla}) \vec{M} - (\vec{M} \cdot \vec{\nabla}) \vec{H}. \quad (1)$$

In the linear approximation the total magnetization \vec{M} and the effective field \vec{H} are decomposed into a static and a small dynamic part, viz. $\vec{M} = \vec{M}_0 + \delta \vec{m}$ and $\vec{H} = \vec{H}_0 + \delta \vec{h}$ with \vec{H}_0 the static exchange field and $\delta \vec{h}$ given by the sum of the dynamic dipolar and exchange fields. Hence, Eq.(2) becomes

$$-\frac{1}{\gamma} \frac{\partial \vec{\omega}_{\text{FM}}}{\partial t} = \vec{M}_0 (\vec{\nabla} \cdot \delta \vec{h}) - (\vec{M}_0 \cdot \vec{\nabla}) \delta \vec{h} + \delta \vec{m} (\vec{\nabla} \cdot \vec{H}_0) - (\delta \vec{m} \cdot \vec{\nabla}) \vec{H}_0 + \vec{H}_0 (\vec{\nabla} \cdot \delta \vec{m}) + (\vec{H}_0 \cdot \vec{\nabla}) \delta \vec{m} + (\delta \vec{h} \cdot \vec{\nabla}) \vec{M}_0, \quad (2)$$

by taking into account that for a flux-closure configuration and for a circular cylinder $\vec{\nabla} \cdot \vec{M}_0 = 0$. In the derivation of Eq.(2) also some well-known vector calculus rules are applied. The physical meaning of each term on the second member of Eq.(2) is discussed. An extension of Eq.(2) to the case of a circular and cylindrical dot in the presence of a vortex core region with out-of-plane magnetization is performed. The equation for the density of chirality is further generalized by including the Gilbert and the spin-transfer torque dampings and the additional physical effects are discussed.

[1] R. Zivieri, in preparation.

Spin glass behavior in $\text{La}_{0.7}\text{Ca}_{0.3}\text{MnO}_3$ nanoparticles

Tran Dang Thanh^{a,b,*}, Do Hung Manh^b, Pham Thanh Phong^c, Nguyen Van Chien^b,
The-Long Phan^a, Nguyen Xuan Phuc^b, Seong-Cho Yu^{a,†}.

^a Department of Physics, Chungbuk National University, Cheongju 361-763, Korea

^b Institute of Materials Science, Vietnam Academy of Science and Technology, Hanoi,
Vietnam

^c Department of Natural Science, Nha Trang Pedagogic College, Khanh Hoa, Vietnam

Electronic mail: *thanhxraylab@yahoo.com; †scyu@chungbuk.ac.kr

Recently, there has been extensive research on nano-scale perovskite manganites materials. Manganites with a typical composition $\text{La}_{0.7}\text{Ca}_{0.3}\text{MnO}_3$ (LCMO) are of interest in this context due to its high colossal magnetoresistance (CMR) in the vicinity of insulator-metal, and paramagnetic(PM) - ferromagnetic (FM) temperatures transitions. The CMR phenomenon, superparamagnetism behavior, freezing temperature has been investigated in nanopolycrystalline LCMO samples, but studies related to the spin glass behavior of nanopolycrystalline LCMO samples are quite rare. In this work, we have investigated the dc magnetization and ac susceptibility of LCMO nanoparticles (~ 7 nm) synthesized by a reactive milling method. Three samples named LCMO1, LCMO2, and LCMO3 were obtained after milling times of 8, 12, and 16 h, respectively. X-ray diffraction patterns show that the samples have a single phase in the perovskite structure. Values of saturation magnetization (M_S) determined at 5 K decreases from 36.8 emu/g for LCMO1 to 14.7 emu/g for LCMO3. They are much smaller than $M_S = 97.5$ emu/g of a bulk sample. The dc magnetization, ac susceptibility, and fitting results indicate an existence of the spin-glass behavior in the samples. This phenomenon originates from the competition between ferromagnetic double-exchange and antiferromagnetic superexchange interactions. Its nature is discussed thoroughly.

The magnetocaloric effect in $\text{La}_{0.7}\text{Ca}_{0.3}\text{MnO}_3$ nanoparticles with different grain sizes

Tran Dang Thanh^{a,b,*}, Peng Zhang^a, The-Long Phan^a, Seong-Cho Yu^{a,†}.

^a Department of Physics, Chungbuk National University, Cheongju 361-763, Korea.

^b Institute of Materials Science, Vietnam Academy of Science and Technology, Hanoi, Vietnam.

Electronic mail: *thanhxraylab@yahoo.com; †scyu@chungbuk.ac.kr

Nanocrystalline $\text{La}_{0.7}\text{Ca}_{0.3}\text{MnO}_3$ (LCMO) samples were synthesized by the combination of the convention solid-state reaction and ball-milling with the milling times of t_m from 0 to 30 minutes. All the samples are orthorhombic without any detectable secondary phase. The unit cell parameters are almost unchanged with increasing t_m . By using the Williamson-Hall method, the average values of the crystallite size obtained are about 72, 54, and 45 nm for $t_m = 10, 20, \text{ and } 30$ minutes, respectively. Magnetic entropy change (ΔS_m) of samples under a magnetic field change of 10 kOe was calculated using the isothermal magnetization data. Its maximum (ΔS_{max}) decreases from 1.99 to 0.67 $\text{J.kg}^{-1}.\text{K}^{-1}$ but the linewidth of ΔS_m curves (δT_{FWHM}) increases from 17 to 57 K with varying t_m from 10 to 30 minutes. The relative cooling power (RCP) is thus in between 34 and 39 J.kg^{-1} . Together with temperature dependences of the saturation magnetization (M_s), the remanent magnetization (M_r) and variations of the coercivity (H_C) for LCMO nanoparticles have been also estimated. The nature of this phenomenon is discussed thoroughly.

Modeling of Hysteresis in Magnetic Multidomains

E. Cardelli^{1,2}, M. Carpentieri³, A. Faba^{1,2}, G. Finocchio⁴

¹Department of Industrial Engineering, Perugia University, Perugia, ITALY, ecar@unipg.it

²Center for Electric and Magnetic Applied Research, University of Perugia, Perugia, Italy

³Dept. of Electrotechnics and Electronics, Polytechnic of Bari, Italy

⁴Dept. of Electronic Engineering, Industrial Chemistry and Engineering, University of Messina, Italy

The complete modeling of magnetic hysteresis at macroscopic scale is a difficult task being the material behavior influenced by different factors such as the grain size, the structural stress, the presence of enclosures, etc. [1]. One idea should be the use of a physical-based model derived for sub-micrometer materials, but its use for macroscopic materials (geometrical dimensions of several millimeters at least) is actually limited by the description scale to use (the exchange length is of the order of 5-8 nm) which gives rise to numerical problems with matrix of more than 200 billions of elements [2]. Differently, the use of phenomenological models [3] is able to reproduce the macroscopic magnetic hysteresis. To this aim the main challenging is the identification of the approximation functions to use in the model. A promising approach to treat the magnetic vector hysteresis is an extension of the Classical Scalar Preisach Model from the 1-d case to the 3-d one. The model is based on the definition of a vector hysterion characterized by a material-dependent Preisach distribution in the \mathbf{H} -space. We have used the results of the nanomagnetic simulations either to identify the parameters of the 3-d Preisach-type vector model, and to identify some possible relationships between physical properties of the material and the properties of the vector model. In this paper, we present the results about our investigation to different structures, where the presence of domains during the switching process of the magnetization is observed. In particular, we discuss about possible useful identification strategies. The material we have investigated is Permalloy (Py) alloy with about 20% iron and 80% nickel content in weight. We studied a system of the above material with rectangular cross section having dimensions of 1200 nm x 400 nm and a thickness of 4 nm. In the Fig. 1 we show some results about the magnetization of the magnetic structure above, along the easy and hard axis.

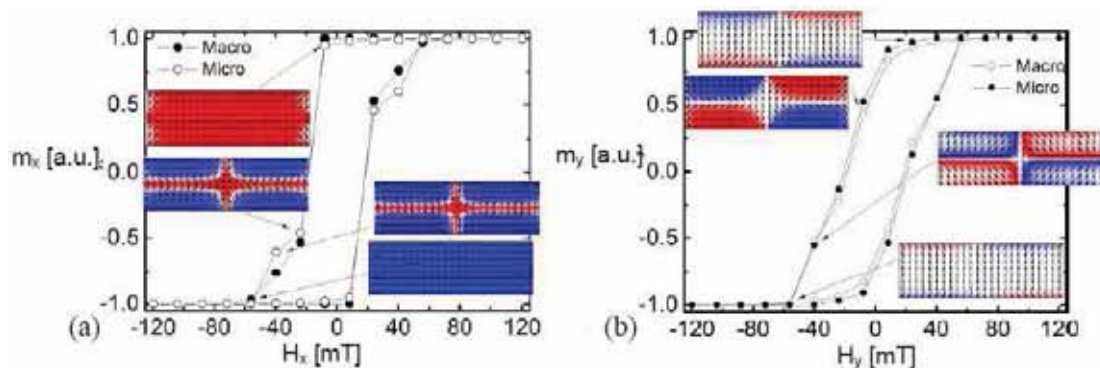


Figure 1: Comparison between Micromagnetic and Macromagnetic computations approach. Magnetization of the structure described above, (a) easy axis, (b) hard axis.

-
- [1] A. Aharoni, Introduction to the Theory of Ferromagnetism, Oxford Press, 1998.
 - [2] W.F. Brown, Micromagnetics, Krieger, New York, 1978.
 - [3] E. Cardelli, E. Della Torre, A. Faba, IEEE Trans. on Magn., Vol. 46, n. 12, 2010.

Micromagnetic simulation of energy consumption in realistic nanomagnetic switches

M. Madami^a, G. Gubbiotti^b, S. Tacchi^b and G. Carlotti^a

^a Dipartimento di Fisica, Università di Perugia, Via A. Pascoli, 06123 Perugia, Italy.

^b IOM-CNR c/o Dipartimento di Fisica, Università di Perugia, Via A. Pascoli, 06123 Perugia, Italy.

It is well known that bistable or multistable nanomagnetic switches can be used to store information, associating each logic state to a different equilibrium orientation of the magnetization [1]. In this context, the question of the minimum energy required to change the logic state of one bit, for instance reversing the nanodot magnetization, is of great current interest to explore the lower energy limits of future devices for Information and Communication Technologies [2].

In this work, we first present micromagnetic calculations of the dissipated energy during magnetization reversal in realistic bistable magnetic switches, consisting of rectangular nanodots with sub-200 nm lateral dimensions. Three different switching strategies are considered and the relative results compared in terms of energy dissipation mechanism, such as the generation of spin waves: i) the irreversible magnetization reversal obtained by the application of an external field along the easy axis, in the opposite direction with respect to the initial magnetization orientation; ii) the quasi-reversible (adiabatic) switching, resulting from driving the magnetization to reverse across the hard axis, by a proper quasistatic sequence of external fields; iii) the precessional switching obtained applying a short pulse of field, oriented perpendicular to the initial magnetization direction.

In the second part of this presentation, we analyse the energy cost of a “Landauer erasure” process [3] at different temperatures T , from 0 K to 400 K, for the same kind of realistic nanomagnetic switches considered above. Following different protocols, it is shown that the minimum expected value of $\Delta E = k_B T \ln(2)$, known as “Landauer limit” [4], is recovered by micromagnetic simulations, independently from the fact that simulations start from a well-defined initial state or not. The only condition to achieve the correct Landauer limit is that the adopted erasure protocol includes a proper time interval where the probability distribution of the nanodot magnetization has the same amplitude in the two possible states.

This work was supported by the European Community’s Seventh Framework Programme (FP7/2007-2013) under Grant No. 318287 “Landauer” and by the Ministero Italiano dell’Università e della Ricerca (MIUR) under PRIN Project No. 2010ECA8P3 “DyNanoMag”.

[1] M.T. Niemier et al., *Condens. Matter* **23**, 493202 (2011)

[2] G. Csaba et al., *J. Comp. Electr.* **4**, 105 (2005)

[3] B. Lambson, D. Carlton, and J. Bokor, *Phys. Rev. Lett.* **107**, 010604 (2011)

[4] R. Landauer, *IBM J. Res. Dev.* **5**, 183-191 (1961)

Effects of the Ti doping on critical behaviours of $\text{La}_{0.7}\text{Ca}_{0.3}\text{MnO}_3$

Dianta Ginting, S. C. Yu, T. L. Phan

Department of Physics, Chungbuk National University, Cheongju 361-763, South Korea

We have studied influences of the Ti-doping on the critical properties of polycrystalline sample of $\text{La}_{0.7}\text{Ca}_{0.3}\text{MnO}_3$ prepared by solid-state reaction. The critical behavior at the paramagnetic to ferromagnetic phase transition in $\text{La}_{0.7}\text{Ca}_{0.3}\text{MnO}_3$ is studied using techniques such as modified Arrott plot, Kouvel-Fisher plot, and critical isotherm analysis. The nature of this transition is found to be second order magnetic transitions. By using the modified Arrott plot method, the critical parameters were obtained to be $T_C \approx 129.66$ K, $\beta = 0.497 \pm 0.013$, and $\gamma = 1.309 \pm 0.013$. With these critical exponents, the isothermal magnetization data of the samples around T_C fall into two branches of a universal function $M(H, \varepsilon) = |\varepsilon|^\beta f_\pm(H/|\varepsilon|^{\beta+\gamma})$, where $\varepsilon = (T - T_C)/T_C$ [1] is the reduced temperature, f_+ for $T > T_C$ and f_- for $T < T_C$. This proves that the critical parameters determined are reliable, and in good accordance with the scaling hypothesis. Comparing with theoretical models, the critical exponents in our case are close to those expected for the mean-field theory [2]. This reflects that the Ti doping leads to the second-order phase transition in $\text{La}_{0.7}\text{Ca}_{0.3}\text{Mn}_{0.95}\text{Ti}_{0.05}\text{O}_3$ while the parent compound of $\text{La}_{0.7}\text{Ca}_{0.3}\text{MnO}_3$ exhibits the first-order phase transition. Such the phenomenon is assigned to changes in the structural parameters, $\text{Mn}^{3+}/\text{Mn}^{4+}$ ratio, and magnetic interaction mechanism caused by Ti dopants.

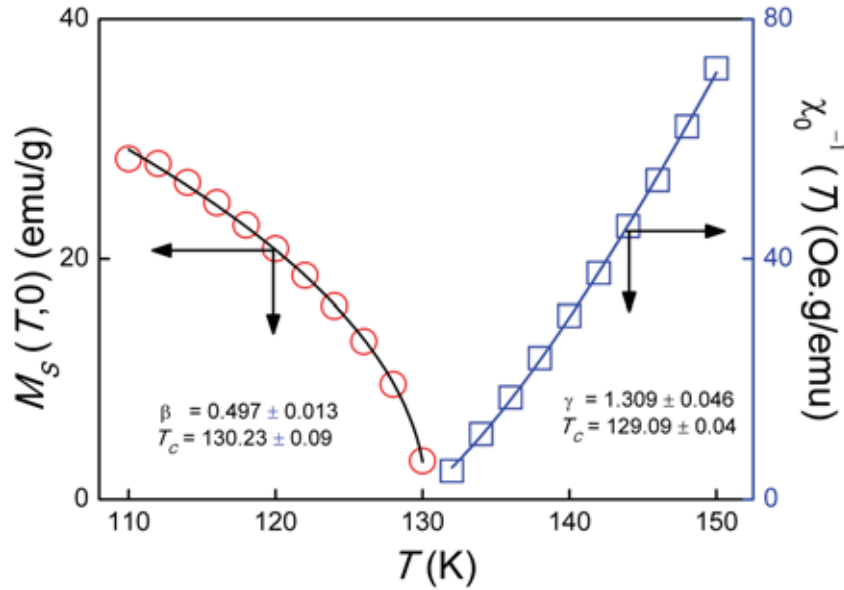


Figure 1: $M_S(T)$ and $\chi_0^{-1}(T)$ data fitted to the critical laws.

-
- [1] H. E. Stanley, *Introduction to Phase Transitions and Critical Phenomena* (Oxford University Press, London, 1971).
- [2] N. Kaul, *J. Magn. Magn. Mater.* 53, 5 (1985).

Magnetic vortex dynamics under a rotational magnetic field

Je-Ho Shim^a, Suhk Kun Oh^a, Seong-Cho Yu^a, and Dong-Hyun Kim^{a*}

^a Department of Physics, Chungbuk National University, Cheongju 361-763, South Korea

Magnetic vortex structure is mostly observed in ferromagnetic patterns on micro- and nanometer scales. Thus, understanding dynamics of the magnetic vortex dynamics becomes more and more essential for future spintronic applications based on the ferromagnetic patterns. Numerous studies have been reported on the magnetic vortex dynamics for the vortex under a pulse or an AC variation of magnetic fields or spin currents. However, few studies have been addressed to the vortex dynamics under a rotating magnetic field. The response function of the magnetic vortex structure under a rotating magnetic field seems to be relatively easy task, but has not yet been clearly solved [2]. In this work, we have carried out micromagnetic simulations based on Landau- Lifshiz-Gilbert (LLG) equation using the public OOMMF software[1] to investigate the motion of vortex core in a ferromagnetic disc under a rotational magnetic field. The exchange coefficient, saturation magnetization and damping constant of the simulation are 1.3×10^{-11} J/m, 8.6×10^5 A/m, and 0.01, respectively.. The amplitude and the frequency of the rotating field ware systematically varied as exemplified in Fig. 1(a). The observed response behavior of the magnetic vortex structure will be discussed within the context of the linear response theory[2].

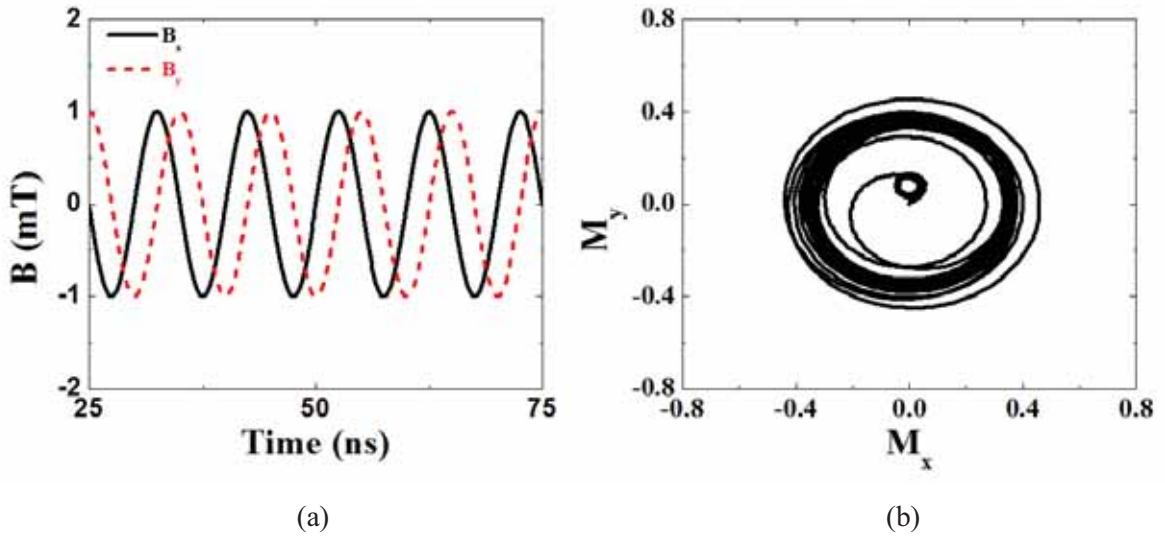


Figure 1: (a) Example of rotating magnetic field profile, where the amplitude and the frequency of the rotating magnetic field are 1mT and 100 MHz, relatively. (b) Vortex core trajectory for the rotating magnetic field.

[1] M. J. Donahue and D. G. Porter, OOMMF User's Guide, from <http://math.nist.gov/oommf> (2002).

[2] S. K. Oh, J. Korean. Phys. Soc. 54, 567 (2009).

Electrical control of magnetisation in magnetostrictive structures

D.E. Parkes^a, S.A. Cavill^b, J. Miguel^b, S.S. Dhesi^b, K.W. Edmonds^a, R.P. Campion^a,
and A.W. Rushforth^a

^a School of Physics and Astronomy, University of Nottingham, Nottingham NG7 2RD,
United Kingdom.

^b Diamond Light Source Chilton, Didcot, Oxfordshire OX11 0DE, United Kingdom.

The electrical control of magnetisation is a key stage in the development of future computer logic and storage devices. Electric fields can be much more localised than magnetic fields, and do not give rise to the Joule heating associated with electric currents. The control of ordered domain patterns forms the basis of a number of different proposed technologies, such as racetrack memory[1]. We combine micromagnetic calculations with experimental investigation of a hybrid ferromagnetic/piezoelectric device to demonstrate and study the strain-mediated electrical control of ordered domain patterns in a microfabricated MBE-grown film of Fe₈₁Ga₁₉[2]. By tuning an applied uniaxial strain anisotropy we can enhance or suppress a flux-closing domain pattern in a 15µm-wide bar.

Magneto-optical Kerr effect images reveal behaviour that can be explored by micromagnetic calculations (see figure 1). We vary the strain-anisotropy coefficient in our calculation and observe how both the domain configuration and the different energy contributions in the system respond. The energy scales involved in the manipulation of these domains are comparable to those required to achieve non-volatile switching of the magnetisation in a similar system [3].

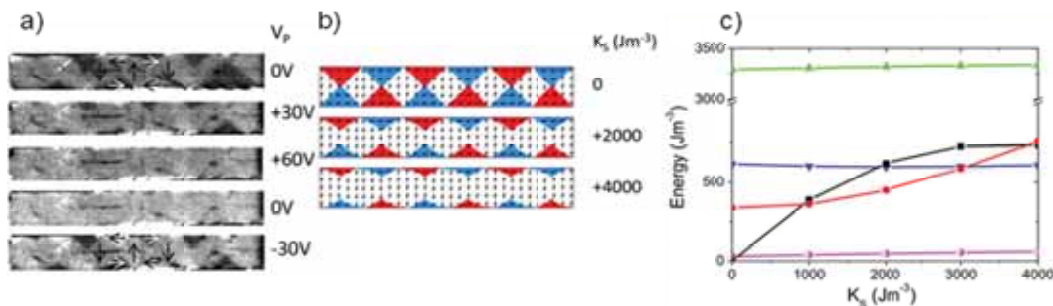


Figure 1 a) Magneto-optic Kerr effect images of the electrical control of ordered domain patterns. V_p is the voltage applied to the piezoelectric part of the hybrid device. b) Domain configuration calculated by micromagnetic simulations for different values of strain-induced magnetic anisotropy. c) The energy contributions in the simulated region as a function of strain anisotropy coefficient, K_s : strain-induced (squares), demagnetization (full circles), cubic magnetocrystalline (down triangles), uniaxial magnetocrystalline (up triangles) and exchange energy (half-filled circles).

This demonstration of strain-mediated electrical control of magnetisation and magnetic order will be important for the development of future computer memory and storage technologies based on magnetoelectric effects.

[1] Parkin, Patent US 6834005; S.S.P. Parkin et al., Science 320, 190 (2008).

[2] Cavill, S.A., Parkes, D.E., Miguel, J., Dhesi, S.S., Edmonds, K.W., Campion, R.P., Rushforth, A.W., Applied Physics Letters, 102, 3 (2013).

[3] D. E. Parkes, S. A. Cavill, A. T. Hindmarch, P. Wadley, F. McGee, C. R. Staddon, K. W. Edmonds, R. P. Campion, B. L. Gallagher, and A. W. Rushforth, Appl. Phys. Lett. 101, 072402 (2012).

Magnetization Reversal in Exchange Spring Media Assisted by Circularly Polarized Microwave Fields

Martino LoBue^a, Claudio Serpico^b, Alexander Pasko^a, Renuka Tayade^a, Georgio Bertotti^c, Federic Mazaleyrat^a

^a Ecole Normale Superier de Cachan, France

^b Dipartimento di Ingegneria Elettrica, Università di Napoli “Federico II, Napoli, Italy

^c Istituto Nazionale di Ricerca Metrologica, strada delle Cacce Torino, Italy

Switching behaviour in exchange-spring media has gained a considerable attention in recent times. It is of major interest due to its application in magnetic recording and storage technologies. In the case of static magnetization, Asti et al. developed a 1-D micromagnetic model for exchange coupled system and presented the analytical expressions for the reversal process ([1] [2] and ref. therein). Dynamic analysis using the Landau-Lifshitz equation has been studied numerically around late 60's for the distributed thin films [3]. More recently, it has received a new attention with emphasis on microwave assisted switching [4] as a perspective for the enhancement of the magnetic writing capabilities. However the dynamics of switching needs to be explored further for the spatially non-uniform cases.

In this article, by using a combination of analytical and numerical techniques, we investigate the influence of microwave fields on the switching of exchange-spring media. In the mathematical model we use, the spring-media is uniaxial and invariant with respect to rotations around a symmetry axis (z-axis of the reference frame) which is orthogonal to the interface separating the two phases. The media is subject to a DC field along the z-axis and to a microwave field circularly polarized in the xy-plane. Spatial variations of magnetization are assumed to occur only along the z direction. The two phases are initially and fictitiously assumed to be not in interaction. In this situation, the magnetization dynamics is spatially uniform in each phase and can be determined analytically in terms of P-modes and Q-modes [5]. Starting from a situation when the two phases are in two distinct spatially uniform modes, we numerically determine the spatial profile of magnetization in presence of the exchange coupling of the phases. By carrying out the above analysis under a slowly varying DC field [6], we demonstrate how the use of circularly polarized fields of appropriate amplitude and frequency lead to a substantial reduction of the DC field necessary to obtain the switching of the spring media.

[1] G.Asti et al., Phys. Rev. B **69** (2004), 174401.

[2] G.Asti et al., Phys. Rev. B **73** (2006), 094406.

[3] H.Chang et al., J. Appl. Phys., **38**, no.5 (1967), 2294-22301.

[4] M. Bashir et al., IEEE Trans. Magn., **44**, no.11 (2008).

[5] G.Bertotti, I.Mayergoyz & C.Serpico, “NON-LINEAR MAGNETIZATION DYNAMICS IN NANOSYSTEMS”, Elsevier (2009).

[6] Bertotti et al. J. Appl. Phys. **105**, 07B712 (2009)

Micromagnetic study of size effect on angular ferromagnetic resonance in nanowires arrays

Laurentiu Stoleriu^a, Dorin Cimpoesu^a, Junjia Ding^b,
Adekunle Adeyeye^b, Alexandru Stancu^a, Leonard Spinu^c

^a Dept. of Physics, Alexandru Ioan Cuza University of Iasi, Romania

^b Dept. of Electrical & Computer Engineering, National University of Singapore, Singapore

^c AMRI and Department of Physics, University of New Orleans, USA

Arrays of similar permalloy nanowires (Fig. 1(a)) with different inter-wire spacing were deposited on top of coplanar waveguides using electron beam lithography followed by electron-beam deposition and lift-off process [1]. The wires were subjected to both an external magnetic field \mathbf{H} and an alternative field \mathbf{h}_r in the GHz range while the FMR spectra were recorded using a network analyser. Polar absorption diagrams were built using spectra for the same ac field frequency but for different orientations and amplitudes of the external field.

In this paper we use the finite element micromagnetic approach as implemented in magpar [2] to explore some of the origins of the FMR absorption angular diagrams features while we extend the discussion to the effect of the wires' size on the resonant absorption.

The samples were described as one or two permalloy parallelepipeds with the same thickness of 30 nm but with different widths – from 50 to 300 nm – and different lengths – from 300 to 4000 nm (Fig. 1(b)). The material parameters for permalloy were chosen similar to those proposed in mumag standard problem #1 with a damping parameter $\alpha=0.01$.

The paper discusses the effect of the ac field frequency, external field value and wire size (length and width) on the shape and features of the absorption diagram as well as on how different segments of the wire – the ends or the middle – contribute to the resonant absorption (Fig. 2).

We find that for smaller widths – below 100 nm – the ends of the wires play an important role in the absorption while for thicker wires this role diminishes in favour of the moments located in the middle of the wire.

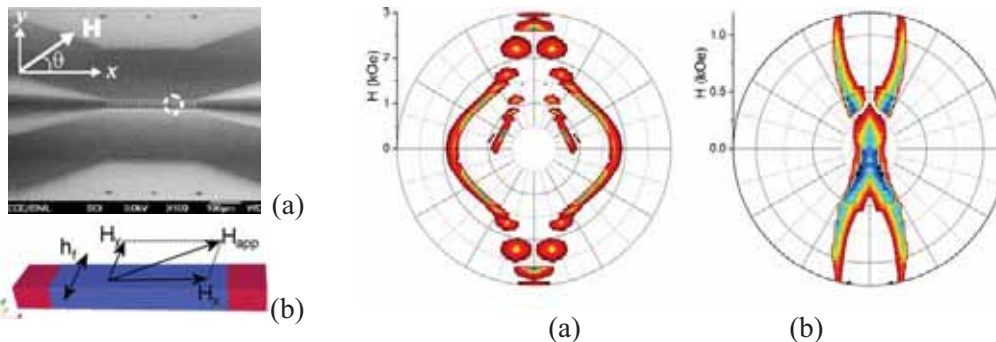


Figure 1: (a) SEM image of permalloy wires arrays and (b) the sample used in FEM micromagnetic simulations. Figure 2: Resonant polar absorption diagrams for a single wire at 7.5GHz frequency of the ac field for two sizes: (a) 300x50x30 nm³ and (b) 2000x300x30 nm³.

[1] J. Ding, M.Kostylev, A.O. Adeyeye, Phys. Rev. Lett. 107, 047205 (2011).

[2] W. Scholz, J. Fidler, T. Schrefl, et. al., Comp. Mat. Sci. 28, 366 (2003).

Static and dynamic magnetic domain configuration in electrodeposited cobalt platinum nanowires

M. Shahid Arshad^a, Kristina Žužek Rožman^a, Matej Komelj^a, Paul J. McGuinness^a, Spomenka Kobe^{a,b}

^aJozef Stefan Institute, Department of nano-structured materials K7, Ljubljana, Slovenia

^bCenter of Excellence on Nanoscience and Nanotechnology (CENN Nanocenter), Ljubljana, Slovenia

We performed magnetic measurements supported by theoretical simulations on an electrodeposited $\text{Co}_{65\pm 0.2}\text{Pt}_{35\pm 0.2}$ nanowire with the length of 5.5 μm and the diameter of 200 nm. The response of the nanowire on the variation of the external magnetic field perpendicular to the nanowire principal axis was investigated. We applied the MFM imaging and simultaneously interpreted the observed patterns on the basis of the magnetization profile calculated within the framework of the micromagnetic modeling (OOMMF).[1] At zero field the MFM image exhibits a multiple domain structure, whereas the micromagnetic simulation predicts the presence of vortices along the length of the nanowire because of competition between crystal anisotropy and demagnetization energy. With an increasing field, the experimental pattern becomes more uniform, and the calculation reveals a decay of the vortices due to alignment of the magnetic moments, mostly in the direction along the nanowire. A further increase of the external-field magnitude yields a gradual reorientation of the moments starting from the edges towards the central axis of the wire, which ends with the majority of the moments parallel to the field direction in the saturation state. Experimentally, this process is characterized by the change in the contrast of the MFM image.

We observed the switching behavior between two interacting CoPt nanowires lying parallel to each other on variation of external perpendicular magnetic field under MFM.

[1] Object Oriented Micromagnetic Framework (OOMMF), freely available at <http://math.nist.gov/oommf/>

Micromagnetics for magnetoelastic strips

F. Reichel^a, T. Schrefl^a, D. Suess^b, G. Hrkac^c, D. Praetorius^c, M. Gusenbauer^a,
S. Bance^a, H. Oezelt^a, J. Fischbacher^a, A. Kovacs^a, L. Exl^a

^a Industrial Simulation, St. Poelten University of Applied Sciences, Austria

^b Institute of Solid State Physics, Vienna University of Technology, Austria

^c Institute for Analysis and Scientific Computing, Vienna University of Technology, Austria

Magnetostrictive amorphous ribbons are used as key components in sensors for electronic stock surveillance [1]. In acousto-magnetic devices the magnetoelastic coupling the mechanical oscillation frequency and the time decay of the vibration are measured. Here we present a finite element micromagnetic model for the combined simulation of the magnetic domain structure and the mechanical motion. We used the general finite element framework “escript” [2] for solving the micromagnetic equations and the wave equation for the mechanical displacement. The magnetoelastic coupling energy is:

$$\Phi_{\sigma} = -\frac{3}{2} \lambda_s \left\{ \sum_{i=1}^3 \sigma_{ii} m_i^2 + \sum_{i \neq j} \sigma_{ij} m_i m_j \right\} \quad (1)$$

Here m_i are the magnetization components and σ_{ij} is the stress tensor. Since the strip dimensions are usually much larger than the domain wall width, the large body thin-film limit is applied [3]. The domain pattern is updated at every time step during the numerical integration of the equation for the displacement:

$$\rho \frac{\partial^2 u_i}{\partial t^2} - \frac{\partial \sigma_{ij}}{\partial x_j} = 0 \quad (2)$$

Here ρ is the density, t and x are the time and space coordinates.

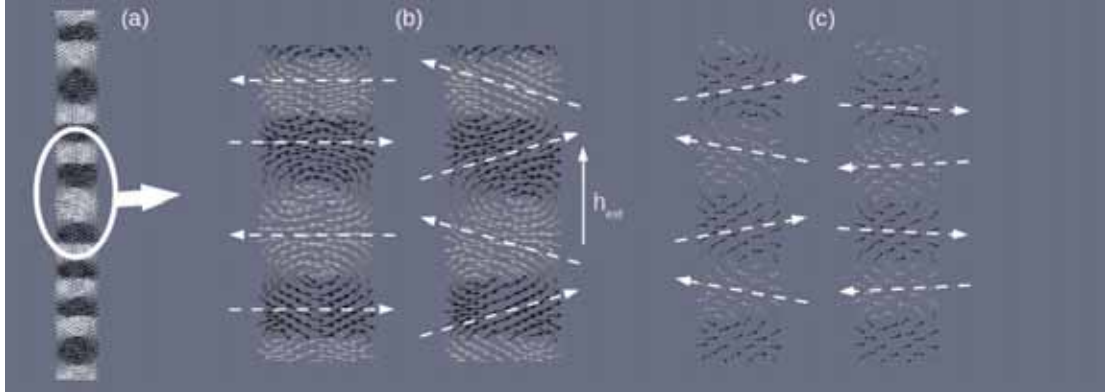


Figure 1: Magnetic domain patterns during the vibration of the platelet. (a) Gives the domain structure for zero applied field. (b) After applying a field parallel to the long axis the magnetisation within the domains rotates towards the field direction. (c) Change of the magnetic domain pattern during mechanical vibrations of the ribbon.

This work is supported by Vienna Science and Technology Fund (WWTF, MA09-029).

[1] G. Herzer, *J. Magn. Magn. Mater.* **254-255** (2003), 598-602.

[2] L. Gross, B. Cumming, K. Steube, D. Weatherley, *Lecture Notes in Computer Science* **4699** (2007), 270-279.

[3] D. Kinderlehrer, L. Ma, *IEEE Trans. Magn.* **30** (1994), 4380-4382.

Self-similarity in $(\partial M/\partial T)_H$ curves for Heusler alloys with ferri-to-ferromagnetic and ferro-to-paramagnetic phase transitions

Maryam Ovichi^a, Yi Jin^a, Mohammadreza Ghahremani^a, Lawrence H. Bennett^a, Edward Della Torre^a, Francis Johnson^b, and Min Zou^b

^a Department of Electrical and Computer Engineering, George Washington University, Washington D.C., 20052, USA

^bGE Global Research, Niskayuna, NY 12309, USA

Heusler alloys display first-order ferri-to-ferromagnetic and second-order ferro-to-paramagnetic transitions. This paper presents a new temperature scaling methodology which exhibits a self-similar field dependence $(\partial M/\partial T)_H$ curve. This methodology, based on temperature, extends Franco's transformation [1] by: (i) adding ferri-to-ferromagnetic transition, (ii) performing the scaling methodology on the $(\partial M/\partial T)_H$ curve instead of $\Delta S_M(T,H)$ curve, and (iii) redefining the arbitrary temperature references used by Franco, by employing constant temperatures which can be determined from $(\partial^2 M/\partial T^2)_H$ and $(\partial M/\partial T)_H$ curves. Using this new computational method, the composition of ferrimagnetic, ferromagnetic and paramagnetic clusters for Heusler alloys exhibiting the first-order and second-order phase transitions can be calculated. The self-similarity phenomenon within the material's $(\partial M/\partial T)_H$ curve then aids in formulating compositions[2].

By applying the self-similarity model, we evaluated the effectiveness of this new analytical approach, the cluster composition functions for $\text{Ni}_{51}\text{Mn}_{33.4}\text{In}_{15.6}$, which exhibits first-order ferri-to-ferromagnetic and second order ferro-to-paramagnetic transitions. Self-similarity, which magnetization vs. temperature at each applied field exhibits, is defined in mathematics as an object that is exactly or approximately similar to a part of itself. By rescaling the modified Franco's transformation, all the $(\partial M/\partial T)_H$ curves collapsed on to the single self-similar curve with a low index of dispersion. Once collapsed, the curve is asymmetric and negatively skewed due to the intrinsic transition differences in the mixed-state region. The mixed-state region of the self-similar curve is distinctly bell-shaped as shown in the figure. The self-similar curves are optimally modelled using the maximum entropy method.

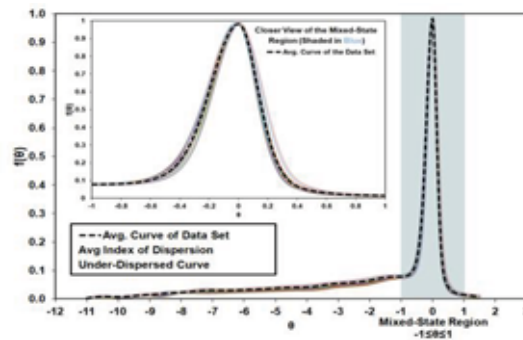


Figure 1: Self-similarity curves collapse onto a single curve. The inset shows a closer view of the mixed-state region.

[1] V. Franco Applied Physics letters 89, 222512(2006)

[2] <http://dx.doi.org/10.1016/j.physb.2011.09.044>

Analysis of noise-assisted phenomena in systems with hysteresis

Mihai Dimian^a and Petru Andrei^b

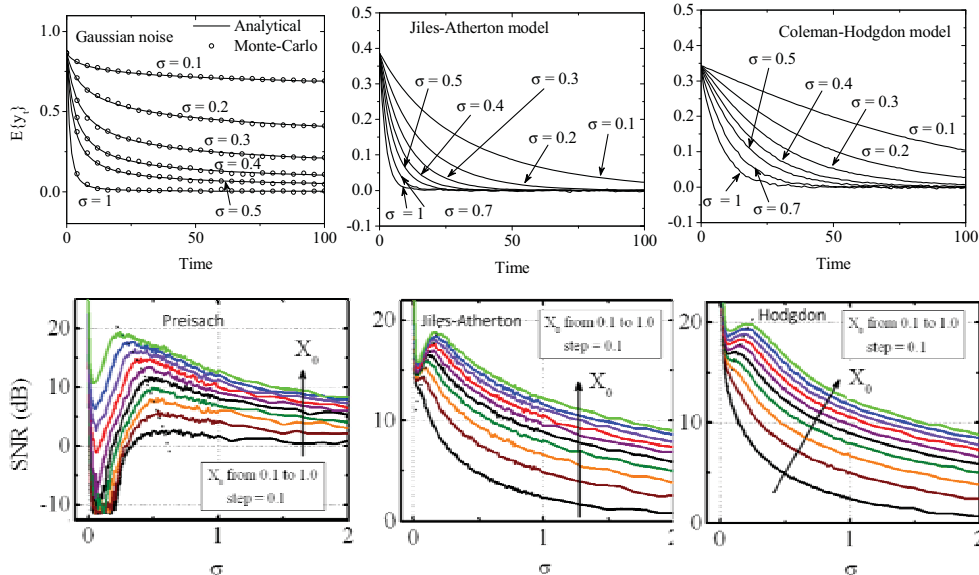
^a Stefan cel Mare University, Suceava, Romania

^b Florida State University, Tallahassee, United States of America

Everybody hates noise while the world tends to become even noisier. While it is jeopardizing the future development of several technologies, such as magnetic data storage, noise may also contribute to novel paradigms used to overcome current limitations, such as heat assisted magnetic recording employed to achieve higher data storage densities. Numerous studies have been recently focused on these constructive roles played by noise in nonlinear systems, including phenomena coined as dithering, coherence or stochastic resonances [1,2]. From theoretical point of view, most of these studies can be theoretically framed into two-state models or simple variants thereof, while complex multi-stable systems are rarely addressed. The extensive experience of hysteretic modeling community [3] can significantly contribute to the analysis of noise benefits in systems with complex metastable configurations.

The purpose of this talk is to provide a unitary framework for studying noise-assisted phenomena in complex hysteretic systems and its implementation in an open-access academic software [4,5]. Various differential, integral, and algebraic models of hysteresis are considered in an arbitrary colored noise environment and both disruptive and constructive effects of noise are analyzed. The emphasis is placed on thermal relaxations, memory losses, noise induced amplifications and stochastic resonances.

The Figure bellow shows representative examples of thermal relaxation curves for different values of the noise strength σ (upper images), as well as signal-to-noise ratio variation with the noise strength σ for different amplitude X_0 of a deterministic sinusoidal input (lower images) in the case of Preisach model, Jiles-Atherton model and Coleman-Hodgdon model of hysteresis. White Gaussian noise is considered in these examples.



- [1] L. Gammaitoni, P. Hanggi, P. Jung, and F. Marchesoni, *Eur. Phys. J. B* **69** (2009), 1-3.
- [2] M. Dimian, O. Manu, and P. Andrei, *J. App. Phys.* **111** (2012), 07D132.
- [3] G. Bertotti and I. Mayergoyz (eds.), *Science of Hysteresis*, Elsevier, New York (2006).
- [4] M. Dimian, P. Andrei, *Noise-driven phenomena in hysteretic systems*, Springer, **in press**.
- [5] *HysterSoft*, User Guide v. 1.8 [online <http://www.eng.fsu.edu/ms/HysterSoft>].

Reaction-diffusion equations containing hysteresis with diffusive thresholds

Pavel Gurevich^a, Dmitrii Rachinskii^b

a Free University Berlin, Berlin, Germany

b University of Texas at Dallas, USA; University College Cork, Cork, Ireland;

The goal of the talk is an attempt to describe a system with fluctuating hysteresis thresholds by means of diffusion equations, where the role of the spatial variable is played by hysteresis threshold.

To illustrate our approach, we suggest a prototype model that describes a population of two-phenotype species in a varying environment. The *first key feature* is that the species can switch between the two phenotypes whenever the environment achieves certain thresholds. Thus, the behavior of each species is characterized by hysteresis (non-ideal relay).

The *second key feature* is that the thresholds for each species can fluctuate. Under the assumption that this fluctuation obeys the Gaussian distribution, we arrive at a system where the density of the population obeys a reaction-diffusion equation with discontinuous hysteresis operators in the right-hand side.

The collective impact of the species on the environment is described in terms of the Preisach operator with a measure given by the population density. The *third key feature* is that this measure becomes time dependent and is now a part of the solution.

In the talk, we formulate a theorem on the well-posedness of the problem and discuss emerging spatial patterns.

Phase transitions and hysteresis: new perspectives and results

Stefano Bosia^a, Michela Eleuteri^b, Jana Kopfová^c, Pavel Krejčí^d

^a Politecnico di Milano, Italy

^b Università di Milano, Italy

^c Mathematical Institute of the Silesian University, Opava, Czech Republic

^d Institute of Mathematics, Academy of Sciences of the Czech Republic, Praha, Czech Republic

The theory of hysteresis operators developed in the recent years has proved to be a powerful tool for solving mathematical problems in various branches of applications, such as solid mechanics, material fatigue, ferromagnetism, phase transitions.

In a series of recent papers [1], [2], [3], we developed a model for thermo-elasto-plastic oscillations of beams and plates with hysteresis and material fatigue. It is well known that plastic deformations lead to energy dissipation and material fatigue, which is in turn manifested by material softening, heat release and material failure in finite time.

In view of engineering applications, it is relevant to account also for the possibility of having decreasing fatigue rate, so that the material can be partially repaired by local melting.

A way to achieve this goal can be to account also for phase transitions in the model, so that the time of failure of the material can be shifted and, possibly considering a sufficiently large time interval of observation, a global solution of the corresponding PDEs system can be found.

In this talk we discuss thermodynamical consistency of the new model which includes, together with the fatigue parameter, also a new parameter of phase transition, describing the degree of melting of the material. We moreover outline some new perspectives and related mathematical results.

[1] M. Eleuteri, J. Kopfová, P. Krejčí: "A thermodynamic model for material fatigue under cyclic loading", Proceedings of the 8th International Symposium on Hysteresis and Micromagnetic Modeling", Physica B: Condensed Matter, **407**, no. 9 (2012), 1415-1416.

[2] M. Eleuteri, J. Kopfová, P. Krejčí: "Non-isothermal cycling fatigue in an oscillating elastoplastic beam", Comm. Pure Appl. Anal., to appear.

[3] M. Eleuteri, J. Kopfová, P. Krejčí: "Fatigue accumulation in an oscillating plate", Discrete and Continuous Dynamical System – Series S, **6**, no. 4, (2013), 909-923.

A representation result for hysteresis operators with vector valued inputs and its application to models for magnetic materials

Olaf Klein^a

^a Weierstrass Institute for Applied Analysis and Stochastics (WIAS), Berlin, Germany

The representation formula for hysteresis operators acting on scalar-valued continuous input functions being piecewise monotone that was derived by Brokate and Sprekels, see [1], has been extended to hysteresis operators dealing with inputs in a general normed vector space V , see [2, 3]. The input functions are requested to be piecewise *monotaffine*, i.e. to be piecewise the composition of a **monotone** with an **affine** function.

Let $C_{\text{p.w.m.a.}}([0, T], V)$ denote the set of all continuous, piecewise monotaffine functions from $[0, T]$ to V , let Y be some set. Let $S_F(V)$ be the set of all convexity triple free strings of elements of V , i.e., the set of all $(v_0, \dots, v_n) \in V^{n+1}$ with n being a natural number such that no component v_i can be written as convex combination of its predecessor v_{i-1} and its successor v_{i+1} .

The representation result in [2,3] leads to

- a) Every function $G: S_F(V) \rightarrow Y$ generates a hysteresis operator \mathcal{H}_G mapping $u \in C_{\text{p.w.m.a.}}([0, T], V)$ to the function $\mathcal{H}_G[u]: [0, T] \rightarrow Y$ defined by

$$\mathcal{H}_G[u](t) = G(u(t_0), u(t)) \quad \text{for all } t \in [t_0, t_1], \quad (1)$$

$$\mathcal{H}_G[u](t) = G(u(t_0), \dots, u(t_{i-1}), u(t)) \quad \text{for all } t \in]t_{i-1}, t_i], \quad i = 2, \dots, n, \quad (2)$$

with $0 = t_0 < t_1 < \dots < t_n = T$ being the *standard monotaffinity decomposition* of $[0, T]$ for u , i.e. the uniquely defined decomposition of $[0, T]$ such that for $i = 1, \dots, n$ the time t_i is the maximal time in $]t_{i-1}, T]$ such that u is monotaffine on $[t_{i-1}, t_i]$.

- b) For every hysteresis operator \mathcal{B} mapping functions in $C_{\text{p.w.m.a.}}([0, T], V)$ to functions from $[0, T]$ to Y , there exists a unique function $G: S_F(V) \rightarrow Y$ such that \mathcal{B} is the hysteresis operator \mathcal{H}_G generated by G .

The representation result allows to formulate a vector version of the forgetting according to Madelung deletion considered in [1] for hysteresis operators with scalar input-functions. Moreover, a mathematical precise formulation of the congruence property of vector minor loops considered in [4] is reformulated as a condition for the representation on $S_F(V)$. These results will be applied to some hysteresis operators arising in models for magnetic materials.

-
- [1] M. Brokate, J. Sprekels, Hysteresis and Phase Transitions, Springer-Verlag (1996)
[2] O. Klein, Physica B, **407** (2012), 1399-1400
[3] O. Klein, Adv. Math. Sci. Appl., in print.
[4] I. D. Mayergoyz, Mathematical Models of Hysteresis and their Applications, Elsevier (2003)

Hysteresis of Magnetostructural Transitions: Reversible and Irreversible Processes

Virgil Provenzano^{a,b}, Edward Della Torre^b, and Lawrence H. Bennett^b

^aNational Institute of standards and Technology (NIST), Gaithersburg, MD 20899 USA

^bGeorge Washington University, Washington, D.C., USA

The polycrystalline compounds of Gd_5Ge_2Si and $MnFeP_{0.5}As_{0.5}$ and the off-stoichiometric $Ni_{50}Mn_{35}In_{15}$ Heusler alloy belong to a group of materials exhibiting first-order crystallographic transitions near room temperature. Coincident with these transitions, these materials display large magnetocaloric effect (MCE) peaks. Because of their complex magnetic behavior and their promise as near-room-temperature magnetic refrigerants, the magnetic properties of this group of materials have been extensively studied. Since first-order transitions are thermally/magnetically driven phenomena, a thermally driven transition can be field-induced in the reverse order by applying a strong enough field. These field-induced transitions are typically accompanied by large magnetic hysteresis; the characteristics of which are complex function of temperature, field, and thermal-magnetic history. In this study we show that the virgin curve, major loop, and first-order reversal curves are the results of both reversible and irreversible processes. For example, the size (area) of the hysteresis loop is the result of the following processes. The first involves the amount of sample field-induced from one phase (Phase1) to another (Phase2), while the second involves the amount that is reversibly transformed from Phase2 to Phase1, as the field is cycled back to zero. The combination of these two processes is the mechanism responsible for magnetic hysteresis and related properties. Connected with these two processes, is the material starting state that can be either single or mixed phase, prior to field cycling. The starting state determines both the extent of the field-induced transition and degree of reversibility; a single phase state resulting in full reversibility and largest hysteresis, whereas a mixed phase state resulting in partial reversibility and smaller hysteresis.

The complex interplay involving the initial state, irreversible and reversible processes is illustrated by the MH loops measured at 270 K and at 280 K on the $Gd_5Ge_2Si_2$ compound and presented in Fig. 1. The loops at each temperature were sequentially measured, referred as the first, second, and third loops. The loops consist of the ascending and sequential descending curves. The first ascending curve at each temperature is the virgin curve. At 270 K, $Gd_5Ge_2Si_2$ is in a mixed phase (orthorhombic majority phase and monoclinic minority phase), whereas at 280 K it is single monoclinic phase. The mixed state at 270 K resulted in the first loop being larger than second loop, while second and third loops are identical and identical to the major loop. The single phase state at 280 K resulted in the three loops being all the same, identical to the corresponding major loop, and larger than those at 270 K. Similar results were obtained on the $MnFeP_{0.5}As_{0.5}$ compound and the off-stoichiometric Heusler alloy, but not shown in this abstract.

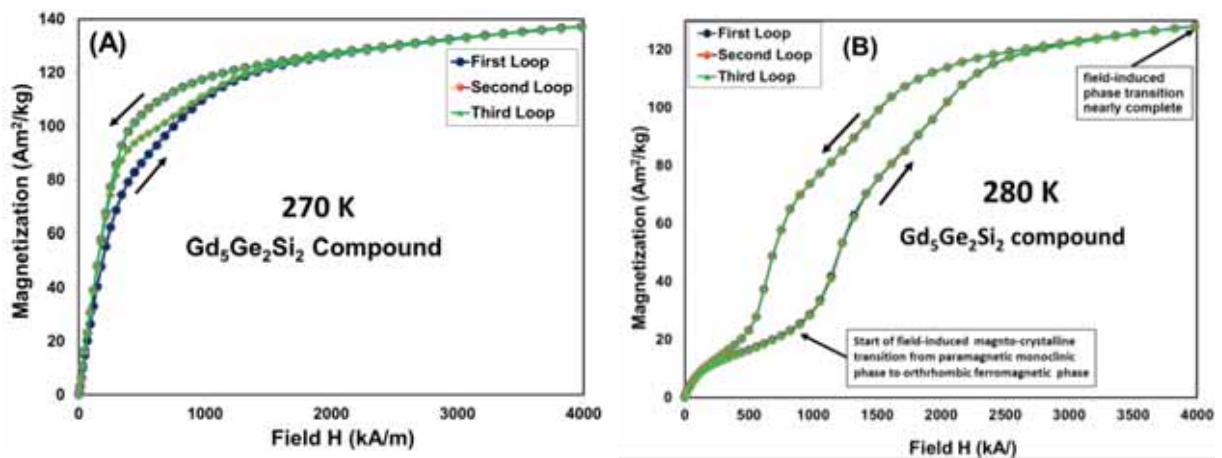


Figure 1 M vs. H loops for $Gd_5Ge_2Si_2$ compound, (A) measured at 270 K and (B) measured at 280 K

FORC experimental technique and the Preisach distribution

Alexandru Stancu

Faculty of Physics & CARPATH, „Alexandru Ioan Cuza“ University of Iasi, Boulevard
Carol I, 11, 700506, Romania

In many laboratories all over the world the First-order Reversal Curves (FORC) diagrams are used systematically as a tool for characterizing various hysteretic processes [1-4]. This technique was initially designed by Mayergoyz as an identification method for the Preisach distribution in ferromagnetic materials. From the beginning it was observed that the physical system should obey certain conditions in order to be correctly described by the Classical Preisach Model and that only when these conditions are rigorously respected this identification method will provide the Preisach distribution. Many other attempts to design identification tools for the Preisach distribution have failed due to the statistical instability of the distribution of coercive and interaction fields in the ferromagnetic systems [5]. The turning point in the use of FORC technique is marked by the idea of transforming this method into a purely experimental tool that can provide a sort of “fingerprint” of the studied hysteretic systems. However, the link between the so called FORC distribution and the well-known Preisach distribution had to be maintained in order to be able to make not only qualitative discussions concerning the measured samples [1]. What really happened was that most of the experimentalists using FORCs assumed that the FORC distribution is a slightly distorted version of the Preisach distribution and consequently they are usually discussing the experimental FORC distribution in terms of real distribution of physical hysterons as a function of coercivity and interaction field. This opens the problem of a profound discussion concerning the distribution of the Preisach hysterons and their relation with the physical fundamental bricks with intrinsic hysteresis. Simple magnetic systems, like the arrays of nanowires in which each element has a characteristic rectangular loop when is isolated from the other wires are ideal *toy models* able to provide insight into the complex relation between the physical elements in interaction and the experimental FORC distribution. The results of such an analysis shows how far from the classical image of the FORC distribution the reality can be [5]. The effect of interactions on the hysteresis loops of the hysterons has to be re-evaluated and clarified. For example, in a typical nanowire system, one can identify two distinct effects of interactions. For the wires with lower coercivity than the average coercivity in the system the interactions are at the origin of the shift of their hysteresis loops that makes them asymmetrical. The interactions acting on higher coercivity wires have a different effect. They are producing an apparent increase of coercivity of the hysterons maintaining the symmetry of the hysteresis loops. This discussion is valid in all the systems with demagnetising mean field interactions. In the full presentation the role of inter-particle interactions will be presented and the effect of this clarification on the interpretation of experimental FORC distributions will be also discussed. *Acknowledgement:* This work was supported by a grant of the Romanian National Authority for Scientific Research, CNCS-UEFISCDI, Project No. PN-II-ID-PCE-2011-3-0794 [IDEI-EXOTIC No. 185/25.10.2011].

-
- [1] A. Stancu et al., J. Appl. Phys. **93** (2003), 6620-6622.
 - [2] A. Stancu et al., Appl. Phys. Lett. **83** (2003), 3767-3769.
 - [3] C. Enachescu et al., Phys. Rev. B **72** (2005), 054413.
 - [4] R. Tanasa et al., Phys. Rev. B **71** (2005), 014431.
 - [5] C. I. Dobrotă, A. Stancu, J. Appl. Phys **113** (2013), 043928.

RARE EARTH AND RARE EARTH FREE FUTURE MAGNETS FOR ENERGY APPLICATIONS

Oliver Gutfleisch, Tino Gottschall, K. Skokov, M. Kuzmin

TU Darmstadt, Material Science, Germany

Due to their ubiquity, magnetic materials play an important role in improving the efficiency and performance of devices in electric power generation, conversion and transportation ¹. Permanent magnets are essential components in motors and generators of hybrid and electric cars, wind turbines, etc. Magnetocaloric materials could be the basis for a solid state energy efficient cooling technique alternative to compressor based refrigeration. Any improvements in magnetic materials will have a significant impact in these areas, on par with many “hot” energy materials efforts (e.g. hydrogen storage, batteries, thermoelectrics, etc.).

The talk focuses on rare earth and rare earth free permanent magnet and magnetocaloric materials with an emphasis on their optimization for energy and resource efficiency. The synthesis, characterization, and property evaluation of the materials will be examined briefly having in mind their critical micromagnetic length scales and phase transition characteristics. Especially the structure-property relationships impacting on coercivity as well as hysteresis properties will be discussed.

For permanent magnet applications we ‘simply’ want to maximize hysteresis, for magnetocalorics one needs to minimize both thermal and magnetic hysteresis. Especially interesting are hysteresis properties in Heusler alloys, which have great potential for solid state refrigeration ² and sensor applications ³, and which are susceptible to multiple stimuli such as pressure, field, strain, field, etc.

¹ O. Gutfleisch, J.P. Liu, M. Willard, E. Brück, C. Chen, S.G. Shankar, *Magnetic Materials and Devices for the 21st Century: Stronger, Lighter, and More Energy Efficient (review)*, *Adv. Mat.* **23** (2011) 821-842.

² J. Liu, T. Gottschall, K.P. Skokov, J.D. Moore, O. Gutfleisch, *Giant magnetocaloric effect driven by structural transition*, *Nature Mat.* **11** (2012) 620-626+suppl.

³ B. Bergmair, J. Liu, T. Huber, O. Gutfleisch, D. Süß, *Wireless and passive temperature indicator utilizing the large hysteresis of magnetic shape memory alloys*, *Appl. Phys. Lett.* **101** (2012) 042412_1-4.

Prof. Oliver Gutfleisch
Institut für Materialwissenschaft
FG Funktionale Materialien
Technische Universität Darmstadt
Petersenstr. 23
64287 Darmstadt, Germany
gutfleisch@fm.tu-darmstadt.de
http://www.mawi.tu-darmstadt.de/fm/funktionale_materialien

High-temperature micromagnetics with the Landau-Lifshitz-Bloch equation.

O. Chubykalo-Fesenko^a, P.Nieves^a, U.Atxitia^b

^a Instituto de Ciencia de Materiales de Madrid, CSIC, Cantoblanco, 28049 Madrid, Spain

^{a,b} Department of Physics, University of York, UK

The Landau-Lifshitz-Bloch (LLB) equation represents a generalization of the standard micromagnetics for high temperature and ultra-fast dynamics applications [1]. Its current domain includes several emerging areas of modern magnetism such as laser-induced ultrafast dynamics, heat-assisted magnetic recording, spin-caloritronics and spin-torque dynamics with Joule heating. In this talk we will review the LLB micromagnetics. Differently to the standard LLG approach, the LLB equation contains in addition to the transverse relaxation term, the longitudinal relaxation term and does not conserve the magnetization modulus. We present classical and quantum LLB equations, their stochastic forms [2] as well as recently derived LLB equation for multi-component magnets, such as ferrimagnetic materials [3]. We will also discuss the conditions when the LLB equation should be used instead of the LLG-based micromagnetics.

As examples of the applications of the LLB micromagnetics, we will present our recent results on modeling of the ultrafast magnetization dynamics in ferromagnetic FePt material and in a ferrimagnetic FeCoGd material. FePt represents an ultimate magnetic material for ultra-high density magnetic recording and thus the study of ultra-fast magnetization dynamics in this material is potentially very important. We perform micromagnetic modeling of laser-induced ultra-fast (sub-ps) demagnetization and subsequent recovery. The modeling allows to demonstrate the change in the demagnetization and recovery speed as a function of the laser pulse intensity. The reason for the observed change is the slowing down of the longitudinal relaxation rate due to the proximity to the Curie temperature.

FeCoGd is a ferrimagnetic material where not only demagnetization but also the magnetization switching has been reported. Importantly, this switching occurs under the heat alone, without any other external stimulus such as applied field [4]. The ferrimagnetic LLB equation explains the observed switching as an angular momentum transfer between longitudinal and transverse motion.

[1] O. Chubykalo-Fesenko et al. Phys. Rev. B 74 (2006), 094436.

[2] R.F.Evans et al., Phys. Rev.B 85 (2012) 014433.

[3] U. Atxitia et al. Phys. Rev. B 86 (2012) 104414.

[4] T.Ostler et al Nature Comm, 3 (2012) 666.

On the route to three dimensional magnetic memory

Yemliha Bilal Kalyoncu, Ozhan Ozatay

Bogazici University, Istanbul, Turkey

Future limitations to the improvements in the data storage density with perpendicular recording act as a driving force for an intensive effort to investigate alternative schemes to reliably store and recall information with ultra-high density on magnetic media. There are several approaches for achieving this goal, such as thermally-assisted recording, microwave assisted recording and ultimately 3-d magnetic storage schemes. IBM has already demonstrated race track memory in which magnetic domains (bits) are moved along a 3D magnetic wire by applying spin-polarized current pulses [1]. Here we will present our investigation of heat-assisted domain transfer in a magnetic multilayer nanowire stack with perpendicular anisotropy using locally applied fields. A recent study in continuous film [CoNi/Pd]/Pd/ [Co/Pd] multilayer stacks has unambiguously shown stray field induced domain replication using element-specific x-ray imaging techniques [2]. For storage device applications it is crucial to understand and gain full control over the conditions that lead to reproducible stray field induced single domain transfer in patterned magnetic nanostructures. For this purpose we have fabricated single magnetic layer (CoNi/Pd) nanowires as well as devices that consist of a SiN-CoNi/Pd-SiN-CoNi/Pd-Ta stack with 50-100 nm constrictions in a cross-wire configuration to study domain transfer between magnetic layers. We use the localized stray field from a magnetic tip to write single-domains in the CoNi/Pd magnetic layer by modulating its coercivity via instantaneous and localized heating from a current pulse [3]. We will present our detailed investigation of the resulting domain structure in nanowires with various widths as a function of the current pulse amplitude and width to vary the local temperature and the tip height to vary the local field. We will also report on the nature of current-induced demagnetization limit and thermally-induced domain transfer between magnetic layers. This study establishes the preliminary conditions for the use of 3-D integrated cross-wires of perpendicular anisotropy magnetic materials to boost the data storage capacity of future magnetic memory devices.

[1] S.S.P. Parkin, M. Hayashi, L. Thomas, *Science* 320, 190(2008)

[2] T. Hauet, C. Günther, B. Pfau, M. Schabes, J.-U. Thiele, R. L. Rick, P. Fischer, S. Eisebitt, and O. Hellwig, *Phys. Rev. B* 77, 184421 (2008).

[3] O. Ozatay and B. D. Terris Read / Write Structures for a Three Dimensional Memory US Patent# 8164940

Analysis of stochastic resonance and thermally-induced synchronization in spin-torque oscillators

M. d'Aquino^a, C. Serpico^b, G. Bertotti^c, I.D. Mayergoyz^d

^a Dipartimento per le Tecnologie, Università di Napoli "Parthenope", Napoli, Italy.

^b Dipartimento di Ingegneria Elettrica, Università di Napoli Federico II, Napoli, Italy.

^c Istituto Nazionale di Ricerca Metrologica, Torino, Italy.

^d ECE Dept. and UMIACS, University of Maryland, College Park, MD, United States.

Magnetic nanodevices known as Spin-Torque Oscillators (STOs) have great potential for advanced wireless applications[1]. Typical STOs are composed of a 'fixed' layer whose magnetization is pinned to a given orientation, a non magnetic spacer and a thin 'free' ferromagnetic layer where the magnetization dynamics takes place. In particular, possible dynamical regimes under dc excitations include large-angle precessional magnetization dynamics. Since STOs have nanoscale dimensions, thermal fluctuations may induce transitions between different dynamical regimes[2,3]. In addition, when STOs are subject to time-varying excitations (ac currents/external fields), the dynamical picture of magnetization dynamics becomes very complex due to the possible onset of nonlinear resonance, quasiperiodicity, synchronization and chaos.

In this work, the synchronization of thermally induced transitions between different magnetization regimes (equilibria, self-oscillations) with 'weak' external ac excitations (for instance, ac spin-polarized injected currents) is analyzed. In the absence of ac excitation, the STO output signal exhibits random transitions between precessional and stationary behavior with transition rates which, at given temperature, are intrinsic of the magnetic nano-system. The transition rates increase monotonically with the temperature and can be moderately low in typical experimental situations for nanoscale devices, whereas the magnetization self-oscillations take place at GHz frequencies.

It is shown that, when a 'weak' ac current with frequency satisfying a special time scale matching condition involving the thermal transition rates is injected, synchronization between the aforementioned thermal transitions and the external signal occurs. This leads to the appearance of a strong response of the system at the frequency of the external signal in the spectrum. To investigate such thermally-induced synchronization, a theoretical approach is developed, based on separation of time scales and averaging techniques, and it is found that the amplitude of the system response at the forcing frequency has a non monotonic dependence on temperature which is the signature of stochastic resonance[4,5]. It is expected that the proposed approach can be instrumental for the comprehensive analysis of experiments on thermally induced synchronization of spin-transfer nano-oscillators. In addition, the analysis presented in this work is very general in character and could be applied to large variety of systems in which steady-state periodic solutions are driven by out-of-equilibrium interactions with the environment.

-
- [1] J. C. Slonczewski, *J. Magn. Magn. Mater.* 159, L1, 1996; S. I. Kiselev et al., *Nature* 425, 380, 2003
 - [2] I.N. Krivorotov et al., *Phys. Rev. Lett.* 93, 166603 (2004).
 - [3] R. Bonin et al., *Eur. Phys. J. B* 59, 435445 (2007).
 - [4] L. Gammaitoni et al., *Reviews of Modern Physics*, Vol. 70, No. 1, 1998.
 - [5] M. d'Aquino et al., *Phys Rev. B* 84, 214415 (2011).

Magnetization dynamics driven by transfer torque from the spin-Hall effect

M. Carpentieri

Department of Ingegneria Elettrica e dell'Informazione, Politecnico of Bari, Bari, Italy.

Recently, several research groups are interested in very simple devices, bi-layer composed by a ferromagnet/heavy-metal with large spin-orbit coupling, that have opened important perspectives for high speed storage and microwave auto-oscillators applications [1-3].

The switching mechanism was explained by means of either the Rashba field (RF), due to the strong Rashba spin-orbit coupling, or the spin-orbit torque from spin-Hall effect (ST-SHE). Liu *et al.*, by studying the effect of the electrical current in different heavy-metal such as Pt, Ta, and W, experimentally demonstrated that RF was negligible and the main contribution to the switching mechanism was the ST-SHE. In fact, the demonstration is related to the fact that spin-Hall angle and consequently the electric current to achieve the switching in presence of Pt has opposite sign than the one used in presence of Ta or W.

In this work, both magnetic switching and dynamics observations are studied by micromagnetic simulations into different experimental devices (for numerical simulations experimental magnetic parameters are used).

The first device is similar to that measured in the experimental framework presented in Ref. 1, a square Co layer (500nm in side) of 0.6 nm in thickness coupled with a 3 nm in thickness of Pt. In this case, three different regions of behaviour as function of the bias field and current are identified: (1) direct switching (DS), (2) switching via an intermediate state (IS), and (3) stochastic switching (SS).

The second one is that studied by Liu and coauthors in Ref. 3, that is a three-terminal device composed by a Ta strip positioned at the bottom of a MTJ of CoFeB/Mgo/CoFeB. The MTJ has an elliptical cross section of 300 nm x 100 nm and it is positioned in order to have the easy axis perpendicular to the current flow. In this way, when a dc current density is applied to the Tantalum, the SHE injects spins into the CoFeB, and when the spin current density is large enough to reduce the net effective damping to zero, we can achieve both switching and spontaneous steady-state magnetic precession. Due to the different sign of the spin-Hall coefficient in CoFeB/Ta with respect to Co/Pt, the switching is achieved considering the opposite sign of the current. In this case, the switching scenario is similar to that already observed for switching driven by spin-polarized current in collinear spin-valves, in other words, the switching occurs via a nucleation process with the presence of complex magnetic pattern including also magnetic vortex states.

In this device, magnetization dynamics is also found when a magnetic field is applied and varying the in-plane angle considered with respect to the easy axis of the ellipse. As expected, the frequency value increases with the field amplitude and its behavior is rather constant with the current. Finally, by fixing the SHE current and the applied field, and varying the MTJ current I_{MTJ} , the oscillation frequency strongly changes. Magnetization dynamics is found just for low positive I_{MTJ} (persistent oscillations are not generated when negative I_{MTJ} is applied) and the effect of the I_{MTJ} is to increase the precession frequency.

[1] I. M. Miron, K. Garello, G. Gaudin, P.-J. Zermatten, M. V. Costache, S. Auffret, S. Bandiera, B. Rodmacq, A. Schuhl, and P. Gambardella, *Nature* 476, 189-193, 2011.

[2] L. Liu, C.-F. Pai, Y. Li, H. W. Tseng, D. C. Ralph, R. A. Buhrman, *Science* 336, 555 (2012).

[3] L. Liu, C.-F. Pai, Y. Li, H. W. Tseng, D. C. Ralph, R. A. Buhrman, *Phys. Review Lett.* 109, 186602 (2012).

LLG and spin accumulation and vortices in magnetic spin valve systems

Gino Hrkac^a, Thomas Schrefl^b, Stephane Durand^c, Marcus Page^d, Dieter Suess^d, Dirk Praetorius^d

^a Univeristy of Exeter, Exeter, UK

^b University of Applied Sciences, St Poelten, Austria

^c University of Ghent, Belgium

^d Vienna University of Technology, Austria

In this paper we investigate the difference in the Slonzewski spin torque approach and the change of spin accumulation based on a diffusion equation derived by Zhang, Levy and Fert and [1,2] at an interface of a magnetic to a non-magnetic material, in a micromagnetic framework, by considering two cases; first a spin-accumulation due to current and second due to field excitation; refereed to as spin-pumping. In spin polarized transport models, the magnetization was assumed to be constant / pinned in one of the layers and the polarization was introduced as an extra field that is part of the effective field. Spin diffusion and interfacial effects were neglected but it was shown that these effects are important in magnetoresistance experiments [3–5]. Zhang et al. introduced a model for the relaxation of a coupled spin-magnetization system, where they considered the one-dimensional case. We start from the following spin dynamics equation

$$\mathbf{s}_t = -\text{div} \mathbf{J}_s - 2D_0(x) \frac{\mathbf{s}}{\lambda_{sf}^2} - 2D_0 \frac{\mathbf{s} \times \mathbf{m}}{\lambda_J^2} \quad (1)$$

with \mathbf{s} being the spin accumulation, \mathbf{m} the magnetization, λ_{sf} the characteristic spin flip relaxation length, λ_J the electron's mean free path and D_0 the diffusion constant. The first term is the divergence of the spin current \mathbf{J}_s (which is a matrix in $\mathbb{R}^{3 \times 3}$), which is defined as

$$\mathbf{J}_s = \frac{\beta \mu_B}{e} \mathbf{m} \otimes \mathbf{J}_e - 2D_0(x) [\nabla \mathbf{s} - \beta \beta' \mathbf{m} \otimes (\nabla \mathbf{s} \cdot \mathbf{m})] \quad \text{with } \nabla \mathbf{s} \in \mathbb{R}^{3 \times 3} \quad (2)$$

with \mathbf{J}_e the applied electric current and β and β' the spin polarization parameters for the magnetic layers. In the first case of our study we assume a constant electric current and mapped the spin-accumulation profiles over the interface and for the second case the first term in equation 2 can be omitted as no electric current is applied and a time varying magnetization is assumed. This leads to a reduced expression of the spin accumulation current in equation 2, as \mathbf{s} is not fully absorbed in the ferromagnet and unabsorbed transverse spin accumulation diffuses over the interface into the metal layer and leads to a modified spin-torque.

Also we will discuss the effect of symmetric and asymmetric spin torque effects on the vortex oscillations in a spin-valve system in the presence of two vortices and its effect on the frequency and linewidth. We will show that the mutual interaction between two vortices, considering a non-linear current distribution, pseudo-diffusion model, can lead to non-linear oscillation regimes.

-
- [1] S. Zhang, P.M. Levy, A. Fert, Phys. Rev. Lett. 88 (2002) 236601.
 - [2] A. Shpiro, P.M. Levy, S. Zhang, Phys. Rev. B 67 (2003) 104430.
 - [3] P.C. van Son, H. van Kempen, P. Wyder, Phys. Rev. Lett. 58 (1987) 2271–2273.
 - [4] M. Johnson, R.H. Silsbee, Phys. Rev. B 37 (1988) 5312–5325.
 - [5] T. Valet, A. Fert, Phys. Rev. B 48 (1993) 7099–7113.

Synchronization of spin-torque nanooscillators: promising ways for long-distance and robust synchronization of STNO arrays

D.V. Berkov, S.G. Erokhin

Innovent Technology Development, Jena, Germany

Non-linear magnetization dynamics in ferromagnetic nanoelements excited by the spin-polarized dc-current is one of the most intensively studied phenomena in solid state magnetism. Despite immense efforts, synchronization of oscillations induced in several such nanoelements (spin-torque driven nanooscillators, or STNO) still represents a major challenge both from the fundamental and technological points of view. In this talk we present two concepts which would allow an advanced synchronization of several STNOs.

In the first scheme, we propose to use magnetization oscillations induced in a thin nanowire by a spin polarized current (SPC) injected via several point contacts placed on the top of this nanowire. We show that an oscillatory mode propagating along the nanowire in this system is possible when a sufficiently strong out-of-plane field is applied [1]. This propagating mode is a promising candidate for obtaining a long-distance synchronization between STNOs, because the nanowire can be viewed as a quasi-1D waveguide. In such a system there is no decay of the spin wave amplitude caused by the wave front expansion (as in 2D and 3D). Indeed, in our simulations we have found that synchronization of two STNOs on such a nanowire is possible up to the intercontact distance as large as $\Delta r = 3$ mkm [2]. However, several qualitatively important features of the synchronization behaviour for this system make the achievement of a stable synchronization in this geometry to a highly non-trivial task. In particular, there exist a *minimal* intercontact distance, below which a synchronization of STNOs can not be achieved. Further, when the current value in the 1st contact is kept constant, the synchronized oscillation power depends *non-monotonously* on the current value in the 2nd contact. Finally, for one and the same current values there might exist several synchronized states (with different frequencies), depending on the initial conditions.

Our second synchronization concept is based on STNOs represented by coupled vortices inside square-shaped magnetic nanoelements [3]. The steady gyration of these vortices is also driven by SPC injected via the point contacts, which are placed in the centers of the nanosquares. We predict that synchronization of two such coupled STNOs is extremely dynamically stable due to a very large coupling energy (up to 1000 kT for a 500 x 500 nm² nanosquares) in a wide region of current values (2 - 7 mA for a point contact diameter of 100 nm). Both 'in-phase' and 'out-of-phase' locking regimes can be obtained in our system due to the strong coupling between STNOs arising from dipolar and exchange interactions. We explicitly prove that inclusion of thermal fluctuations does not disturb the synchronization regime. Further, we show that for this system the synchronization of any number of STNOs can be achieved, demonstrating that within our concept we can easily synchronize 10 nanooscillators, even in the case when diameters of their current supplying point contacts have a broad distribution.

[1] D.V. Berkov, C. T. Boone, and I. N. Krivorotov, Phys. Rev. B **83**, 054420 (2011)

[2] D.V. Berkov, Phys. Rev. B **87**, 014406 (2013)

[3] S.G. Erokhin, D.V. Berkov, [arXiv:1302.0659](https://arxiv.org/abs/1302.0659) [cond-mat.mes-hall] (2013)

Spin-torques and switching voltages in MgO-based magnetic tunnel junctions

Ciaran Fowley^a, Kerstin Bernert^{a, b}, Yuriy Aleksandrov^{a, b}, Volker Sluka^a,
Ewa Kowalska^{a, b}, Wen Feng^{a, b}, Jürgen Lindner^a, Jürgen Fassbender^{a, b},
and Alina M. Deac^{a, b}

^a Helmholtz-Zentrum Dresden-Rossendorf, Dresden, Germany

^b Technical University Dresden, Dresden, Germany

A spin-polarized current flowing through a ferromagnet can exert a torque on the local magnetization, thereby providing means of manipulating it [1]. Current-induced switching is currently being investigated as potential writing scheme for magnetic random access memory (MRAM), for which the structure of choice is based on magnetic tunnel junctions (MTJ) with an MgO barrier, due to their large magnetoresistance signals. MgO-based MTJs are known to exhibit a finite anisotropy along the direction normal to the plane of the layers, as well as a non-trivial dependence of the spin-transfer torques on the applied bias. Here, we present analytical solutions for the switching voltages for MgO-MTJs for the generalized case where the free layer has two generic “intrinsic” fields oriented along orthogonal directions. The magnetization of the reference layer and the applied field are assumed to be parallel to one of the two intrinsic field axis. Both the in-plane and the field-like spin-torque terms are taken into account, with the field-like torque assumed to have a quadratic dependence on the applied voltage and to favor the antiparallel state [2]. The switching voltages thus determined can be expressed for different geometries by replacing the two generic intrinsic field terms with the appropriate expressions for the anisotropy and demagnetizing fields, according to the specific free and reference layer configuration considered. For in-plane MgO-based magnetic tunnel junctions, one of the two intrinsic fields of the free layer corresponds to the (negative) demagnetizing field, which pulls the magnetization of the free layer towards the film plane. The orthogonal intrinsic field component is the easy-axis anisotropy, parallel to the current polarization and the external field direction. We demonstrate that in this configuration the quadratic dependence of the field-like torque on the applied voltage can cause back-hopping (a behavior characteristic to tunnel junctions, whereby reliable switching to the desired state is achieved for applied voltages of the order of the critical voltage, but a larger applied bias induces a telegraph-noise behavior [3]). For perpendicular anisotropy tunnel junctions without in-plane shape anisotropy, the only intrinsic field present in the free layer is parallel the effective anisotropy, parallel to the reference layer direction. In this case, we find that neither back-hopping, nor spin-transfer driven steady state precession are expected, as evidenced by experimental results [4]. Finally, if an in-plane shape anisotropy is considered in addition to the effective perpendicular anisotropy, a variety of canted states are predicted.

[1] J.C. Slonczewski, *J. Magn. Magn. Mater.* 159, L1 (1996); L. Berger, *Phys. Rev. B* 54, 9359 (1996).

[2] C. Heiliger and M. Stiles, *Phys. Rev. Lett.* 100, 186805 (2008).

[3] J. Z. Sun, *J. Appl. Phys.* 105, 07D109 (2009); T. Min et al., *J. Appl. Phys.* 105, 07D126 (2009).

[4] J.J. Nowak, et al. *IEEE Magn. Lett.* 2, 3000204 (2011).

Spin torque generated magnetic droplet solitons

Johan Åkerman^{a,b}

^a Physics Department, University of Gothenburg, Fysikgränd 3, 412 96 Gothenburg, Sweden

^b Materials Physics, School of Information and Communication Technology, KTH Royal Institute of Technology, Electrum 229, 164 40 Kista, Sweden

The theoretical prediction, by Ivanov and Kosevich [1], of ‘magnon drop’ solitons in thin films with perpendicular magnetic anisotropy (PMA) and zero damping, dates back to the 1970s. More recently, Hofer, Silva and Keller [2], demonstrated analytically and numerically that related ‘magnetic droplet’ solitons should be possible to excite in nano-contact spin-torque oscillators (NC-STOs) based on PMA materials, where spin transfer torque locally realizes the zero-damping condition required in [1].

In my talk, I will present the first experimental demonstration of such magnetic droplets, realized using 50-100 nm diameter nano-contacts (NCs) fabricated on top of orthogonal GMR stacks of Co8/Cu/Co0.3[Ni0.8/Co0.4]x4 (thicknesses in nm). The nucleation of a magnetic droplet manifests itself as a dramatic 10 GHz drop in microwave signal frequency at a drive-current dependent critical perpendicular field of the order of 0.5 - 1 T. The drop in frequency is accompanied by a simultaneous sharp resistance increase of the device and a sign change of its magnetoresistance, directly indicating the existence of a reversed magnetization in a region of the [Co/Ni] free layer underneath the NC. As predicted by numerical simulations, the droplet exhibits rich magnetodynamic properties, experimentally observed as auto-modulation at approximately 1 GHz and sometimes sidebands at 1/2 and 3/2 of the fundamental droplet frequency. The 1 GHz modulation can be shown numerically to be related to the drift instability of the droplet [2], albeit with enough restoring force to make the droplet perform a periodic motion instead of leaving the NC region. The sidebands at 1/2 and 3/2 of the droplet frequency are related to eigenmodes of the droplet perimeter.

Magnetic droplet nucleation is found to be robust and reproducible over a wide number of NC-STOs with different NC sizes, making this new nanomagnetic object as fundamental and potentially useful to nanomagnetism as e.g. domain walls and vortices..

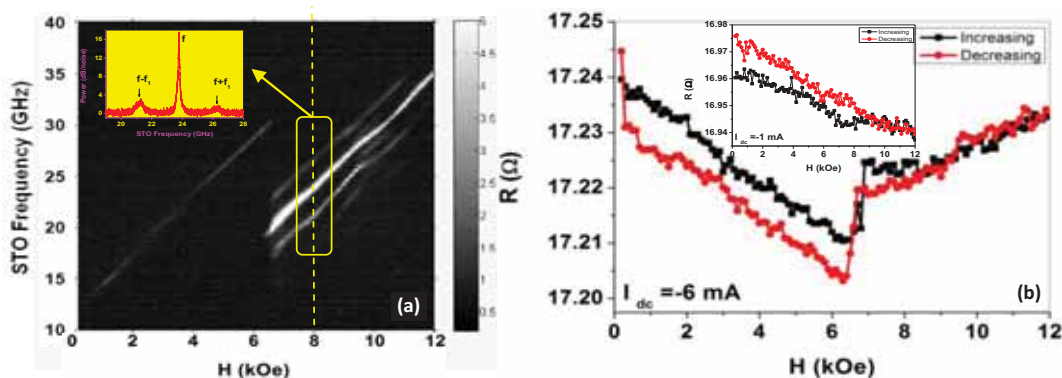


Figure 1: (a): Field dependent STO frequency at $I = -6$ mA with a dramatic frequency drop at about 0.65 T. Inset: complex self-modulated dynamics at $\mu_0 H = 0.8$ T; (b): Resistance vs. field at $I = -6$ mA showing a jump in resistance coincident with the frequency drop. Inset: featureless data for $I = -1$ mA.

[1] B. A. Ivanov and A. M. Kosevich, Zh. Eksp. Teor. Fiz. **72**, 2000 (1977)

[2] M. A. Hofer, T. J. Silva, and M. W. Keller, Phys. Rev. B **82**, 054432 (2010)

Micromagnetic simulation of permanent magnets

Simon Bance^a, Harald Oezelt^a, Thomas Schrefl^a, Gergely Zimanyi^b

^a St Poelten University of Applied Sciences, St Poelten, Austria

^b UC Davis, Davis CA, USA

Permanent magnets find applications in many modern technologies and are crucial components in hybrid vehicles and wind turbines. It is an ongoing challenge to design permanent magnets with better performance, from alternative materials with adequate supply.

Experimentally there are two main ways to characterise permanent magnets; the angular dependence of the coercive field and first-order reversal curve (FORC) measurements [1]. Numerical micromagnetics is a powerful tool that can be used to simulate these same measurements, providing insight into the reversal mechanisms and their causes.

We give an overview of some of the techniques used to perform these calculations and present recent results where they have been fruitful in revealing the nature of hysteretic behaviour.

Modern sintered magnets have a granular structure of polyhedral grains. Experimental measurements and molecular dynamics simulations have shown the existence of edge defect regions of around 1nm thickness [2]. To simulate we need finite element meshes that resolve the defect region sufficiently. When these defects are taken into account, micromagnetics simulations can explain the observed angular dependence of the coercive field. Finite temperature studies highlight the connection between reversal and thermal activation processes (see fig. 1). FORC diagrams show that reversal proceeds by collective processes.

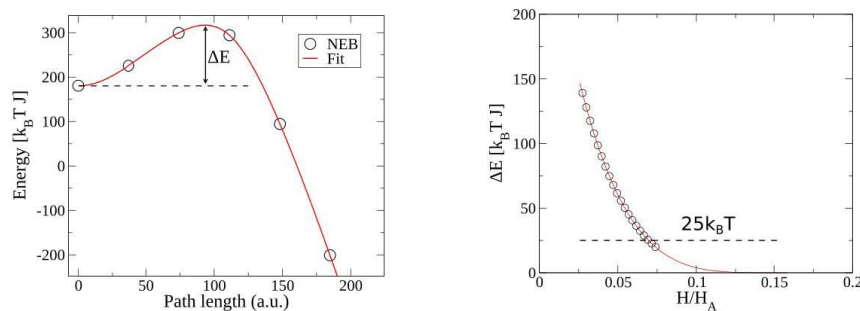


Figure 1: Left: Energy barriers between magnetization states can be calculated using the nudged elastic band method [3]. Right: The thermally-activated coercive field at room temperature corresponds to a barrier height of $25 k_B T$, according to the Arrhenius-Neel law.

[1] Roberts, A. P., Pike, C. R., & Verosub, K. L. (2000). First-order reversal curve diagrams: a new tool for characterizing the magnetic properties of natural samples. *J. geophys. Res.*, 105(28), 461-28.

[2] G. Hrkac, T. Woodcock, C. Freeman, A. Goncharov, J. Dean, T. Schrefl, O. Gutfleisch, The role of local anisotropy profiles at grain boundaries on the coercivity of Nd₂Fe₁₄B magnets, *Applied Physics Letters* 97 (23) (2010) 232511–232511.

[3] Dittrich, R., Schrefl, T., Suess, D., Scholz, W., Forster, H., & Fidler, J. (2002). A path method for finding energy barriers and minimum energy paths in complex micromagnetic systems. *Journal of magnetism and magnetic materials*, 250, 12-19.

Micromagnetic study of ferromagnetic resonance spectra from ferromagnetic nanoelement arrays

H.-G. Piao^{a,b}, X. Zhang^a, D.-H. Kim^b, S. K. Oh^b, and S.-C. Yu^{b*}

^a Department of Materials Science and Engineering, Tsinghua University, Beijing 100084, China

^b Department of Physics, Chungbuk National University, Cheongju 361-763, South Korea

Recently, a spin wave excitation on a nanometer scale has been attracting much attention due to its possible applications such as spintronic devices and microwave communications[1–4]. In particular, collective excited mode of spin waves mutually coupled by each ferromagnetic element forming an array is considered to be one of promising candidates for future application thanks to the tunability of the properties by changing the structural parameters of the array. Thus, it becomes clear that understanding of the spin wave dynamics in nanostructured ferromagnetic materials is a key to the realization of future spintronic applications based on the array of nanomagnetic elements. In this work, we report our micromagnetic simulation result on the collective excited spin wave modes of a finite array of elongated circular-shaped ferromagnetic nanoelements. With a systematic variation of the array geometry such as the interdot separation and the nanoelement diameter, the spectra of collective spin wave modes are carefully investigated by the Fourier analysis, together with detailed observation of the spin configurations, where a possibility of the tunable magnonic crystal structure is conjectured based on the ferromagnetic nanoelement array structure.

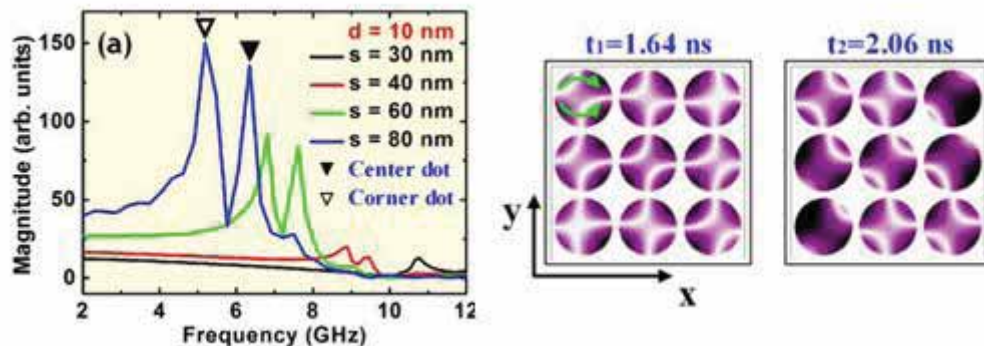


Fig. 1. Spin wave modes analyzed by the fast Fourier transform (a) for a fixed interdot distance $d = 10$ nm with variation of S from 30 to 80 nm and (b) for a fixed shorter diameter $S = 40$ nm with variation of d from 10 to 40 nm.

[1] H. Kronmüller and S. S. P. Parkim, Handbook of Magnetism and Advanced Magnetic Materials

(John Wiley & Sons Ltd, England: West Sussex, 2007).

[2] A. Khitun, M. Bao, and K. L. Wang, IEEE Trans. Magn. 44, 2141 (2008).

[3] K.-S. Lee and S.-K. Kim, J. Appl. Phys. 104, 053909 (2008).

[4] A. Slavin, Nature Nanotech. 4, 479 (2009).

Study of the spin excitations in antidot lattices with line defects

M. Madami¹, G. Gubbiotti^{1,2}, S. Tacchi², G. Carlotti^{1,3}, S. Jain⁴

¹ CNISM - Unità di Perugia and Dipartimento di Fisica, Università di Perugia, Via A. Pascoli, I-06123 Perugia, Italy.

² IOM-CNR c/o Dipartimento di Fisica, Università di Perugia, Via Pascoli, 06123 Perugia, Italy.

³ Centro S3, CNR - Istituto di Nanoscienze, Via Campi 213A, I-41125 Modena, Italy.

⁴ Materials Science Division, Argonne National Laboratory, Argonne, Illinois 60439, USA

The propagation of spin waves in antidot lattice (ADL) samples with line defects has been studied by both micro-focused Brillouin light scattering (μ -BLS) and micromagnetic simulations. The samples under investigation are NiFe square ADLs with circular holes of 250nm of diameter, the period of the structure is 700nm and the thickness of the NiFe layer is 60nm. Line defects have been introduced in the samples removing either a line or a column (or both) of holes every three lines (columns) as shown in the scanning electron microscopy (SEM) images of Figure 1. An ADL without line defects is used as reference sample.

The results from micromagnetic simulations, performed with OOMMF and using 2D periodic boundary conditions, show the appearance of new eigenmodes extending along the line defect areas, as shown in Figure 1. Moreover the frequencies of the other eigenmodes are also modified because of the different intensity of internal field due to the presence of the line defects.

Micro-focused BLS has been used in order to map out the intensity profile of these eigenmodes which are excited by a microwave current injected into a coplanar waveguide deposited on top of the sample surface (as shown in the SEM images of Figure 1). The comparison between micromagnetic simulations and μ -BLS measurements shows a good overall agreement in all samples investigated.

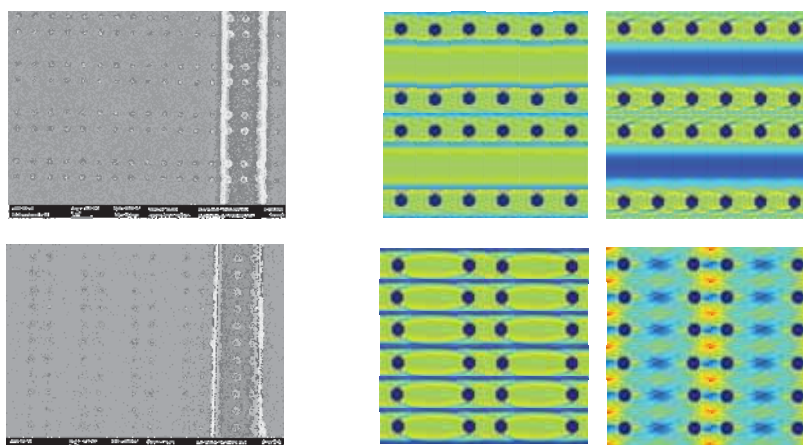


Figure 1. (left column) SEM images of two of the samples studied, with horizontal and vertical line defects respectively. (right columns) spatial profiles of two selected eigenmodes for each ADL as obtained from micromagnetic simulations.

This work was supported by the European Community's Seventh Framework Programme (FP7/2007-2013) under Grant No. 318287 "LANDAUER" and by the Ministero Italiano dell'Università e della Ricerca (MIUR) under the PRIN2010 project (No. 2010ECA8P3).

Nonlinear Thiele approach to the magnetic vortex dynamics under spin polarised current

R. Hernández Heredero^a, O. Chubykalo-Fesenko^b, K.Y. Guslienko^{c,d}

^a Escuela Técnica de Telecomunicaciones, Universidad Politécnica de Madrid, Spain

^b Instituto de Ciencia de Materiales de Madrid, CSIC, Madrid, Spain

^c Universidad del País Vasco, San Sebastian, Spain

^d IKERBASQUE, The Basque Foundation for Science, Bilbao, Spain

Nonlinear effects in magnetic vortex dynamics have recently attracted attention due to their manifestations, for example, in spin-transfer vortex nano-oscillators [1]. A powerful model to predict vortex dynamics is the generalized Thiele approach, where for the vortex core position \mathbf{X} an ansatz for the magnetisation, $\mathbf{m}(\vec{r}, t) = \mathbf{m}[\vec{r}, \mathbf{X}(t)]$, is assumed. This assumption has allowed to calculate the vortex gyrotropic frequency under applied magnetic field or spin polarised current, as well as its nonlinear corrections [1,2]. The nonlinearities are normally taken into account assuming small deviations from the equilibrium of the vortex displacement $\mathbf{X}(t)$. An alternative, more phenomenological approach, is to consider nonlinear vortex dynamics within a general nonlinear oscillator formalism [3].

In this work we derive the dynamical Thiele equation for the vortex dynamics in a thin circular magnetic dot, evaluating the spin-torque, damping, gyrotropic and nonlinear potential terms. For the vortex parameterization, we consider both the “rigid” and the “side charge free” models of displaced vortex [4]. The calculations are performed using complex variables and are more exact than the previously reported. We show that in the rigid model the exact result is that the spin-torque term is linear in the vortex displacement, while it is not so for the side charge free model. For the damping tensor we calculate both diagonal and non-diagonal elements. The damping form for the nonlinear vortex dynamics, followed from the Thiele approach, does not allow in the most general case its representation in the standard form of the nonlinear oscillator as in Ref. [3]. The obtained equations can serve as a theoretical basis for interpretation of the experiments on the magnetization dynamics in nanopillars and their arrays.

-
- [1] A. Dussaux et al. Phys. Rev. B 86 (2012), 014402.
 - [2] K.Y. Guslienko et al., Phys. Rev. B 82 (2010), 014402.
 - [3] J.-V- Kim et al., Phys. Rev. Lett. 100 (2008), 017207.
 - [4] K.Y. Guslienko, J. Nanosc. Nanotech. 8 (2008), 2745-2760.

Heat-assisted solutions in spin transfer driven magnetic recording: functionality of a macrospin model

Eugen Oniciuc, Laurentiu Stoleriu and Alexandru Stancu

Faculty of Physics & CARPATH, „Alexandru Ioan Cuza“ University of Iasi, Boulevard
Carol I, 11, 700506, Romania

Writing by polarized currents has been already successfully introduced in magnetic recording industry [1]. Such a promising fast and non-volatile universal memory still implies some challenges for the future theoretical and experimental researches, especially regarding cost-density ratio and new architecture concepts. Increasing density means smaller bits and superparamagnetic limit become hard to avoid [2]. The best solution for this problem seems to be heat/energy assisted writing.

Traditionally, magnetization dynamics models are based on various forms of Landau-Lifshitz-Gilbert equation which may contain fluctuation fields in order to describe thermal effects. In this work, we simulate some heat assisted writing solutions with a macrospin dynamic model which already contain the thermodynamics within the Landau-Lifshitz-Bloch form of dynamic equation [3-6]. We prove that such approach have some incontestable advantages by simplicity, robustness, flexibility and numeric efficiency in certain dimension scales used today in technological applications. We provide new switching phase diagrams, critical curves and specific trajectories of macrospin in the presence of polarised current. Spin transfer term in macrospin dynamic equation comes in a natural and simple form proposed by Slonczewski [7]. Also, thermally assisted magnetization reversal is discussed and explained for several geometrical and material configurations. The agreement between our simulations and published experimental data is very good and justify the use of macrospin models in certain conditions. Limits of macrospin models in heat assisted problems are also discussed and complementary functionalities in relation to other models are emphasized.

Acknowledgement: This work was supported by a grant of the Romanian National Authority for Scientific Research, CNCS-UEFISCDI, Project No. PN-II-ID-PCE-2011-3-0794 [IDEI-EXOTIC No. 185/25.10.2011].

-
- [1] Everspin's invited talk, MMM-INTERMAG 2013, Chicago, USA
<http://www.everspin.com/>
 - [2] S. H. Charap, P. L. Lu, Y. He, IEEE Trans. Mag. **33** (1997), 978
 - [3] D. A. Garanin, Phys. Rev. B **55** (1997), 3050
 - [4] P. M. Haney and M. D. Stiles, Phys. Rev. B **80** (2009), 094418
 - [5] C. Schieback, D. Hinzke, M. Kläui, U. Nowak, and P. Nielaba, Phys. Rev. B **80** (2009), 214403
 - [6] E. Oniciuc, L. Stoleriu and A. Stancu, Appl. Phys. Lett. **102** (2013), 022405
 - [7] J. Slonczewski, J. Magn. Magn. Mater. **159** (1996), L1-L7.

GPU enabled high-resolution computation of dispersion relations in 2D magnonic crystals

Ben Van de Wiele^a, Federico Montoncello^b, Arne Vansteenkiste^c

^a Department of Electrical Energy, Systems and Automation, Ghent University, Belgium

^b Dipartimento di Fisica e Scienze della Terra, Università degli Studi di Ferrara, Italy

^c Department of Solid State Physics, Ghent University, Belgium

Magnonic crystals have gained increasing interest to carry and manipulate information represented by magnonic waves. By adjusting the 1D or 2D periodicity, it is possible to tailor the spin-wave propagation properties as required in future spintronic devices. To fully understand the rich dispersion relations in these magnetic metamaterials as obtained from experiments [1], one needs theoretical models [2] and/or micromagnetic simulations. While the application of numerical simulations was restricted to only small portions of the structures, large scale simulations can now be conducted using Graphical Processing Units [3] offering the possibility of in-depth numerical studies on magnonic crystals.

In most numerical studies, dispersion relations are obtained by first applying a short, localized pulse and then computing the spatial and temporal Fourier transform of the magnetization in one simulation. Contrary to this approach we study the dispersion relations by combining several simulations in which a localized sinusoidal excitation with fixed frequency is continuously applied onto the system. The corresponding k-spectrum is obtained by a spatial Fourier transform. Contrary to a pulse excitation, resonant magnonic waves with the same frequencies are continuously excited in the system increasing the damped magnetization signal throughout the magnonic crystal and resulting as such in a higher k-space resolution. Furthermore, using a pulse excitation, the complete frequency spectrum is obtained with a resolution that is limited by the Gilbert damping and the simulation time. In our method, by optimizing the frequencies selected in the simulations, one can control the accuracy throughout frequency space.

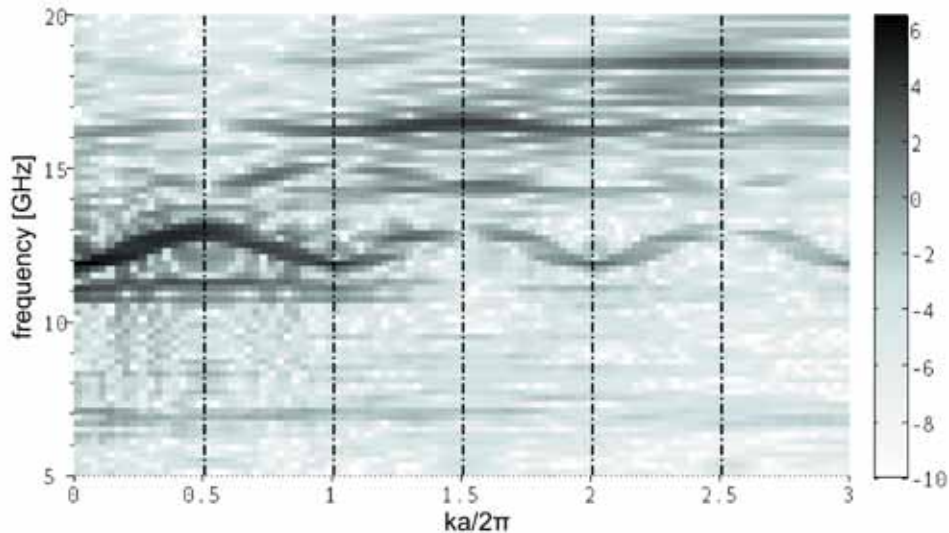


Figure 1. Dispersion for the 2D magnonic crystal described in [1], a is the period length. The k-space resolution is limited by the propagation properties of the waves rather than on numerical limits.

-
- [1] S.Tacchi, M. Madami, G. Gubbiotti, *et.al*, Phys. Rev. B, Vol. 82, 024401 (2010).
 - [2] L. Giovannini, F. Montoncello, and F. Nizzoli, Phys. Rev. B, 75 , 024416 (2007).
 - [3] A. Vansteenkiste and B. Van de Wiele, J. Magn. Magn. Mat., 323, No. 21 (2011).

Size effects on spin dynamics in 2D ferromagnetic antidot lattices

Roberto Zivieri^a, Perla Malagò^a, Loris Giovannini^a

^aDipartimento di Fisica e Scienze della Terra, Università di Ferrara, Ferrara, Italy

The size effects on frequencies of collective modes in two-dimensional (2D) arrays of periodic circular antidots (holes) embedded into a ferromagnetic Permalloy material are investigated. The study is performed by calculating the frequency behaviour as a function of the intensity H of the external magnetic field applied in the plane of the system along the y -direction for vanishing Bloch wave vector. The antidot periodicity is $a = 420$ nm, the thickness is $L = 30$ nm, whereas the diameters of the holes are $d_1 = 140$ nm, $d_2 = 180$ nm, $d_3 = 220$ nm and $d_4 = 260$ nm, respectively [1]. The two relevant modes, having an appreciable calculated scattering cross-section, are: 1) the resonant mode of the spectrum, the so-called Fundamental (F) mode, whose spatial profile is confined in the channels; 2) the equivalent mode mainly localized in the horizontal rows of ADs, the F^{loc} mode. Frequencies of collective modes monotonically increase with increasing the mean internal field. However, at a fixed external field the frequencies of F and F^{loc} mode have on opposite behavior as a function of the hole size as shown in Figure 1. Indeed, the mean demagnetizing field experienced by the F mode is anti-parallel to the external field lowering the mean internal field, while for the F^{loc} mode it is parallel and has the effect to increase the internal field.

Moreover, at the centre of the first Brillouin zone, the two lowest spin-wave mode frequencies, namely the edge mode (EM) localized at the antidot borders [2] and the F mode, become soft at a given critical field showing a deep minimum as illustrated in Figure 1. The intensity of the critical field depends on the hole size and both soft modes do exhibit a finite gap. The softening mechanism is strictly related to the rotation of the static magnetization from the hard to the easy axis marking a reorientational and continuous phase transition [3].

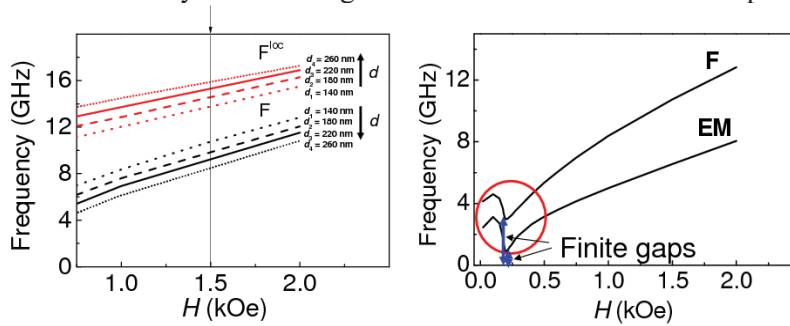


Figure 1. Left panel. Frequencies vs. the magnetic field for the F and F^{loc} collective modes at different diameters. Right panel: Frequencies of the two-lowest collective modes, EM and F, respectively vs. the magnetic field at $d = 140$ nm. The softening region together with the finite gaps are highlighted.

[1] J. Ding, D. Tripathy, A. O. Adeyeye, J. Appl. Phys. **109**, (2011) 07D304-1-3.

[2] S. Tacchi, M. Madami, G. Gubbiotti, G. Carlotti, A.O. Adeyeye, S. Neusser, B. Botters, D. Grundler, IEEE Trans. Magn. **46**, (2010) 172-178.

Magnetization dynamics driven by spin-Hall effect in three-terminal MTJ devices

R. Tomasello¹, M. Carpentieri²

¹ Department of Computer Science, Modeling, Electronics and System Science, University of Calabria, Rende (CS), Italy

² Department of Ingegneria Elettrica e dell'Informazione, Politecnico of Bari, Bari, Italy.

Very recently, Liu *et al.* have used a giant spin Hall effect (SHE) in tantalum to generate large spin current and to obtain steady state magnetic oscillations [1]. The system is a three-terminal device, as described in Fig. 3(a) of Ref. 1 (we set the same magnetic parameters of Ref. 1, main values are: saturation magnetization of 1000×10^3 A/m, exchange constant of 2.0×10^{-11} J/m, spin Hall angle of 0.15), where the switching was achieved through the spin-transfer torque due to the SHE. This effect gives advantages both in Magnetic Random Access Memories, reducing the switching current density, and in oscillators, inducing steady-state magnetic oscillations, with low damping and small saturation magnetization.

Here, we numerically demonstrate, by means of micromagnetic simulations, the possibility to excite permanent precessional modes in the free magnetic layer of the Magnetic Tunnel Junction (MTJ).

When a dc current density (J_{Ta}) is applied along the Ta strip, the SHE injects spins into the CoFeB, and when the SHE spin current density (J_{SHE}) is large enough to reduce the net effective damping to zero, spontaneous steady-state magnetic precession is obtained.

We applied a magnetic field (H_{app}) up to values of 50 mT, varying the in-plane angle ϕ , considered with respect to the easy axis of the ellipse. We found the magnetization dynamics when $\phi=15^\circ$ and 30° .

Fig. 1a reports the oscillation frequency (f) as function of the J_{SHE} for different H_{app} and for $\phi=30^\circ$ (the graph for $\phi=15^\circ$ is not represented). As shown, the frequency value depends on the field amplitude and its behavior is rather constant with the current. As expected, the precession frequency increases with the field value (in our case it is $f=3.76$ GHz and 4.59 GHz for $H_{app}=30$ mT and 40 mT respectively). In addition, for this angle ϕ no stable dynamics are observed when increasing the field amplitude.

Finally, we fixed J_{SHE} , H_{app} and ϕ and swept the MTJ current density (J_{MTJ}) between -5.1×10^6 A/cm² and $+5.1 \times 10^6$ A/cm². Persistent oscillations are not generated when negative J_{MTJ} is injected. Vice versa, we found magnetization dynamics for low positive J_{MTJ} . The effect of the J_{MTJ} is to increase the frequency value from about 3.8 GHz to 6 GHz and, as expected, the frequency rises when increasing the J_{MTJ} (see Fig. 1a-b).

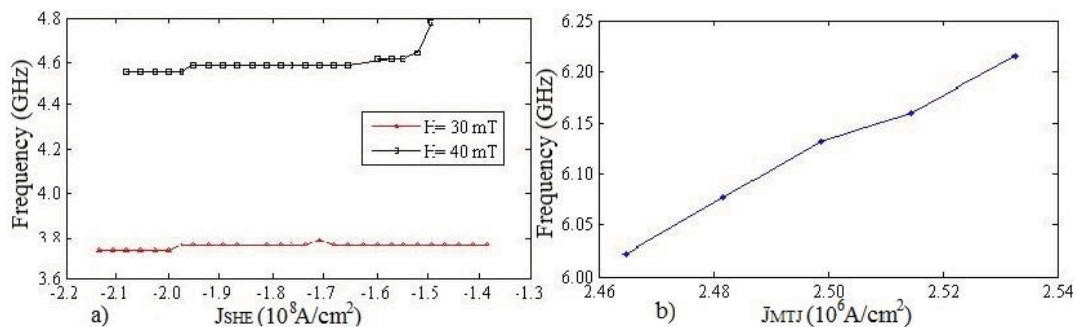


Figure 1: a) f in dependence on the J_{SHE} for $\phi=30^\circ$ and for $H_{app}=30$ mT and 40 mT. b) f as a function of the J_{MTJ} , for $H_{app}=30$ mT $J_{SHE}=-1.39 \times 10^8$ A/cm² and $\phi=30^\circ$.

[1] L. Liu, C.-F. Pai, Y. Li, H. W. Tseng, D. C. Ralph, R. A. Buhrman, *Science* 336, 555 (2012).

[2] L. Liu, C.-F. Pai, Y. Li, H. W. Tseng, D. C. Ralph, R. A. Buhrman, *Phys. Review Lett.* 109, 186602 (2012).

Numerical and experimental studies of current-induced magnetization switching and back-hopping in magnetic tunnel junctions with MgO barriers

Piotr Ogrodnik^{a,b}, Witold Skowroński^d, Tomasz Stobiecki^d, Renata Świrkowicz^a,
Józef Barnas^{b,c}

^a Faculty of Physics, Warsaw University of Technology, Warsaw, Poland

^b Institute of Molecular Physics, Polish Academy of Science, Poznań, Poland

^c Faculty of Physics, Adam Mickiewicz University, Poznań, Poland

^d Department of Electronics, AGH University of Science and Technology, Kraków, Poland

Current Induced Magnetization Switching (CIMS) due to Spin Transfer Torque (STT) in magnetic tunnel junctions (MTJs) has been extensively studied in recent years. This was stimulated by possible applications of the effect in the next generation of non-volatile magnetic random access memory cells (STT-RAM). An important issue of the current studies concerns the design of voltage-controllable and thermally stable structures. Non-deterministic behavior of MTJ-based memory cells may occur at higher bias voltages as multiple returns from the parallel (P) to the antiparallel (AP) states [1,2]. Such a behavior is clearly visible in experimentally measured resistance vs. bias voltage loops, and is referred to as the back-hopping effect.

In this paper we will present a comparison of experimental and simulation data for MTJs with different MgO barrier thicknesses. The probability of back-hopping can be significantly enhanced by an antiferromagnetic coupling between the reference and free layers of a MTJ. Such a situation has been observed experimentally in the case of a MTJ with 1 nm thick MgO tunnel barrier. Experimental results have been compared with numerical macrospin simulations, based on the Landau-Lifshitz-Gilbert (LLG) equation with additional STT terms. The results have been also supported by an additional linear stability analysis. From the analytically calculated eigenvalues of the linearized LLG equation, the stability conditions for the P and AP states have been determined for arbitrary magnitudes of the in-plane as well as out-of-plane (field-like) components of the spin torque. These conditions have been checked for STT components and other parameters of MTJs estimated from the experimental data [3]. In turn, for a MTJ with thinner MgO tunnel barrier of 0.76 nm, a strong ferromagnetic coupling has been observed. For this specific tunnel barrier thickness, a single switching event from the AP to P state takes place, without any back-hopping, as observed in the experiment as well as in the macrospin simulations. In addition, analytical and numerical stability diagrams have been calculated for each sample. Based on our studies, one can identify the parameters of MTJs, for which the back-hopping effect is reduced. This may be important for a proper STT-MRAM cell design.

Acknowledgement: This work was supported by Swiss Contribution, NANOSPIN PSPB-045/2010 grant.

[1] J. Z. Sun et al., J. Appl. Phys. 105, 07D109, 2009

[2] S.-C. Oh et al. Nat.Phys., vol. 5, 2009

[3] W. Skowronski et al. arXiv:1301.7186.

Influence of dipolar interactions on the low temperature magnetic states and hysteresis of single-wall zigzag nanotubes

Hernán Salinas^a, Johans Restrepo^a, Oscar Iglesias^b.

^aGrupo de Magnetismo y Simulación G+ y Grupo de Instrumentación Científica y Microelectrónica, Instituto de Física, Universidad de Antioquia. A.A. 1226, Medellín, Colombia

^bDpt. de Física Fonamental and Institut de Nanociència i Nanotecnologia, Facultat de Física, Universitat de Barcelona, Av. Diagonal 645, 08028 Barcelona, Spain

Magnetic nanostructures can be synthesized with different shapes such as disks, cylinders, rings and nanotubes. Owing to their specific geometry and nanoscale size that have found distinctive applications due to their peculiar magnetic orderings. In this work, we have studied the low temperature magnetic equilibrium configurations and hysteretic properties of magnetic nanotubes. The results have been obtained by Monte Carlo simulations of a lattice of Heisenberg magnetic moments residing on the cylindrical lattice of single-wall zigzag nanotubes which interact via competing short-range exchange (J) and long-range dipolar interactions (D). In order to ensure that the low temperature magnetic states correspond to the true ground states, a simulated annealing protocol was followed complemented by a two different single spin flip dynamics: one based on trial changes inside a cone around the actual spin direction with a temperature dependent reduction of its aperture, and the other one based on the free movement of the spins within a unit sphere. Results reveal the occurrence of different low-temperature magnetic states depending of the degree of competition between the exchange and dipolar energies. Thus, collinear ferromagnetic states can be observed for dominant exchange interactions whereas vortex states are obtained above a certain threshold value of $\gamma=D/J$ when dipolar interactions dominate. For intermediate values of γ , interesting non-collinear helical states are obtained. We have found convenient to use as an order parameter the rotational of the spin configurations (together with the different magnetization components) in order to characterize properly these three different states and to propose a magnetic phase diagram as a function of γ , radius and length of the nanotube. Moreover, some analytical expressions are developed in order to obtain the energies of a wide set of spin configurations in terms of a polar angle and to justify the validity of the simulation results. Finally, low temperature hysteresis loops have been obtained nanotubes with the three different kinds of ground states. The reversal mechanisms have been studied by direct visualization of the intermediate magnetic states and analyzed by using convenient order parameters.

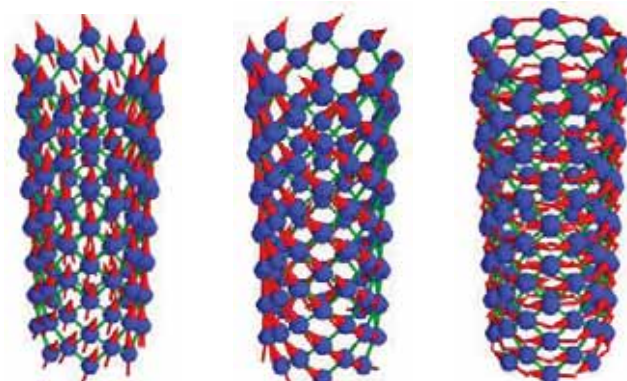


Figure 1: Low temperature magnetic configurations of a zig-zag nanotube with $\gamma=0.01, 0.036, 0.05$ (left, center, right).

Magnetisation dynamics based on the Landau-Lifshitz equation with Baryakhtar damping term

Weiwei Wang^a, Mykola Dvornik^b, Marc-Antonio Bisotti^a, Dmitri Chernyshenko^a,
 Marijan Beg^a, Maximilian Albert^a, Arne Vansteenkiste^b,
 Bartel V. Waeyenberge^b, Volodymyr V. Kruglyak^c, Hans Fangohr^a

^a Engineering and the Environment, University of Southampton, Southampton, UK

^b DyNaMat Lab, Ghent University, Gent, Belgium

^c School of Physics, University of Exeter, Exeter, UK

The Landau-Lifshitz-Gilbert (LLG) equation is the fundamental equation of motion in micromagnetics governing magnetisation dynamics. However, some results given by the LLG equation are in contradiction with experimental data and microscopic calculations. For instance, a microscopic calculation gives the dependence of spin wave decrement for short-wave magnons proportional to k^4 while the LLG equation shows a relation proportional to k^2 , where k is the wavevector [1]. Baryakhtar generalized the LLG equation by starting from Onsager's relations, considering the symmetry of the relaxation processes, and dropping the requirement for the equation of motion to preserve the length of the magnetisation – in contrast to the established LLG equation. Compared to the LLG equation, Baryakhtar's modification contains an extra damping term (Baryakhtar term) proportional to the Laplace operator of the total effective field.

In this work, the Baryakhtar term was implemented and the spin wave propagation characteristics and dispersion relation in a Permalloy rod were studied by micromagnetic simulations. A spin wave excited at one end of the rod decays as a function of distance x , so that its amplitude is proportional to $\exp(-\lambda x)$, where λ is the decay coefficient. The simulation results confirm that the Baryakhtar term enhances the spin wave amplitude decay coefficient λ at high frequencies while it has no significant impact on the spin wave dispersion relation. Analytical analysis of a simplified model shows that λk (the product of spin wave decay coefficient and wavevector) has an additional term that scales with k^4 (due to the Baryakhtar term) in addition to the linear dependence of the spin wave frequency. The spin wave linewidth is calculated, which gives an extra contribution proportional to k^4 introduced by the Baryakhtar term. We acknowledge financial support from EPSRC's DTC grant EP/G03690X/1.

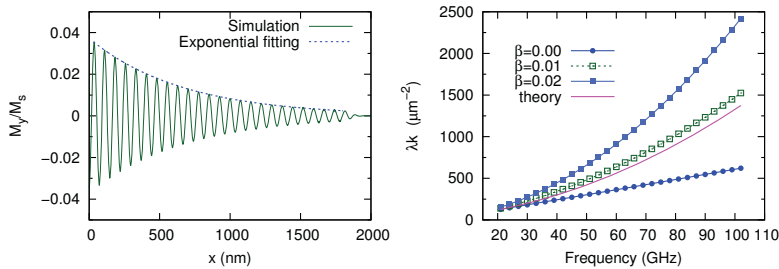


Figure 1: Left: The spatial spin wave amplitude decaying (normalized M_y component). Right: λk as a function of the frequency for a Permalloy rod, and β measures the strength of the Baryakhtar term ($\beta=0$ corresponds to the conventional LLG equation). The magenta solid line shows the corresponding analytical result for $\beta=0.01$ case.

[1] V. Baryakhtar *et al.*, Physical Review B, **56**, 619 (1997)

Comparison between advanced time–frequency analyses of nonstationary magnetization dynamics in spin-torque oscillators

Giulio Siracusano^a, Aurelio La Corte^b

^a Dipartimento di Fisica della Materia e Ingegneria Elettronica, University of Messina, Salita Sperone, 31 - 98166 Messina, Italy

^b Dipartimento di Ingegneria Informatica e delle Telecomunicazioni, University of Catania, Viale Andrea Doria, 6 – 95125 Catania, Italy

We report a time-frequency analysis of measurements of the voltage signal related to a spin-torque oscillator [1] investigating on non-stationary dynamics using different techniques. Wavelet [2], compared to the traditional Fourier analysis, has the advantage of revealing time and frequency domain information simultaneously, especially for nonlinear and non-stationary signals. Huang -Hilbert- Transform (HHT) [3] is a novel non-linear signal analysis method. In this study, analysis based on HHT and Morlet wavelet scalogram (MWS) (computed as described in [4]) were performed and compared.

With Wavelet analysis, we identify nonstationary magnetization dynamics revealing the existence of intermittent and independent excited modes while by means of the HHT we are able to accurately extract the time domain traces of each independent mode.

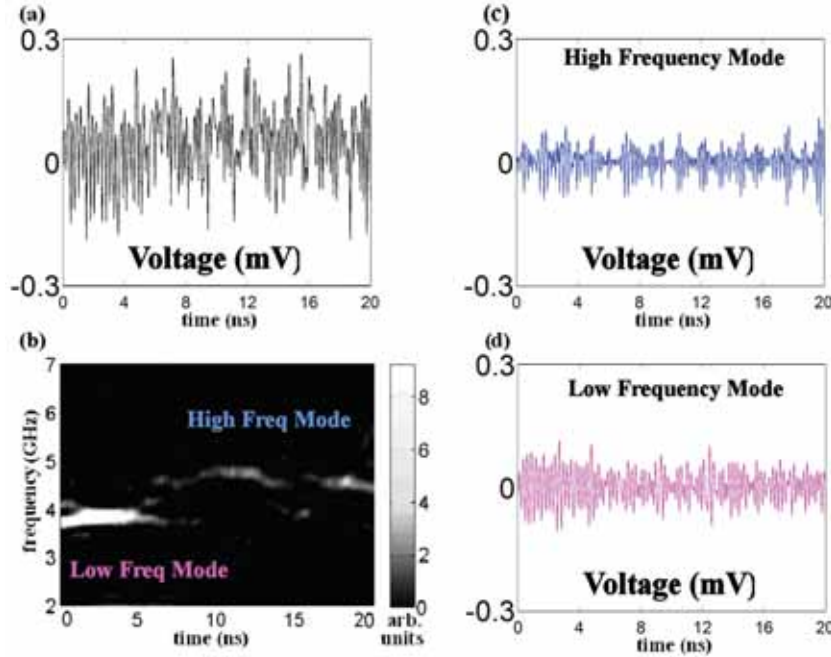


Figure 1: (a) Voltage signal $x(t)$ in [1]. (b) MWS of $x(t)$ [4]. (c) Time-domain plots of high frequency mode in $x(t)$ as extracted using HHT and (d) low frequency mode in $x(t)$.

Figure 1 (a) shows a time domain representation of the signal $x(t)$, while in Figure 1(b) with the MWS there are identified two sources of excitation, identified as low and high frequency modes. Figure 1(c) and (d) show a time-domain representation of high frequency (blue) and low frequency (magenta) harmonics as extracted using the HHT. The HHT demonstrate the ability to extract independent modes and instantaneous variables enabling to completely investigate the time-frequency dynamics.

-
- [1] I. N. Krivorotov et al, Phys. Rev. B **77**, 054440 (2008).
 - [2] I. Daubechies, CBMS-NSF Reg. Conf. (SIAM, Philadelphia, 1992).
 - [3] Huang, N.E. et al, Proc. Royal Society, **454**, 903–995 (A), (1998).
 - [4] G. Siracusano, G. Finocchio, A. La Corte, et al, PHYS. REV. B **79**, 104438 (2009).

Micromagnetic modelling on superparamagnetic microbeads manipulation and detection using spin-valve PHE sensors

M. Volmer^a, M. Avram^b

^a Transilvania University of Brasov, Eroilor 29, Brasov 500036, Romania

^b National Institute for Research and Development in Microtechnologies, Str. Erou Iancu Nicolae 32B, Bucharest 72996, Romania

Superparamagnetic (SPM) microbeads are widely used to tag, manipulate, and detect chemical and biological species. There is great interest in exploiting this functionality in what is known today as lab-on-a-chip devices (LOC). Microscale orthogonal layers of parallel microwires [1], electromagnets and arrays of soft magnetic microstructures are used to transport microbead ensembles and even individual beads across the surface of a chip. Recently, it has been shown that the strong, localized stray field from domain walls (DWs) in submicrometer ferromagnetic tracks can trap individual SPM beads with forces up to hundreds of pN and manipulate them [2].

In this contribution we present a micromagnetic analysis of the interaction between the SPM microbeads and the planar Hall effect (PHE) sensor surface. The simulated system consists of a circular Permalloy structure, 2 μm in diameter and 10 nm thick, placed above a conductive nonmagnetic stripe 6 μm long and 2 μm , Fig. 1(a). The current which is flowing through the conductive stripe creates a biasing field, H_{bias} , parallel with the driving current, I_{sens} , inside the sensor. A magnetic field, H_{appl} , can be applied perpendicular to the sensor's surface. This field is used to magnetize the SPM microbeads. In turn, these beads create a magnetic field which is detected by the PHE sensor.

Considering this setup we have obtained the magnetic energy distribution of a SPM bead of 200 nm in diameter placed above the sensor surface at a distance of 200 nm. Effects like large magnetic field gradients and field amplification in the sensor's vicinity have been

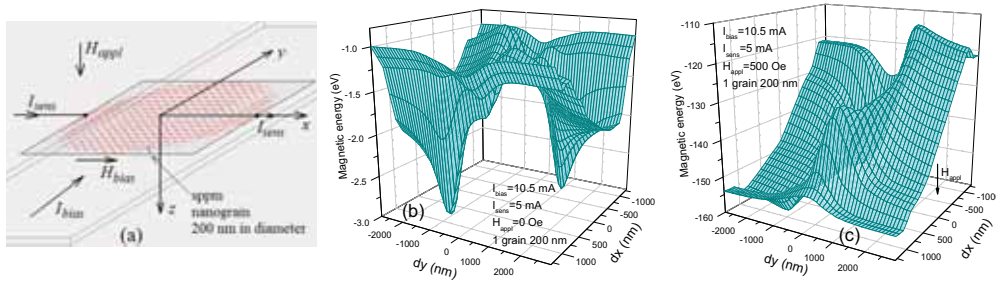


Figure 1: (a) The geometry of the simulated system, (b) the magnetic energy distribution of a SPM microbead when $H_{appl}=0$ and (c) when $H_{appl}=500$ Oe.

observed. A magnetic force which is position dependent appears and is responsible for the beads distribution. From the plots, presented in Fig. 1(b) for $H_{appl}=0$ and in Fig. 1(c) for $H_{appl}=500$ Oe, respectively, we observe regions with minimum energy in which the SPM beads will be captured. These positions can be tuned by changing the fields and currents amplitudes and polarities. The output of the PHE sensors when the SPM microbeads are localized in these positions will be obtained by micromagnetic simulations. The results will be compared with experimental data.

[1] P. Rinclin, H. J. Krause and B. Wolfrum, Appl. Phys. Lett. 100 (2012) 014107

[2] E. Rapoport, D. Montana and G. S. D. Beach, Lab Chip, 12 (2012), 4433-4440

The influence of the spatial current distribution on the domain wall depinning from a single notch

M. A. Hernández^a, V. Raposo^a, E. Martínez^a, L. López-Díaz^a and L. Torres^a

^a Dpto. Física Aplicada, Universidad de Salamanca, Salamanca, SPAIN.

The position of a Domain Wall (DW) in a thin ferromagnetic strip can be controlled by means of notches, which act as pinning potential wells by locally lowering its magnetostatic energy. The analysis of the DW depinning is of interest, not only because of the fundamental physics involved [1], but also due to its potential application for logic and memory devices [2]. In particular, the study of the critical depinning current as a function of the applied field provides quantitative information on non-adiabaticity, and for applications, reducing this critical current is mandatory to avoid unwanted Joule heating effects. Traditionally, the experimental measurements are interpreted by means of micromagnetic simulations which consider that the current is spatially uniform and directed along the strip axis ($\mathbf{j}_a = j_a \mathbf{u}_x$). However, in real experiments, where the current is injected through two metallic contacts (Fig. 1(a)), the current direction deviates from the strip axis and it reaches high values inside the constriction (Fig. 1(b)).

In the present work, micromagnetic modeling is used to characterize the current-induced DW depinning from a triangular notch in a thin Permalloy strip with emphasis on the influence of the non-uniform spatial distribution of the injected current, which has been calculated using a finite element solver (COMSOLTM). Our results indicate that this non-uniform current distribution do influence the dynamics. For instance, a uniform current of 51mA is required to promote the DW depinning, whereas this value is significantly reduced to 36mA if the real spatial distribution of the current is taken into account (Fig. 1(c)). This observation, along with the details of our model and its implications for the estimation of the non-adiabaticity, will be discussed in the presentation.

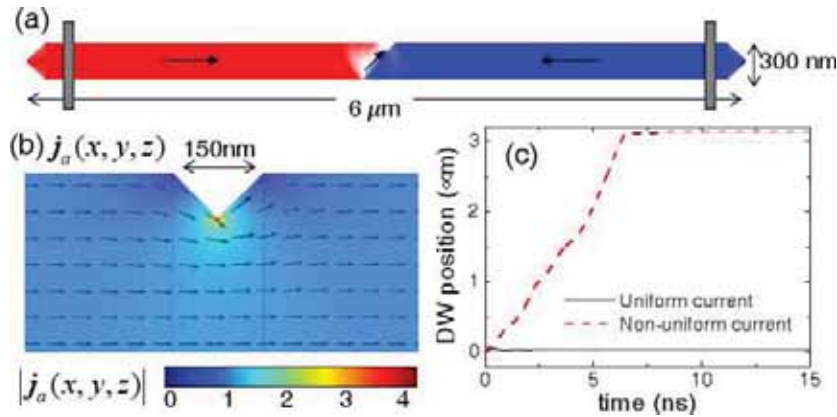


Figure 1: (Color on-line) (a) Geometry of the analyzed Permalloy strip. (b) Spatial distribution of the current density as computed by COMSOLTM, where the color scale represents the strength. (c) Temporal evolution of the DW position under uniform (solid) and non-uniform (dash) currents of 36mA

[1] see for example, G. S. D. Beach et al. J. Magn. Magn. Mater. 320, 1272, (2008).

[2] S. S. Parkin, U.S. Patent No. 6834005 (2004).

Estimating the thermal rate and mechanism of magnetic transitions

Pavel F. Bessarab^{a,b}, Valery M. Uzdin^b, and Hannes Jónsson^a

^a University of Iceland, Reykjavík, Iceland

^b St. Petersburg State University, St. Petersburg, Russia

The energy surface of a magnetic system gives the energy as a function of the angles determining the orientation of the magnetic moments. Minima on the energy surface correspond to stable or metastable magnetic states and can represent parallel, antiparallel or, more generally, non-collinear arrangements (Fig. 1). A rate theory has been developed for systems with arbitrary number, N , of magnetic moments, to estimate the thermal stability of magnetic states and the mechanism for magnetic transitions based on a transition state theory approach [2]. The minimum energy path is determined using the NEB method [1] to identify the transition mechanism and estimate the activation energy barrier. A pre-exponential factor in the rate expression is obtained from the Landau-Lifshitz equation for spin dynamics. The velocity is zero at saddle points so it is particularly important in this context to realize that the transition state is a dividing surface with $2N-1$ degrees of freedom, not just a saddle point (Fig. 1).

A harmonic approximation to the rate constant gives [2]

$$k^{HTST} = \frac{v}{2\pi} \sqrt{\frac{\det H_m}{\det H_s}} e^{-(E^s - E^m)/k_B T} \quad \text{where} \quad v = \frac{\gamma}{(1 + \alpha^2)} \prod_{i=1}^D \frac{M_{s,i}^2 \sin \theta_{s,i}}{M_{m,i}^2 \sin \theta_{m,i}} \sqrt{\sum_{i=2}^D \frac{\alpha_i^2}{\epsilon_i}} \quad (1)$$

where $\det H_m$ and $\det H_s$ denote the determinants of the Hessian matrices at the minimum and at the saddle point, ϵ_i are eigenvalues of the Hessian at the saddle point and θ_s , θ_m and M_s , M_m are polar angles and magnitude of magnetic moments at the saddle point and at the minimum. The determinants are computed as a product of the eigenvalues and the prime means that the negative one, ϵ_1 , is omitted. A comparison of this HTST with direct dynamical simulations using the Landau-Lifshitz-Gilbert equation show good agreement for a wide range of coupling constant (Fig. 1). Dynamical corrections can then be applied to get the exact rate constant.

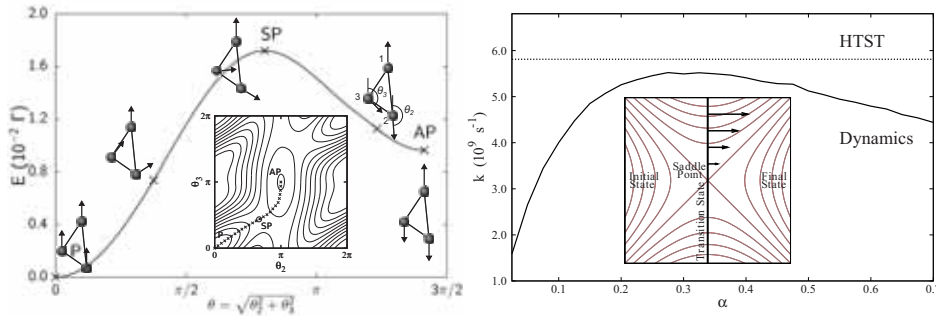


Figure 1: Left: Energy landscape for a transition in Fe trimer. *Inset*: The energy surface. Right: Comparison of the HTST transitions rate (dotted line) and direct Landau-Lifshitz-Gilbert dynamics as a function of the damping constant α at $T = 23$ K (solid line). *Inset*: The energy surface near a saddle point, the HTST transition state (thick line) and spin velocity (arrows).

[1] G. Henkelman, B. Uberuaga and H. Jónsson, *J. Chem. Phys.* **113**, 9901 (2000).

[2] P.F. Bessarab, V.M. Uzdin, and H. Jónsson, *Phys. Rev. B* **85** (2012), 184409.

Analysis of random magnetization switching using monte carlo simulations

Andrew Lee^a, Ziyu Liu^a, Giorgio Bertotti^b, Claudio Serpico^c, Isaak Mayergoyz^a

^a University of Maryland, College Park, Maryland, USA

^b Istituto Nazionale di Ricerca Metrologica, Torino, Italy

^c Università of Naples "Federico II", Napoli, Italy

A new approach to stochastic magnetization dynamics driven by interactions with a thermal bath has been proposed in [1-3]. In this approach, thermal bath effects (damping as well as fluctuations) are described by a jump-noise process. A Monte Carlo technique for numerical modeling of such stochastic magnetization dynamics has been discussed in [4] where the concept of “self-scattering” has been used to achieve time-homogenization of the jump-noise process and appreciably simplifies numerical calculations. In this paper, the Monte Carlo technique is used for the detailed numerical study of random magnetization switching in uniaxial magnetic particles. The focus of this study has been two-fold. First, the numerical analysis of random switching (exit) time has been performed, and cumulative distribution functions of the exit time have been computed for various magnetic energy barriers, jump-noise process characteristics and temperatures. It has been observed from simulations that the cumulative distribution function depends, as expected, on the ratio of the energy barrier to kT rather than on each of these quantities separately. The second focus of our study has been the numerical testing of the Kramers-Brown approximation from [5,6]. The essence of this approximation is that the (truncated) Boltzmann distribution is established in an energy well long before random magnetization switching from this well occurs. This approximation is valid for a “sufficiently” large ratio of energy barrier to kT . The purpose of our numerical study has been to identify this ratio in more precise terms and to explore how this ratio depends on the properties of the jump-noise process. The identification of this barrier ratio is important because the Kramers-Brown approximation is frequently used and, in particular, this approximation is the foundation for the derivation of the stochastic master equation for thermal switching that has been carried out in [7]. In this sense, our numerical calculations establish the limits of applicability of this master equation.

-
- [1] I. Mayergoyz, G. Bertotti and C. Serpico, *Physical Review B* 83, 020402(R) (2011).
 - [2] I. Mayergoyz, G. Bertotti and C. Serpico, *J. Appl. Phys.* 109, 07D312 (2011).
 - [3] I. Mayergoyz, G. Bertotti and C. Serpico, *J. Appl. Phys.* 109, 07D327 (2011).
 - [4] A. Lee, Z. Liu, C. Serpico, G. Bertotti and I. Mayergoyz, *J. Appl. Phys.* 111, 07D501 (2012).
 - [5] W.F. Brown, *Physical Review*, 130 (5) (1963), 1677–1686.
 - [6] H.A. Kramers, *Physica*, 7 (1940), 284-304.
 - [7] Z. Liu, A. Lee, G. Bertotti, C. Serpico and I. Mayergoyz, *J. Appl. Phys.* 111, 07D108 (2012).

Mutual Demagnetizing Tensor for Patterned Dots with Rhomboid Lattice Geometries

Omar Khan ^{a,c}, Carlo Ragusa ^a, Fiaz Khan ^b, Bartolomeo Montrucchio ^b

Dipartimento {^a Energia, ^b Informatica e Automatica}, Politecnico di Torino, Italy
^c omar.khan@ieeee.org

Dot patterned magnetic media have important applications in nanotechnology. Classical fabrication methods for them may result in regular, rhomboid (Fig.1), or honeycomb shaped lattices. However, conventional micromagnetic numerical tools dealing with such lattices in simulation software treat them as a single body with embedded non-magnetized regions. These numerical approaches are not favourable computationally as the patterned-media can cover large areas. It is widely understood that the major contribution to this computation time is the demagnetizing field calculations. Hence, in this paper, we propose performance driven numerical refinements in the form of a new tensor component; the **mutual demagnetizing tensor \mathbf{N}** , for representing magnetostatic interactions between different dots. The demagnetizing field in an n-body rhomboid patterned grid is given as:

$$\mathbf{h}_p(\mathbf{i}, \mathbf{j}) = - \sum_{b=1}^2 \sum_{c=1}^{K/2} \sum_{j'} \sum_{i'} \mathbf{N}_{p,b,c}(\mathbf{i} - \mathbf{i}', \mathbf{j} - \mathbf{j}') \cdot \mathbf{m}_{b,c}(\mathbf{i}', \mathbf{j}'), \quad (1)$$

where, \mathbf{h}_p is the field in body p , b is the grid identifier, K is the total number of bodies identified using indices b, c , and \mathbf{m} is the magnetization. Here, two sub-grids are sufficient for rhomboid lattices. Since position \mathbf{i}, \mathbf{j} of each dot are dependent on the concerned sub-grid, i.e., $\mathbf{f}_g(\mathbf{i}, \mathbf{j})$, we can treat the above equation as:

$$\mathbf{h}[\mathbf{f}_g(\mathbf{i}, \mathbf{j}), \mathbf{g}] = - \sum_{g'} \sum_{j'} \sum_{i'} \mathbf{N}[\mathbf{f}_g(\mathbf{i} - \mathbf{i}', \mathbf{j} - \mathbf{j}'), \mathbf{g} - \mathbf{g}'] \cdot \mathbf{m}[\mathbf{f}_g(\mathbf{i}', \mathbf{j}'), \mathbf{g}'], \quad (2)$$

where \mathbf{g} represents the sub-grid as a pseudo-axial component because it lies in the same \mathbf{xy} plane. The application of the convolution theorem is apparent in the above expression, hence by applying the Fast Fourier transform to both tensor \mathbf{N} and magnetization \mathbf{m} , we obtain:

$$\tilde{\mathbf{H}}(\mathbf{I}_\omega, \mathbf{J}_\omega, \mathbf{G}_\omega) = -\tilde{\mathbf{N}}(\mathbf{I}_\omega, \mathbf{J}_\omega, \mathbf{G}_\omega) \cdot \tilde{\mathbf{M}}(\mathbf{I}_\omega, \mathbf{J}_\omega, \mathbf{G}_\omega) \quad (3)$$

This will reduce the complexity in Eq. 2 from $O(\mathbf{n}^2)$ to $O(\mathbf{n} \log \mathbf{n})$, where \mathbf{n} is the number of data points, leading to considerable speedup and memory savings.

- [1] A. O. Adeyeye and N. Singh. Large area patterned magnetic nanostructures. *Journal of Physics D: Applied Physics*, 41(15):153001+, 2008.

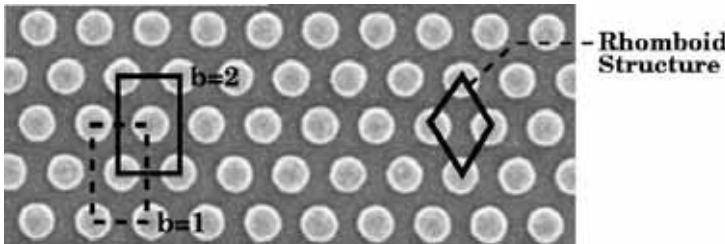


Figure 1: Scanning electron micrograph of resist patterns for rhomboid lattice geometry (adapted from [1]). The imposition of sub-grids on the geometry conforms to Eq. 1

Magnetic vortex based biosensor

Giovanni Finocchio^a, Vito Puliafito^a, Nicola Donato^a, Luis Torres^b,
Mariangela Latino^c, Bruno Azzerboni^a

^a Department of Electronic Engineering, Industrial Chemistry and Engineering, University of Messina, C.da Di Dio, 98166 Messina, Italy

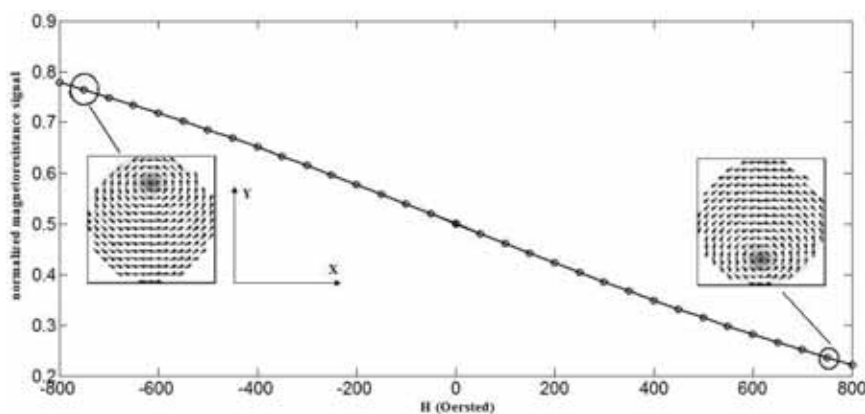
^b Department of Applied Physics, University of Salamanca, Plaza de la Merced, 37008 Salamanca, Spain

^c CNR Catania, Italy

Magnetic particles (beads) have been studied because of their many promising biomedical applications. Those are suitable to be used in biosensor applications, since their magnetic properties allow relatively easy (and remote) detection, large surface to volume ratio and mobility, but one of the most important advantages is that the magnetic background of even complex biological fluids is very low. Here we propose a GMR (TMR) biosensor [1] where at least the ground state of the “free layer” of the sensor is a magnetic vortex configuration of any chirality (clockwise or counter-clockwise) and any polarity (positive or negative) [2]. The magnetization of the polarized layer can be either in non-uniform (for example vortex configuration) or in uniform configuration. The two ferromagnets can be separated by a normal metal (GMR-vortex biosensor) or by an insulator (TMR-vortex biosensor).

The magnetic field due to the magnetic beads is detected via a change in the GMR (TMR) signal related to a motion of the vortex core with respect to its equilibrium position. The magnetic vortex sensor is able to detect the presence of the field in any direction, in particular the magnetization parallel to the field expands while the antiparallel is compressed. The response of the sensor is linear in a wide range of field, and it is related to the shift of the vortex core. The figure displays an example of magnetic vortex response to an external field applied along the x direction. The computations have been performed by means of micromagnetic simulations (Permalloy free layer of 250 nm-diameter and 60 nm-thickness) [3].

If used in an array configuration the magnetostatic coupling between the vortex sensors is sensibly reduced with respect to sensors with uniform magnetic state.



-
- [1] G. Finocchio and B. Azzerboni, patent pending.
 - [2] V.S. Pribiag, et al., *Nature Physics* **3**, 498-503 (2007).
 - [3] Y. Liu, et al. *Journ. Appl. Phys.* **99**, 08G102 (2006).

Synchronization of propagating and localized spin-wave modes in a double-contact spin-torque oscillator: a micromagnetic study

V. Puliafito^a, G. Consolo^b, L. Lopez-Diaz^c, B. Azzerboni^a

^a Department of Electronic Engineering, Industrial Chemistry and Engineering, University of Messina, Contrada Di Dio, 98166 Messina, Italy

^b Department of Mathematics and Informatics, University of Messina, Viale F. Stagno D'Alcontres 31, 98166, Messina

^c Department of Applied Physics, University of Salamanca, Plaza de los Caidos, 37008 Salamanca, Spain

The possibility of synchronizing two or more interacting spin-transfer oscillators (STO) has been studied with the aim of amplifying the overall output power and spectral purity [1]. Here, we numerically characterize a double nanocontact STO within a computational region of $1 \mu\text{m} \times 1 \mu\text{m}$ [2]. The study is performed in the cases of normal and in-plane external bias field, where the corresponding excited modes are propagating and localized, respectively. Synchronization phenomena are examined as a function of the applied current and the distance between the contacts, deriving the characteristic locking bandwidth in each case. To realize the physical phenomenon responsible for the synchronization (dipolar or spin-wave coupling), simulations are also performed by cutting the ferromagnetic material separating the two contacts [3,4]. Interestingly, we observe that in the case of in-plane field a frequency pulling can take place between localized modes excited by closely-positioned contacts but no kind of interaction occurs in the cut geometry.

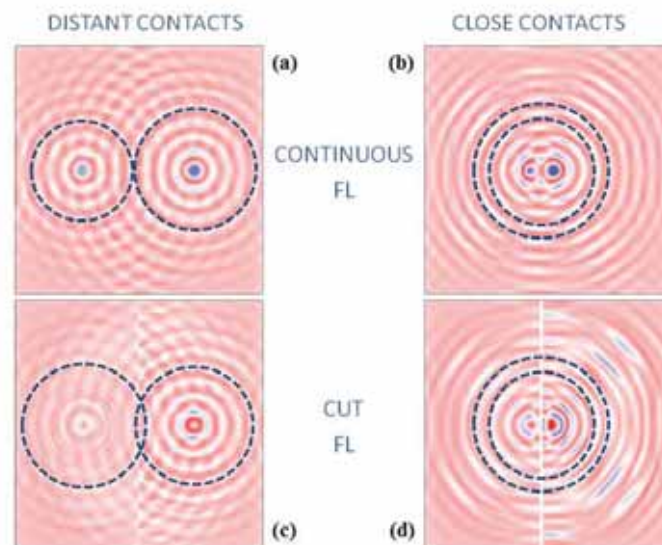


Figure 1: Spin-wave dynamics in presence of a perpendicular-to-plane external field for distant (left) and close (right) contacts. (bottom) The case of a cut between the contacts.

-
- [1] S. Kaka, et al., *Nature* **437**, 389 (2005).
 - [2] S. Bonetti, et al., *Phys. Rev. Lett.* **105**, 217204 (2010).
 - [3] A. Slavin and V. Tiberkevich, *IEEE Trans. Magn.* **45**, 1875 (2009).
 - [4] M. R. Pufall, et al., *Phys. Rev. Lett.* **97**, 087206 (2006).

Micromagnetic modelling of soliton mode in in-plane ferromagnets

A. Giordano,^a S. Komineas,^b L. Torres,^c B. Azzerboni,^a G. Finocchio^a

^a Department of Electronic Engineering, Chemistry and Industrial Engineering, University of Messina, Messina, Italy

^b Department of Mathematics, Heraklion University, Heraklion, Greece

^c Department of applied Physics, Universidad de Salamanca, Salamanca, Spain

Non uniform magnetization configurations have been found to be the underlying cause of most of the phenomena arising in the field of magnetic nanostructures in the last years. Non-uniform configurations are presented not only in the micrometer sized sensors, or open point contact spin-transfer driven nano-oscillators (STNOs), but also in spin valves (SVs) with dimensions in the range of a hundred nanometers. Injection of a direct electrical current through SVs offers the possibility to induce microwave steady-state magnetization precession by the action of the spin transfer torque. In particular, circular vortex and antivortex motion can be excited by a direct spin-polarized current as recently demonstrated both experimentally and by means of micromagnetic simulations.[1] Here, we present a complete full micromagnetic study on the vortex dipole dynamics in different kinds of sub-micrometer SVs where the current is injected through a nano-aperture of tenths of nanometers(fig1 top-left). All the features predicted by the first analytical models are reported, including vortex dipole rotation or translation depending on the shape (elliptical (fig.1a), circular(fig.1b), rectangular(fig.1c)) and size of the SV and also on the field and/or current.

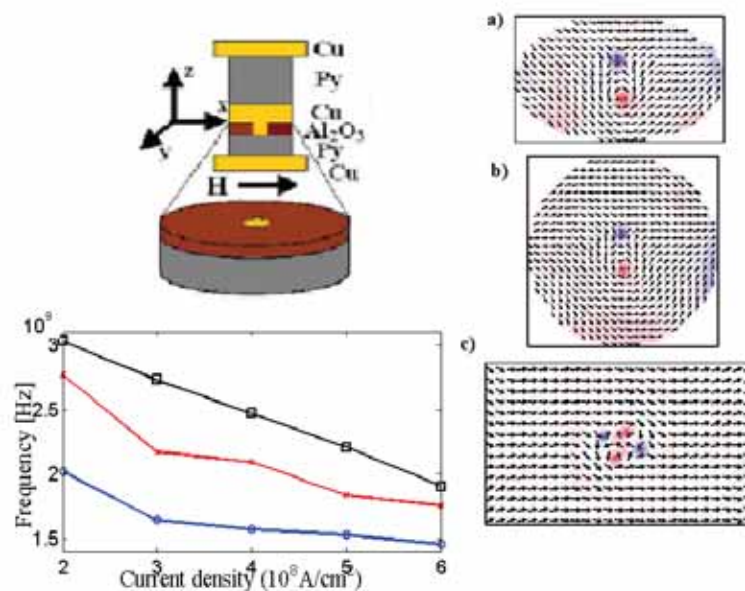


Figure 1

- [1] G. Finocchio, O. Ozatay, L. Torres, R. A. Buhrman, D. C. Ralph, and B. Azzerboni, Phys. Rev. B **78**, 174408 (2008).

A soliton mode excited by the spin-Hall effect

A. Giordano^a, M Carpentieri^b, A. Laudani^c, G. Finocchio^a

^a Department of Electronic Engineering, Chemistry and Industrial Engineering, University of Messina, Messina I-98166, Italy

^b Department of Ingegneria Elettrica e dell'Informazione, Politecnico of Bari, Bari, Italy

^c Department of Engineering, Roma Tre University, Rome, 00146 Italy.

A different way to excite self oscillations in a ferromagnet is given by the transfer torque from spin-orbit interaction. In a recent experiment[1], this modes remindful of the nonlinear self-localized spin wave-'bullet'. Our results based on micromagnetic simulations including the implementation of the spin-transfer torque from spin-Hall effect are in qualitative agreement with the experimental data and indicate that the excited mode is localized near the region where the current is injected ($J=4.25 \times 10^8 \text{ A/cm}^2$). The detail of the simulated device are displayed in Fig.1(a), it is composed by two disks with 2 μm -diameter and thickness of 8 nm (Platinum) on the bottom and 5 nm (Permalloy) on the top. On the top layer there are two pointed Au(150) electrodes separated by a 100 nm gap.

Fig. 1(b) and the inset of Fig.1(c) show the current density distribution as it is injected from the gold electrodes.

As shown in Fig. 1c, micromagnetic simulations indicate that the oscillation frequency decreases when increasing the current amplitude following a red shift behaviour, typical of bullet modes. By analyzing the spatial distribution of the magnetization, (see Fig (1d)) we find out that the auto-oscillations are localized with a periodic expansion and compression of the mode.

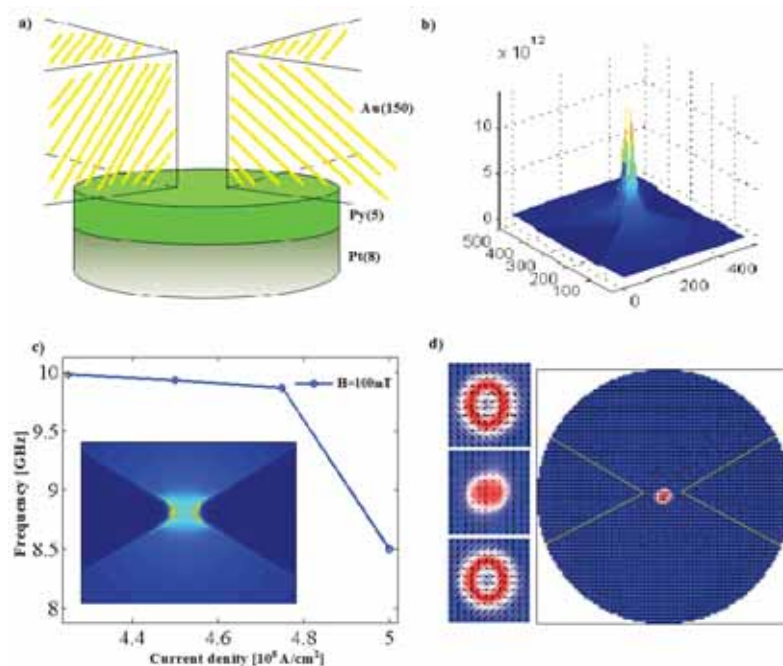


Figure 1

- [1] V. E. Demidov *et al*, Magnetic nano-oscillator driven by pure spin current, Nature Materials, Nature Materials 11,1028–1031,(2012).

Micromagnetic and magneto-transport simulation of MgO-based junctions for sensing and memory applications

Z. Hou^a, A. V. Silva^{a,b}, D. C. Leita^a, R. Ferreira^c, S. Cardoso^{a,b} and P. P. Freitas^{a,b}

^a INESC-MN and IN, Lisbon, Portugal

^b Instituto Superior Técnico (IST), Av. Rovisco Pais, 1000-029 Lisbon, Portugal

^c INL, Av. Mestre José Veiga, 4715-31 Braga, Portugal

Major advances in MgO-barrier magnetic tunnel junctions (MTJs) have made them excellent candidates for spin electronic devices, such as spin-torque magnetic random access memory [1], magnetic field sensors [2], or logic devices [3]. In this paper, we present a three-dimensional micromagnetic method using commercial Spinflow3D software, to study a complex multilayer structure towards a customization of its properties for particular applications. As a model system, the MTJ pillar consists of antiferromagnet/ferromagnet /spacer / ferromagnet /barrier/ ferromagnetic with circular and elliptical geometries. Input simulation parameters [uniaxial anisotropy (H_k), magnetic moment, exchange coupling, magnetoresistance, and resistance], were obtained from experimental data of a CoFeB/MgO stack with a Co-based synthetic-antiferromagnetic pinned layer (PL). H_k of all ferromagnetic layers is always set parallel to the external applied field (H_{ap}). However, for memories H_k is also parallel to the ellipse longest axis, thus giving a squared behavior, while for sensors H_k is perpendicular to the ellipse longest axis leading to a linear curve (Figure 1).

Figure 1(a) shows the magnetic [$M(H)$] behavior for circular and elliptical nanopillars with different dimensions suitable for memory applications. The simulation suggests a decrease in coercive field (H_c) with increase in size for ellipses with fixed aspect ratio (AR). Furthermore, a degradation of the memory capability (square shape) is visible for very small sizes, due to the decrease of the free-layer (FL) effective anisotropy. However, increasing FL H_k can prevent such behavior, which can be experimentally done by tuning the material and its thickness. Figure 1(b) shows the change saturation field (H_{sat}) for the elliptical sensor devices, following the expected trend of the demagnetizing field which will set the sensitivity of the device. Finally, a full TMR (FL and PL) curve for $20 \times 40 \text{ nm}^2$ pillar displays a linear FL behavior, and a PL with no hysteresis as no rotational anisotropy [4] was considered.

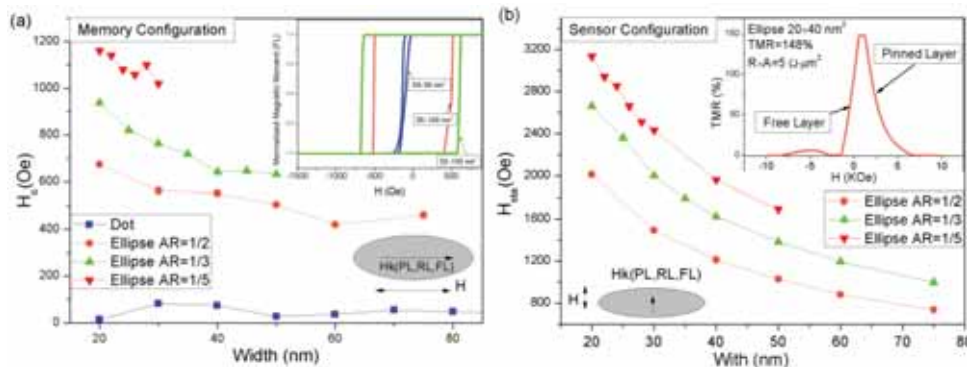


Figure 1:(a) H_c and (b) H_{sat} dependence on the width of the nanopillar. Inset of (a) compares $M(H)$ of nanopillars with width=50 nm and (b) shows TMR curve of a nanopillar with inversion of the FL and PL.

-
- [1] W. J. Gallagher and S. S. P. Parkin, IBM J. Res. Dev. 50, 5(2006).
 [2] P. P. Freitas, R. Ferreira, S. Cardoso et al J. Phys.: Condens.Matter 19, 165221 (2007).
 [3] S. Matsunaga, J. Hayakawa, S. Ikeda, K. Miura et al. , Appl. Phys. Exp. 1, 091301 (2008).
 [4] J. Olamit and K.Liu, J. Appl. Phys. 101, 09E508 (2007)

Simulation tool for studies on magnetic tunnel junction switching dynamics, including local current density

Marek Frankowski, Maciej Czapkiewicz, Witold Skowroński, Tomasz Stobiecki

Department of Electronics, AGH University of Science and Technology, al. Mickiewicza 30, 30-059 Kraków, Poland

We present Object Oriented MicroMagnetic Framework (OOMMF) [1] extension, with Landau-Lifshitz-Gilbert equation and Slonczewski's component [2,3], for the micromagnetic simulation of Magnetic Tunnel Junction (MTJ) switching dynamics. The following models of physical effects were implemented: magnetoresistance of vertical channels calculated from the local spin arrangement, local current density used to calculate in-plane and perpendicular components of spin transfer torque (STT) [4] and Oersted field caused by the junction current. Local current density distribution is calculated from a model of current perpendicular to MTJ plane, consisting of vertical channels (built of discretization cells) connected in parallel. Resistance of each channel depends on the tunnel magnetoresistance (TMR) effect. The Oersted field for each simulation stage can be calculated as a sum of contributions from Biot-Savart law using two alternative methods: from each simulation cell or each column, assuming that they are longer than thickness of simulated layers.

In this work, we analyze the simulation data of exchange biased MTJ in two modes: quasistatic (magnetic field hysteresis loop) and dynamic (current induced magnetization switching CIMS). Developed software allows analysis of all listed components separately, therefore, the contribution of each physical phenomenon in dynamic behaviour of MTJ magnetisation is discussed. Examples of CIMS hysteresis loops simulations are depicted in Fig. 1. Simulation results of the CIMS will be compared with experimental data measured in MTJ nanopillars.

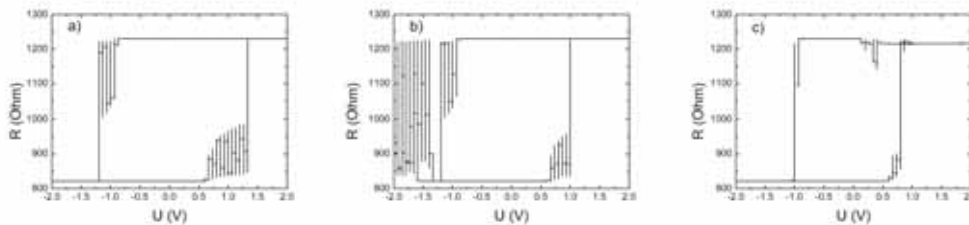


Figure 1: The example of CIMS loop simulation of CoFeB 2 nm/MgO 1 nm/CoFeB 2 nm elliptical 250×150 nm MTJ nanopillar with implemented: (a) in-plane torque alone (b) in-plane and perpendicular torque – note backhopping effect [5], (c) in-plane torque and Oersted field – note decrease of critical voltage.

Project was co-financed by the Polish Ministry of Science and Higher Education - Diamond Grant DI2011001541, statutory activity 11.11.230.016, Foundation for Polish Science MPD Programme co-financed by the EU European Regional Development Fund and Swiss Contribution by NANOSPIN PSPB-045/2010 grant.

-
- [1] Donahue M.J., Porter D.G., OOMMF User's Guide, Version 1.0, NIST report (1999).
 - [2] Berger L., Phys. Rev. B 54, 9353 (1996).
 - [3] Slonczewski J. C., J. Magn. Magn. Mater. 159, L1 (1996).
 - [4] Skowroński W., et al., arXiv:1301.7186.
 - [5] Sun J.Z., et al., JAP 105, 07D109 (2009).

Soliton dynamics driven by spin-transfer torque in perpendicular ferromagnets

V. Puliafito^a, S. Komineas^b, O. Ozatay^c, L. Torres^d, T. Heaut^e,
B. Azzarboni^a, G. Finocchio^a

^a Department of Electronic Engineering, Industrial Chemistry and Engineering,
University of Messina, Italy

^b Department of Applied Mathematics, University of Crete, Heraklion, Greece

^c Department of Physics, Bogazici University, Istanbul, Turkey

^d Department of Applied Physics, University of Salamanca, Spain

^e Institut Jean Lamour, Université De Lorraine-CNRS UMR, Nancy, France

In a ferromagnetic thin film with strong perpendicular anisotropy we refer to a magnetic bubble as a small area, delimited by a domain wall, where the spins are pointing opposite to the ferromagnetic state of the rest of the film. The complexity of the bubble structure is mostly related to the shape and the magnetic configuration of the domain wall. With this regard, the mathematical instruments that are used to describe the properties of a magnetic bubble are the topological density and the skyrmion number. They are connected one each other and the latter always turns out an integer value for magnetic bubbles. More in detail, the higher is the skyrmion number the more complex is the bubble, including the possibility to have non circular magnetic bubbles. A particular bubble structure is also referred to as bubble-antibubble pair.

Our micromagnetic analysis has demonstrated the possibility to nucleate a magnetic dynamical bubble in a confined point-contact geometry by means of the local injection of a spin-polarized current. With the addition of a large enough in-plane external field, moreover, it is possible to achieve a microwave giant-magnetoresistive signal through the persistent magnetization precession. Our results indicate that the magnetization dynamics is characterized by a rotation of the in-plane magnetization component near the bubble boundary and by expansion/compression of the dynamical bubble itself. By determining the topological density associated to our obtained magnetic configuration, we have noticed that it represents two pairs of bubble-antibubble. Last, similarly to what theoretically observed in point-contacts, we also find an hysteretic behavior in the nucleation of the bubble as a function of the applied current.

-
- [1] G. Finocchio, et al. Phys. Rev. B **78**, 174408 (2008)
 - [2] M. A. Hofer and M. Sommacal, Phys. D **241**, 890 (2012)
 - [3] S. M. Mohseni, et al., Science **339**, 1295 (2013)

Mesh size and damped edge effects in FEM simulations of spin waves

G. Venkat^a, M. Franchin^b, H. Fangohr^b and A. Prabhakar^a.

^a Dept. of Electrical Engineering, Indian Institute of Technology, Madras

^b Engineering and the Environment, University of Southampton

Micromagnetic simulations have, of late, been used for investigating spin wave dynamics in magnetic nano structures [1]. In order to simulate the wave phenomena as accurately as possible, a proper understanding of the effect of the simulation parameters is essential. This is especially true for FEM simulations, where a variety of parameters have to be optimized keeping in mind the computational resources available for the simulation.

We considered a stripe of permalloy having dimensions $400 \times 100 \times 5$ nm³. Spin waves were excited and the spin wave dispersion probed along the length of the pad using the procedure described in [1]. It was observed that the dispersion curve lost clarity at a cut-off frequency (Fig. 1(a)). This was investigated further and it is shown that the cut-off follows the analytic formulation ([1]):

$$\omega = \sqrt{\left(\omega_0 + \omega_M \lambda_{ex} k^2\right) \left(\omega_0 + \omega_M \lambda_{ex} k^2 + \omega_M \frac{1 - e^{-kc}}{kc}\right)}, \quad (1)$$

where $k = p/l_{av}$ and l_{av} is the average mesh length used. The value of $p = 1.97$ was extracted by fitting the values of f_c to (1), shown in Fig. 1(b).

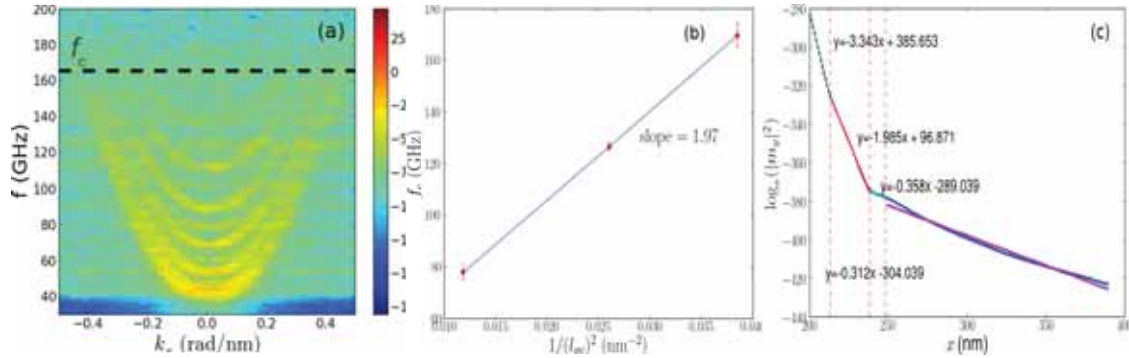


Figure 1: (a) Dispersion plot showing a cutoff at $f=f_c$, (b) dependence of f_c on $(1/l_{av})^2$ and (c) spatial variation of $\log_e(|m_y|^2)$ in the damped stub.

We reduce reflections from the boundaries by introducing a highly damped stub at the end of the stripe [2]. The damping coefficient was set as $\alpha = 1.0$ for $200 < x \leq 400$ nm. To mitigate the abruptness of the change from $\alpha = 0$ in the stripe to $\alpha = 1.0$ in the stub, we set $\alpha = 0.5$ at $x = 200$ nm. This results in a non-uniform effective damping of the spin wave amplitudes, as shown in Fig. 1(c). A stub length of about 50 nm appears sufficient to dampen the spin waves and eliminate reflections from the ends of the stripe.

-
- [1] G. Venkat et al., "Proposal for a standard micromagnetic problem: Spin wave dispersion in a magnonic waveguide", IEEE Trans. Magn., vol. 49, pp. 524-529, 2013.
 [2] G. Consolo et al., "Boundary conditions for spin-wave absorption based on different site-dependent damping functions," IEEE Trans. Magn., vol. 43, pp. 2974 – 2976, 2007.

Effective quantities and effective rules in 2D ferromagnetic antidot lattices

Roberto Zivieri^a

^aDipartimento di Fisica e Scienze della Terra, Università di Ferrara, Ferrara, Italy

The effective properties of two-dimensional (2D) square arrays of antidots are studied according to micromagnetic and analytical calculations. Micromagnetic calculations were performed by using the Hamiltonian-based Dynamical Matrix Method (HDMM) extended to periodic systems. The nanometric systems are composed by periodic square arrays of circular antidots (holes) embedded into a Permalloy ferromagnetic film. In the calculations the diameter d of the holes varies between 10 nm and 120 nm, the array periodicity is $a = 800$ nm and the thickness is $L = 22$ nm. The external field \mathbf{H} is applied along the y direction and perpendicularly to the Bloch wave vector \mathbf{K} placed along the x direction in the sample plane. From the inspection of spatial profiles of collective modes it is possible to identify a characteristic wavelength which is commensurable with the periodicity a of the system [1]. Since collective modes are mainly affected by the finite size of the holes rather than the periodicity and since the characteristic wavelength is much larger than d , the dynamics is described in terms of effective properties and an effective medium approximation is used. These properties are those that characterize the 2D arrays of antidots as metamaterials [2].

In this way, the characteristic wavelength can be regarded as an effective wavelength λ_{eff} related to the scattering from the antidots of the given spin-wave mode. Interestingly, the effective wavelength, which can be defined for each mode of the spectrum, is not necessarily equal to the Bloch wavelength and, in the geometry studied, assumes either the value a or the value $2a$. In the cases studied the ratio $d/\lambda_{\text{eff}} \ll 1$ for the whole range of Bloch wave vectors investigated. Correspondingly, also a small wave vector is introduced and important effective rules are derived. As an example, in Figure 1 the spatial profiles of two spin-wave modes localized along the horizontal rows of antidots, the $DE_{3\text{BZ}}^{\text{loc}}$ and $DE_{4\text{BZ}}^{\text{loc}}$ modes (the superscript “loc” denotes localized), respectively, at the border of the third Brillouin zone are depicted. For this couple of modes λ_{eff} is three times larger than the Bloch wavelength λ_{B} .

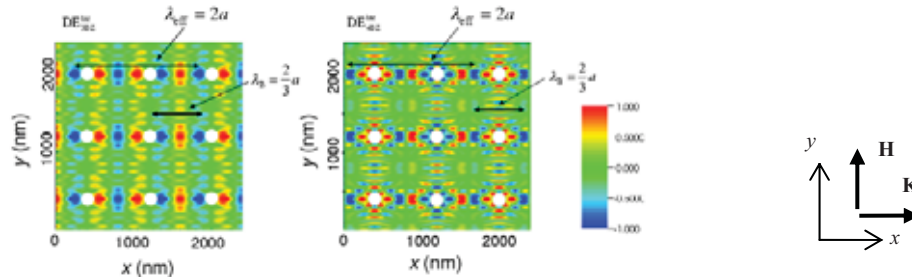


Figure 1: Calculated spatial profiles of $DE_{3\text{BZ}}^{\text{loc}}$ and $DE_{4\text{BZ}}^{\text{loc}}$ modes in 3×3 primitive cells with $a = 800$ nm and $d = 120$ nm according to DMM. λ_{eff} and λ_{B} are indicated. A reference frame with the direction of \mathbf{H} and \mathbf{K} is also shown.

[1] R. Zivieri, Proceedings of Metamaterials '2012, 6th International Congress on Advanced Electromagnetic Materials in Microwave and Optics (2012), 624-626.

[2] R. Zivieri and L. Giovannini, “Metamaterial properties of ferromagnetic antidot lattices” in press in Photonics and Nanostructures - Fundamentals and Applications.

Collective magnetic vortex dynamics in pairs, chains and two-dimensional arrays of circular nanodots

Oksana Sukhostavets^a, Julián Gonzalez^a, Konstantin Guslienکو^{a,b}

^a Dpto. Física de Materiales, Universidad del País Vasco UPV/EHU, San Sebastián, Spain

^b IKERBASQUE, The Basque Foundation for Science, Bilbao, Spain

The patterned magnetic films in the form of regular arrays of small flat particles (*e.g.*, circular dots) with different lateral arrangements (1D and 2D dot lattices) are kinds of artificial magnonic crystals. The isolated dots reveal their own discrete spin excitation spectra due to geometrical confinement. The interdot magnetostatic coupling leads to collective spin excitation spectra of the dot lattices. Such ferromagnetic dots can be in a vortex state. The vortices are characterized by in-plane curling magnetization in the main dot area and a small vortex core (~ 10 nm) with the perpendicular magnetization. If the vortex core is shifted by external magnetic field or electric current, it oscillates providing the narrow frequency linewidth and quite high power output [1]. Coupled vortex oscillators are now under intensive investigation as promising candidates for spin-torque nano-oscillators emitting microwaves or transferring the microwave signals in magnonic crystals. The need of close packing of such dots leads to the increasing influence of interdot magnetostatic interaction on their dynamics.

In the present work we perform the micromagnetic calculations of vortex dynamics in a pair of magnetic dots and in 1D and 2D dot arrays. Traditionally, the interaction is described within dipolar approximation, while high order multipole moments (quadrupolar, octupolar, etc.) can exist for finite size particles, even if they are uniformly magnetized. There is more room for appearance of such moments for strongly inhomogeneous magnetization distributions like ones in the vortex state dots. The calculations of the interaction energy for vortex dot pair [2] show that with decreasing distance higher magnetic multipole moments and their interaction indeed start playing important role. The general multipole expansion of the interaction energy between the magnetic particles of arbitrary shape is conducted and then applied to consider a typical case of the cylindrical magnetic dots in a vortex state [2]. This expansion shows a significant role of not only the dipole-dipole, but also dipole-octupole, octupole-octupole, and other high order interactions for dense dot arrays. The quadrupolar interaction is considerably small for thin dots and can be neglected. The interdot interaction leads to a frequency splitting of degenerated vortex gyrotropic modes.

We calculated the vortex gyrotropic eigenfrequencies in coupled 2D dot arrays (square and hexagonal) and 1D dot chains on the basis of the multipole decompositions of the interdot coupling integrals. The vortex eigenfrequencies do not depend on the vortex chiralities, but strongly depend on the vortex core polarizations. The vortex frequencies of isolated dots form the collective excitation bands with decreasing the interdot distances as a result of the interdot magnetostatic interactions. The group velocity for transferring the total microwave magnetic energy from one dot to another is proportional to the dot thickness. The velocity can reach 500 m/s for the typical dot sizes and closely packed (hexagonal) dot arrays or linear dot chains with alternative polarizations. The presented calculations can serve as a benchmark for interpretation of experiments (*e.g.*, Ref. [3]) on the magnetic vortex dynamics in coupled dot arrays and chains.

[1] A. Dussaux et al., *Nature Commun.* **1** (2010), 8.

[2] O. Sukhostavets et al., *Phys. Rev. B* **87** (2013), in press.

[3] A. A. Awad et al., *Appl. Phys. Lett.* **97** (2010) 132501; A. Vogel et al., *Phys. Rev. Lett.* **105** (2010), 037201.

Competition between surface effects and dipolar interactions in an assembly of nanomagnets

O. Iglesias^a, Z. Sabsabi^b, F. Vernay^b, H. Kachkachi^b

^a Dpt. de Física Fonamental and IN²UB, Universitat de Barcelona, Spain

^b Laboratoire PROMES (UPR-8521) & Université de Perpignan Via Domitia, Perpignan, France

From a fundamental point of view, it remains crucial to have an experimental access to single particle intrinsic properties of nanomagnets. Such a characterization provides information on intra-particle quantities like exchange, anisotropy but also on surface effects that become predominant at the nanoscale. Yet, most of the current experimental data are not relevant to individual particles but rather to assemblies of nanomagnets. In this case, collective effects can no longer be neglected as the magnetic properties of the assembly are a result of the interplay between intrinsic properties of the individual entities and inter-particle interactions, which must be taken into account in any theoretical interpretation of experimental data. Taking into account solely dipole-dipole interactions (DDI), we investigate the competition between intrinsic and collective effects in monodisperse assemblies of nanomagnets with oriented anisotropy in the low-density limit. We show that surface anisotropy can be incorporated in the established perturbative approach to DDI [1] within the scope of the effective one-spin problem [2], establishing a new theoretical framework to study the competition between both. In particular, we derive approximate formulas for the thermal and field dependence of the assembly magnetization. In order to establish the range of validity of the analytics results are compared to those obtained from Heisenberg Monte Carlo simulations of two models: a) macrospin ensemble with DDI and uniaxial and cubic anisotropies; b) interacting ferromagnetic particles atomistic spins. The results allow to clarify the distinct influence of surface and interaction effects on measured magnetization curves in real samples with different degrees of concentrations and particle sizes.

[1] M. Azeggagh and H. Kachkachi, Phys. Rev. B 75, 174410 (2007); Eur. Phys. J. B 44, 299 (2005).

[2] R. Yanes, O. Fesenko-Chubykalo, H. Kachkachi, D.A. Garanin, R. Evans, R. W. Chantrell, Phys. Rev. B 76, 064416 (2007).

Micromagnetic simulations of spin torque driven magnetization oscillations in magnetic tunnel junctions

Maciej Czapkiewicz, Marek Frankowski, Witold Skowroński, Tomasz Stobiecki

Department of Electronics, AGH University of Science and Technology, al. Mickiewicza 30, 30-059 Kraków, Poland

Microwave generation observed in Magnetic Tunnel Junctions (MTJ) is a well-known effect, although its spectral purity and linewidth depend strongly on external magnetic field and junction parameters: size, interlayer exchange coupling (IEC), and magnetic anisotropy. For example, as was shown in [1], additional frequency modes are observed for strong ferromagnetic IEC whereas suppression of secondary peak is related to low coupling (for thicker tunneling barrier).

We present an approach to the micromagnetic simulation of an AC voltage signal excited in MTJ nanopillars by DC current due to spin transfer torque (STT) effect and spectral analysis of this signal. Simulations are performed by means of Object Oriented MicroMagnetic Framework (OOMMF) [2] extension, with Slonczewski's component [3] added to the Landau-Lifshitz-Gilbert equation and magnetoresistive term taken into account to calculate a local current density. Excitation of MTJ free layer magnetisation due to field pulse or STT effect is depicted by modulation of junction resistivity due to simulated TMR effect. Obtained resistivity response is analyzed by means of FFT. Presented simulation tools allow to understand influence of MTJ parameters and alignment of magnetization direction on resonance frequency, peak width and additional resonant modes. For example, simulation of simple model of Pseudo-Spin Valve (PSV) junction, excited by external magnetic field pulse, show monochromatic spectrum for anti-parallel alignment of magnetizations in free and reference layer (Fig.1a) whereas additional "parasite" mode is observed in case of parallel alignment (Fig.1b), due to different configuration of demagnetizing field. Used simulation tool allow us to analyze modulation of resistivity separately for each discretization cell, therefore spatial resolved analysis of additional modes can be performed to better understand origin of line broadening or spectral impurity. More complex example of simulation analysis of STT-driven excitation of elliptical PtMn/CoFe/Ru/CoFeB/MgO/CoFeB MTJ nanopillar with tilted external magnetic field applied, is presented in Fig. 1c.

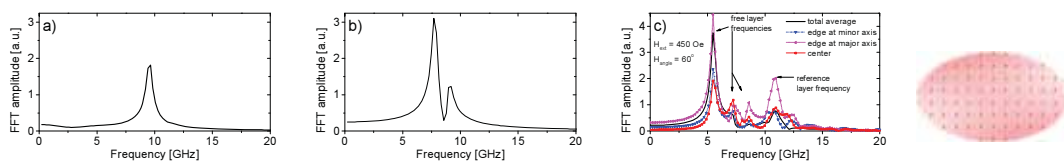


Figure 1: Spectral analysis of simulation results from: MTJ PSV nanopillar with antiparallel (a), parallel (b) magnetization alignment; average and localised response of elliptical MTJ (c).

Project was co-financed by the Polish Ministry of Science and Higher Education - Diamond Grant DI2011001541, statutory activity 11.11.230.016, Foundation for Polish Science MPD Programme co-financed by the EU European Regional Development Fund and Swiss Contribution by NANOSPIN PSPB-045/2010 grant.

[1] Skowroński W., et al., arXiv:1301.7186

[2] Donahue M.J., Porter D.G., OOMMF User's Guide, Version 1.0, NIST report (1999).

[3] Slonczewski J. C., J. Magn. Magn. Mater. 159, L1 (1996).

Computing the demagnetising tensor for finite difference micromagnetic simulations via numerical integration

Dmitri Chernyshenko^a, Hans Fangohr^a

^a Engineering and the Environment, University of Southampton, UK

In the finite difference method which is commonly used in computational micromagnetics [1], the demagnetising field is usually computed as a convolution of magnetisation with the demagnetising tensor that describes the magnetostatic field of a cuboid cell with constant magnetisation. An analytical expression for the demagnetising tensor is available [2], however at distances far from the cuboid cell, numerical evaluation of it can be very inaccurate [3].

Due to this, at distances close to the originating cell numerical packages such as OOMMF compute the demagnetising tensor using the explicit formula, but at distances far from the originating cell a formula based on an asymptotic expansion has to be used [3]. In this work, we describe a method to calculate the demagnetising field by numerical evaluation of the multidimensional integral using a sparse grid integration scheme. This method substantially improves the accuracy of computation at intermediate distances between the cells (Figure 1(a)).

This is of particular importance for GPU-based calculations where single precision floating point numbers can be the only supported type or may be preferred for performance reasons, resulting in significant loss of accuracy (Figure 1(b)).

We describe the method, show the measurements of accuracy and execution time, and make recommendations for the choice of scheme order and integrating coefficients.

We acknowledge financial support from EPSRC's DTC grant EP/G03690X/1.

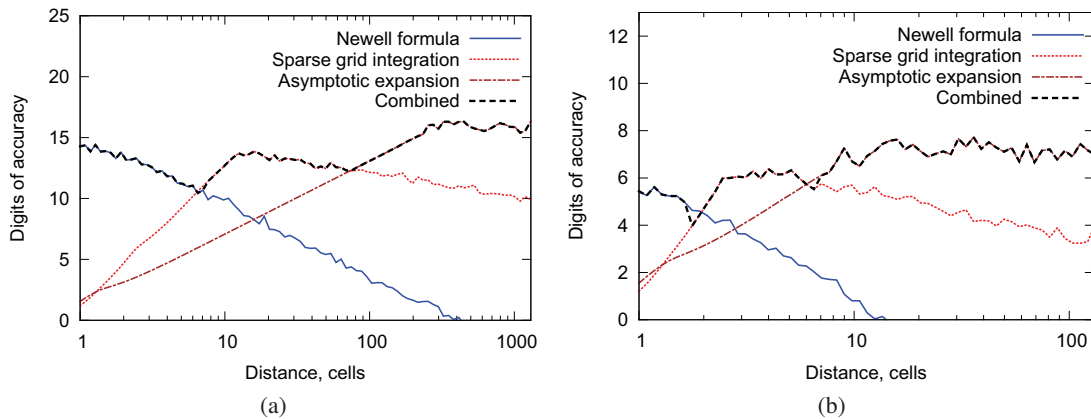


Figure 1: Number of accurate digits in the computation of the demagnetising tensor as a function of the distance between the interacting cuboids: (a) double precision, (b) single precision

-
- [1] M.J. Donahue et al., OOMMF User's Guide, Version 1.0, , Interagency Report NISTIR 6376, NIST, Gaithersburg, MD (1999), <http://math.nist.gov/oommf>
 - [2] A.J. Newell et al. Yu, X. Z. et al., A generalization of the demagnetizing tensor for nonuniform magnetization, *Journal of Geophysical Research* **98** 9551-9555 (1993)
 - [3] M.J. Donahue, Accurate computation of the demagnetization tensor, 6th International Symposium on Hysteresis Modeling and Micromagnetics HMM-2007, Naples, Italy (2007)

Micromagnetic simulations of ferromagnetic resonance in patterned permalloy films and stripes

G. R. Aranda^a, G. N. Kakazei^{b,c}, J. González^a, K. Y. Guslienko^{a,d}

^a Dpto. Física de Materiales, Universidad del País Vasco (UPV/EHU), San Sebastian, Spain

^b IFIMUP-IN (Institute for Nanoscience and Nanotechnology) and Departamento de Física, Universidade do Porto, Porto, Portugal

^c Institute of Magnetism, National Academy of Sciences of Ukraine, Kiev, Ukraine

^d IKERBASQUE, The Basque Foundation for Science, Bilbao, Spain

We performed real time micromagnetic simulations of ferromagnetic resonance (excitation frequency being 9.85 GHz) in different patterned permalloy structures. Applying an in-plane dc field and an ac field perpendicular to it, we identified the fields with maximum response of the dynamical magnetization [1] (resonance fields) for different in plane orientations of the dc field. The simulated samples were infinite permalloy stripes of 20 nm thick and 250 nm width, interacting and non interacting, and striped - patterned 20 nm thick films, with infinitely long rectangular structures with thick and thin zones of 250 nm width and period of 500 nm, and different thicknesses of the patterning ($t=5$ nm, 10 nm, 15 nm), see fig. 1. We used OOMMF code for simulations, with the 1D and 2D extensions for periodical conditions in the case of materials with one or two infinite dimensions [2], and extracted the dynamical magnetization profiles related to the various resonance peaks.



Figure 1: Patterned permalloy film lateral cross-section.

The resonance field values for non-interacting infinite stripes with different direction of the applied dc field can be fitted using a modified Kittel formula. In this formula, resonance field value changes with the angle of application of the saturating field because of the demagnetizing field variation induced by the change of orientation of the static magnetization. The dynamical magnetization is not uniform. For thin stripes and small angles of the dc applied field with the stripe axis, the dynamical magnetization has its maximum amplitude in the central zone of the stripe. For angles of the applied field bigger than 80° , we find the so called edge localized modes, in which the zones of maximum amplitude of the dynamical magnetization are located at the stripe edges. However, for thicker samples, both peaks are merged into one peak with maximum dynamical magnetization in an intermediate zone (neither centre nor edge of the stripe). The effect of magnetostatic interaction between stripes on the resonance field value changes depending on the peak eigenmode distribution. Patterning increases the number of excited resonance peaks (all of them with smaller amplitude). Every new peak in this case can be associated to a zone of different internal field because of the demagnetizing effects.

[1] S. Jung, J. B. Ketterson, and V. Chandrasekhar, Phys. Rev. B **66** (2002), 132405.

[2] **OOMMF User's Guide, Version 1.0**, M.J. Donahue and D.G. Porter, Interagency Report NISTIR **6376**; K.M. Lebecki, M.J. Donahue, M.W. Gutowski, J. Phys. D. 41 (2008), 175005; <http://math.nist.gov/oommf/contrib/oxsext/>

Micromagnetic simulation of exchange coupled ferri-/ferromagnetic heterostructures

Harald Oezelt^a, Thomas Schrefl^a, Christian Schubert^b, Manfred Albrecht^b, Laura Heyderman^c

^a Industrial Simulation, St. Poelten University of Applied Sciences, St. Poelten, Austria

^b Institute of Physics, Chemnitz University of Technology, Chemnitz, German

^c Laboratory for Micro- and Nanotechnology, Paul Scherrer Institute, Villigen PSI, Switzerland

In order to improve data density of magnetic storage devices new nano-scale exchange-coupled composite (ECC) magnets are investigated by computing their hysteresis loops. The ECC media is modelled as a bilayer consisting of a ferrimagnetic Fe-Tb phase and a ferromagnetic Co/Pt multilayer (see Fig. 1a). While the finite element simulation of ferromagnets is a common task, ferrimagnets have so far only been simulated on their own and in two dimensions, for the application in magneto-optical recording [1].

Ferrimagnets have different sublattices with unequal opposing magnetic moments hence the mathematical model has to be adapted. By assuming that the sublattices of Fe-Tb alloy are strongly coupled antiparallel, the usual Landau-Lifshitz-Gilbert equation with the effective intrinsic properties and damping values can be used [1]. The effective values can be taken from preliminary experimental work [2]. With this method the effective net-magnetization of the ferrimagnetic layer can be computed. In our experiment we use a continuous CoPt ferromagnetic layer, which is exchange-coupled to an amorphous ferrimagnet. Following Mansuripur [1] we model the amorphous ferrimagnet by a set of patches, whereby each patch has its own anisotropy axis (see Fig. 1a). The coupling energy between the layers is given by

$$E_{ex} = J_{int} \sum S_i S_j \approx \frac{J_{int} S^2}{a^2} \int u_i u_j dF = \frac{A_{int}}{a} \int u_i u_j dF . \quad (1)$$

In (1) the transition from a discrete spin model with spins $S_{i,j}$ to a continuous description with a unit magnetization vector u is made. To model the roughness of the interface between the two phases a variation of the exchange constant A_{int} is implemented throughout the contact surface. Fig. 1b shows the computed hysteresis for different exchange coupling strength and the experimentally measured hysteresis loop of the Fe-Tb/CoPt bilayer.

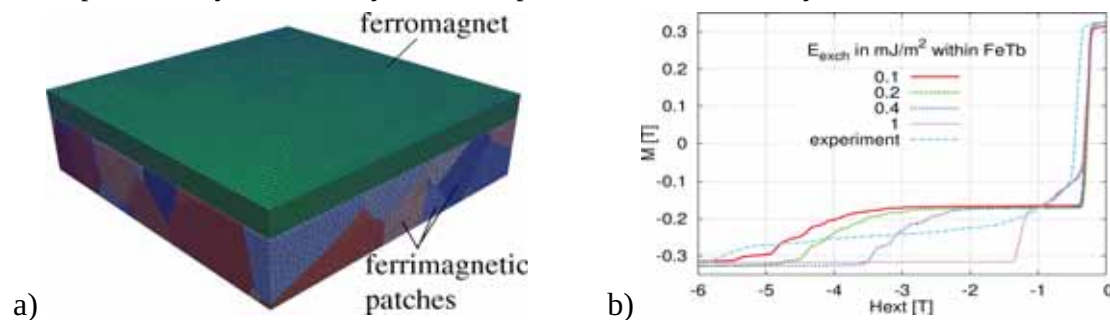


Figure 1: a) Geometric model and b) the hysteresis of different ECC models.

We gratefully acknowledge the financial support of Austrian Science Fund FWF (I821).

[1] M. Mansuripur, (1995). The physical principles of magneto-optical recording, Cambridge University Press. <http://dx.doi.org/10.1017/CBO9780511622472>.

[2] C. Schubert et al., Phys. Rev. B **87** 5 (2013), 054415.

Simulation of nanocomposites: new micromagnetic methodology

Sergey Erokhin^a, Dmitry Berkov^a, Nataliya Gorn^a, Andreas Michels^b

^a Innovent Technology Development, Jena, Germany

^b Laboratory for the Physics of Advanced Materials, University of Luxembourg, Luxembourg

We developed a new micromagnetic methodology for numerical simulations of magnetic nanocomposites, which allows to calculate the magnetization distribution of a nanocrystalline material, corresponding small-angle neutron scattering (SANS) cross-section and to model hysteresis loop.

The objects of our interest are nanocomposites, where both phases are ferromagnetic (Nanoperm, NdFeB). For example, composites of the Nanoperm type [1] consist of the iron-based crystallites with typical size of 10 nm, embedded in an amorphous soft magnetic matrix. These alloys with very high permeability show the unusual angular anisotropy in the SANS cross-section. In order to prove that this phenomenon can be attributed to the magnetic structure, it is necessary to perform numerical simulations on the micromagnetic level.

The micromagnetic modelling in this area is rare, because finite difference and finite elements approaches are not really suitable for large-scale simulations of nanocomposites.

The main components of our new method are:

- (a) Generation of the mesh consisting of polyhedral finite elements, using the model of interacting spheres with short-ranged potential. This procedure assures that the shape of each polyhedron is close to spherical and that their spatial arrangement is random.
- (b) Calculation of the magnetodipolar energy in the dipolar approximation. This approximation is exact only for spherical particles, but in our case, where the shape of polyhedra is close to spherical, its accuracy is sufficient.
- (c) The exchange interaction is computed using the standard Heisenberg form, where the exchange constant is proportional to the volumes of neighbouring finite elements and the spacing between their centres.

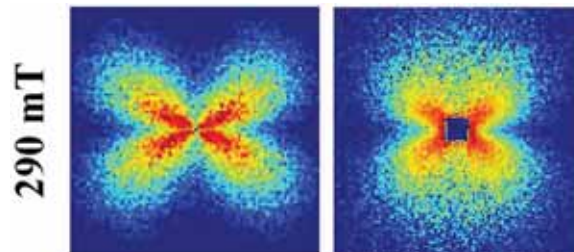


Figure 1: SANS cross-sections of Nanoperm calculated by our modeling (left) and obtained experimentally (right).

SANS cross-sections (Fig. 1), calculated from the Fourier components of simulated magnetization distributions [1], reproduce very well the experimentally measured data. Also we have found that magnetodipolar interaction is of special importance for all bulk nanomagnets with spatially fluctuating magnetic parameters and in the case of Nanoperm is responsible for unusual angular pattern in the SANS cross section.

Support by DFG under the project BE 2464/10-1 is acknowledged.

[1] A. Michels, C. Vecchini, O. Moze, K. Suzuki, P.K. Pranzas, J. Kohlbrecher and J. Weissmüller, Phys. Rev. B, 74, 134407 (2006)

Magnetization dynamics induced by spin transfer effects: Self-consistent finite element approach

Magali Sturma^{a,b}, Daria Gusakova^a, Jean-Christophe Toussaint^b, François Alouges^c

^a SPINTEC, 17 rue des Martyrs, 38054 Grenoble, France

^b Institut Neel, 25 rue des Martyrs, BP 166, 38042 Grenoble cedex 9, France

^c CMAP –Ecole Polytechnique, Route de Saclay, 91128 Palaiseau, France

Usually the spin transfer effects are introduced in micromagnetism by means of two local contributions: Slonczewski and “field-like” terms in the case of magneto-resistive stacks, or adiabatic and non-adiabatic terms when describing the domain wall motion. Most of the theoretical models are applied for simple geometries with homogeneous current flows. In order to design realistic spintronic devices (e.g. RF oscillators, magnetic memories) with strong current and magnetization gradients imposed by system properties or geometry, the additional length scales as well as self-consistent interaction between transport and dynamics equations should be considered.

We present the advanced model which couples Landau-Lifshitz-Gilbert equation (LLG) for magnetization dynamics with the diffusive transport equations introduced in [1]. At each time step the local torque is determined from the spin accumulation distribution and then injected into the LLG equation. In this self-consistent treatment all non-linear diffusive terms are taken into account [2]. The implementation was realized as an add-on module to our micromagnetic finite element (FE) software FEELGOOD [3] which faithfully describes any complex geometry (nanoconstrictions, circular cross-sections etc...). This code deals with vector test functions belonging to the tangent plane to the local magnetization. Thus, it overcomes the problem of the magnetization renormalisation proper to most existing FE software and treats correctly the magnetization dynamics for realistic damping factors. Furthermore, stability and convergence of the integration scheme ensure the reliability of our code [4].

We present the comparative study between simplified and coupled models by choosing for a start a moving domain wall under the action of a homogeneous or a non-homogeneous spin-polarized current. We show that spin diffusion terms are not negligible contrary to the hypotheses made in the basic model [1]. We discuss how the accounting of mutual interaction between the local magnetization and the electron spins in a self-consistent way affects the wall motion and its velocity. The described self-consistent model applied to the single ferromagnetic material is the first step towards the understanding of the behavior of more complex structures comprising several magnetic and non-magnetic layers (e.g. spin transfer nano-oscillators, magnetic memories).

[1] S. Zhang, P.M. Levy, A. Fert, Phys. Rev. Lett. **88**, 236601 (2002).

[2] D. Claudio-Gonzalez, A. Thiaville, Jacques Miltat, Phys. Rev. Lett. **108**, 227208 (2012).

[3] F. Alouges, E. Kritisikis, J.C. Toussaint, Physica B **407**, 1345 (2012).

[4] F. Alouges, E. Kritisikis, J. Steiner, J.C. Toussaint, arxiv:1206.0997 (2012).

A Preisach type model for temperature driven hysteresis memory erasure in shape memory materials

Jana Kopfová^a, Pavel Krejčí^b

^a Mathematical Institute of the Silesian University, Opava, Czech Republic

^b Institute of Mathematics, Academy of Sciences of the Czech Republic, Praha, Czech Republic

Classical models for shape memory materials ([1, 2, 5]) can be alternatively described by a constitutive equation involving hysteresis operators. The best known example is the stress-strain law in the Souza-Auricchio model ([1, 5]), which is very popular in the engineering community for its simplicity and a small number of model parameters, which can easily be identified. The ATL model of [2] is more complex and involves a nonlinear modification of the play operator.

A mathematical analysis of the Souza-Auricchio model carried out in [4] shows that even in the quasistatic case, the energy balance is ill-posed and a regularization is necessary for the thermodynamic consistency. The problem of well-posedness in the fully dynamical case (momentum and energy balance) is completely open.

To account for the memory erasure during the austenite-martensite phase transition, we propose here a different regularization inspired by the Preisach model.

We will show, ([3]) that the model is thermodynamically consistent and we will discuss its properties and applications.

[1] F. Auricchio and L. Petrini, A three-dimensional model describing stress-temperature induced solid phase transformations. Part II: thermomechanical coupling and hybrid composite applications," *Internat. J. Numer. Methods Engrg.*, vol. 61, 716-737, 2004.

[2] F. Auricchio, R.L. Taylor, and J. Lubliner, Shape-memory alloys: macromodelling and numerical simulations of the superelastic behavior, *Comput. Methods Appl. Mech. Engrg.*, vol. 146, 281-312, 1997.

[3] J. Kopfová and P. Krejčí, A thermodynamically consistent temperature-dependent Preisach hysteresis model, *Continuum Mechanics and Thermodynamics*, Volume 23, Number 2, 125–137, 2011.

[4] P. Krejčí and U. Stefanelli, Existence and nonexistence for the full thermomechanical Souza-Auricchio model of shape memory wires, *Mathematics and Mechanics of Solids* 16, 349-365, 2011.

[5] A. C. Souza, E. N. Mamiya, and N. Zouain, Three-dimensional model for solids undergoing stress-induced phase transformations, *European J. Mech. A Solids*, vol. 17, 789-806, 1998.

Modelling mixed clockwise and counter-clockwise hysteresis in multi-layer materials by using a generalized Jiles-Atherton model

Petru Andrei^a, Mohit Mehta^a, Mihai Dimian^b

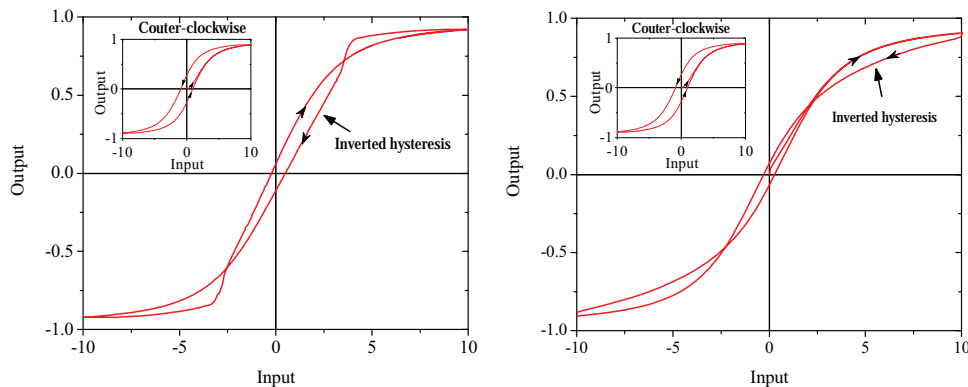
^a Florida State University, Tallahassee, United States of America

^b Stefan cel Mare University, Suceava, Romania

Several recent investigations of magnetization reversals in multilayers and superlattices with antiferromagnetic interlayer coupling and positive exchange bias have proved a mixed hysteretic behaviour of counter-clockwise and clockwise loops [1-3]. Due to the physical inconsistency of clockwise hysteresis in homogeneous magnetic materials, the hysteresis modelling of such behaviour has been ignored for a long time. However this anomalous behaviour is thermodynamically possible in magnetic multi-layers as long as the overall work done in the mixed hysteresis cycle is positive. In addition, the clockwise loops are quite often exhibited by hysteretic systems from other areas, such as elasto-plasticity and pharmacology, which led to the development of several naturally clockwise models, such as Bouc-Wen [4].

By using an inverting technique for the classical (counter-clockwise) Jiles-Atherton model [5], we have recently developed a clockwise model that describes the input-output relation in the form of a first-order differential equation [6]. Here, a unitary framework for studying mixed clockwise and counter-clockwise hysteresis in magnetic multi-layer materials is proposed by using a weighted superposition of classical and inverted Jiles-Atherton (JA) models. The small number of parameters and relatively simple numerical implementation and identification procedures make this generalized JA model very appealing to describe these unconventional magnetization reversals when compared to other approaches that could be developed, as will be discussed in the full paper.

Fig. 1 shows representative examples of mixed clockwise and counter-clockwise hysteresis JA model for different superposition weights with the following parameters $a = 1$, $k = 1$, $c = 0$, $\alpha = 0$, and $y_{sat} = 1$. The significance of these parameters is known from the classical counter-clockwise JA hysteresis (which is shown in the inset of the figures).



- [1] M. Ziese, I. Vrejoiu, D. Hesse, *Appl. Phys. Lett.* **97** (2010), 052504.
- [2] S. Jammalamadaka, J. Vanacken, V. Moshchalkov, *EuroPhys. Lett.* **98**, (2012) 17002.
- [3] J. Park, D. R. Lee, Y. Choi, *et al.*, *Appl. Phys. Lett.* **95** (2009), 102504.
- [4] M. Ismail, F. Ikhouane, J. Rodellar, *Arch. Comput. Methods Eng.* **16** (2009), 161–188.
- [5] D. C. Jiles, D. L. Atherton, *J. Appl. Phys.* **55**, (1984) 2115-2120.
- [6] P. Andrei, M. Dimian, *IEEE Trans. Magn.* (2013) in press.
- [7] I.D. Mayergoyz, P. Andrei, *J. Appl. Phys.* **91** (2002), 7645-7647.

Memory characteristics of hysteresis and creep in multi-layer piezoelectric actuators: an experimental analysis

Matteo Biggio^a, Mark Butcher^b, Alessandro Giustiniani^{b,c}, Alessandro Masi^b,
Marco Storace^a

^a DITEN, University of Genoa, Via Opera Pia 11A, I-16145, Genova, Italy

^b Engineering Department, CERN, Geneva, Switzerland

^c Dept. of Engineering, University of Sannio, Piazza Roma, 21 I-82100 Benevento, Italy.

Piezoelectric actuators (PEA's) are widely employed in micro-positioning applications because of their high stiffness and resolution [1]. Unfortunately, they usually display undesirable properties such as hysteretic and creep nonlinearities that can result in loss of positioning precision and repeatability. In order to reduce these undesired effects, feed-forward compensation approaches are a very attractive choice, because of their sensorless nature; however, these techniques require accurate modelling of the PEA dynamical behaviour, including its hysteresis and creep. While there is an extensive literature on mathematical models and memory characteristics of rate-independent hysteresis, this is not so for creep. Several phenomenological models of varying complexities have been proposed [2,3], but the relationship, if any, between the hysteresis and creep memory structures has never been fully characterized experimentally nor explicitly taken into account in the models.

In this paper, we give an experimental characterization of the creep and hysteresis characteristics of multi-layer PEA, taking into account the relationships in terms of memory structure. We measure the creep characteristics of the actuator on the major hysteresis loop, on several minor loops, and on several first-order reversal curves (see Figure 1 for an example), fitting the creep response with the well-known log-t type time dependence [3]. We determine experimentally to what extent the hysteresis and creep dynamics satisfy the cancellation and congruence properties, and hence they can both be captured by Preisach-like models. We finally give experimental insights on the range of validity and/or adequacy of several well-known phenomenological models of creep, including simple linear models [1] and models with independent hysteresis and creep memory structures [2].

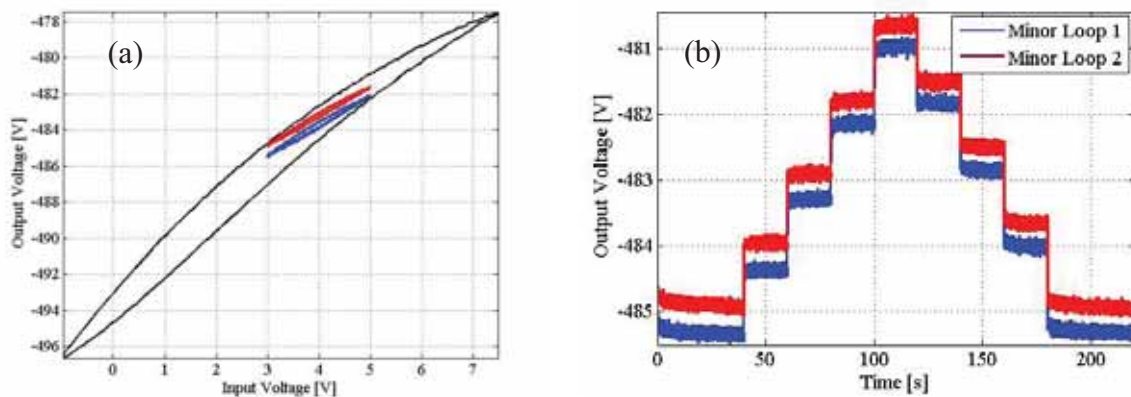


Figure 1: (a) Major hysteresis loop (black) and two minor loops (red and blue). (b) Creep dynamics on the minor loops shown in panel (a), obtained by driving the PEA with a piecewise constant signal.

- [1] S. Devasia et al, IEEE Trans. Ctrl. Sys. Tech., **15**, (2007), 802-823.
- [2] P. Krejci, K. Kuhnen, IEEE Proc. Ctrl. Theory and App., **148**, (2001), 185-192.
- [3] R. Changhai, S. Lining, Sensors and Actuators A: Physical, **122**, (2005), 1439.

Controlling the controller: differential equations with hysteresis and delay

Eyal Ron

Free University of Berlin, Germany

Our talk revolves around parabolic equations with hysteresis and delay terms on the boundary. In particular, we will focus on stability analysis of periodic solutions of such equations.

A thermal control model consisting of a parabolic equation with hysteresis on the boundary was first suggested by Glashoff and Sprekels [1,2] in the beginning of the eighties. An important topic for this model was periodic solutions. Gurevich and Tikhomirov [3] recently showed the existence of both stable and unstable periodic solutions. Their result naturally raises the question of whether it is possible to change the stability properties of such solutions.

We use the well-known Pyragas control to change the stability of periodic solutions of the thermal control model. Using this method, one adds an additional delay term to the boundary without destroying the known periodic solution. This results in a parabolic equation with both hysteresis and delay terms on the boundary. We reduce the stability analysis of periodic solutions of such equations to the analysis of a kernel of a finite-dimensional operator. In addition, we demonstrate specific cases in which the Pyragas control indeed changes the stability of periodic solutions.

-
- [1] K. Glashoff and J. Sprekels, *SIAM J. Math. Anal.*, **12(3)** (1981), 477–486.
 - [2] K. Glashoff and J. Sprekels, *J. Integral Equations*, **4(2)** (1982), 95–112.
 - [3] P. Gurevich and S. Tikhomirov, *J. Dynam. Differential Equations*, **23(4)** (2011), 923–960.

Genetic Algorithm Identification of a H-moving Vector Hysteresis Model

Ermanno Cardelli, Antonio Faba

Department of Industrial Engineering, Perugia University, Perugia, ITALY, ecar@unipg.it
Center for Electric and Magnetic Applied Research, University of Perugia, Perugia, Italy

Recently a vector hysteresis model based on a generalization of the Preisach theory has been presented [1]. This model uses a mathematical operator called vector hysteron which is able to reproduce physical phenomena with vector hysteresis. This model can be used for the prediction of magnetization in magnetic materials. One of the possible applications is the simulation of magnetic steels used in electrical machines. In general, the model parameters need to be identified by measurements. In this paper we apply a genetic algorithm GA for the numerical identification of the parameters of the model of a not oriented grain Si-Fe magnetic steel, typical material used for the manufacturing of rotating electrical machines. The vector model computes the total magnetization state of a magnetic material as the sum of the contribution of vector hysterons distributed in the applied magnetic field plane, described in a Cartesian coordinate system. Each hysteron is defined by its shape, or critical curve, and its position in the \mathbf{H} -plane. The moving model concept was introduced to remove the congruency property of the classical Preisach model [2], because many experiments show that actual hysteresis phenomena in magnetic materials often don't obey this property. In general the moving model concerns the variation of the distribution function P in function of the magnetization. This approach is physically reasonable but can be almost difficult to apply in practice, because the value of the magnetization at a given applied field is unknown apriori.

We present here an attempt to solve this problem for the case investigated, namely \mathbf{H} -moving model where the distribution function of the hysteron is less general and not directly magnetization dependent, but it is only function of the angle of the applied magnetic field.

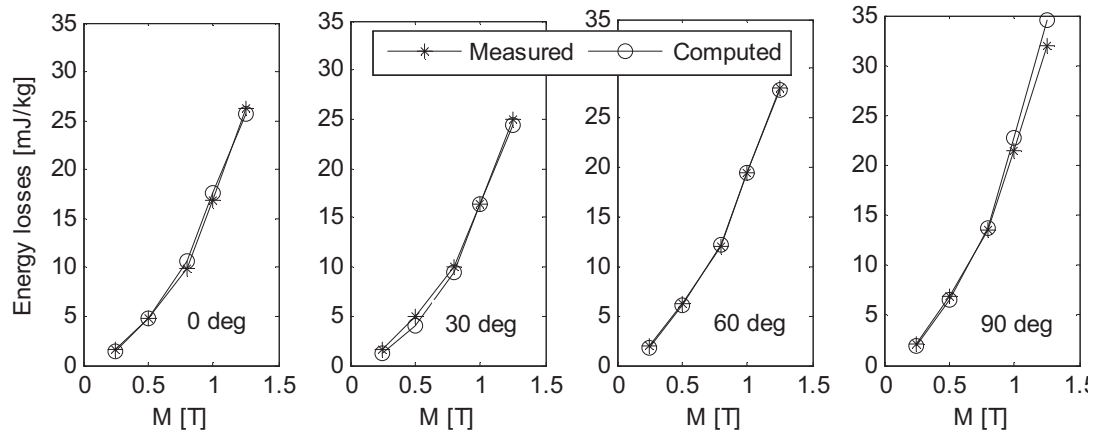


Figure 1: Comparison between the hysteresis losses measured experimentally on a FeSi NOG steel and computed using the \mathbf{H} -moving model proposed. The hysteresis loops are scalar along different directions respect the rolling one.

-
- [1] E. Cardelli, E. Della Torre, A. Faba, IEEE Trans. on Magn., Vol. 46, n. 12, (2010).
 - [2] E. Della Torre, **Magnetic Hysteresis**, Wiley-IEEE Press, (2000).

Thermal Hysteresis of the Virgin Curve for a Heusler Alloy

Edward Della Torre, Virgil Provenzano and Lawrence H. Bennett
George Washington University, Washington, D.C., USA

The giant magnetocaloric effect in certain Heusler alloys is caused by a critical change in the lattice parameter, which permits a change in the sign of the exchange energy. We report here on the factors governing this phenomenon. Thermal hysteresis occurs near a given temperature at which the two states are stable, a low-magnetization state and a high magnetization state. The transformation from one state to the other is asymmetrical and can be field induced in one direction only. Under the same conditions, the material can be in different states at the same temperature depending upon whether it was cooled down or heated up to that temperature. When the low-magnetization state transforms to the high-magnetization state, some adjacent spins must reverse. This near-neighbor exchange reversal is the principal loss mechanism in these materials.

If a temperature above the Curie temperature is applied, the material will be demagnetized. When the temperature is lowered to the Kittel temperature, the majority of the spins will be ferromagnetically coupled. If the temperature is lowered well below the Kittel temperature and then raised to the Kittel temperature, the majority of the spins will be ferrimagnetically coupled. This can be tested by applying an increasing magnetic field to the two cases. It is seen that the state that has a majority of ferromagnetically coupled spins will have a smaller number of conversions than the other state, however, they will both achieve the same magnetization in high fields and will behave the same afterwards.

Figure 1 shows the magnetization behavior of the virgin curve starting from zero field, saturating the material and then returning to zero. It is seen for the specimen that approached the Kittel temperature from below, **the lowest curve**, the ascending magnetization loop lies well below the other. However, that when the Kittel temperature was approached from above, **the middle curve**, the ascending curve lies well above it. The descending curves for all cases starting from saturation are identical. These curves were fitted to the model described in a previous paper¹. On the basis of that model, we conclude that about 1/3 of the spins is ferromagnetically coupled when the material approaches the Kittel from below and more than 2/3 when it is approached from above, i.e., there is thermal hysteresis in the virgin curve.

This paper explores the factors that affect the magnetization behavior of the material. It is seen that the two ascending curves describe the limits of the magnetization process. Intermediate behavior is possible by generating first order reversal curves by starting with the material in the state corresponding to the lowest curve and field inducing a reversal of some of the spins from the ferrimagnetic state to the ferromagnetic state. It is noted that this process is irreversible.

References

1.V. Provenzano, E. Della Torre, L.H. Bennett, "Magnetizing processes in Heusler alloys," *IEEE Trans. Magn.* (2013) in press.

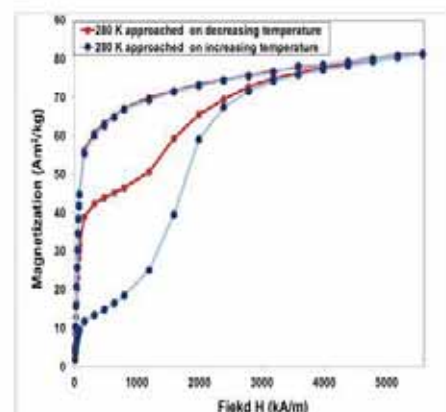


Fig. 1. Magnetizing curves for a Heusler alloy at the Kittel temperature.

Magnetostriction measurements of high strength steel under the influence of bi-axial magnetic fields

Christopher Burgy^{a,b}, Marilyn Wun-Fogle^a, J.B. Restorff^a, Edward Della Torre^b

^a Naval Surface Warfare Center Carderock Division, West Bethesda, MD, USA

^b The George Washington University, Washington, DC, USA

A detailed knowledge of a material's microscopic texture is required in order to produce a realistic model of the magnetization process under applied fields. Previous studies on the magnetostriction in high strength steels have ignored the internal anisotropies due to previous material handling. The process of cold-rolling steels leave magnetic domains stretched in the direction of rolling, allowing for an additional easy axis to exist along with the six crystalline axes found in body-centric-cubic lattices [1]. We have devised an experiment to interrogate the magnetic domains of a sample in order to characterize their sizes, shapes, and distributions for use as future Preisach modelling parameters.

The samples tested were the same cylinders used in our previous paper, which determined magnetostriction characteristics of high strength steel with respect to rolling direction [2]. A sample holder was constructed which would position a steel rod, which was wrapped in longitudinal field induction and pickup coils, between the pole faces of a large transverse field coil. Strain gauges were attached to each side of the rod as outlined in [3].

During the experiment, a constant transverse field (H_t) was applied to the sample, while simultaneously oscillating the longitudinal field. The major B-H loops are shown for varying transverse fields for one of the steel rods in fig. 1. These measurements were repeated for rods in each of the three rolling directions outlined in [2].

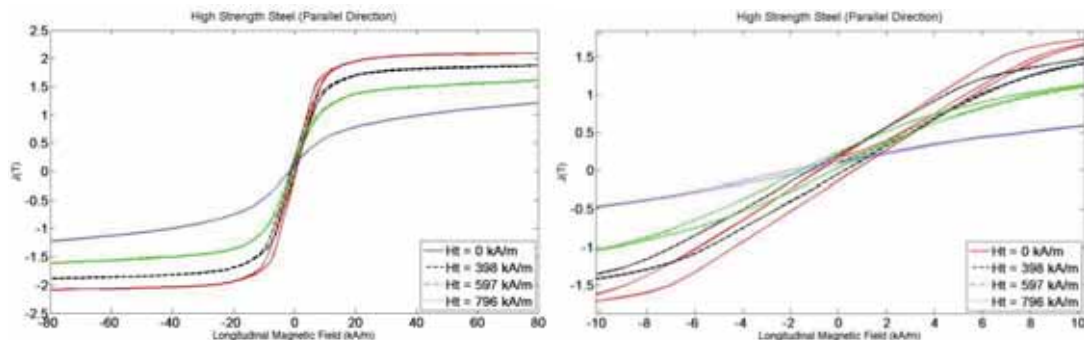


Figure 1: Left: Major B-H for values of constantly-applied transverse field (H_t). Right: B-H for values of constantly-applied transverse field (H_t) zoomed in

The samples measured show interesting relationships between the transverse fields applied and the subsequent change in major loops. Increasing the transverse field decreased the saturation magnetization (M_s). Future efforts will focus on identifying the distributions and shapes of magnetic domains which will dictate these behaviours in a Preisach model.

-
- [1] R. M. Bozorth, Ferromagnetism. Piscataway, NJ: IEEE, 1993. 638. Print.
 - [2] C. D. Burgy, E. Della Torre, M. Wun-Fogle, J. B. Restorff, IEEE Trans. Magn. **48** (2012), 3088-3091.
 - [3] M. Wun-Fogle, J. B. Restorff, J. M. Cuseo, I.J Garshelis and S. Bitar, IEEE Trans. Magn. **45** (2010), 4112-4115.

Modelling of hysteresis losses in assemblies of magnetic nanoparticles for hyperthermia cancer treatment

David Serantes^{a,b}, Oksana Chubykalo-Fesenko^a, Daniel Baldomir^b and Carlos Martínez-Boubeta^c

^a Instituto de Ciencia de Materiales de Madrid, CSIC, Cantoblanco, ES-28049 Madrid, Spain

^b Instituto de Investigaciones Tecnológicas, Universidade de Santiago de Compostela, 15782 Santiago de Compostela, Spain

^c Departament d'Electrònica and IN2UB, Universitat de Barcelona, 08028 Barcelona, Spain

Magnetic-hyperthermia cancer treatment uses the heat generated by magnetic nanoparticles under the application of an external magnetic field to cause the death of malignant cells. From the clinical perspective it is desirable to achieve a rapid and controlled temperature rise by using the smallest possible dosage of magnetic entities. Nanoparticle-assembling constitutes a promising route for magnetic hyperthermia based on the possibility to enhance the effective anisotropy of the array (and thus the hysteresis losses, HL) by tuning the interparticle dipolar coupling. However, technical difficulties in practical induction devices to achieve large magnetic field amplitudes and high frequencies over large volumes (as human bodies), impose the use of relatively low values of H_{\max} . For the clinical usage of nanoparticle assemblies in hyperthermia treatment it is therefore crucial to know the dependence of the HL on H_{\max} as a function of the characteristics of the magnetic system.

Here, we present a Monte Carlo modelling of the hyperthermia properties of arrays of nanomagnets (chains, rings, hexagons, and cubes). Our aim is to address how the geometry and size of the array, together with the orientation of the anisotropy of the particles, determine the heating properties of the system as a function of H_{\max} . We have found that i) the higher hyperthermia output is that of the chain-like arrangement; ii) there is a particular chain length that optimizes the heating efficiency; iii) it is possible to correlate the chain length and anisotropy of the particles with the amplitude of the applied magnetic field in order to have optimized hyperthermia properties. We believe that this knowledge may be very useful for improving the efficiency of magnetic hyperthermia.

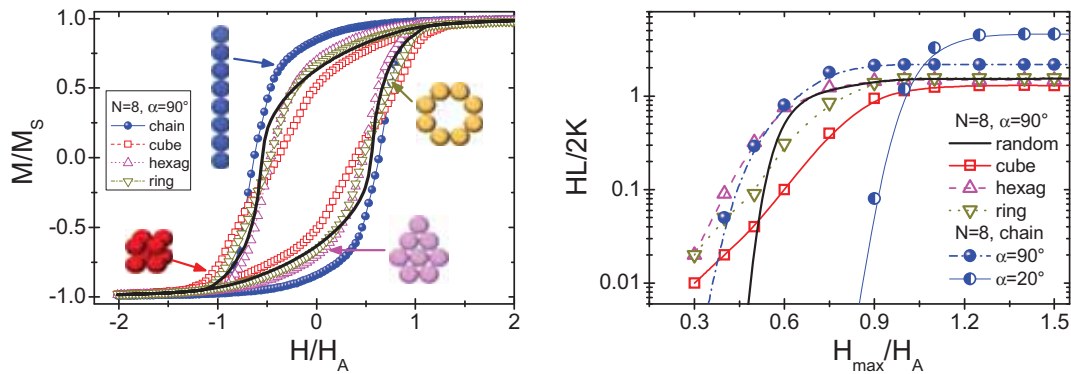


Figure 1: Left panel: $M(H)$ curves corresponding to different spatial arrangements (chain, ring, hexagon, and cube) of the same amount of particles, $N = 8$. Right panel: HL vs. H_{\max} data corresponding to cases displayed in the left panel; in addition it is also shown how the alignment of the easy-axes of the particles enhances the HL for the chain. In both cases, the black line stands for the randomly-distributed non-interacting system.

Parameter identification of the hysteresis of a bell tower

Peter Ivanyi^a, Amalia Ivanyi^b

^{a,b} Pollack Mihaly Faculty of Engineering and Information Technology
University of Pecs, Hungary

Hysteresis phenomena occur not only in magnetic materials but in several other fields of research. In this paper a Preisach model [1] of mechanical hysteresis is evaluated from measurements and a parameter identification is presented.

In Pécs, city of Hungary, there is a Turkish style mosque on the main square of the city centre. To the north-east corner of the mosque a St. Bartholomew bell tower has been designed by two architects Zoltan Bchman and Balint Bachmann [2]. Three slender steel columns surround the three different bells, positioned at different height between the columns. The bell tower has a moving telescopic structure, which can hydraulically rise to become a tower during the tolling period (fig. 1).



Figure 1: The measurement

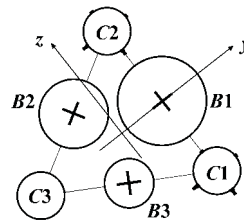


Figure 2: The cross section of the system and column 1

To model the behaviour of this dynamic system during the tolling period a measurement for mechanical hysteresis $\varphi = \mathcal{H}\{M\}$ is developed, where φ [rad] is the declination angle and M [Nm] is the bending moment. The measurement was realized on column 1 (C1) and 2 (C2) (fig. 2) by an elctro-mechanical system and controlled by geodesic measurement at column 1 (C1) and 3 (C3). In the mechanical measurement after the calibration of the rotation indicator the declination angle was measured in principal axes y and z of the cross section. At the same cross section of the column surface strain gage pairs measured the bending moments and the axial forces. In this paper the measured results of column 1, under tolling bell 1 (B1) are presented in direction of principal axis y .

Some periods of the bending moments, the declination angle and hysteresis resulting from the filtered measured data can be seen in Fig. 3. In the full paper the parameter identification of Gaussian-Gaussian type Preisach distribution [1] is presented and the deviation of the measured and the simulated characteristics is presented.

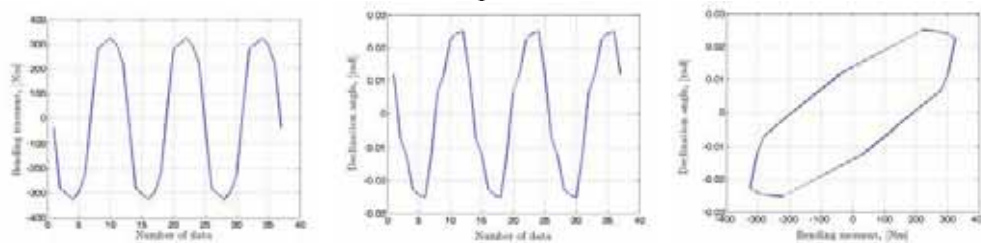


Figure 3: The measured data

[1] G. Bertotti, Hysteresis in Magnetism, Academic Press, 1998.

[2] B. Bachmann, Z. Bachman, Pollack Periodica, 5 (3) (2010), 19-26.

FORC diagrams interpretation: bit pattern media *versus* nanowire arrays

Costin-Ionuț Dobrotă, Alexandru Stancu

Faculty of Physics & CARPATH, „Alexandru Ioan Cuza“ University of Iasi, Boulevard Carol I, 11, 700506, Romania

One of the most appealing experimental techniques for magnetic characterization of the hysteretic samples is the first-order reversal curves (FORC) method that provides a diagram that can be linked to the distribution of interaction and coercive fields. In out of plane applied field, arrays of small nanopillars (Bit Patterned Media - BPM) or nanowires (NW) are producing mean field interactions of demagnetizing-type that strongly influences magnetization reversals of the individual elements. In this paper we present a comparative study concerning FORC diagrams aiming to supply the fundamental understanding of the interplay between the intrinsic coercivities and state dependent interaction fields in perpendicular ferromagnetic structures. Although the two types of networks are very similar, the representative FORC diagrams are quite different. BPM diagrams have a two branch configuration (usually named “wishbone” structure) [1] while for NW the typical FORC diagram take the form of a wide extension along the interaction field axis with a narrow distribution of coercive fields [2]. In addition, an unexpected second distribution less prominent than the first one but extended along the coercive field axis is also present in the case of the NW, being apparently associated with non-interacting nanowires. During the magnetization processes, interaction field distribution changes in a different way in the two cases (see. fig. 1.) Using a 0K-Ising-Preisach model we explain FORC diagrams accounting for specific evolution of the interaction fields [3]. We also present the way in which FORC diagrams provide Preisach-type information about the system: the inter-particle interaction intensity, the intrinsic coercive field distribution and the real switching sequence of the nanopillars/nanowires. *Acknowledgement:* This work was supported by a grant of the Romanian National Authority for Scientific Research, CNCS-UEFISCDI, Project No. PN-II-ID-PCE-2011-3-0794 [IDEI-EXOTIC No. 185/25.10.2011].

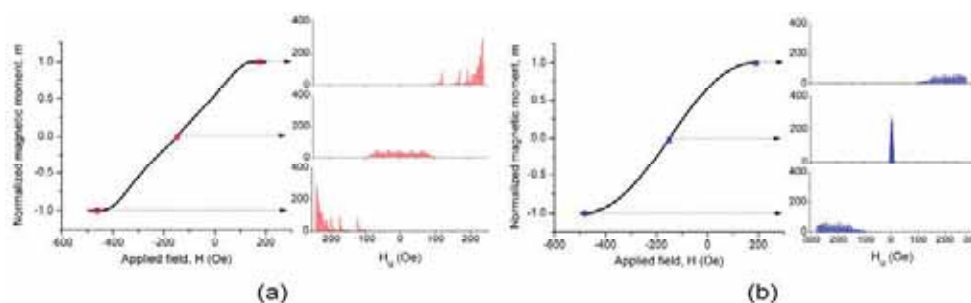


Figure 1: Interaction field distribution in states on the descending branch of the major hysteresis loop for BPM (a) and NW (b).

-
- [1] C. R. Pike, C. A. Ross, R. T. Scalettar, G. Zimanyi, Phys. Rev. B **71** (2005), 134407.
 - [2] A. Rotaru, J. H. Lim, D. Lenormand, A. Diaconu, J. B. Wiley, P. Postolache, A. Stancu, L. Spinu, Phys. Rev. B **84** (2011), 134431.
 - [3] C. I. Dobrotă, A. Stancu, J. Appl. Phys **113** (2013), 043928.

Magnetic relaxation in dipolar magnetic nanoparticle clusters

Ondrej Hovorka^a, Joe Barker^a, Gary Friedman^b, Roy Chantrell^a

^a Department of Physics, The University of York, York, UK

^b Electrical and Computer Engineering Department, Drexel University, Philadelphia, PA, USA

Understanding the role of dipolar interactions on thermal relaxation in magnetic nanoparticle (MNP) systems is of fundamental importance in magnetic recording, for optimizing the hysteresis heating contribution in the hyperthermia cancer treatment in biomedicine, or for biological and chemical sensing, for example.

In this talk, we discuss our related efforts to quantify the influence of dipolar interactions on thermal relaxation in ensembles of small clusters of MNPs. Setting up the master equation and solving the associated eigenvalue problem [1], we identify the observable relaxation time scale spectra and the related effective barrier distributions for various types of MNP clusters. This approach allows accounting for the collective thermal excitations ignored by the classical approach [2,3], which reveals qualitatively different interaction induced behaviour dependent on the hysteresis process applied during the preparation of the initial state. Our findings provide insight into the open questions related to magnetic relaxation in bulk interacting MNP systems, and may prove to be also of practical relevance, e.g., for improving robustness of methodologies in biological and chemical sensing.

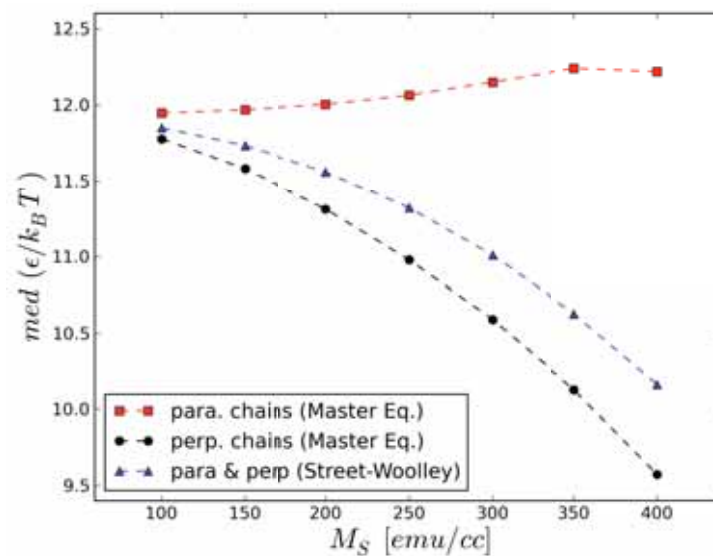


Figure 1: Median of the effective barrier distribution as a function of the interaction strength (tuned by increasing the particles' M_S), computed for an ensemble of 10^5 9-particle chains oriented parallel (■) and perpendicular (●) with respect to the external field direction applied during the preparation of the initial state for relaxation. Comparison with the classical approach is added (Δ), showing the independence on the chain orientation. Particles forming chains are Stoner-Wohlfarth-like and identical, except for the random anisotropy axis orientations (spherical distribution). Parameters: p. diameter 10 nm, anisotropy constant 10^6 erg/cc, $T = 300$ K.

-
- [1] I. Klik, C.-R. Chang, Phys. Rev. B 52 3540 (1995)
 - [2] R. Street, J. C. Woolley, Proc. Phys. Soc. A **62**, 562 (1949)
 - [3] R. Kodama, J. Magn. Magn. Mater. **200**, 359 (1999)

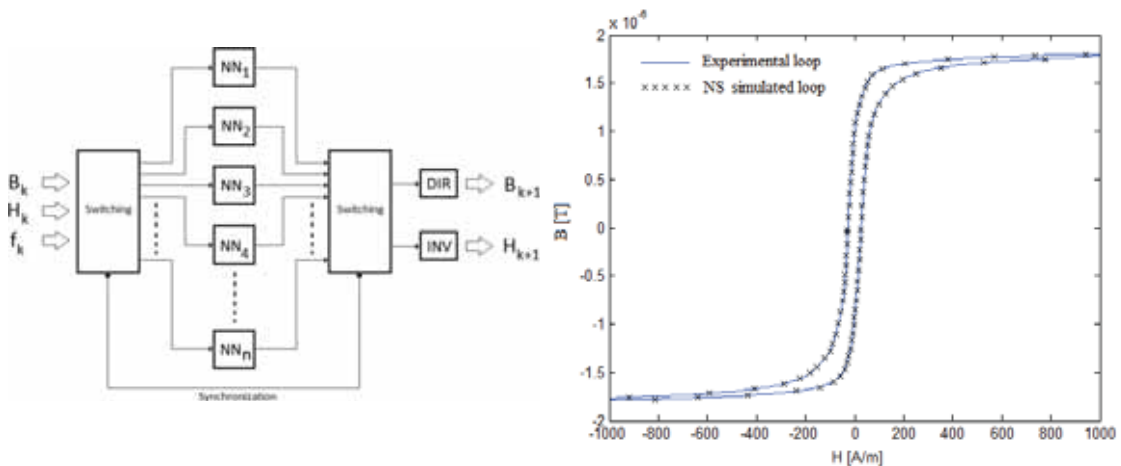
Experimental Testing of a Neural Network approach for Dynamic Ferromagnetic Hysteresis

Antonio Laudani¹, Francesco Riganti Fulginei¹, Carlo Ragusa², Alessandro Salvini¹

¹Department of Engineering, Roma Tre University, Rome, 00146 Italy

²Dipartimento Energia, Politecnico di Torino, Torino, 10129 Italy

The present work focuses on the validation of the Neural Network approach proposed in [1] on suitable experimental data. Dynamic hysteresis loops are simulated by means of an ad-hoc Neural System (NS) based on an array of 3-input 1-output Feed Forward NNs (Fig. 1.a) without using specific hysteresis models [2], [3]. The input pattern of the NNs is the vector (B_k, H_k, f_k) , where B_k , H_k , and f_k are the flux density, the magnetic field and the frequency of the excitation at the k -th step. The output of the NS is B_{k+1} (predicted value at $k+1$ -th step) if the excitation is H (direct case) and H_{k+1} (predicted value at $k+1$ -th step) if the excitation is B (inverse case).



(a) Neural System (NS)

(b) Comparison with the measured loop

Figure 1: The proposed Neural Network approach.

Figure 1.b shows an example of validation of the Neural System results compared with the data obtained by measuring a saturated and symmetric hysteresis loop. The measurement has been performed on a non-oriented Fe-(3 wt%)Si laminations (thickness ~ 0.35 mm) under sinusoidal flux density B and excitation at frequency $f = 5$ Hz. In the full paper the simulations on symmetric/asymmetric and saturated/non-saturated dynamic hysteresis loops will be showed for different types of excitations and several values of frequencies.

-
- [1] F. Riganti Fulginei, A. Salvini, "Neural Network Approach for Modelling Hysteretic Magnetic Materials under Distorted Excitations", IEEE Transactions On Magnetics, vol. 48, p. 307-310, 2012.
 - [2] D. C. Jiles and D. L. Atherton, "Theory of ferromagnetic hysteresis," J. Magn. Magn. Mater., vol. 61, pp. 48-60, 1986.
 - [3] F. Riganti Fulginei, A. Salvini, "Hysteresis model identification by the Flock-of-Starlings Optimization", International Journal Of Applied Electromagnetics And Mechanics, vol. 30, p. 321-331, 2009

Phase Analysis of Lean-Duplex Stainless Steel by Hysteresis Modelling Technique

István Mészáros

Budapest University of Technology and Economics
Department of Materials Science and Technology,
H-1111 Bertalan L. street 7, Budapest, Hungary.

The Lean-Duplex duplex stainless steels (LDSS) are characterized by ferritic-austenitic microstructure. Their metastable austenite phase can transform to a strain induced martensite phase due to cold working. The diffusionless transformation from paramagnetic γ -phase into ferromagnetic α' -martensite phase can be detected studying the magnetic properties of the cold worked LDSS. In the present work the microstructural changes due to cold rolling in a lean duplex stainless steel have been investigated by magnetic testing. For the evaluation of the measured data the multiphase-hyperbolic hysteresis model (MHM) was used.

In this work V2101Mn lean duplex stainless steel was investigated. The phase transformation of the metastable austenite (γ) to the thermodynamically more stable α' -martensite due to cold rolling was studied. Samples were cold rolled to 20%, 40%, 60% and 80% thickness reduction. The phase identification was done by optical and scanning electron microscope. Vickers hardness tests were also performed on each specimen.

The magnetization curves were measured by a permeameter-type AC magnetic property analyzer which was controlled by a 16 bit input-output data acquisition card. The magnetic measurements were carried out by using sinusoidal excitation at a frequency of 5 Hz. The applied maximal excitation field strength was 2500 A/m. The series of symmetrical minor hysteresis loops and the saturation loop were measured.

Our data evaluation technique was applied for data evaluation of the magnetic measurements [1, 2]. This method is based on the multiphase-hyperbolic model of magnetization and it is called model based data evaluation (MBDE) technique. The MBDE method allows us to separate the magnetic contribution of different magnetic phases of the tested alloy. The multiphase-hyperbolic model was fitted to the measured normal magnetization curves and the magnetic contribution of ferrite and strain induced α' -martensite phase phases were determined. Not only their relative phase ratios were determined by this unique phase decomposition technique but the magnetization curves of the individual contributory phases were calculated as well.

This procedure is based on the multiphase hyperbolic model and it is called model based data evaluation (MBDE) technique. The individual magnetization curves of ferrite and α' -martensite were determined by MBDE method. The MBDE technique was applied for studying the plastic strain induced phase transformations in LDSS.

It was demonstrated that the model based data evaluation technique can be used for separating the magnetic phases in lean-duplex stainless steels for determining their phase ratio. Moreover, the model made it possible to determine each of the magnetization curves of the separate magnetic phases. The possibility of magnetic phase decomposition is unique and has great importance in the evaluation of the results of magnetic measurements and in NDT application as well.

[1] I. Mészáros, Materials Science Forum, 589 (2008) 245-250.

[2] J. Takacs, I. Mészáros, Physica B – Cond. Matter, (2008) 403, 3137-3140.

Dynamic magnetic hysteresis of a uniaxial superparamagnet: kinetic theory and the semi-adiabatic approximation

Igor S. Poperechny, Yuri L. Raikher, Victor I. Stepanov

Institute of Continuous Media Mechanics, Ural Branch of Russian Academy of Sciences,
Perm, 614013, Russia

Superparamagnetism is the inherent feature of subdomain ferromagnetic particles. The magnetic state of a superparamagnet is described by the orientational distribution function W that obeys the rotatory diffusion (Brown) equation:

$$\frac{\partial W(\mathbf{e}, t)}{\partial t} = \hat{L}(t)W(\mathbf{e}, t), \quad (1)$$

where \mathbf{e} is a unit vector of the particle magnetic moment. On the basis of equation (1) a kinetic theory of the dynamic magnetic hysteresis (DMH) of ferromagnetic nanoparticles was recently developed [1]. It was shown that in single-domain ferromagnetic particles three qualitatively different regimes of cyclic magnetization reversal are possible, namely, quasi-equilibrium, intermediate and polarization. In a general case, to find the full solution of equation (1) is rather a complicated procedure, due to what in the literature several approximate methods were proposed. For the low-frequency range the most used one is the so-called two-level model [2], which is quite easy to use. However, the simplicity is achieved at the expense of accuracy: the real distribution function is replaced by just a sum of two δ -functions. A more adequate description is provided by the semi-adiabatic approximation proposed in [3]. But in its original form the theory [3] is applicable only in the case of the magnetic field directed along the easy-magnetization axis.

Hereby, we describe the extension of the semi-adiabatic approach for any orientation of the external field. The basic idea is that the first eigenvalue λ_1 of operator \hat{L} is much smaller than all the other ones and, thus, it solely determines the relaxation process at low frequencies. With allowance for that, we expand the distribution function W in a series of instant eigenfunctions and retain just the first two terms:

$$W(\mathbf{e}, t) = F_0(\mathbf{e}, t) + A(t)F_1(\mathbf{e}, t), \quad \hat{L}F_0 = 0, \quad \hat{L}F_1 = -\lambda_1 F_1. \quad (2)$$

Substitution of (2) in (1) reduces the problem to a single differential equation for the coefficient $A(t)$. Calculations for the particles with diameter about 10 nm in the frequency range $f < 1$ MHz reveal very good agreement between the DMH loops found from the exact solution of equation (1) and those obtained in the semi-adiabatic approximation (2). We note also one more important merit of the approach developed: it is applicable for arbitrary temperatures and not only for low ones, as it is for the two-level model.

In the built up framework we analyze the effective coercive force (ECF) defined as the absolute value of the field that zeroes out the average projection of the particle magnetic moment on the field direction. The derived expression for ECF proves to be very robust. It takes in not only the temperature behavior of ECF, as the previous ones do [4], but also delivers the explicit dependence of ECF on the applied field frequency and amplitude. Comparison with the numerical calculations show that our formula works fine for the ensembles of aligned as well as randomly oriented nanoparticles.

The work was done under auspices of RFBR grants 12-02-31319 and 12-02-00897.

-
- [1] I. S. Poperechny, Yu. L. Raikher, V. I. Stepanov, *Phys. Rev. B* **82** (2010) 174423-14.
 - [2] N. A. Usov, Yu. B. Grebenshikov, *J. Appl. Phys.* **106** (2009) 023917-11.
 - [3] Yu. L. Raikher, V. I. Stepanov, *J. Magn. Magn. Mater.* **300** (2006) e311–e314.
 - [4] J. Carrey, B. Mehdaoui, M. Respaud, *J. Appl. Phys.* **109** (2011) 083921-17.

Experimental Verification and Modeling Rate-Dependent Hysteresis Nonlinearities of a Magnetostrictive Actuator

Omar Aljanaideh^a, Subhash Rakheja^a, C-Y Su^a

^a Department of Mechanical and Industrial Engineering Concordia University, Montreal, Canada

Magnetostrictive actuators are increasingly being explored for micro/nano scale actuations attributed to material deformations in the presence of an external magnetic field [1, 2]. These actuators, however, exhibit strong hysteresis nonlinearities that tend to be asymmetric and dependent on the rate of the input [2]. Furthermore, these show output saturation under moderate and high magnitude excitations. In this study, the hysteresis and output saturation nonlinearities of a magnetostrictive actuator were characterized under different amplitudes of simple and complex harmonic excitations over a wide range of frequencies (10-200 Hz) and magnetic bias levels (35 and 75 kA/m). A schematic of the experimental set-up is shown in Figure 1 together with a sample of measured output-input characteristics. The measurements revealed asymmetric output-input characteristics and strong dependence on the magnetic bias, amplitude and frequency of the input. Output saturation was also observed under moderate to high amplitude excitations. The variations in the peak-peak output displacement and the area bounded by the hysteresis loop were further analysed in order to investigate the influence of each experimental factor on the hysteresis nonlinearity.

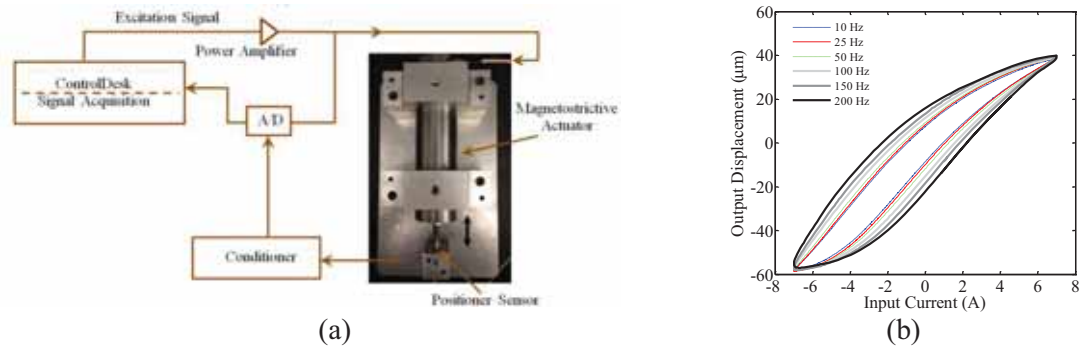


Figure 1: (a) Schematic representation of the experimental setup; and (b) Measured output-input characteristics under excitations in the 10-200 Hz range (amplitude = 7 A bias = 44.1 kA/m).

The measurements revealed that the area bounded by the hysteresis loop increased nearly linearly with the excitation frequency, irrespective of the input amplitude, while the magnetic bias excitation significantly affected both the peak-peak output displacement and the hysteresis loop area. A rate-dependent Prandtl-Ishlinskii model with a memoryless function, suggested in [3], was subsequently formulated to describe both the rate-dependent asymmetric hysteresis and output saturation properties of the actuator over a wide range of inputs. The parameters of the rate-dependent model and the memoryless function were identified on the basis of the measured data. Comparisons of the model responses with the measured data suggested that the proposed model can effectively characterize the nonlinear output-input properties of the magnetostrictive actuator over a broad range of excitation amplitudes and frequencies. Owing to continuous nature of the Prandtl-Ishlinskii model and the memoryless function, a model inverse could be formulated analytically so as to compensate for the rate-dependent hysteresis nonlinearities in an efficient manner.

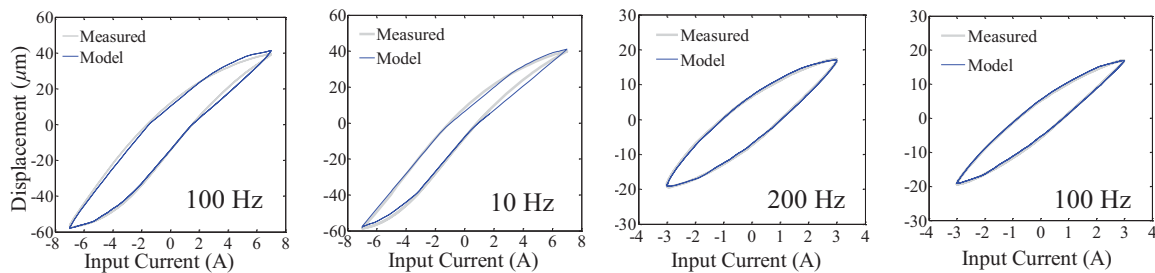


Figure 2: Comparisons of model responses with the measured data under different excitation frequencies and amplitudes.

References

- [1] G. Engdahl, Handbook of Giant Magnetostrictive Materials, Academic, New York, 2000.
- [2] D. Davino, A. Giustiniani, C. Visone, Physica B **407** (2012) 1427–1432
- [3] C. Visone, Journal of Physics: Conference Series **138** (2008), 1-25.

Frequency dependent Preisach model: measurement, identification and application in FEM

Miklós Kuczmann

Széchenyi István University, Győr, Hungary

The aim of this work is to study the losses inside ferromagnetic materials, as well as the loss separation technique [1], and the development of a dynamic hysteresis model [2]. The device under test is a ferromagnetic ring, and a computer controlled measurement system has been realized (fig. 1) to measure data for the identification of the dynamic Preisach model.

The axial symmetry arrangement has been simulated by a 2D FEM procedure (eddy current field simulation), and the hysteresis nonlinearity represented by the inverse Preisach model has been handled by a fixed point procedure. Sinusoidal flux, triangular flux and many other time function of flux have been realized by a controller. Comparison between measured and simulated data results in a training set for the identification of frequency dependent models.

The realized model will be used in FEM routines to simulate motors of electric vehicles;

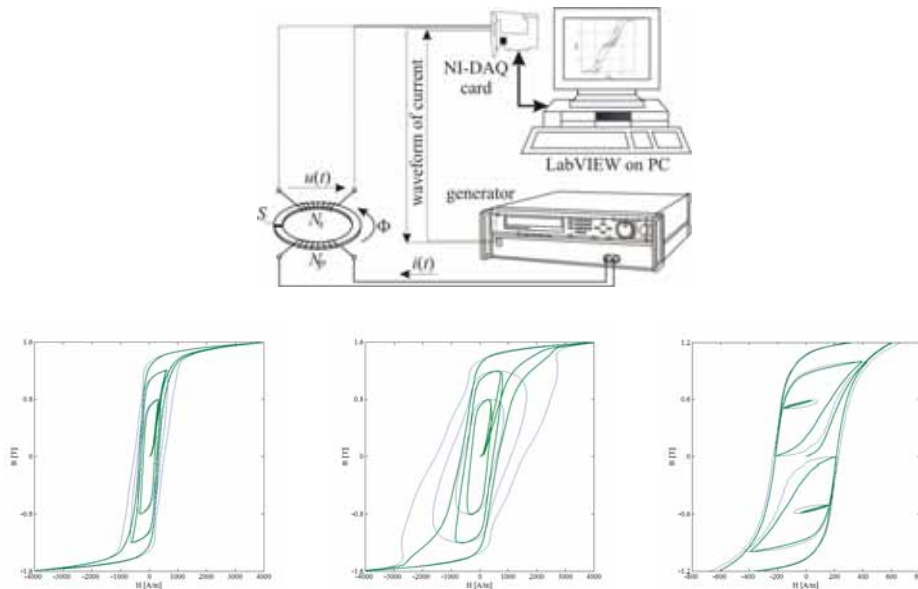


Figure 1: The dynamic hysteresis measurement setup and comparisons between measured data and BH curves obtained from eddy current field simulations without excess field term (50Hz, 200Hz, minor loops).

the aim is to decrease losses via the geometry of the motor.

This paper is sponsored by the Széchenyi István University (15-3202-08), and by “TÁMOP-4.2.2.A-11/1/KONV-2012-0012: Basic research for the development of hybrid and electric vehicles - The Project is supported by the Hungarian Government and co-financed by the European Social Fund”.

-
- [1] G. Bertotti, **Hysteresis in Magnetism**, Academic Press, 1998.
 - [2] M. Kuczmann, A. Iványi, **The Finite Element Method in Magnetics**, Budapest: Academic Press, 2008.

Hysteresis phenomena in permalloy-niobium bilayer films

Ludmila Uspenskaya, Sergei Egorov

Institute of Solid State Physics, Russian Academy of Sciences, Chernogolovka,
Russia

Multilayered hybrid films are considered as promising for applications in many aspects. Hard-soft magnetic multilayers are known as synthetic materials with colossal magnetoresistance effects [1]. Superconductor-ferromagnet hybrids demonstrate huge low temperature magnetoresistance in fields about 1 Oersted [2,3], current phase inversion [4] under relatively low fields and other interesting properties [5]. The ferromagnet layer in these structures is responsible for switching behaviour of structures. Accordingly, the ferromagnetic material is selected based on the facts that it must meet the following requirements: it should have low spontaneous magnetization, low coercitivity, and be able for fast switching of magnetization. However, the magnetic properties of ferromagnetic films depend upon many factors, like substrate quality, lateral sizes of the films, geometrical ratio.

In this work we paid main attention to direct observation of magnetization reversal process in hybrid permalloy-niobium films. We have found that magnetization reversal of permalloy in hybrids and in the free permalloy layers differs not only by the value of coercitivity, by the duration of time of domain wall nucleation and by the rate of magnetization reversal, but in a qualitative sense. Next, we have observed the dependence of kinetics of magnetization reversal upon the structures sizes and aspect ratios; smart rotational modes appear with the reduction of structure sizes below some critical size L . The surprise was not only the emergence of new modes of reversal, but the dimension of the structure under which the transition to new modes of reversal occurs; the critical size L was found much larger than the width of the domain wall in permalloy; it was of the order of several micrometers. We have seen that the coercitivity and the delay of magnetization reversal depend upon the size and shape of the structure. And finally, we have found the memory effect of the structure upon the magnetic state of permalloy, which survive till heating sample over T_c^{Nb}

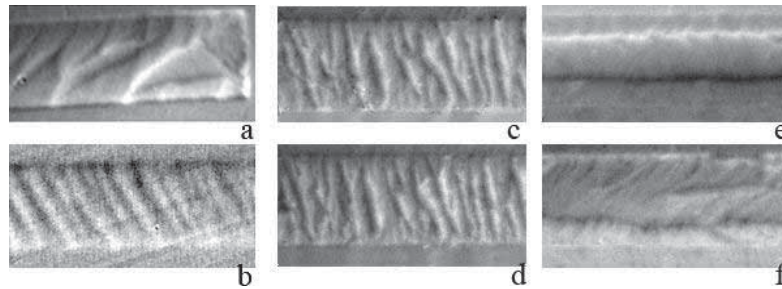


Figure 1: a,b – magnetization reversal of permalloy film fabricated on 60 and 100 nm niobium sublayer; c,d and e,f – frozen-in magnetic domain structure and reproduced one in low temperature reversal process after many cycles of saturating field switching in the same hybrid permalloy-niobium film

- [1] J.M.D. Coey. Magnetism and magnetic materials. Cambridge University Press, New York, 2010.
- [2] V. V. Bol'ginov, V. S. Stolyarov, D. S. Sobanin, A. L. Karpovich, V. V. Ryazanov., JETP Letters, **95** (2012), 366-371.
- [3] V. V. Ryazanov, V. A. Oboznov, A. S. Prokofiev and S. V. Dubonos, JETP Lett. **77** (2003), 39.
- [4] V.V. Ryazanov, V.A. Oboznov, V.V. Bol'ginov, A.S. Prokof'ev, A.K. Feofanov. Phys. Usp. **47**, 732 (2004).
- [5] M.Yu. Kupriyanov, A.A. Golubov, and M. Sigel, Proc. Of SPIE **6260** (2006), 62600S.

Description of inverted hysteresis loops based on the Preisach and Jiles-Atherton Theories

Yevgen Melikhov^a, Arun Raghunathan^b

^a Wolfson Centre for Magnetics, School of Engineering, Cardiff University, Cardiff, U.K.
^b GE-Global Research, JFWTC, Bangalore, India

Materials consisting of several magnetic phases (paramagnetic, soft and/or hard ferromagnetic, antiferromagnetic) often exhibit “strange” dependence of magnetisation on the external applied field: even inverted hysteresis loops with negative coercivity due to presence of the antiferromagnetic coupling between magnetic phases can be observed (see for example [1-3]). Based on the energetic consideration, we extend the applicability of the Jiles-Atherton (JA) and Preisach models to describe the above-mentioned *strange* hysteresis.

Jiles-Atherton (JA) Model --- Starting with the assumption that under ideal conditions of no losses, the magnetic response of the material to variation of external magnetic field is anhysteretic, the total energy density with the losses E_{LOSSES} can be calculated as shown in Eq.(1), where M_{irr} is the irreversible contribution to the total magnetisation M , M_{an} is the anhysteretic function representing anisotropy of the material, and $H_e (B_e)$ is the effective magnetic field with the mean field term in it. Introducing the reversible term M_{rev} and expressing it through M_{irr} completes the formulation of the classical JA model [4].

Preisach Model --- The Preisach model assumes that a system is represented by a set of bistable units, allowing each unit to be in only one of the two possible states $m=\pm\Delta m$ (i.e., magnetisation "up" or "down"), with an energy barrier between the states [5]. The Gibbs energy $G_P(m;H)$ determines the stability of the unit as shown in Eq.(2) with the free energy of the unit $F_P(m)$ and the coupling of the unit to the external magnetic field $k(m;H)$. Magnetisation of the system is then calculated by double integral over the known probability of the bistable units.

Inverted Hysteresis --- The situation becomes “complex” in *strange* magnetic materials in which there could be several loss mechanisms or antiferromagnetic coupling can be present. This can be accounted for in the JA model changing E_{LOSSES} term and in the Preisach model changing $k(m;H)$ term. Such modifications of the models allow successful description of inverted hysteresis loops with negative coercivity (see Fig. 1). Such curves are observed experimentally and the behaviour is attributed to the presence of the ferromagnetic or antiferromagnetic coupling between magnetic phases (see for example [1-3]).

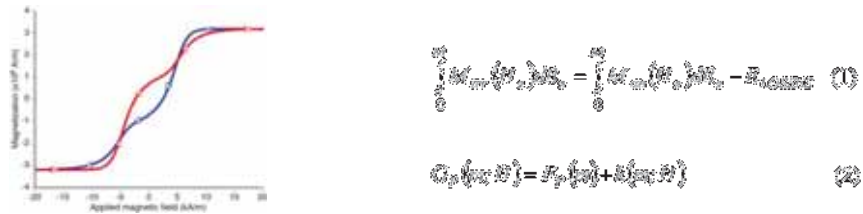


Figure 1. Major hysteresis loop for materials with antiferromagnetic coupling (see e.g. [3]).

[1] Y. Melikhov et al., *JMMM* **215**, 27, 2000.
 [2] D. Miyagi et al., *IEEE Trans. Magn.* **46**, 318, 2010.
 [3] Y. Z. Wu et al., *PRB* **64**, 214406, 2001.
 [4] D. C. Jiles et al., *JMMM* **61**, 48, 1986.
 [5] G. Bertotti, *Hysteresis in magnetism* (chapter **13**), Academic Press, 1998.

Comparison of losses due to capillary-effect hysteresis and viscous damping on a plate moving on a liquid

Bhagya Athukorallage and Ram Iyer
Texas Tech University, Lubbock, Texas, USA

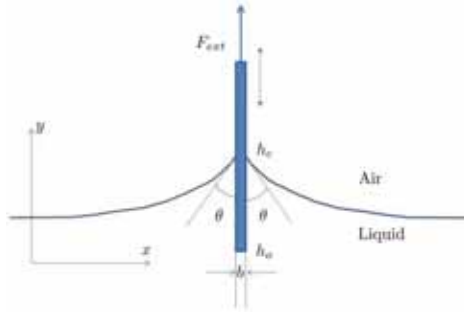


Figure 1: Capillary surfaces attached to a thin plate with contact angle θ .

In this study, we consider a thin rectangular plate that is moving with respect to a liquid under the influence of a periodic force F_{ext} as shown in Figure 1. We consider the case of capillary numbers $0 \leq Ca \leq 2 \times 10^{-2}$ ($Ca = \frac{\mu v}{\gamma}$, where μ , γ are the viscosity and surface tension of the liquid, and v is the speed of the plate). For a human wearing a rigid contact lens, $Ca = 2 \times 10^{-2}$ represents the maximum achieved during a typical blink.

The contact angle between the liquid and the wall takes values between two limiting values $\theta_R \leq \theta \leq \theta_A$ - the receding and advancing angles [1]. In prior work [2], we showed that contact-angle hysteresis contributes to static stability of a contact lens-tear layer system. To investigate the dynamics of this system, it is essential to determine the relative contributions of the energy dissipation due viscous drag of the liquid on the wall boundary and contact lens hysteresis. This is the purpose of this paper.

The motion of the plate is modelled by:

$$\rho \frac{D\mathbf{u}}{dt} = \rho g - \nabla p + \mu \nabla \cdot \left(\frac{\nabla \mathbf{u} + \nabla \mathbf{u}^T}{2} \right); \quad (1)$$

$$F_{ext}(t) = W + 2\gamma(b+w)\cos(\theta) + \mu \frac{\partial \mathbf{u}_2}{\partial x} - bwp(h_0), \quad (2)$$

where p is the pressure, W is the weight of the plate, $\mathbf{u} = (\mathbf{u}_1, \mathbf{u}_2)$ are the components of the velocity, and w is the width of the plate. $F_{ext}(t)$ is assumed to be sinusoidal in t with frequency ω . The last term in (2) represents the force due to buoyancy. The equations above have to be solved for θ together with the Young-Laplace equation [1] describing the capillary surface f :

$$p_{atm} - p(h_c) = \gamma \frac{f_{xx}}{(1+f_x^2)^{\frac{3}{2}}}. \quad (3)$$

Recently [3], very interesting stick-slip behavior for just unidirectional motion of a plate was observed in experiments. The liquid sticks to the plate and the contact angle decreases from θ_A to θ_R as the plate moves upward. Upon reaching θ_R , the contact angle almost instantaneously switches to θ_A and the cycle repeats. Due to this stick-slip behavior, the losses due to hysteresis is higher than what would otherwise be expected. In this study, we will compute the losses due to hysteresis in the contact angle and compare it against the losses due to viscous drag for various values of ω .

References

- [1] de Gennes, P-G., Quere, D., (2004), Capillary and Wetting Phenomena, Springer, New York.
- [2] Athukorallage, B. and Iyer, R., (2013), Model of a contact lens and tear layer at static equilibrium, *Proceedings of American Control Conference*, to appear.
- [3] Nelson, W. C., Sen, P., and Kim, C-J. (2011), Dynamic Contact Angles and Hysteresis under Electro-wettin-on-Dielectric, *Langmuir*, Vol 27, pp 10319–10326.

Vector hysteresis measurements and modeling of electrical steels under stress

Aphrodite Ktena^a, Daniele Davino^b, Ciro Visone^b, Evangelos Hristoforou^c

^a Department of Electrical Engineering, TEI of Chalkida, Greece

^b Engineering Department, University of Sannio, Italy

^c Laboratory of Physical Metallurgy, NTUA, Greece

The dependence of macroscopic magnetic properties on applied and residual stresses is promising for developing new magnetic non-destructive evaluation (NDE) techniques in steels. Increased residual stress is believed to lead to dislocation density distribution changes, grain size and shape changes and increased dispersion of local easy axes which partially explains the observed decrease in remanent and maximum magnetization, and susceptibility. Vector magnetic properties, measured on electrical steels after unloading from tensile stress, offer useful insight in the effect of residual stress on the anisotropy dispersion. Hysteresis loops have been measured at 0°, 30°, 45°, 60° and 90° to the direction of the applied stress and the magnetization vector has been recorded (Fig. 1). The VSM loops at 0° are compared against measurements obtained with ac magnetometry at 0.1 Hz. The results reveal a stress-related anisotropy component, more pronounced at higher strain levels, *eg* 14%, and corroborate previous findings [1] about the effect strain has on the susceptibility, especially as the material approaches remanence, which is of special importance in magnetic NDE.

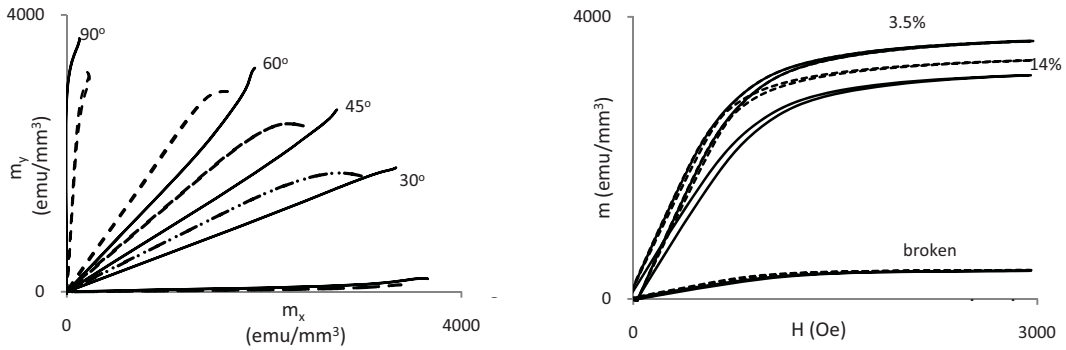


Figure 1. Transverse (m_y) vs parallel (m_x) to applied stress magnetization for fields applied at 0°, 30°, 45°, 60° and 90° at 3.5% (solid) and 14% (dashed) strain, on the left; first quadrant hysteresis loop with the field at 0° and magnetization measured parallel to applied stress (dotted) and the field at 90° and measured transverse to applied stress (solid) for various strain levels, on the right

The hysteresis model in [1], whose vector properties are tested against the vector VSM measurements, accounts for the effect of residual stress on macroscopic magnetic parameters based on the assumptions that residual stress leads to increased anisotropy dispersion and internal demagnetizing fields which become more prominent approaching remanence. The relationship between applied field \mathbf{H} and the magnetization \mathbf{M} is modeled using a vector formulation of the Preisach construction with the Stoner-Wohlfarth mechanism of the coherent rotation of the magnetization as the elementary hysteresis operator $\gamma(a,b)$; angular dispersion of easy axes $\rho(\theta)$; and a characteristic density $\rho(a,b)$ constructed as the weighed sum of normal probability density functions:

$$\mathbf{M}(t) = \int \rho(\theta) d\theta \iint \rho(a,b) \gamma(a,b) \mathbf{H}(t) da db, \quad \rho(a,b) = \sum_i w_i \rho_i \quad (1)$$

[1] Ktena, A. Hristoforou, E., Stress Dependent Magnetization and Vector Preisach Modeling in Low Carbon Steels, 48 (4) (2011) 1433 - 1436

Modeling the effects of stress on the magnetic properties of ferromagnetic materials

Hatem ElBidweihy, Mohammadreza Ghahremani, Edward Della Torre

The George Washington University, Washington, DC, USA

Several theories and models have been presented over the years to evaluate the effect of mechanical stresses on the magnetic properties of ferromagnetic materials. A simple form of the Preisach model will be used to support a hypothesis explaining two magnetization features of steel; (1) the coincident point or the stress crossover, and (2) the bulge or the kink.

In related high strength steel studies, the measurements of magnetization and magnetostriction under different uniaxial compressive stresses have been presented [1-2]. We reasoned that the two aforementioned magnetization features are interdependent with the magnetostriction data, specifically the region of minimum magnetostriction.

The DOK model approximates the Preisach function by a Gaussian distribution and is given by [3]: $M_{irr} = S * M_s * \text{erf}\left(\frac{H - \bar{h}_k}{\sigma}\right)$, where M_{irr} is the irreversible component of the

magnetization, S is the squareness, M_s is the saturation magnetization, h_k is the mean switching field (also the mean of the Gaussian distribution), and σ is the standard deviation of the switching fields (also the standard deviation of the Gaussian distribution). The model can simulate the effect of compressive stresses without adding any additional parameters. The measurements showed that increasing the magnitude of the compressive stress (1) increases the coercive field (increases h_k in the DOK model), and (2) spreads out the changes in magnetization over a broader range of fields (increases σ in the DOK model).

Figure 1 shows several magnetization major loops generated by the DOK model for different values of h_k and σ . The model simulates the coincident point only when such values are linearly-related, as shown in the legend. The point of coincidence, lying in the proximity of the region of minimum magnetostriction, occurs at a magnetic field of 0.8 kA/m which corresponds to the coercive field of an ideal square hysteresis loop.

The cumulative density functions (CDF) corresponding to the h_k and σ values used are shown in Fig. 2. A point of coincidence arises at the same field of 0.8 kA/m. From the basics of statistics, at this point the portion of the material with switching fields less than or equal to 0.8 kA/m is the same regardless of the compressive stress.

A preliminary attempt to model the bulge follows by adding to the magnetization model a scaled factor of the magnetostriction data at regions of deflection (Fig. 3).

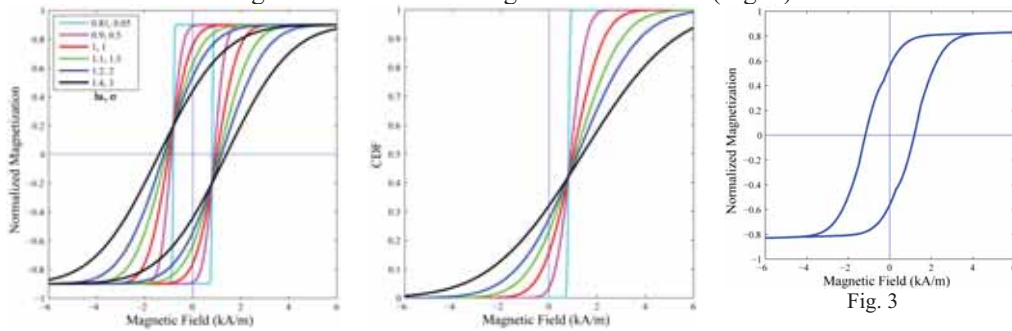


Fig. 1

Fig. 2

Fig. 3

- [1] H. ElBidweihy, C. D. Burgy, E. Della Torre, M. Wun-Fogle, J. B. Restorff, *J. Appl. Phys.* (submitted), (2013).
 [2] C. D. Burgy, E. Della Torre, M. Wun-Fogle, J. B. Restorff, *IEEE Trans. Magn.* **48** (2012), 3088-3091.
 [3] E. Della Torre, J. Oti, and G. Kadar, *IEEE Trans. Magn.* **26** (1990), 3052-3058.

How to fit hysteresis curves obtained from Monte Carlo simulations to those obtained from the master equation approach?

Suhk Kun Oh^{*}, Seong-Cho Yu, Dong-Hyun Kim

Department of Physics, Chungbuk National University, Cheongju, South Korea

Hysteresis curves obtained from both Monte Carlo (MC) simulations and master equation approach via the Tome and de Oliveira equation [1][2] for the infinite-range Glauber kinetic Ising model in the presence of time-dependent external oscillating magnetic fields are compared. The Tome-de Oliveira equation is obtained from the Hamiltonian

$$H = -\frac{J}{2N} \sum_{i,j=1}^N s_i s_j - h_0 \cos \omega t \sum_{i=1}^N s_i, \quad (1)$$

where s_i denotes the Ising spin variable with $s_i = \pm 1$ at site i , J the positive exchange coupling constant, N the total number of spins, h_0 the magnetic field amplitude, and Ω the oscillation frequency, respectively. Then, in terms of dimensionless variables $\xi = \omega t$, $K = \beta J$, and $\Omega = \omega \tau_0$, the equation is given in the form

$$\Omega \frac{d}{d\xi} m(\xi) = -m(\xi) + \tanh\left[K \left\{ m(\xi) + \frac{h(\xi)}{J} \right\}\right]. \quad (2)$$

The solution is of the form

$$m(\xi) = P(\xi - \phi), \quad (3)$$

where P denotes some periodic function, and ϕ denotes delayed phase of magnetization owing to external oscillating magnetic field. We solved the above equation numerically and compared the results with those obtained through MC simulations. We found that the hysteresis curves cannot be related by simply introducing a re-scaled time ξ . The difference between lagged phases of Eq. (3) and MC simulation turn out to be another piece of information, which is necessary to relate both curves.

[1]T. Tome and M. J. de Oliveira, Phys. Rev. A **41** (1990), 4251-4254.

[2]B. K. Chakrabarti and M. Acharya, Rev. Mod. Phys. **71** (1999), 847-859.

*Poster preferred

Influence of pressure and interactions strength on hysteretic behavior in two-dimensional polymeric spin crossover compounds

Daniel Chiruta^{a,b}, Jorge Linares^a, Pierre Dahoo^a, M. Dimian^b

^a Université de Versailles Saint-Quentin-en-Yvelines, Versailles, France

^b Stefan cel Mare University, Suceava, Romania

The design and fabrication of new spin crossover compounds (SCO) with potential applications in various spintronic and photonic devices (memories, sensors, displays) have attracted significant research interests over the last few years [1-2]. Versatility of these materials under various factors such as light, magnetic field, pressure or temperature, has generated substantial research on explaining and controlling their behavior. While the single-step phase transitions were considerably analysed, two-step and three-step transitions with or without hysteresis have been recently reported [3-5] and their explanations are still under scrutiny.

By taking into account the short-range antiferromagnetic type interaction (with strength J) and long-range ferromagnetic interaction (with strength G) into a temperature-dependent Ising-type Hamiltonian, we were able to describe various multi-step behavior consistent with the experimental results. By applying a Monte Carlo entropic sampling technique to generate the state configurations of the system, the Ising-type Hamiltonian has been solved. The results obtained for chain systems have been reported in [6] while here we focus on the interplay between short-range and long-range interactions in explaining the switching behavior in two-dimensional SCO compounds and we study how the pressure influences these multi-step thermal transitions with hysteresis. In Fig. 1, relevant examples of high-spin fraction n_{HS} variation with the temperature are presented for various values of short range and long-range interaction strengths.

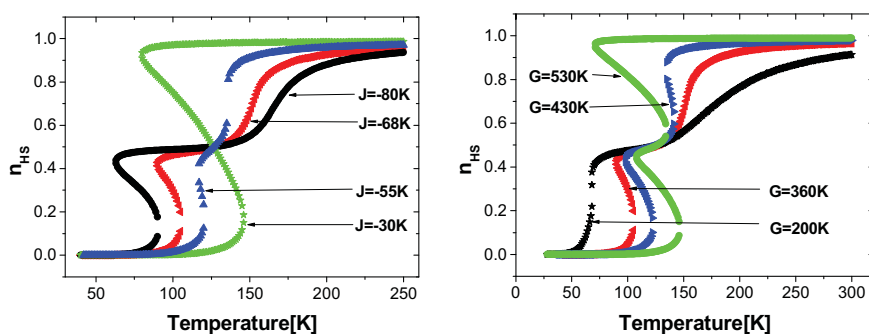


Figure 1: Samples of temperature dependence of high spin fraction for different strengths of short-range (left) and long-range (right) interactions in a 2-D polymeric SCO system.

-
- [1] A. Bousseksou, G. Molnár, L. Salmon, W. Nicolazzi, *Chem. Soc. Rev.* **40** (2011), 3313-3335
 - [2] P. Gutlich and H.E. Goodwin (eds), *Spin Crossover in Transition Metal Compounds I, II, and III, Topics in Current Chemistry* **233, 234, 235**, Springer (2004).
 - [3] H.B. Duan, X.M. Ren, L.J. Shen, et al., *Dalton Trans.* **40** (2011), 3622-
 - [4] N.F. Sciortino, K.R. Scherl-Gruenwald, G. Chastanet, et al., *Angew. Chem. Int. Ed.*, **51** (2012), 10154–10158.
 - [5] K. Nishi, H. Kondo, T. Fujinami, et al., *Eur. J. Inorg. Chem.* in press.
 - [6] D. Chiruta, J. Linares, P.R. Dahoo, M. Dimian, *J. App. Phys.* **112** (2012) 074906

Demagnetization current evaluations using Finite Element Method & magnetic equivalent circuit modelling and optimum design in a pole changing memory motor

Jung Ho Lee, Jung Woo Kim, Pil Won Lee

Hanbat National University, Daejeon, Korea

Memory motors combine the flux controllability of a PM(permanent magnet) machine with the high power density of conventional electric machine [1]-[2].

Memory motors can be built either as variable-flux or pole-changing machines. In both machine types, the magnetization of PMs can be simply varied by using a short current pulse, with no need for permanent demagnetizing current as in a conventional internal PM machine operating in at flux weakening mode. The operation of a memory motor is based on its ability to use a small stator current to change the magnetization of its magnets. This study illustrates how the magnetization of rotor magnets can be continually varied by applying a short pulse of stator current.

In this paper, we introduce the magnetic equivalent circuit modeling and parameter calculation method for the selection of fundamental design variables for a pole changing memory motor (PCMM). A demagnetizing current evaluation method for a PCMM are presented and a characteristic analysis are performed in the situation of pole changing due to the demagnetizing short pulse current. And this paper presents, finally, the optimum design relative to the torque density and ripple on the basis of the design variables of magnet thickness and current in order to improve performance of a PCMM. More detailed design procedure, results and discussion will be given in final paper.

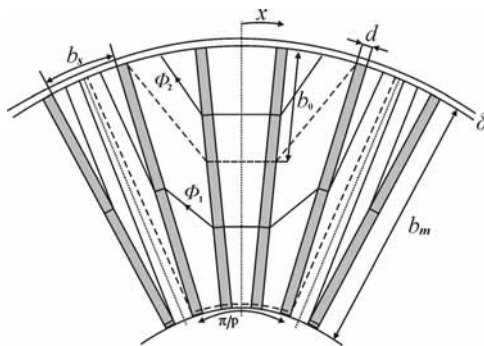


Figure 1: Cross-sectional view of the PCMM with four magnets per pole.

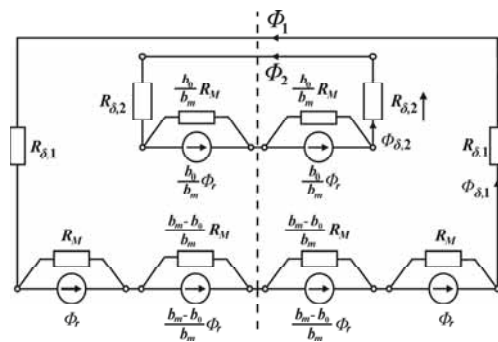


Figure 2: Magnetic equivalent circuit of proposed model.

-
- [1] V.Ostovic, "Memory motor-A new class of controllable flux PM machines for a true wide speed operation," in Conf. Rec. IEEE-IAS Annu. Meeting, 2001, pp. 2577-2584.
 - [2] V. Ostovic, "Pole changing permanent magnet machines," *IEEE Trans. on Industry Applications*, vol. 38, no.6, pp.1493-1499 Dec. 2002.
 - [3] V. Ostovic, *Dynamics of Saturated Electric Machines*. New York: Springer Verlag, 1989.
 - [4] V. Ostovic, *Computer-Aided Analysis of Electric Machines—A Mathematica Approach*. Englewood Cliffs, NJ: Prentice-Hall, 1994.

Optimum design of CW-SynRM and loss & efficiency evaluations by coupled Preisach models & FEM and experiment

Jung Ho Lee, Jun Ho Lee, Young Hyun Kim

Hanbat National University, Daejeon, Korea

Synchronous Reluctance Motor (SynRM) has advantage such as low cost and higher efficiency than induction machines. If stator windings of a SynRM are not a conventional distributed type but the concentrated type, a decrease in copper loss and the production cost due to the simplification of winding in factory, is obtained. However, the vibration and noise of Concentrated Winding SynRM (CW-SynRM) caused by torque ripple are relatively greater than other machines.

Therefore, it is important to select an appropriate combination of design parameters to reduce torque ripple. There are two earlier approaches for the CW-SynRM.

The first approach is the stator design, which the stator teeth, open width of slot, slot depth are the design variables relative to torque ripple reduction, under the condition of fixed optimum designed rotor structure in the 24 slot SynRM [1].

The second is the rotor design, in which are the design variables are flux barrier number, flux barrier width relative to torque ripple reduction, under the condition of fixed optimum designed stator structure in Ref [2].

The torque ripple is slightly decreased by these earlier researches. However, it is insufficient for commercial use and the physical properties of CW-SynRM cannot be accurately predicted and improved by these individual considerations.

The focus of this paper is, finally, the optimum design relative to torque ripple on the basis of the design variables of stator and rotor in order to improve performance and production cost problem of a SynRM.

Comparisons are given with loss evaluations characteristics of normal distributed winding SynRM (24 slot) and CW-SynRM (6 slot) using coupled Finite Element Method (FEM) & Preisach model, respectively. To prove the propriety of the proposed method, the DSP installed experimental devices are equipped and the experiment is performed. More detailed design procedure, results and discussion will be given in final paper.

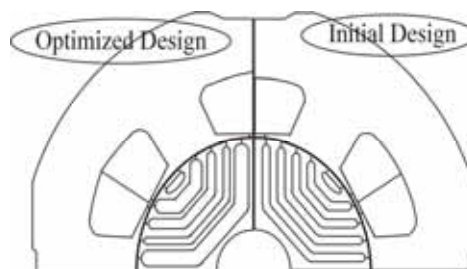


Figure 1: Configurations of optimized and initial design model for stator & rotor design.

-
- [1] S. J. Park, S. J. Jeon, J. H. Lee, "Optimum design criteria for a synchronous reluctance motor with concentrated winding using response surface methodology", *Journal of Applied Physics(MMM)*, vol.99, issu 8, April. 2006.
 - [2] J. M. Park, S. I. Kim, J. P. Hong, J. H. Lee, "Rotor design on Torque Ripple Reduction for a synchronous reluctance motor with concentrated winding using response surface methodology", *IEEE Transactions on Magnetics*, vol. 42, No. 10, pp.3479-3481. Oct. 2006.

PM magnetization characteristics analysis of a post-assembly line start permanent magnet motor using coupled Preisach modeling and Finite Element Method

Jung Ho Lee, Won Gee Byen, Young Hyun Kim

Hanbat national University, Deajeon, Korea

The Line Start Permanent Magnet Motor (LSPMM) combines a permanent magnet rotor for a better motor efficiency during synchronous running with an induction motor squirrel cage rotor to permit the motor starting by direct coupling to an AC power source.

This solution may lead to important technical advantages such as reduced manufacturing costs and or better performances as well as reduced running costs if the space of the rotor is properly negotiated between permanent magnets and squirrel cage. The fact that the magnetizing field is generated by the permanent magnets means that no magnetizing current is drawn from the line finally leading to a much higher power factor in full load operation and lower losses in the stator winding. The LSPMM can replace the common induction motor in many applications, one of the most appropriate being the centrifugal applications (fans and pumps driving) due to their known torque-speed characteristic.

To simplify the manufacturing process and reduce the manufacturing cost, it is necessary to magnetize the permanent magnet in the post-assembly magnetization method [1]. However, the eddy current occurring in the rotor bar during magnetization disturbs the magnetization of Nd-Fe-B.

This paper deals with the PM magnetization characteristics evaluations in a post-assembly LSPMM using a coupled Finite Element Method (FEM) and Preisach modeling, which is presented to analyze the magnetic characteristics of permanent magnets.

The coupled Finite Elements Analysis (FEA) & Preisach model have been used to evaluate the nonlinear solution [2]-[4]. More detailed analysis procedure, results and discussion will be given in final paper.

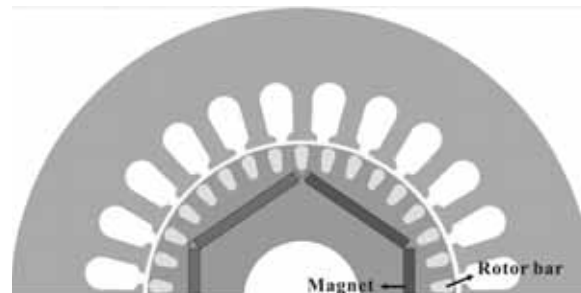


Figure 1: Cross section of single phase LSPMM

-
- [1] G. W. Jewell and D. Howe, "Computer-aided design of magnetizing fixtures for the post-assembly magnetization of rare-earth permanent magnet brushless DC motors," *IEEE Trans. Magn.*, vol. 39, no. 3, pp. 1499-1452, May 2003.
 - [2] A. Ivanyi, *Hysteresis Models in Electromagnetic Computation*, AKADEMIAI KIADO, BUDAPEST
 - [3] I. D. Mayeroyz, "Mathematical Models of Hysteresis," *IEEE Trans. In Magnetism*, Vol. MAG-22, No.5, pp.603-608 Sept. 1986.
 - [4] A. Visintin, *Differential models of hysteresis*, Applied Methematical Sciences, Springer, 1994.

Vector Hysteresis Measurements of Not Oriented Grain SiFe Steels by a Biaxial Hall Sensors Array

Ermanno Cardelli, Antonio Faba

Department of Industrial Engineering, Perugia University, Perugia, ITALY, ecar@unipg.it
Center for Electric and Magnetic Applied Research, University of Perugia, Perugia, Italy

This work discusses the vector measurement of the effective magnetic field inside a not oriented grain SiFe steel sample, taking in to account the effect of the demagnetizing field. We propose to use an array of biaxial Hall sensors, placed up to the sample surface. The calibration of the system and an extrapolation from the values of the magnetic field measured by the biaxial Hall sensors strongly reduce the uncertainties of the direct measurement and provide an accurate evaluation of the magnetic field inside the material sample. Although the approach proposed can be also used for industrial frequencies, 50-60 Hz or more, the analysis is limited here to the static case, because we are mainly interested in static magnetic measurements. These measurements are especially useful for the vector characterization of soft magnetic materials and, in particular, for the identification and the experimental validation of vector hysteresis models [1]. The experimental analysis presented in the paper deals with commercial not oriented grain SiFe steels but it can be extended to any other soft magnetic material under the condition that the dimension of the magnetic domains is smaller than the dimensions of the hall cells used.

In figure 1 we show the rotational magnetic losses measured using a Round Rotational Single Sheet Tester [2] and the biaxial Hall sensor array. The extrapolated data, are the actual losses that take into account the actual magnetic field inside the sample. The figure show the displacement between these data and the losses obtained by the directly measurement of the magnetic field at different distances from the sample surface.

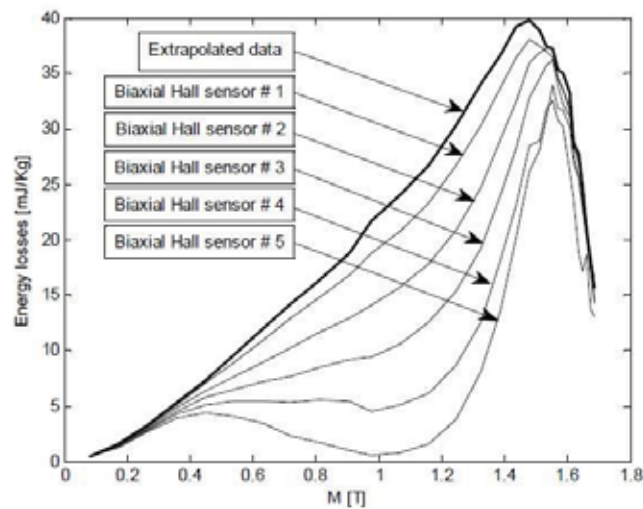


Figure 1: Rotational magnetic losses of a FeSi steel sample using the biaxial Hall sensor array presented in this work.

-
- [1] E. Cardelli, E. Della Torre, A. Faba, IEEE Trans. on Magn., Vol. 46, n. 12, (2010).
 - [2] E. Cardelli, A. Faba, Physica B, Vol. 372, pp. 143-146, 2006.

Numerical Modelling of Transformer Inrush Currents

Ermanno Cardelli, Antonio Faba

Department of Industrial Engineering, Perugia University, Perugia, ITALY, ecar@unipg.it
Center for Electric and Magnetic Applied Research, University of Perugia, Perugia, Italy

Inrush currents are high value transient currents generated when a magnetic core is driven into saturation during initial excitation. They have many undesirable effects, such as damage or reduction of life of the transformer, opening of the power circuit by means of protective relays, and this fact can strongly reduce the quality and the continuity of the power systems, especially in the case of networks with uninterruptible power supplies. The effects of inrush currents can be mitigated by using suitable late-closing relays, over-size fuses, or other passive components. Although reduction in inrush currents magnitudes has been achieved with this hardware, active controls, such as the controlled closing ones, seem to be promising in order to reduce the complexity and the cost of the power system. An open question is about their complexity, that means how much must they have memory of the power system previous history, in order to ensure the desired degree of reliability and robustness of the protection system. Usually the control strategies are based on the prediction of the residual magnetic flux acting in the transformer in order to avoid a transient overshoot in the current, by selecting the closing time correspondent to the given residual flux [1], [2]. The evaluation of the residual flux with accuracy is a very difficult and complex problem to solve, for the two following reasons: the effects of the eddy currents in the laminated cores are in general considerable; the hysteresis in the magnetic materials must be taken into account. In this paper we approach the general problem of the prediction of the inrush currents and of the optimal closing time in no-load transformers, introducing a model of hysteresis in the analysis of the transient during the transformer switching [3]. In the Fig. 1 we show a result about the inrush current prediction by using the proposed approach in comparison with experimental measurements.

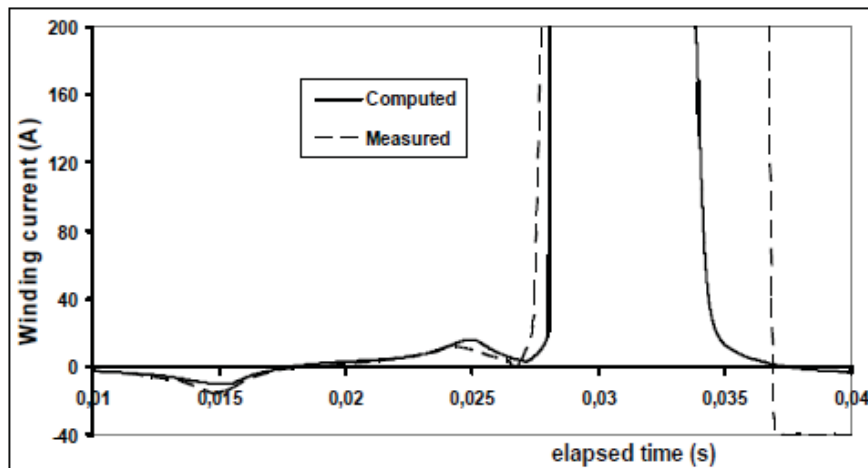


Figure 1: Comparison between the predicted current computed by means the proposed approach and the actual one measured by a suitable experimental set-up.

-
- [1] John H. Brunke, Klaus J. Frölich, IEEE Trans. on Power Delivery, Vol. 16, NO.2, 2001.
 - [2] S. G. Abdulsalam, W. Xu, IEEE Trans. on Power Delivery, Vol. 22, NO.1, 2007.
 - [3] E. Cardelli, E. Della Torre, A. Faba, IEEE Trans. on Magn., Vol. 46, n. 12, 2010.

Comparative Analysis Between the Jiles-Atherton and the Bouc-Wen Models for Saturated and Symmetric Hysteresis Loops in Ferromagnetic Materials by using MeTEO algorithm

F. Riganti Fulginei, A. Laudani, A. Salvini

Department of Engineering, Roma Tre University,
Via della Vasca Navale, 86, 00146, Rome, Italy

The aim of this work is comparing the well know Jiles-Atherton [1] and the Bouc-Wen [2] hysteresis models for saturated and symmetric hysteresis loops in ferromagnetic materials in order to emphasize their different features. The hysteretic Bouc-Wen model [2] is a nonlinear system described by following differential equations:

$$\begin{cases} \ddot{x} + 2\xi\omega_n\dot{x} + \alpha\omega_n^2x + (1-\alpha)\omega_n^2z = u(t) \\ \dot{z} = -\gamma|\dot{x}||z|^{n-1}z - \beta\dot{x}|z|^n + A\dot{x} \end{cases} \quad (1)$$

where $u(t) = B\cos(\omega t)$ and $(\alpha, \xi, \omega_n, A, \beta, \gamma, n, B, \omega)$ are the nine characteristic parameters to be found. Metric-Topological-Evolutionary Optimization (MeTEO) algorithm [3] has been utilized to find characteristic parameters of the two models. It is based on a hybridization of three modern heuristics running on a parallel architecture. Fig. 1 shows an example of comparison for a given device [4]. In the full paper the dissimilarities between the two models will be show by considering different points of view: dynamic generalization, type of loop shape and so on.

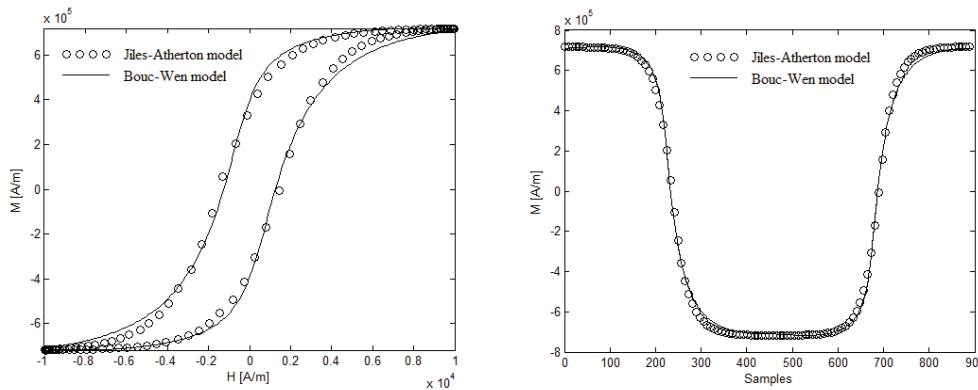


Figure 1: Example of comparison between the Jiles-Atherton and the Bouc-Wen hysteresis models for a static, symmetric and saturated loop on a given device.

-
- [1] D. C. Jiles and D. L. Atherton, "Theory of ferromagnetic hysteresis," J. Magn. Mater., vol. 61, pp. 48–60, 1986.
 - [2] M. Ismail, F. Ikhouane and J. Rodellar, "The Hysteresis Bouc-Wen Model, a Survey", Archives of Computational Methods in Engineering, Volume 16, Issue 2, pp 161-188, June 2009
 - [3] F. Riganti Fulginei, A. Salvini and G. Pulcini, "Metric-topological-evolutionary optimization". Inverse Problems in Science & Engineering (IPSE), vol. 20, p. 41-58, 2012
 - [4] F. Riganti Fulginei, A. Salvini, "Neural Network Approach for Modelling Hysteretic Magnetic Materials under Distorted Excitations", IEEE Transactions On Magnetics, vol. 48, p. 307 -310, 2012.

Fast analysis of ferromagnetic shields by means of Fixed Point iterative technique

L. Giaccone, C. Ragusa

Dip. Energia, Politecnico di Torino, C.so Duca degli Abruzzi 24, 10129 Torino, Italy.

The modelling of thin ferromagnetic shields subjected to strong applied field requires taking into account the non linear characteristic of the material, because the operating points can lie between the Rayleigh and the linear region. To this end, the iterative scheme proposed in [1] is extended in order to handle the nonlinear behaviour of the magnetic characteristic. Here, the nonlinearity is managed by means of the Fixed Point (FP) technique [2] by which the constitutive relation of the material is expressed as

$$H = \frac{1}{\chi_{FP}} M + H_{RES}, \quad (1)$$

where the susceptibility χ_{FP} is a constant and H_{RES} is the nonlinear residual to be updated iteratively throughout the solution process. Let us assume that the iterative scheme proposed in [1] is summarized by the function f that gives the magnetization at iterative step $k+1$ by knowing the magnetization and the residual at the previous step: $M^{k+1} = f(M^k, H_{RES}^k)$. By knowing M^{k+1} , eq. (1) is employed for the computation of H^{k+1} . This quantity is entered in the nonlinear characteristic of the material in order to get the corresponding magnetization that we call \bar{M}^{k+1} . Eventually eq. (1) is used for updating the residual $H_{RES}^{k+1} = H^{k+1} - (\bar{M}^{k+1} / \chi_{FP})$. The process is iterated until the residual reach a fixed value under a

given tolerance. In Fig. 1 is shown the nonlinear characteristic used in the following example. A simulation for the simple case study represented in the inset is performed. The dotted line of Fig. 1 points out that some elements work in the Rayleigh zone whereas others work in the linear zone. In Fig. 2 the magnetic flux density is computed along the inspection line represented in Fig. 1. The shielded field is represented by the black line for the nonlinear material and by the red line under linear assumption. It is apparent the overestimation of the shielding efficiency in the second case. Finally, a Finite Element simulation is performed in order to validate the result as shown by the dotted line.

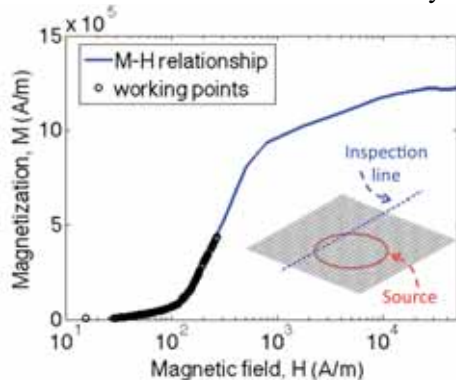


Figure 1: Example on nonlinear material characteristic. The inset represents a simple case study: source (red), shield (black) and inspection line (blue). The dotted curve represents the working point of each element.

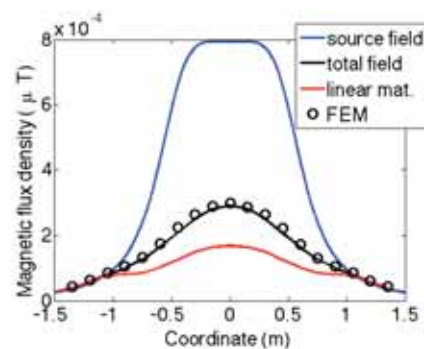


Figure 1: Magnetic flux density along the inspection line represented in Fig.1. Blue line: source field. Black line: nonlinear shield. Red line: linear shield. Finally, the dotted line is obtained by a standard Finite element code for the solver validation.

- [1] L. Giaccone, C. Ragusa, O. Khan. and M. Manca, IEEE Trans. Magn. 49 (7), (2013).
 [2] O. Bottauscio et al., IEEE Trans. Magn. 49 (7), pp. 726—729, (2004)

A computationally effective dynamic hysteresis model for taking into account the skin effect in magnetic laminations

O. de la Barrière^a, C. Ragusa^b, C. Appino^c, F. Fiorillo^c, M. LoBue^a, F. Mazaleyrat^a

^a SATIE, ENS Cachan, CNRS, UniverSud, 61 av du President Wilson, Cachan, France.

^b Dip. Energia, Politecnico di Torino, C.so Duca degli Abruzzi 24, 10129 Torino, Italy.

^c Istituto Nazionale di Ricerca Metrologica (INRIM), Torino, Italy

The authors of [1] have calculated the magnetic loss and dynamic cycles in 0.35 mm thick Iron Silicon laminations, taking into account skin effects, up to a frequency of 800 Hz. The Dynamic Preisach Model (DPM), representing the material $\mathbf{B}(\mathbf{H})$ law, is coupled with a finite element method (FEM) to solve the diffusion equation on the lamination thickness. Although accurate, this approach is computationally time consuming because it requires the application of the full DPM at each finite element. On the other hand, the author of [2] has pointed out that the switching magnetic objects in the Preisach plane are confined in an interval around the dynamic field $\mathbf{H}(t)$. If a boxlike Preisach distribution is assumed [2] and a constant field rate is considered, the dynamic field can be obtained from the static field $\mathbf{H}_{\text{stat}}(t)$ (i.e. the field that would give under static conditions the same polarization $\mathbf{J}(t)$) by the equation

$$H(t) = H_{\text{stat}}(t) + \text{sign}(\dot{H}_{\text{stat}}) \frac{4}{3} \sqrt{\frac{\dot{H}}{\kappa_d}}, \quad (1)$$

where κ_d is the parameter of the DPM. In this paper, equation (1) is extended to a generic $\mathbf{H}(t)$ waveform by assuming that the Preisach distribution be locally constant on the dynamic field interval. Moreover, a further simplification of (1) is obtained if the time derivative of $\mathbf{H}(t)$ is approximated to the one of $\mathbf{H}_{\text{stat}}(t)$. Thus, the following Simplified Dynamic Model (SDM) for the dynamic field is eventually obtained:

$$H(t) = H_{\text{stat}}(t) + \text{sign}(\dot{H}_{\text{stat}}) \frac{4}{3} \sqrt{\frac{\dot{H}_{\text{stat}}}{\kappa_d}} \quad (2)$$

Here, eq. (2) can be considered as a non-linear dynamical system able to provide the static field $\mathbf{H}_{\text{stat}}(t)$, given the dynamic field $\mathbf{H}(t)$, at a very reduced computational cost. Once the static field is obtained, a static hysteresis model (here the static Preisach model) allows to compute the corresponding polarization $\mathbf{J}(t)$. This method provides the dynamic constitutive law $\mathbf{B}(\mathbf{H})$ for the material, which can be coupled to FEM to solve the diffusion equation on the lamination thickness. This model is diagrammatically showed in Fig. 1. The SDM has been compared with the full DPM (for the same dynamic constant κ_d), and with experimental results in the frequency range 100Hz-1kHz. The model provides results in good agreement with the method of [1], where the full DPM is used, both in terms of loss results (Fig. 2) and hysteresis loops. A computational speed-up of ~ 50 is also recorded.

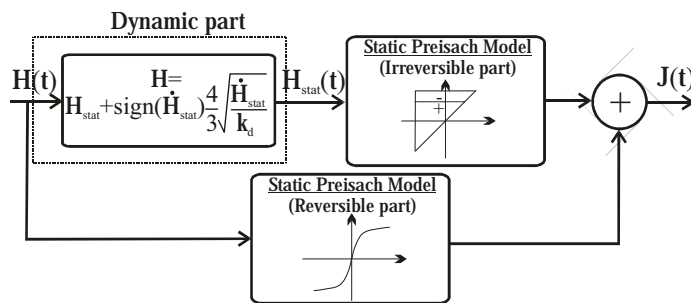


Figure 1: Simplified Dynamic Model (SDM)

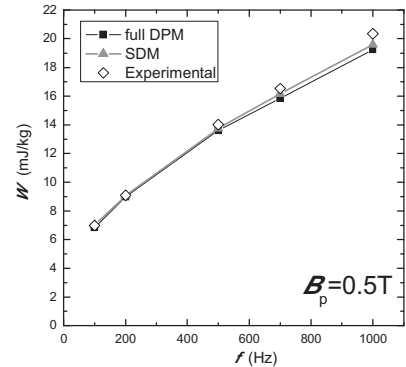


Figure 2: Loss results (sinusoidal induction waveform of mean peak value $B_p=0.5$ T)

[1] L. Dupré and al., IEEE Trans. Magn. 35 (5), pp. 4171-4184 (1999).

[2] G. Bertotti, J. Appl. Phys. 69 (8), pp. 4608-4610 (1991).

Hysteresis losses computation by using DME solver in electrical machines

S. Vergura, M. Carpentieri, F. Lattarulo

Department of Electrical Engineering and Information, Technical University of Bari, via E. Orabona 4, I-70125 Bari, Italy

An open issue is the computation of the hysteresis losses of the magnetic materials used in the electrical machines. Several mathematical models have been proposed in order to study the hysteresis behavior [1]. For this aim, the Magnetic Equivalent Circuits (MECs) technique is a powerful tool for machine analysis. As is known, a magnetic circuit can be modeled by means of the electrical analogy, where the reluctance has the role of a resistance, the flux has the role of a current, and the Magnetic Force (MF) has the role of a voltage source [2]. In this paper we use the Diagonal Mesh Equivalent (DME) to solve the equivalent electrical circuit. DME is a circuital interpretation of the gaussian elimination used to solve the mesh-based equations system. It consists in two steps: the former one transforms the coefficient matrix of the magnetic equivalent circuit in a triangular one, while the latter one transforms the triangular coefficient matrix in a diagonal one. By using DME, the mesh fluxes are calculated, whereas the branch fluxes are successively evaluated by means of the equivalent magnetic Kirchhoff's Current Law (KCL) at the nodes. These branch fluxes are related to the several parts of the machine, e.g. air gap, stator, rotor etc. By using the geometrical parameters of the machine, the flux density B of each branch can be evaluated. In this way, we are able to compute the hysteresis loop of each magnetic part of the machine.

Fig. 1a shows the equivalent magnetic circuit of the claw-pole magnetic device as that reported in Fig. 1 of Ref. [2] and used as a sample in this paper. This is a claw-pole alternator used in automotive applications with outer diameter of 140 mm and stator diameter of 70 mm. The magnetic materials in this specific case is SiFe (3% in weight) with magnetization saturation $M_s=2T$ when the applied field is $H_s=120000$ A/m and coercive field of $H_c=20000$ A/m. Fig. 1b shows the major loop related to the stator of the studied electrical machine. The hysteresis loop is obtained directly from the fluxes computed by the DME. By calculating the loop area we can obtain the energy losses related to that part of the electrical machine; this is a fundamental aspect for the design of electromagnetic power devices.

The full paper will show the details of the algorithm and the results will be also compared to the semi-analytical models.

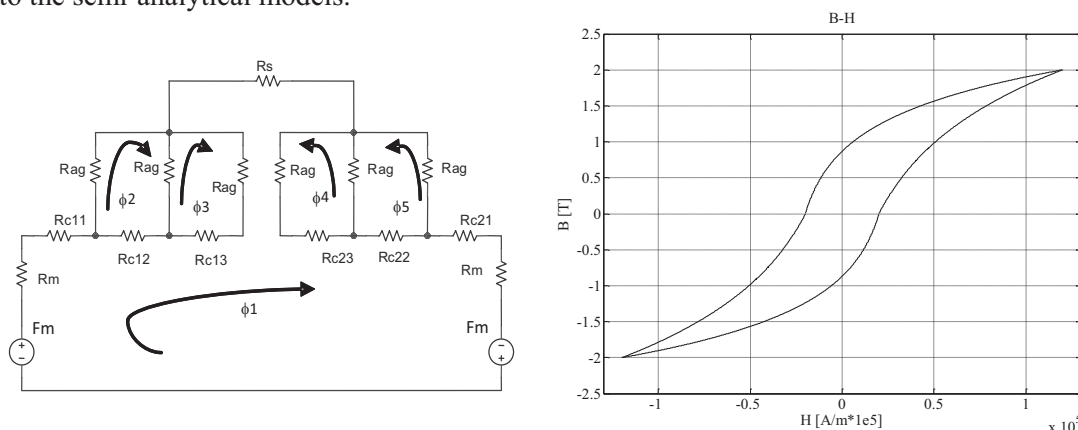


Fig 1. a) magnetic equivalent circuit b) hysteresis loop computed by using MEC approach

[1] M. Carpentieri, G. Finocchio, F. La Foresta, B. Azzerboni, J. Magn. Magn. Mat. 280, 158-163, 2004.

[2] Derbas, H.W., Williams, J.M., Koenig, A.C., Pekarek, S.D., IEEE Transactions on Energy Conversion 24, 388-396, 2009.

Mean field modeling with Preisach-Krasnosels'kii-Pokrovskii hysterons for arrays of ferromagnetic nanowires

Costin-Ionuț Dobrotă, Alexandru Stancu

Faculty of Physics & CARPATH, „Alexandru Ioan Cuza“ University of Iasi, Boulevard Carol I, 11, 700506, Romania

First-order reversal curves (FORC) method has been extensively used in recent years as experimental characterization technique of hysteretic materials. Typical ferromagnetic nanowire arrays FORC diagram has a specific shape in an axial applied field, constantly appearing as a high extension along the interaction field axis with a narrow dispersion of coercivities, and an unexpected supplemental distribution of larger coercive fields with weak interactions [1]. A mean field model introduced through a mechanical analogy and based on Preisach-Krasnosel'skii-Pokrovskii (PKP) hysterons is able to explain the interplay between interactions and critical fields in nanowire arrays [2]. Physical phenomena behind of FORC diagram are highlighted using sets of PKP hysterons describing the effect of the demagnetizing-type mean field on the switching events. One single PKP hysteron is representative for an ideal interacting nanowire array in which every wire is in the local interaction mean field created by all the other wires from the system [3]. Using a small number of PKP hysterons one obtains a FORC diagram with specific distributions that represents the basic diagram for ferromagnetic nanowire arrays, as shown in fig. 1. Generally, a negative mean field characterizes a nanowire array and switching events are evidenced in the AB feature of the diagram. Switching events of the nanowires with slightly higher intrinsic coercive fields take place when these nanowires feel the mean field with a magnetizing effect that leads to larger apparent coercive fields (C_0C branch) experimentally observed for nanowire arrays. In the full paper we present the details of the model based on PKP hysterons, an identification procedure and the limits of this approach. *Acknowledgement:* This work was supported by a grant of the Romanian National Authority for Scientific Research, CNCS-UEFISCDI, Project No. PN-II-ID-PCE-2011-3-0794 [IDEI-EXOTIC No. 185/25.10.2011].

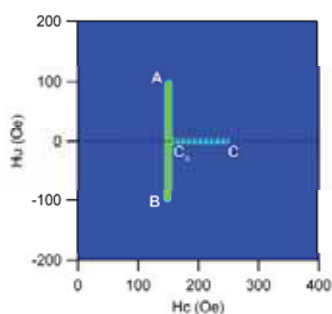


Figure 1: Basic shape of the nanowire arrays FORC diagram simulated with PKP hysterons.

-
- [1] A. Rotaru, J. H. Lim, D. Lenormand, A. Diaconu, J. B. Wiley, P. Postolache, A. Stancu, L. Spinu, Phys. Rev. B **84** (2011), 134431.
 - [2] C. I. Dobrotă, A. Stancu, J. Phys.: Condens Matter **25** (2013), 035302.
 - [3] C. I. Dobrotă, A. Stancu, Physica B **407** (2012), 4676.

Exchange coupling influence on hysteresis loops and magnetization reversal of permalloy thin films

L.S. Uspenskaya^a, M.V. Indenbom^b

^a Institute of Solid State Physics RAS, Chernogolovka, Russia

^b Laboratory of magnetism of Brittany CNRS, Brest, France

Possibility to use ferromagnetic-antiferromagnetic multilayers as spin-valves, resistivity switching elements or miniature sensors of magnetic field stimulates experimental study of artificial hybrid structures and theoretical interpretation of observed phenomena.

Principal understanding is achieved that interfacial exchange interaction between adjacent layers determines the hysteresis loop shift and the enhanced coercivity of multilayered structures. The existence of interface-related spin-exchange spring was experimentally proved by observation of the nucleation of domain walls at different film spots due to field reversal, by finding of rotary hysteresis, and by observation of variation of hysteresis loops after field rotation. Recently, some dynamic consequences from the existence of exchange enhanced anisotropy were discussed. It was predicted that induced anisotropy could affect on domain wall motion, on resonance and magnetic precession limited switching, and the reversal time could depend on damping parameter and induced anisotropy. Besides, dynamic hysteresis loops were found reveal distinct reversal asymmetry that was not observed in the corresponding static loops.

The present work addresses the direct study of kinetics of magnetization reversal in the bilayer hybrid film with exchange bias. The variation of magnetization reversal with alteration of direction of external field is observed, and direct correspondence between the asymmetry of hysteresis loops and magnetization kinetics is established. The kinetics of domain walls nucleation and the dependence of dynamic characteristics of domain wall motion on the magnetic field direction and strength are considered. Unexpected anisotropy of dynamic characteristics of domain wall motion at magnetic field reverse relative unidirectional anisotropy is found.

This work was supported by UBO CNRS, by grant of Russian Foundation of Basic Research, and by the program of Russian Academy of Science.

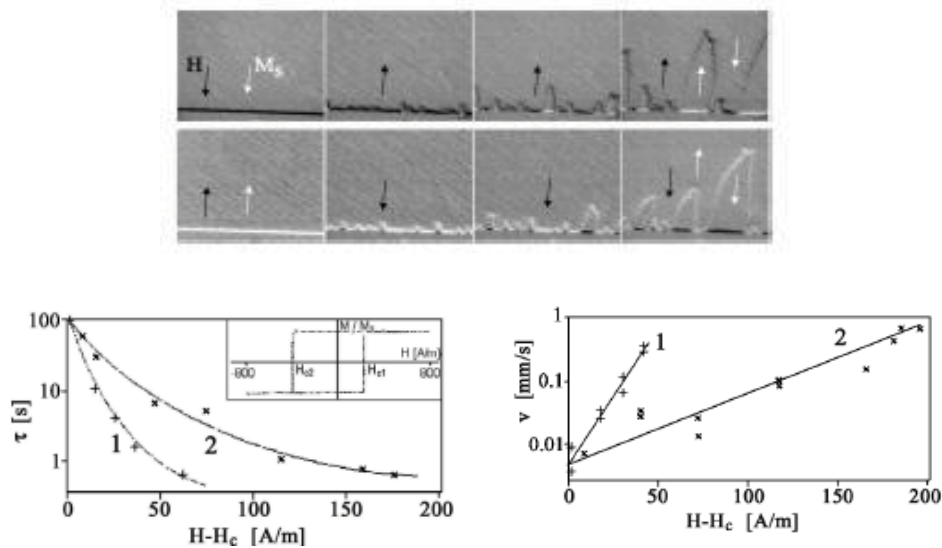


Figure 1: Magnetization reversal of permalloy film under oppositely directed field, and dependences of time of nucleation of domain walls τ and their velocity V upon the field strength for two opposite directions of the applied field.

Combined first order reversal curve analysis of magnetization and magnetoresistance

Randy K. Dumas^{a,b}, Peter K. Greene^a, Dustin A. Gilbert^a, Li Ye^a, Chaolin Zha^c,
Johan Åkerman^{b,c,d}, Kai Liu^{a,*}

^a Department of Physics, University of California, Davis, USA

^b Department of Physics, University of Gothenburg, Gothenburg, Sweden

^c Materials Physics, Royal Institute of Technology (KTH), Stockholm-Kista, Sweden

^d NanOsc AB, Kista, Sweden

Uncovering the mechanisms that govern hysteretic reversal is critical to their basic understanding and potential applicability. Of particular interest are ferromagnetic/non-magnetic layered structures exhibiting magnetoresistance (MR). While the first order reversal curve (FORC) technique [1] has historically been applied to a variety of magnetic systems, its applicability has been recently extended to systems exhibiting thermal, electrochemical, ferroelectric, and resistive hysteresis [2]. In addition to providing a useful qualitative “fingerprint” of the reversal mechanisms, FORC analysis has shown the ability to probe a wealth of quantitative information regarding reversible/irreversible switching, interactions, and distributions of key magnetic parameters not readily accessible from standard major loop investigations. Here, we provide a *combined* FORC analysis of the magnetization, termed M-FORC, and magnetoresistance, termed MR-FORC, to provide a comprehensive picture of the reversal mechanisms in a multilayered [Co/Cu]₈ film stack.

Families of M-FORCs and MR-FORCs are shown in Fig. 1(a) and 1(c), respectively. Interestingly, MR values up to 4.83% are found along selected MR-FORCs, larger than the 4.25% MR maximum of the major loop. Furthermore, the MR-FORC distribution, Fig. 1(d), reveals a different irreversibility landscape as compared to the M-FORC distribution, Fig. 1(b), as further verified in the FORC switching field distributions (FORC-SFDs), Fig. 1(e). Unlike the M-FORC measurements, which are sensitive to the macroscopic changes in magnetization, the MR-FORCs probe the microscopic domain configurations and the net spin disorder, as those are most important in determining the resultant MR value.

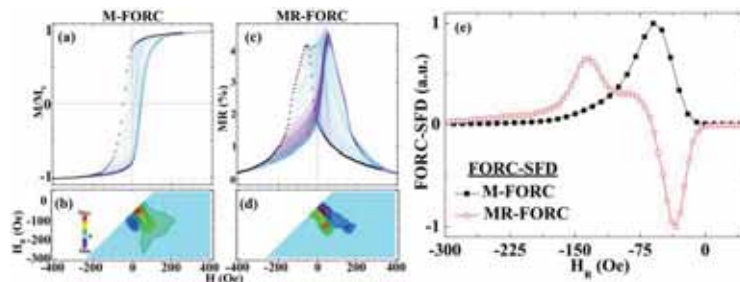


Figure 1: Families of (a) M-FORCs, (c) MR-FORCs, and corresponding FORC distributions are shown in (b) and (d), respectively. (e) FORC-SFDs.

[1] C.R. Pike, *et al.*, J. Appl. Phys. **85**, 6668 (1999); J.E. Davies, *et al.*, Phys Rev B **70**, 224434 (2004); R.K. Dumas *et al.*, Phys. Rev. B **75**, 134405 (2007).

[2] C. Enachescu, *et al.*, Phys. Rev. B **72**, 054413 (2005); D. Ricinchi, *et al.*, J. Optoelectron. Adv. M **6**, 623 (2004); J.M. Pomeroy, *et al.*, APL **95**, 022514 (2009).

* Work at UCD supported by NSF (ECCS-0925626 and DMR-1008791). The Swedish Research Council (VR), The Swedish Foundation for Strategic Research (SSF), and the Knut and Alice Wallenberg Foundation are also gratefully acknowledged.

Permanent magnets NdFeB based for orthodontic applications

F. Fabiano^a, F. Celegato^b, A. Giordano^a, C. Borsellino^c, L. Bonaccorsi^a, L. Calabrese^a,
P. Tiberto^b, G. Cordasco^d, G. Matarese^d, V. Fabiano^c, B. Azzerboni^a

^a Department of Electronic Engineering, Industrial Chemistry and Engineering, Messina, Italy

^b INRIM Electromagnetism Division, Torino, Italy

^c Department of Civil Engineering, Computing, Construction, Environmental and Applied Mathematics, Messina, Italy

^d Department of Experimental, Specialized Medical-Surgical and Odontostomatological Sciences Messina, Italy

Since 1980s, neodymium-iron-boron (NdFeB) based magnets were used to produce extremely high magnetic flux densities with a smaller size compared to other permanent magnet solutions[1]. The origin of this high efficient behavior is related to the rare earth metals incorporated in those magnets. They give rise to a magnetization along the C-axis[2] (large magnetocrystalline anisotropy) with a significant improvement of the maximum energy product (BHMAX), high coercivity, and a dramatic reduction in the magnet dimensions. This last property makes those permanent magnets very promising for dental applications.

In orthodontics, they have been used for treatment of unerupted teeth, tooth movement along archwires, expansion, fixed retention, in the correction of anterior open bite, functional appliances and for positioning a multi-stranded wire retainer in lingual retention[4]. One of the main problems limiting their final success is the fact that neodymium-iron-boron magnets are subject to a severe corrosion in the oral environment. For this aim, it is necessary a coating with a material that is not subject to frictional wear and it is able to prevent the possible side effects of corrosion. In the past, the magnets were coated with teflon (polytetrafluoroethylene), parylene, acrylic and composite resin, but it was demonstrated these coating materials are insufficient for the aim proposed [5,6]. Differently, here we show results achieved when the coated of the magnets is done with a hybrid silane based coating [7]. Aim of this study is to investigate how the presence of the coating affects the magnetic properties, with this purpose several tests on the magnetic force, for different coating compositions and thicknesses, have been performed. Finally, we tested how the coating protects the magnet for corrosive products by immersing it in a system consisting of synthetic saliva.

[1] G. P. Mancini, J. H. Noar and R. D. Evans. "The physical characteristics of neodymium iron boron magnets for tooth extrusion". *European Journal of Orthodontics* 21 (1999) 541-550.

[2] Harris, I.R. "Hard magnets". *Materials Science and Technology* 6 (1990) 962-966.

[3] A.M. Blechman, "Magnetic force systems in orthodontics". *American Journal of Orthodontics* 87 (1985) 201-210.

[4] Hahn W., Fricke J., Fricke-Zech S., Zapf A., Guber R. and Sadat-Khonsari R. " 433-436.

[5] Wilson M., Kpendema M., Noar J.H., Hunt N.P. and Mordan N.J. "Corrosion of intra-oral magnets by biofilms of *Streptococcus sanguis*". *Biomaterials* 16 (1995) 721-725.

[6] Wilson M., Patel H., Kpendema M., Noar J.H., Hunt N.P. and Mordan N.J. "Corrosion of intra-oral magnets by multi-species biofilms in the presence and absence of sucrose". *Biomaterials* 18 (1997) 53-57.

[7] Bonaccorsi L.M., Borsellino C., Calabrese L., Cordasco G., Fabiano F., Fabiano V., Matarese G., Mavilia G., Proverbio E. "Performances evaluation of a Bis-GMA resin-based composite for dental restoration". *Acta Medica Mediterranea*, 2012, 28, 163.

Hysteresis in Economics – future research directions

Yevgen Melikhov

Wolfson Centre for Magnetism, School of Engineering, Cardiff University, Cardiff, U.K.

The idea that economics is a developing system is one of the main ideas in econophysics, the new direction of theoretical economics. Theory of dynamic systems (with friction/dissipation/hysteresis) has to be used in this case. This presentation proposes some of the research directions in which the Preisach model, which is widely used in magnetism as one of the mathematical tools from enormous mathematical apparatus available to describe hysteretic behaviour [1], can be utilised.

In the ‘agent-based’ Preisach model of economics, the whole macroeconomic system is represented by the assemblage of economic agents (e.g., individual consumers or firms), which are represented by a hysteron in mathematical form, and which can be in two states only (sell or buy, for example), where switching from one state into the other is prevented by the barrier (waiting for the right news, for example) [2]:

Interactions between elementary agents and macrohysteresis --- Assuming that the most important feature, i.e. losses, is present in the system (an agent on a micro-scale with microhysteresis), another feature, i.e. interaction between the agents, can be added, which will lead to a collective response of the system being more susceptible to change of input. Importance of this is clearly seen in booms, busts and runs, where collective behaviour makes the response exaggerated. In ferromagnetism interaction is a function of temperature and this leads to the existence of the so-called Curie temperature (or critical temperature) above which hysteresis is removed fully. In economics, ‘herding’ could resemble temperature and its influence on an economic system is worth of studying.

Issue with the complexity of identification of modelling coefficients --- The parameters of the models in economics have to be identified. Such a procedure is called calibration in economics, where the case (i.e. experiment in magnetism) is selected and then a model is calibrated against that particular experiment. As opposed to magnetism (where one can carefully control almost everything allowing better understanding of physics and models), in economics we are deprived of that. One wants, however, employment of these models as “means of calibration, prediction and control” rather than just simple “tools of thought” which is still a challenge [2, 3].

Change of number of elementary agents and macrohysteresis --- The situation could be even more complicated compared with magnetism if we allow parameters of agents to vary in time under external influence; for example, values of barriers could change due to decision changes at different market prices, and/or the probability distribution function could change due to some firms going bust or due to increase of importance of some firms

Variation of experimental timescales and macrohysteresis --- Variation of experimental timescales in magnetism leads to study of different properties covering everything from micro- to macro-scale. The same can be projected on economics: the time of the observation of the system (i.e. time of the experiment) and characteristic time of a part (showing hysteresis) of that system, have to be compared and taken into account.

The author acknowledges the support from the EPSRC through the “Discipline Hopping: Engineering and Physical Sciences and Economic and Social Sciences” programme 2011-2012, as well as fruitful discussions with Dr. S. Selim, Cardiff Business School, Cardiff University.

[1] I. D. Mayergoyz, *PRL* **56**, 1518-1521, 1986.

[2] R. Cross et al., *IEEE Con. Sys. Mag.* **2**, 30-43, 2009.

[3] R. Cross et al., *Phys. B* **403**, 231-236, 2008.

Barkhausen Noise as a microstructure characterization tool

Aphrodite Ktena^a, Evangelos Hristoforou^b, Gunther J. L. Gerhardt^c, Frank P. Missell^c
^dFernando J.G. Landgraf, ^dDaniel L. Rodrigues-Jr, ^dM. Alberteris-Campos

^aTEI of Chalkida, Greece

^bLaboratory of Metallurgy, NTUA, Greece

^cCCET, Universidade de Caxias do Sul, Brazil

^dEPUSP, USP, Sao Paulo, Brazil

Barkhausen noise is known to be related to magnetization reversal mechanisms and the underlying microstructure in magnetic materials. Stochastic by nature though, its application to quantitative material characterization is not straightforward. This paper is an attempt to unlock the information held by Barkhausen noise pertaining to grain size and residual strains. A series of electrical steel samples have been prepared with controlled grain size (11 μm – 148 μm) and strain (0% - 29%) and have been characterized with respect to Barkhausen noise in three different laboratories using surface and bulk measurements. Hysteresis measurements have also been carried out to determine macroscopic magnetic parameters. Barkhausen noise (BN) increases with strain, as expected, and varies inversely proportional to grain size. Of special interest, is the correlation of the BN voltage vs strain curve with the stress-strain curve of the material and the variation of the double-peak BN envelope with the grain size (Fig. 1) as well as the dependence of the material's differential permeability on strain which also features a double-peak, a main one around coercivity and a secondary around remanence. The paper compares the data collected in the three laboratories and presents an overview of modelling approaches, evaluating them against the collected data in an attempt to correlate Barkhausen noise with microstructural parameters.

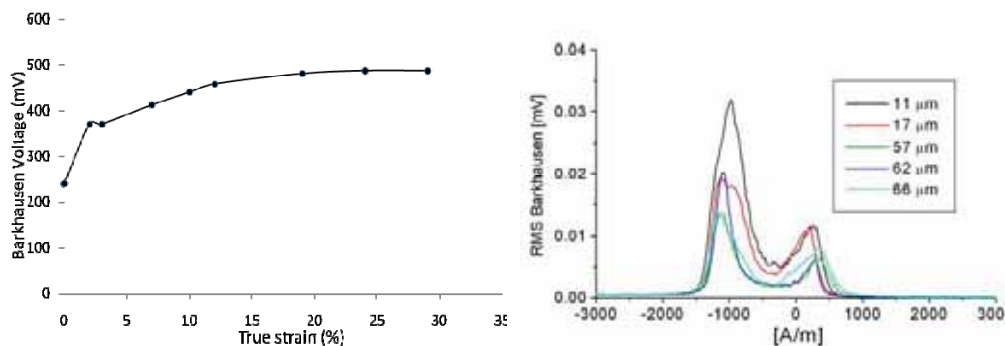


Figure 1 – Barkhausen noise voltage vs strain (left) and for various grain sizes (right)

-
- [1] F. Bohn, A. Gundel, F.J.G. Landgraf, A.M. Severino, R.L. Sommer, Magnetostriction in non-oriented electrical steels, *Physica B* 384 (2006) 294–296

MWCNT/Fe₃O₄ hybrid composites: synthesis, characterization and magnetic properties

A. Pistone^a, D. Iannazzo^a, A. Piperno^b, M. Fazio^a, F. Celegato^c, G. Barrera^c, P. Tiberto^c,
A. Giordano^a, B. Azzerboni^a, S. Galvagno^a

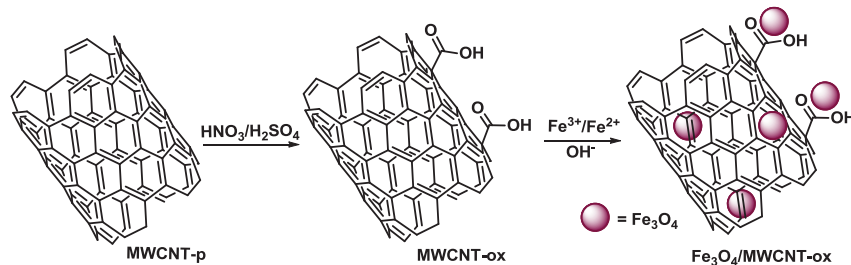
^a Department of Electronic Engineering, Chemistry and Industrial Engineering, University of Messina, Messina I-98166, Italy

^b Department of Chemical Sciences, University of Messina, Messina I-98168, Italy

^c INRIM Electromagnetism Division, Torino, Italy

Carbon nanotubes (CNTs) receive great attention because of their outstanding electronic, mechanical, thermal, chemical properties and significant potential applications in nanoscience and nanotechnology [1]. In recent years, many researches focus on a new type of CNT-inorganic hybrids. The CNTs are coaxially coated with the inorganic compound through synergistic effect and charge transfer in CNT-hybrids, which impart CNTs with tunable electrical, magnetic and optical properties arising from the nanoscale coupling [2, 3]. Fe₃O₄ nanoparticles based nanocomposites have received a lot of attention because of their promising magnetic properties and potential applications in color imaging, electromagnetic shielding, magnetic recording media, soft magnetic materials and ferrofluids [4].

In order to combine the advantages of the CNTs and magnetite nanoparticles, a novel multi walled carbon nanotubes/Fe₃O₄ inorganic hybrid material was prepared through deposition-precipitation and wet-impregnation methods and fully characterized by SEM, TEM, EDS, XRD, VSM. The deposition-precipitation method proved to be a general and effective procedure to decorate pristine and functionalized MWCNTs with Fe₃O₄ nanoparticles at mild conditions of pH and temperature; magnetic hysteresis loops were measured at room temperatures on carbon nanotubes containing various fraction of magnetite using a vibrating sample magnetometer (VSM) operating in the magnetic field range -10 kOe - H - 10 kOe. The diamagnetic contribution of sample holder was subtracted from the measured curves.



Characterization analyses indicated the presence of magnetite clusters with size of about 100 nm that are composed by very small particles with a mean size of 5-10 nm uniformly self-assembled along the surface of the carbon nanotubes; furthermore, the saturated magnetization (M_s), remanence (M_r) and coercivity (H_c) of the decorated MWCNTs are much larger than those of MWCNTs, and the Fe₃O₄ decorated MWCNTs exhibit well magnetic properties.

-
- [1] R.H. Baughman, A.A. Zakhidov, W.A. de Heer, *Science* **297** (2002) 787–792.
 - [2] E. Dominik, *Chem. Rev.* **110** (2010) 1348–1385.
 - [3] R. Zhao, K. Jia, J.J. Wei, J.X. Pu, X.B. Liu, *Mater. Lett.* **64** (2010) 457–459.
 - [4] J. Amici, M. U. Kahveci, P. Allia, P. Tiberto, Y. Yagci, M. Sangermano, *J. Mater. Sci.* **47** (2012) 412–419.

U. Kilic^{1,2}, G. Finocchio³, T. Hauet⁴, S. H. Florez⁵, G. Aktas¹ and O. Ozatay¹

1: Bogazici University, Department of Physics, Istanbul, Turkey

2: Istanbul Bilgi University, Electrical and Electronics Engineering Department, Istanbul, Turkey

3: University of Messina Dipartimento di Fisica della Materia e Ingegneria Elettronica, Messina, Italy

4: Institut Jean Lamour, Université De Lorraine-CNRS UMR, Nancy, France

5: HGST, a Western Digital Company-San Jose Research Center, San Jose, USA

Reaching higher areal densities by means of the conventional recording methods is limited by the superparamagnetic effect which can be pushed back by using materials with high perpendicular magnetic anisotropy [1]. Whilst this preference improves the thermal stability, it requires very high magnetic field application to trigger magnetization reversal, so-called “the writability problem”. Yet, it can be tackled with the sequential application of a laser pulse and a magnetic field pulse to enable low coercivity and fast switching in the data recording process. This forms the basis of a recently proposed data recording method, namely Heat assisted magnetic recording (HAMR). The nature of such switching dynamics of magnetic bits close to Curie temperature can be substantially different from the low temperature regime and requires a formalism that takes into account both longitudinal and transverse magnetization relaxation mechanisms in addition to temperature dependent damping parameters. In our study, the significant changes in the switching process at elevated temperatures close to Curie temperature were investigated within the stochastic Landau-Lifshitz-Bloch formalism [2] which considers thermal excitations at elevated temperatures by including Gaussian stochastic processes. The essential motivation of the current work is to develop a Stochastic-LLB based macrospin model, using experimentally measured temperature dependence of intrinsic parameters for CoNi/Pd multilayers as realistic material parameters [1]. Such a model enables us to determine the temperature dependence of longitudinal susceptibility from single fit simulations of experimental switching data consistent with previous ab-initio calculations [2,3,4]. A map of switching time distribution as a function of magnetic field and heating pulses together with a visualization of the granular switching process will be presented for the evaluation of the above mentioned multilayer system and similar recording media for thermally assisted recording applications. On the one hand, coherent motion of spins is well-described by the macrospin LLB model. On the other hand, a detailed analysis of the spin system behavior corresponding to the applied heat and magnetic field pulses can be achieved with a micromagnetic model which takes into account the interactions between the magnetic moments on sub-micrometer length scales. Such a study is under progress.

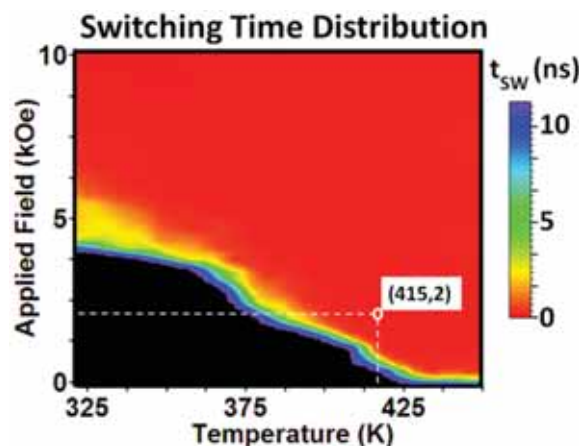


Figure 1: Entire switching time distribution (color gradient) for different combinations of heating and magnetic field pulses. Black region shows the non-switching part.

[1]. APPLIED PHYSICS LETTERS 95, 172502 .2009.

[2]. PHYSICAL REVIEW B 85, 014433. 2012.

[3]. PHYSICAL REVIEW B 74, 094436 .2006.

[4]. JOURNAL OF APPLIED PHYSICS 112, 013914 (2012).

Modeling partial phase transitions in 1st order magnetocaloric material MnFe(P,As)

L.v. Moos^a, C.R.H. Bahl^a, K.K. Nielsen^a, K. Engelbrecht^a, M. Küpferling V. Basso^b

^aDepartment of Energy Conversion and Storage, Technical University of Denmark, Denmark

^bIstituto Nazionale di Ricerca Metrologica, Italy

With the global focus on energy and advances in room temperature Magnetocaloric Materials (MCM), the field of magnetic refrigeration has grown a lot within the last 15 years. Magnetic refrigeration utilizes the magnetocaloric effect (MCE), where a temperature change in the MCM is induced when a magnetic field is applied adiabatically. The MCE can be exploited and magnified in Active Magnetic Regenerators (AMR), where MCM undergo thermodynamic cycles through magnetization, demagnetization and heat exchange in order to cool a system.

The magnetic refrigeration process has previously been modeled, using 2nd order materials with single-valued magnetization, $M(H,T)$, and heat capacity, $c_p(H,T)$, functions, governing the MCE [1]. However, generally 1st order MCMs show a larger MCE, but at the cost of varying degrees of hysteresis. This makes both material characterization and modeling non trivial. The characterization of the MCE, peaking around the magnetic phase transition, is often done indirectly through measuring c_p or M across a broad range of temperatures and magnetic fields, mapping out the complete phase transition [2]. In an AMR cycle the MCM will rarely undergo a complete phase transition, but only cycle through minor loops in c_p and M , the shape of which is determined by the hysteresis.

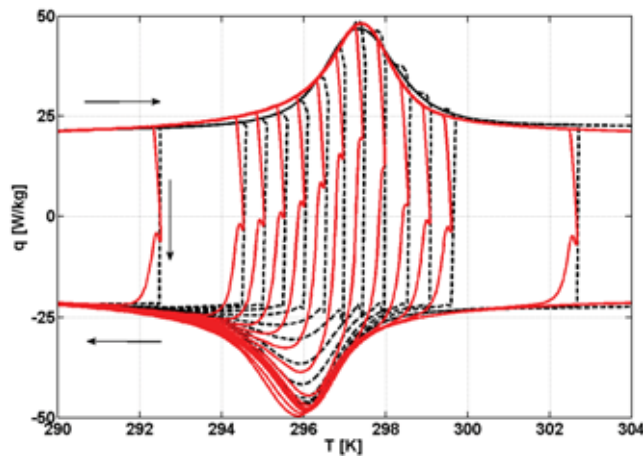


Figure 1: DSC measurements of heat flux, measured through heating and cooling (solid curve) the sample and model simulations of the experiment (dashed curve).

Here we investigate how the 1st order MCM MnFe(P,As) behaves under partial phase transitions, measured through partial $M(H,T)$ and $c_p(H,T)$ curves, as illustrated in figure 1. The experimental results are compared simulations of a Preisach-type model, appropriate to describe the out-of-equilibrium thermodynamic aspects of hysteresis [3]. We discuss how hysteresis affects AMR performance and what experimental material data is required to obtain a satisfactory material model.

-
- [1] K. K. Nielsen et al., Int. J. Refrig. **34** (2011).
 - [2] A. Smith et al., Adv. Energy Mater. **2** (2012).
 - [3] V. Basso et al., J. Magn. Magn. Mater **316** (2007)

Cooling factor for magnetocaloric temperature effect in polycrystalline gadolinium

Mohammadreza Ghahremani, Lawrence H. Bennett, and Edward Della Torre, and Hatem ElBidweihiy

Department of Electrical and Computer Engineering, The George Washington University, Washington, DC 20052, USA

In the last two decades, there have been hundreds of research papers on the magnetocaloric effect (MCE) in materials, for magnetic refrigeration close to room temperature. Most of them have been on hysteretic materials comparing their results to that of gadolinium. Despite its iconic nature, gadolinium exhibits complex magnetic behaviour, including the question of whether it is ferromagnetic [1]. This paper reveals some new interesting MCE features of polycrystalline gadolinium.

The adiabatic temperature change (ΔT) during the magnetization and demagnetization processes of polycrystalline gadolinium is directly measured [2] for several applied magnetic fields near the Curie temperature. The area under the ΔT vs. ambient temperature curves determines the cooling factor (CF). We previously showed a new interpretational approach of plotting ΔT as a function of the average temperature (T_{avg}) instead of the initial temperature (T_i), which emphasizes the reversibility of the MCE [3].

The current paper demonstrates (Fig. 1) that defining the CF as the area under the curve ΔT vs. T_i gives a measurably different CF compared to the area under the curve of ΔT vs. T_{avg} . The use of T_{avg} provides a more accurate cooling performance than using T_i . Although the effect is not very large in gadolinium, it is outside of the experimental error. Such an improved coefficient could be more significant for other materials.

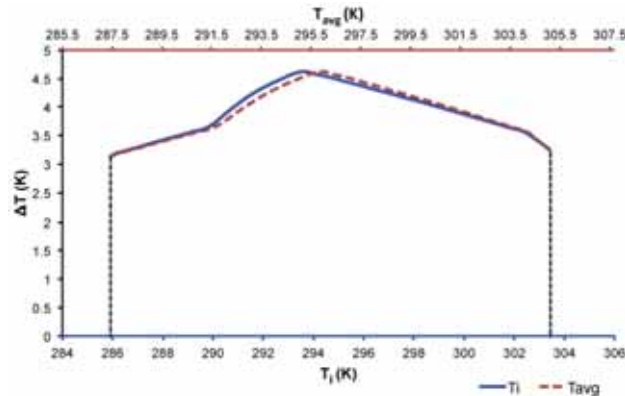


Fig 1: A comparison of gadolinium adiabatic temperature change as a function of initial temperature and average temperature with 2 T applied field near the Curie temperature. The computed areas under these to curves are different.

- [1] J. M. D. Coey, V. Skumryev, K. Gallagher, Nature, vol 401, 2 (1999).
- [2] M. Ghahremani, Y. Jin, L. H. Bennett, E. Della Torre, H. ElBidweihiy and S. Gu, IEEE Trans. Magn. 48, 11 (2012).
- [3] M. Ghahremani, H. M. Seyoum, H. ElBidweihiy, E. Della Torre and L. H. Bennett, AIP Advances, 2, 032149 (2012).

Finding the mechanism and rate of thermal spin transitions

Pavel F. Bessarab^{a,b}, Valery M. Uzdin^b, and Hannes Jónsson^a

^a University of Iceland, Reykjavík, Iceland

^b St. Petersburg State University, St. Petersburg, Russia

Modern technology has made it possible to create, study and control magnetic systems at the nanoscale. Systems with two or more spin states are of particular interest since they can, in principle, be used for magnetic recording. In recent experiments [1], thermal switching of magnetization in nanoscale islands of Fe-atoms on a W(110) surface has been studied by means of spin-polarized scanning tunneling microscopy. Both activation energy barrier and Arrhenius prefactor were found to strongly depend on the island size and shape.

We apply recently developed multi-dimensional transition state theory for magnetic degrees of freedom [2] in order to explain the experimental data [1]. The method involves a calculation of the minimum energy path which is needed for finding the activation barrier and revealing the mechanism of the spin transition. The calculations [3] were carried out for monolayer islands of rectangular shape. The islands have two degenerate states, with spins aligned parallel to the anisotropy axis. The dependence of the energy barrier and Arrhenius prefactor on the size and shape of the islands is illustrated in Fig. (1). Three regions, corresponding to three different mechanisms of magnetization reversal, are marked. Region I corresponds to relatively small clusters where magnetization reversal occurs via coherent rotation of spins. For the larger clusters, a domain wall forms and propagates during the transition. The domain walls are either parallel (region II) or perpendicular (region III) to the anisotropy axis.

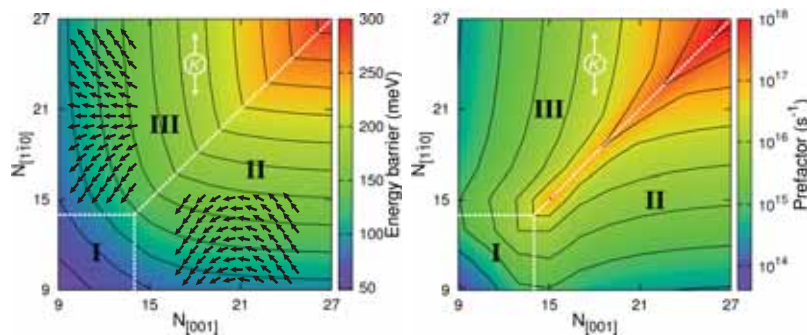


Figure 1: Activation barrier (left) and Arrhenius prefactor (right) versus the number of atomic rows along the [001] and $[1\bar{1}0]$ directions. The easy axis anisotropy is along the $[1\bar{1}0]$ direction. Insets show the spin configurations for different transition mechanisms.

The calculated results agree well with the experimental data. In particular, we could explain a maximum in the Arrhenius prefactor for square islands, which correspond to a crossover between different transition mechanisms. The transition state of the islands in the crossover region has an increased entropy and that leads to a larger value of the Arrhenius prefactor.

[1] S. Krause, G. Herzog, T. Stapelfeldt, L. Berbil-Bautista, M. Bode, E.Y. Vedmedenko, and R. Wiesendanger, *Phys. Rev. Lett.* **103** (2009), 127202.

[2] P.F. Bessarab, V.M. Uzdin, and H. Jónsson, *Phys. Rev. B* **85** (2012), 184409.

[3] P.F. Bessarab, V.M. Uzdin, and H. Jónsson, *Phys. Rev. Lett.* **110** (2013), 020604.

Spin torque in the framework of random magnetization dynamics driven by a jump-noise process

Giorgio Bertotti^a, Claudio Serpico^b, Ziyu Liu^c, Andrew Lee^c, Isaak Mayergoyz^c

^a Istituto Nazionale di Ricerca Metrologica, Torino, Italy

^b Università of Naples "Federico II", Napoli, Italy

^c University of Maryland, College Park, Maryland, USA

Recently, random magnetization dynamics driven by a jump-noise process has been proposed in [1-3] as a unifying approach to the description of damping and fluctuation effects caused by interactions with the thermal bath. The main contribution of this paper is to demonstrate that the Slonczewski spin-torque term can be naturally derived from this approach in the case of spin-polarized current injection. The central idea of this derivation is to modify the expression for the transition probability rate $S(\mathbf{M}, \mathbf{M}')$ which defines a jump-noise process. It was shown in previous papers [1-3] that in the absence of spin-polarized current injection $S(\mathbf{M}, \mathbf{M}') = \varphi(\mathbf{M}, \mathbf{M}') \exp\{[g(\mathbf{M}') - g(\mathbf{M})]/2kT\}$, where $\varphi(\mathbf{M}, \mathbf{M}')$ is a symmetric function of \mathbf{M} and \mathbf{M}' . The non-conservative nature of spin-torque effects results in the breaking of symmetry of $\varphi(\mathbf{M}, \mathbf{M}')$. This symmetry breaking accounts for the physical fact that, in the presence of spin-polarized current injection, the random magnetization scattering events are biased toward the direction of the vector $\mathbf{u} = \beta \mathbf{M} \times (\mathbf{M} \times \mathbf{e}_p)$, where \mathbf{e}_p is the unit vector whose direction coincides with the spin-polarization of injected electrons and β is proportional to the injected spin-polarized current density. By using this bias in the mathematical structure of $S(\mathbf{M}, \mathbf{M}')$, it is demonstrated that the expected (mean) value of the jump-noise process has two distinct terms: one that can be identified with damping and another that corresponds to spin-torque. This second term has a mathematical form similar to the one proposed by J. Slonczewski in [4]. It is also remarkable that this derivation results in a damping coefficient expression which is affected by the presence of spin-polarized current injection. This is natural on physical grounds because the spin-polarized current injection affects overall thermal interactions, which are ultimately responsible for relaxation and damping. According to the Helmholtz decomposition theorem, any magnetization dynamics on the sphere $|\mathbf{M}(t)| = M_s$ can be fully described in terms of two potentials. The interpretation of the derived expressions for damping and spin-torque in terms of these potentials will be discussed in the paper as well.

-
- [1] I. Mayergoyz, G. Bertotti and C. Serpico, Physical Review B 83, 020402(R) (2011).
 - [2] I. Mayergoyz, G. Bertotti and C. Serpico, J. Appl. Phys. 109, 07D312 (2011).
 - [3] I. Mayergoyz, G. Bertotti and C. Serpico, J. Appl. Phys. 109, 07D327 (2011).
 - [4] J. C. Slonczewski, Journal of Magnetism and Magnetic Materials 159, L1 (1996).

Guided self-assembly of magnetic beads for biomedical applications

Markus Gusenbauer^a, Ha Nguyen^{b,c}, Martin Brandl^b, Thomas Schrefl^a

^a Industrial Simulation, St. Poelten University of Applied Sciences, St. Poelten, Austria

^b Center for Biomedical Technology, Danube University, Krems, Austria

^c Institute for Microelectronics and Microsensors, Johannes Kepler University, Linz, Austria

The analysis of circulating tumor cells (CTCs) supports the monitoring of tumor growth and can be used to control the success of cancer therapies. Microfluidic chips help to detect, identify and count these cells in peripheral blood. In these devices the distinct properties (size, affinity, density) of the tumor cells are used to filter them. The technical challenge is to detect, count and isolate one CTC in one billion blood cells (1–100 tumor cells per ml blood). A promising approach from Saliba et al. uses self-organizing chains of ferromagnetic biofunctionalized beads [1]. An array of magnetic traps is prepared by microcontact printing in a microfluidic channel. Single particle chains line up to create a sieve like structure. This method is limited by flow rate due to decreasing chain stability with higher velocity. Our proposed chip technology uses very thin Ni seeding points with a diameter several times larger than the bead diameter. Once magnetized by the field of a permanent magnet the seeding points induce a magnetic gradient field in the microfluidic channel. The beads will arrange themselves at positions where the sum of all the forces created by the stray fields of the Ni discs, the permanent magnet and the magnetic beads is zero.

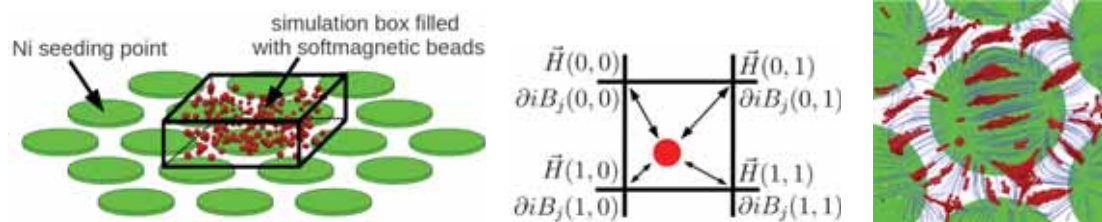


Figure 1: FEM micromagnetics setup to calculate stray field from Ni seeding points in simulation box (left). Discrete particle dynamics simulate micromagnetic beads using particle-in-cell interpolation (center). Simulation result from top view (right).

The simulation consists of two consecutive cycles. (a) We compute the stray field from the Ni seeds. Several permanent magnets create the external field which magnetizes the Ni array. The magnetization within the Ni seeding points is computed using a finite element calculation [2]. The stronger the permanent magnets the higher the perpendicular magnetization component in the Ni array will be. In addition we obtain the magnetic field distribution in the fluid channel. (b) Afterwards we compute the arrangement of the beads in the total magnetic field. We apply the particle-in-cell method to compute the forces on the magnetic beads with $\vec{F} = \vec{\nabla}(\vec{m} \cdot \vec{B})$. The field gradients are obtained by numerical differentiation on a regular grid. The very same grid is used to calculate the force acting on the micromagnetic beads. Magnetic particle dynamics simulations show the resulting structures close to the seeding points (see fig. 1).

Acknowledgements: The authors gratefully acknowledge the financial support of Life Science Krems GmbH, the Research Association of Lower Austria.

[1] A. Saliba et al., Proc. of the Nat. Acad. of Sciences **107(33)** (2010), 14524–14529

[2] FEMME software, <http://suessco.com/simulations/solutions/femme-software>

Domain wall dynamics in out-of-plane magnetized magnetic tracks in the presence of Dzyaloshinskii-Moriya interaction

O. Boulle^a, S. Rohart^b, L. D. Buda-Prejbeanu^a, E. Jué^a, M. Miron^a, S. Pizzini^c, J. Vogel^c, A. Thiaville^b, G. Gaudin^a

^a SPINTEC, CEA/CNRS/UJF/INPG, INAC, 38054 Grenoble Cedex 9, France

^bLab. Physique des Solides, Univ. Paris-Sud, CNRS UMR 8502, 91405 Orsay, France

^c Institut Néel, CNRS, 25 avenue des Martyrs, B.P. 166, 38042 Grenoble Cedex 9, France

Current-induced magnetization dynamics in ultrathin magnetic multilayers with structure inversion asymmetry and perpendicular anisotropy, such as Pt/Co/AlOx multilayers, has recently attracted much attention. Very fast current induced domain wall motion (DW) [1] and current-induced magnetization reversal [2] were recently demonstrated in such multilayers and attributed to the presence of a Rashba spin-orbit interaction as well as to the Spin Hall effect. The presence of inversion asymmetry in an ultrathin magnetic layer may also lead to an additional anti-symmetric exchange magnetic energy term, namely the Dzyaloshinskii-Moriya interaction (DMI), which can strongly affect the magnetization pattern, leading for example to chiral spin spirals for large DMI [3].

In this study, we have explored the influence of the DMI on the DW structure and DW dynamics in ultrathin films with perpendicular anisotropy. We have considered the Fert form [4,5] of the DMI induced by an adjacent layer that reads in continuous form

$$E_{\text{DMI}} = D \left[\mathbf{m}_z \frac{\partial \mathbf{m}_x}{\partial x} - \mathbf{m}_x \frac{\partial \mathbf{m}_z}{\partial x} + \mathbf{m}_z \frac{\partial \mathbf{m}_y}{\partial y} - \mathbf{m}_y \frac{\partial \mathbf{m}_z}{\partial y} \right] \quad (1)$$

where z is the film normal direction (oriented from the adjacent layer to the film), $\vec{\mathbf{m}}$ the unit magnetization vector, and D (units J/m²) the DMI constant in micromagnetic notation. We show that for sufficiently large DMI, this form leads to Néel-like domain walls. Depending on the value of the DMI constant, these walls can move in stationary conditions at large velocities under large fields. We have also studied the current-induced domain wall motion under the spin Hall effect which leads to very high domain wall velocity due to a torque maximised in the Néel DW configuration. Our results shed light on the DW dynamics in ultrathin magnetic layers and should help to interpret recent experiments of current and field- induced DW dynamics.

[1] M. Miron et al., Nat. Mater., **10**, (2011) 419-423

[2] M. Miron et al., Nature, **476**, (2011) 189-193

[3] M. Bode et al., Nature, , **447**, (2007), 190-193

[4] A. Fert, Mater. Science Forum **59-60**, 439 (1990); A. Fert, P.M. Levy, Phys. Rev. Lett. **44**, 1538 (1980).

[5] A. Thiaville et al., Europhysics Letters, **100**, (2012), 57002

Influence of disorder on vortex domain wall mobility in magnetic nanowires

Jonathan Leliaert^{a,b}, Ben Van de Wiele^a, Arne Vansteenkiste^b, Lasse Laurson^c, Gianfranco Durin^{d,e},
Bartel Van Waeyenberge^b, Luc Dupré^a,

^a Department of Electrical Energy, Systems and Automation, Ghent University, Ghent, Belgium

^b Department of Solid State Physics, Ghent University, Ghent, Belgium

^cCOMP Centre of Excellence, Department of Applied Physics, Aalto University, Espoo, Finland

^dIstituto Nazionale di Ricerca Metrologica Torino, Italy

^eISI Foundation, Torino, Italy

A large amount of future spintronic devices is based on the control of the static and dynamic properties of magnetic domain walls in magnetic nanowires. For these applications, understanding the domain wall mobility under the action of spin polarized currents is of paramount importance. Numerous studies describe the spin-current driven domain wall motion in nanowires with ideal material properties, while only some authors take into account the influence of the nanowire edge roughness [1]. In this contribution we numerically investigate the influence of distributed disorder on the vortex domain wall mobility in Permalloy nanowires.

To this aim, we use the GPU based micromagnetic software package MuMax[2] to simulate the propagation of vortex domain walls in nanowires with cross sectional dimensions of 400x10 nm². We apply spin polarized currents acting on the domain wall by means of the Spin Transfer Torque (STT) mechanism, considering a system with perfect adiabaticity ($\beta=0$) and with non-adiabatic STT contributions ($\beta=\alpha$ and $\beta=2\alpha$, α is the Gilbert damping). As in [3], the disorder is simulated as a random distribution of 3.125x3.125nm² sized voids. For each current value, average domain wall velocities are computed considering 25 different realisations of the disorder.

We find that even very small disorder concentrations have a huge impact on the domain wall mobility. In the non-adiabatic case ($\beta=2\alpha$), the domain wall velocity is largely suppressed below the Walker breakdown since the disorder is able to pin the vortex structure hindering the formation of the transverse domain wall, characteristic to the movement in this current region. In the adiabatic case ($\beta=0$), the intrinsic depinning threshold is largely reduced. Even very small disorder densities disable the domain wall to internally balance the Landau-Lifshitz-Gilbert torques with the STT torques, resulting in a non-zero domain wall speed. At low currents, the disorder pins the domain wall structure.

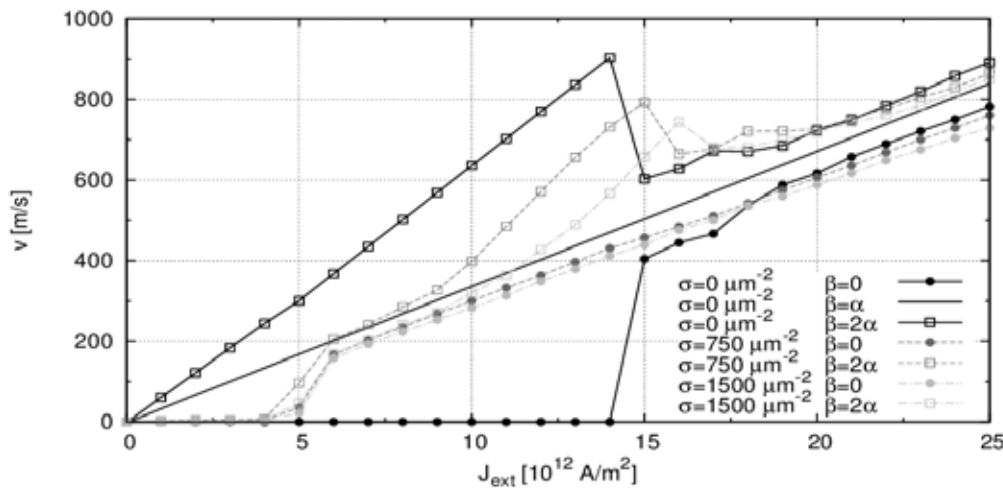


Figure 1: Average speed versus applied current for adiabatic ($\beta=0$) and non-adiabatic ($\beta=2\alpha$) case with varying disorder density σ . The curves tend to converge to the ($\beta=\alpha$) case without disorder, $\sigma=0$, which could explain the large variety of experimentally obtained values for β .

[1] A. Thiaville, *et al. J. Appl. Phys.*, 95, 7049-7051 (2004).

[2] A. Vansteenkiste and B. Van de Wiele, *J. Magn. Magn. Mat.*, 323, No. 21 (2011).

[3] B. Van de Wiele, *et al. Phys. Rev. B* 86, 144415 (2012).

Magnetic droplet driven domain-wall injection in spin-valve nanowires with perpendicular magnetic anisotropy

Ezio Iacocca^a, Majid Mohseni^b, Sunjae Chung^{a,b}, Randy K. Dumas^a, Mark Hofer^c,
Johan Åkerman^{a,b}

^a Physics Department, University of Gothenburg, Gothenburg, Sweden

^b Material Physics, School of ICT, Royal Institute of Technology, Kista, Sweden

^c Department of Mathematics, North Carolina State University, Raleigh, USA

Recent developments in magnetic nanowires have encouraged research on domain-wall (DW) based memory and computation applications [1]. A major drawback of these technologies is found in the DW nucleation methods. In fact, common procedures involve large applied fields, patterned nanostrip antennas, and large sample areas used as magnetic reservoirs. Such techniques limit device miniaturization and the DW nucleation reliability.

An attractive solution relies on spin-torque excited magnetic dissipative droplets [2]. These dynamical modes are localized in nature and its large amplitude precession induces a local magnetization reversal. Therefore, its controlled collapse ensures the stabilization of a nanosized domain and its related DW. By means of micromagnetic simulations [3], we report the injection of DWs in nanowires with perpendicular magnetic anisotropy (PMA) via the excitation and collapse of a novel, quasi-one-dimensional (quasi-1D) droplet (fig. 1.a). In contrast to the dissipative droplet, the quasi-1D droplet is reminiscent of a one dimensional soliton [4] and its oscillation is sustained by fields as low as 0.02 T. Moreover, its controlled collapse is achieved by removing both the bias field and current.

These results suggest a reliable and localized method to inject DWs in PMA nanowires. As a proof of concept, we perform simulations of a notched nanowire, where the notches act as pinning sites for the DWs. As shown in fig. 1.b, a train of DWs are reliably injected by our proposed method and driven into the notches by an in-plane bias current. In summary, we believe that this domain wall injection method will play an important role in the development of high density all-magnetic logic applications.

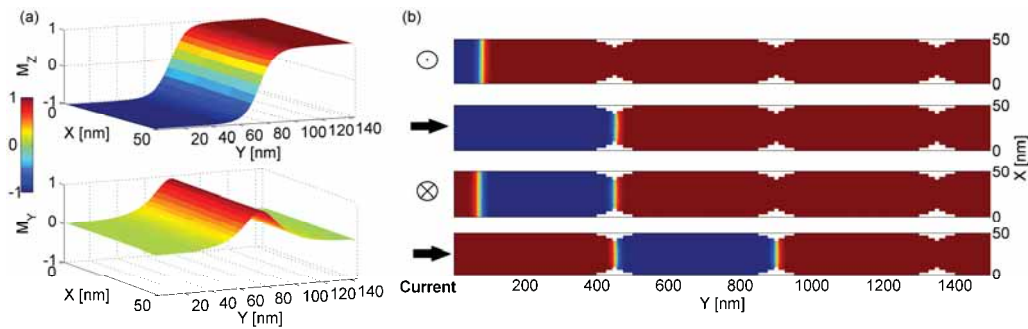


Figure 1: (a) Snapshot of the Z and X magnetization component of the quasi-1D droplet. (b) Colorplots of the Z magnetization component where a train of droplet-driven domain walls are nucleated and driven into the pinning sites.

-
- [1] Allwood et al. *Science* **309**, 1688 (2005); Parkin et al. *Science* **320**, 190 (2008).
 - [2] Mohseni et al. *Science*, **accepted** (2013); Hofer et al. *Phys. Rev. B* **82**, 054432 (2010).
 - [3] Vansteenkiste and de Wiele, *J. Magn. Magn. Mater.* **323**, 2585 (2011).
 - [4] Akhmediev et al. *Phys. Rev. E* **63**, 056602 (2001).

Spontaneous magnetization reversal by domain walls interaction in magnetic uniaxial film elements

Vladimir A. Skidanov, Petr M. Vetoshko and Alexander Stempkovskiy

Institute for Design Problems in Microelectronics RAS, Moscow, Russia

In most cases domain structure reduces magnetostatic energy so that total magnetic moment of magnetic specimen tends to be zero in absence of external magnetic field. But if magnetization M is small enough to maintain monodomain state when specimen size L is more than domain wall (DW) width magnetic sample can exhibit unexpected behaviour in magnetization process. Such a situation takes place in elements etched in uniaxial diluted garnet film with artificially formed single domain DW between two domains with opposite magnetization directions normal to film plane [1].

In the present paper asymmetrical domain structure with more DWs is investigated experimentally by magneto-optical registration of magnetization reversal process. It is shown that strong magnetostatic interaction between domain walls leads to negative total magnetic moment after sub-saturation in positive direction as it is seen in graph in Fig. 1. Stray field formed by DW exceeds stray field formed by garnet boundary due to double equivalent current. As a result of magnetostatic repulsion between two parallel DWs rectangular element is self-magnetized even in zero external field as it is shown in Fig. 1 (upper row).

The second mechanism of magnetization reversal after external field removing is related to DW's surface energy which tends to reduce domain wall length. The result of joint action of magnetostatic repulsion and DW length shortening mechanisms is shown for four pinned domain walls in lower row photos in Fig. 1. This case magnetostatic energy increase may take place due to reduction of DW surface energy in total free energy balance.

Magnetization curve exhibits negligible hysteresis (less than experimental error) due to DW coercive force suppression by high gradient of effective field whereas intrinsic coercive field of garnet film is found to be $H_c \sim 0.7$ Oe with Barkhausen jumps length up to 10 mcm.

Due to high Faraday rotation and low switching field such structures can be used as magnetically controlled high speed valves for optical information treatment.

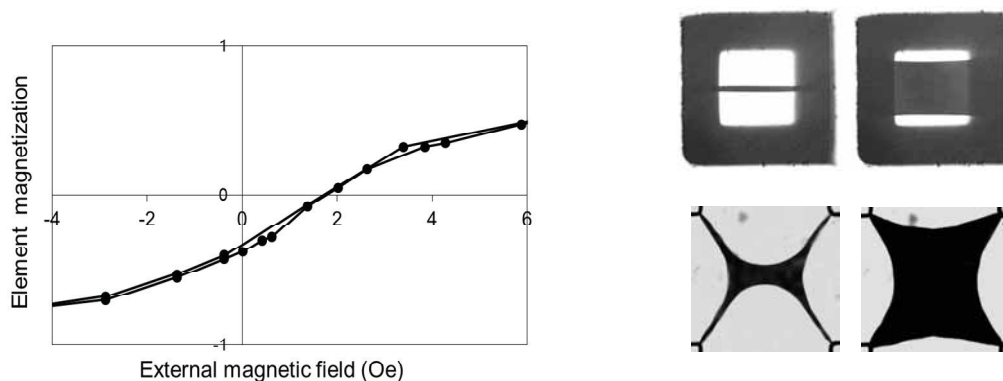


Figure 1: Typical magnetization curve and domain structures in square elements with two free DWs (upper row) and four pinned DWs (lower row) in external field $H = 10$ Oe (left column) and zero field (right column). Garnet film magnetization $4\pi M = 50$ G, DW coercivity field $H_c \sim 0.7$ Oe, thickness $h = 8.5$ mcm, square side $L = 60$ mcm.

[1] V. Skidanov, P. Vetoshko, A. Stempkovskiy, Journal of Phys.: Conf. Series, **266** (2011), 012125.

Dynamics of a magnetic skyrmion in a thin film disk with perpendicular anisotropy

B. Krüger^a, F. Büttner^{a,b}, C. Moutafis^c, I. Makhfudz^d, O. Tchernyshyov^d, M. Schneider^b, C. M. Günther^b, J. Geilhufe^e, J. Mohanty^b, C. v. Korff Schmiesing^b, J. Franken^f, M. Foerster^a, T. Schulz^a, H. Swagten^f, S. Eisebitt^{b,e}, and M. Kläui^a

^a Institut für Physik, Johannes Gutenberg-Universität Mainz, Mainz, Germany

^b Institut für Optik und Atomare Physik, Technische Universität Berlin, Berlin, Germany

^c Swiss Light Source, Paul Scherrer Institut, Villigen, Switzerland

^d Johns Hopkins University, Baltimore, USA

^e Helmholtz-Zentrum Berlin für Materialien und Energie, Berlin, Germany

^f Technische Universiteit Eindhoven, Eindhoven, Netherlands

In the past decade, the dynamics of magnetic vortices has been intensively investigated but much less is known about the dynamics of the magnetic bubble, a skyrmion spin structure in a magnetic medium with high perpendicular anisotropy. The magnetization inside a bubble points out-of-plane and antiparallel to the magnetization in the surrounding domain as shown in fig. 1(a). These two domains are separated by a Bloch-type domain wall.

Micromagnetic simulations predict that even for small excitations a magnetic bubble moves on a non-circular trajectory [1]. This is in contrast to observations on magnetic vortices where the motion is circular [2]. These differences can be explained by our recent analytical model [3], which describes the displacement of the bubble in terms of two waves that travel along the domain wall confining the bubble. These waves have different frequencies and move in opposite directions. Their superposition determines the position of the bubble resulting in a finite momentum of the bubble. The analytical model further shows that the sense of free gyration of a bubble depends on its initial state, that is, the wave with the largest amplitude dominates.

We investigate bubble states in disc-shaped CoB/Pt multilayer elements experimentally using X-ray holographic imaging. The two bubble state in fig. 1 is excited by a bipolar out-of-plane field pulse. The trajectory of the center of the bubble that is highlighted in image (b) is plotted in (c). In response to the field, the bubble is displaced from its equilibrium position. The relaxation back to the equilibrium position is a cycloidal motion. This is the first direct observation of the GHz gyrotropic motion in a magnetic bubble system. The observed

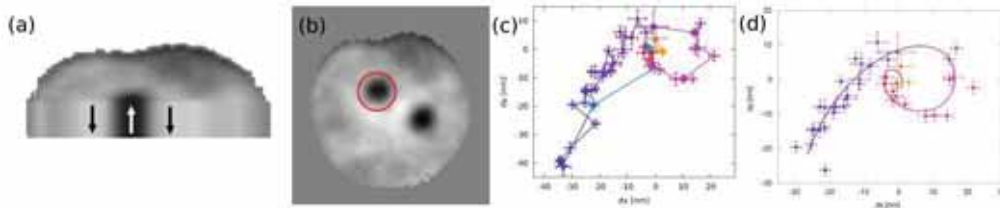


Figure 1: (a) Cross section and (b) top view of a magnetic bubble state in a 550 nm diameter disc. The gray scale indicates the out-of-plane magnetization. (c) Measured trajectory of the magnetic bubble and (d) fit with the analytical expression [3].

trajectory is in excellent agreement with our theoretical model, as shown by a fit in fig. 1, and allows us to determine the eigenfrequencies and the effective mass of the bubble domain.

[1] C. Moutafis, S. Komineas, and J. A. C. Bland, Phys. Rev. B **79**, 224429 (2009).

[2] B. Krüger et al. Phys. Rev. B **76**, 224426 (2007).

[3] I. Makhfudz, B. Krüger, and O. Tchernyshyov, Phys. Rev. Lett. **109**, 217201 (2012).

Numerical investigation of skyrmion formation in geometrically confined MnSi thin film structures

Marijan Beg^a, Justin Diviney^a, Dmitri Chernyshenko^a, Marc-Antonio Bisotti^a,
Weiwei Wang^a, Maximilian Albert^a, Robert Stamps^b, Hans Fangohr^a

^a University of Southampton, Southampton, United Kingdom

^b University of Glasgow, Glasgow, United Kingdom

Apart from some trivial magnetic orders, spins can align in some highly complicated spin textures. One of these nontrivial spin textures is the topologically stable skyrmion pattern which forms in magnetic systems with lack of inversion symmetry [1]. It has been observed that skyrmions form only in a narrow region of the B - T phase diagram, which is mainly occupied by helical and ferromagnetic phase regions. Most experimental and theoretical studies were performed on thin film samples which, relative to their thickness, can be considered as infinitely large in the film layer. For the realisation of electronic devices it is required to know under what circumstances skyrmions are formed in thin films of finite size.

We have conducted an extensive numerical investigation of essential phase diagram parameters in geometrically confined thin film samples. Simulations were performed using the Metropolis Monte Carlo algorithm based on Heisenberg exchange, Dzyaloshinskii-Moriya and Zeeman energy contributions. We report that the critical external fields, which define the edges of skyrmion region in B - T phase diagram, strongly depend on the sample geometry. As the sample size is decreased, the critical external field B_{C_1} – which defines the transition from the skyrmion phase into the helical order phase – moves towards lower values, whereas B_{C_2} – which divides skyrmion and ferromagnetic order – increases when the sample size is reduced. We thus demonstrate that range of external field values for which the skyrmion phase exists grows as the sample size decreases. In particular, we find that B_{C_1} reduces to 0T below some value of sample size; opening the door for zero-field skyrmionic states in confined nano structures.

We acknowledge financial support from EPSRC's DTC grant EP/G03690X/1.

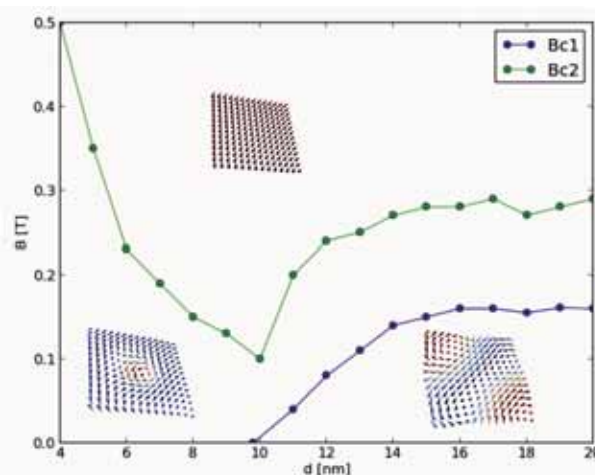


Figure 1: Dependence of critical field values B_{C_1} and B_{C_2} on sample size d .

[1] Yu, X. Z. et al. "Real-space observation of a two-dimension skyrmion crystal", Nature **465** 901-904 (2010)

Measurement of magnetization process for magnetic grain region in austenitic stainless steel using μ -MOKE magnetometer

Kenichi Terashima, Hidetoshi Ueno, Makoto Ishiwata, Katsuhiko Yamaguchi

Fukushima University, Fukushima, Japan

Austenitic stainless steels SUS304 have slight magnetism affected by degradations such as strain hardening, although they show non-magnetism originally. The magnetic properties as bulk have been investigated well with an expectation for a development of new magnetic non-destructive evaluation method. On the other hand, the magnetization process of a specified magnetic grain surrounded by non-magnetic region in SUS304 has not been studied sufficiently, because of the difficulty for measurement. In this paper, the magnetization processes for the magnetic grain in SUS304 are reported using the measured data by micro magneto-optical Kerr effect (μ -MOKE) magnetometers combined with a magnetic domain scope.

Figure 1(a) shows an optical microscope image for the surface of optical polished SUS 304 sample. Magnetic grains in the same area are revealed using magnetic domain scope as shown in Fig.1(b), that is, magnetic regions are shown as dark colored area in Fig.1(b) which is differential image between the applied magnetic field ± 300 Oe. Magnetization process as a major loop within ± 0.5 kOe at the laser spot in Fig.1(b) was measured by μ -MOKE magnetometer as shown in Fig.2. Furthermore, minor loops at the same spot also can be measured.

As the results, magnetization measurement including minor loop is possible used to μ -MOKE, and suggest that magnetic behaviour of each magnetic grain in non-magnetic region is analysed.

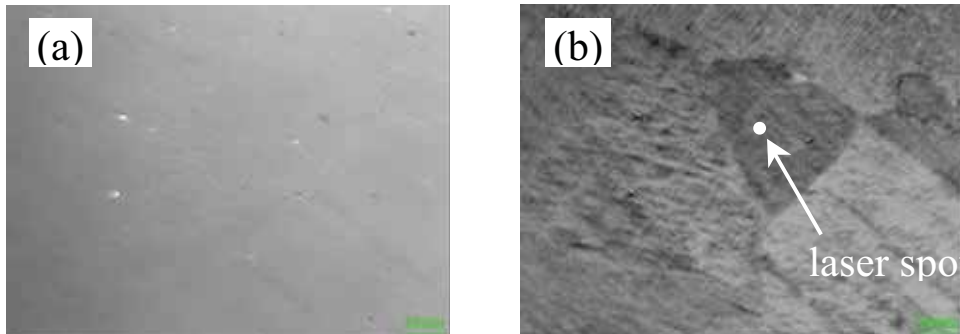


Fig. 1: (a) Optical microscope image and (b) magnetic domain observation differential image between the applied magnetic field ± 300 Oe of SUS 304.

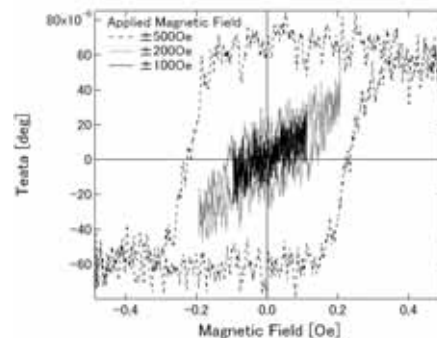


Fig. 2: Magnetic hysteresis curves at laser spot shown in Fig.1(b).

Magnetic properties and EXAFS study of nanocrystalline $\text{Fe}_2\text{Mn}_{0.5}\text{Cu}_{0.5}\text{Al}$ synthesized using mechanical alloying technique

Dwi Nanto^a, Dianta Ginting^a, Dong-Seok Yang^b, Seong-Cho Yu^a

^a Dept. of Physics, Chungbuk National University, Cheongju, 361-763, South Korea

^b Physics Division, School of Science Education, Chungbuk National University, Cheongju, 361-763, South Korea

Nanotechnology has attracted many advanced research fields because the impact on many wide different scientific areas. It is the fact that nanocrystalline materials exhibit physical properties that are much different comparing the former bulk shape. Magnetic nanocrystalline has gained interest for applications in various fields and can be exploited in a vast variety of different applications. In our work, we use Fe_2MnAl (FMA), one of Heusler alloy, as parental. Bradley and Rodgers explained briefly that transformation crystal structure of Cu_2MnAl during heat treatment become entirely body-centered cubic, with a face-centered superlattice, is the main reason why Heusler alloy of Cu_2MnAl exhibits ferromagnetism even though the elements constructed has no ferromagnetic behavior [1].

In this work, nanocrystalline $\text{Fe}_2\text{Mn}_{0.5}\text{Cu}_{0.5}\text{Al}$ (FMCA) alloy was prepared by mechanical alloying technique. The magnetic properties were investigated by using vibrating sample magnetometer (VSM). The result shows that nanocrystalline FMCA alloy has better hysteresis loop squareness and much larger coercivity than nanosized FMA [2]. The magnetic saturation estimates more than two times higher than it. In current work, FMCA is also a good candidate of high density recording media. The enhancement of magnetic saturation by Cu-doped on Mn site of FMA presumably due to site competes between Mn and Cu elements which have a similar atomic radius and their electron valance.

In accordance to the magnetic results, it is interesting to discuss in detail the structure of nanocrystalline FMCA. Influence of milling time on local ordering around the central atom was studied by using extended X-ray absorption fine structure (EXAFS) beamline at Pohang Accelerator Laboratory, South Korea. The first shell of the Fourier transformed spectra changed with milling time, indicating a change in the local ordering around the central Fe atom. The study of crystal structure nanocrystalline (FMCA) alloy is also important to explain its ferromagnetism phenomenon. This work, therefore, is significant in explaining physical background that indicates an enhancement of magnetization on copper doped Heusler alloy.

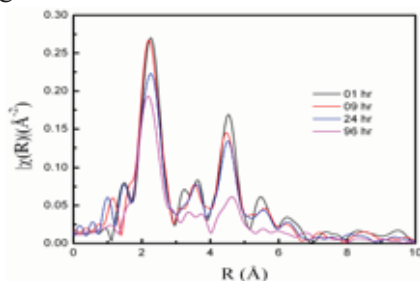


Fig. 1 EXAFS spectra of nanocrystalline $\text{Fe}_2\text{Mn}_{0.5}\text{Cu}_{0.5}\text{Al}$ as function of milling time.

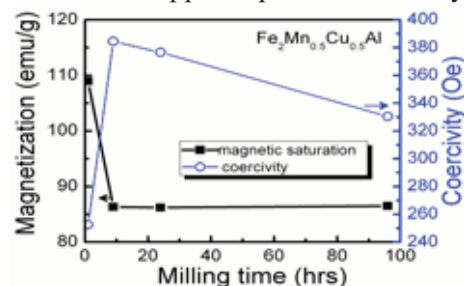


Fig. 2 Magnetic properties of $\text{Fe}_2\text{Mn}_{0.5}\text{Cu}_{0.5}\text{Al}$ nanocrystalline as function of milling time.

References

- [1] A. J. Bradley and J. W. Rodgers, Proceedings of the Royal Society of London. 144, 340 1934.
- [2] A. Vinesh, Hina Bhargava, N. Lakshmi, and K. Venugopalan, J. Appl. Phys. 105, 07A309, 2009.



Ordine degli Ingegneri
Provincia di Messina



investiamo nel vostro futuro

"P.O.N. Ricerca e Competitività" 2007-2013 per le Regioni di Convergenza
Codice Progetto PON01_01322 finanziato a valere sull'ASSE I – Sostegno ai mutamenti strutturali
Obiettivo Operativo 4.1.1.4 "Potenziamento delle strutture e delle dotazioni scientifiche e tecnologiche"
Azione I: "Rafforzamento Strutturale"



Università degli Studi
di Messina

